NIKHEF NATIONAL INSTITUTE FOR NUCLEAR PHYSICS AND HIGH-ENERGY PHYSICS

2001

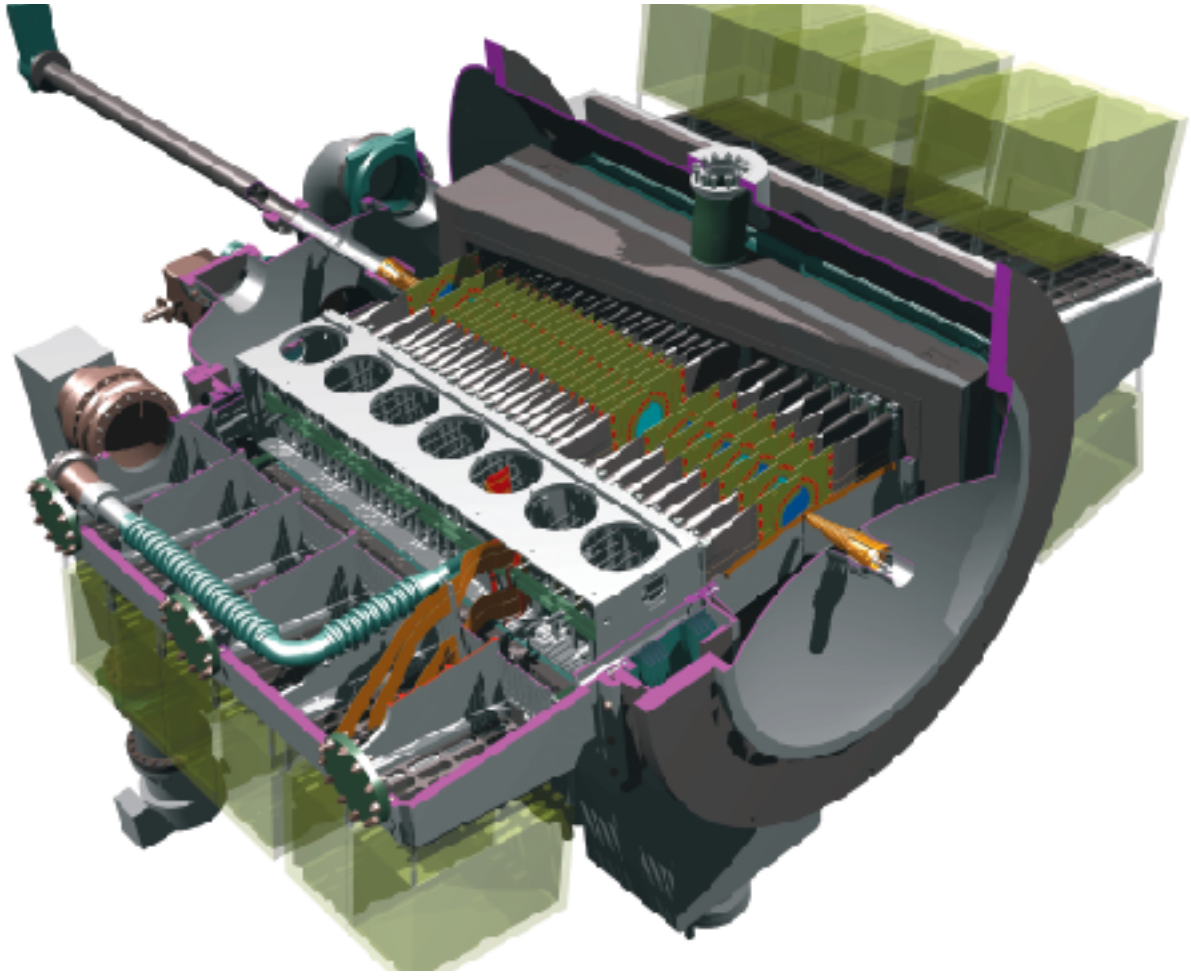

ANNUAL REPORT

NIKHEF

NATIONAL INSTITUTE FOR NUCLEAR PHYSICS AND HIGH-ENERGY PHYSICS

ANNUAL REPORT

2001

Kruislaan 409, 1098 SJ Amsterdam
P.O. Box 41882, 1009 DB Amsterdam

Colofon

Publication edited for NIKHEF:

Address:	Postbus 41882, 1009 DB Amsterdam Kruislaan 409, 1098 SJ Amsterdam
Phone:	+31 20 592 2000
Fax:	+31 20 592 5155
E-mail:	directie@nikhef.nl
Editors:	Louk Lapikás & Marcel Vreeswijk
Layout & art-work:	Kees Huyser
Organisation:	Anja van Dulmen
Cover Photograph:	A 3-D drawing of the LHCb Vertex detector
URL:	http://www.nikhef.nl

The National Institute for Nuclear Physics and High-Energy Physics (NIKHEF) is a joint venture of the Stichting voor Fundamenteel Onderzoek der Materie (FOM), the Universiteit van Amsterdam (UVA), the Katholieke Universiteit Nijmegen (KUN), the Vrije Universiteit Amsterdam (VUA) and the Universiteit Utrecht (UU). The NIKHEF laboratory is located at the Science and Technology Centre Watergraafsmeer (WCW) in Amsterdam.

The activities in experimental subatomic physics are coordinated and supported by NIKHEF with locations at Amsterdam, Nijmegen and Utrecht. The scientific programme is carried out by FOM, UVA, KUN, VUA and UU staff. Experiments are done at the European accelerator centre CERN in Geneva, where NIKHEF participates in two LEP experiments (L3 and DELPHI), in a neutrino experiment (CHORUS) and in SPS heavy ion experiments (NA57 and NA49). NIKHEF participates in the Tevatron experiment D0 at Fermilab, Chicago. At DESY in Hamburg NIKHEF participates in the ZEUS, HERMES and HERA-B experiments. Research and development activities are in progress for the future experiments ATLAS, ALICE and LHCb with the Large Hadron Collider (LHC) at CERN.

NIKHEF is closely cooperating with the University of Twente. Training and education of students are vital elements in the research climate of the laboratory.

Contents

Preface

In this Annual Report we look back at the achievements of NIKHEF in the year 2001, a year that unfortunately was overshadowed by the tragic death of Cees Bakker who we commemorate with thankfulness.

In the year 2001 important progress was made towards the technical realisation of the large-scale hardware projects for the future LHC experiments. The production of the Atlas muon-chambers was successfully started and the first vacuum vessel of the huge end-cap toroids was produced in industry and delivered at CERN. The development and production of the state-of-the art instrumentation for Atlas, LHC-b and Alice will continue to make great demands on the professional skills and dedication in our technical departments during the coming years. As has been the case in 2001 we will have to solve complex technical and planning problems within tight constraints imposed by limited resources – I am convinced we will be able to do so, motivated by the fact that the LHC is the most important project in high energy physics on a world-scale for at least the coming decade. Computing in the LHC era will put unprecedented demands on CPU and storage capacity. NIKHEF plays a leading role in various pilot projects aiming at developing GRID technology, the new approach to large scale computing.

Wonderful results continue to emerge from the Delphi and L3 experiments at LEP and from ZEUS and Hermes at HERA. The latter two have undergone major upgrades in 2001 with important contributions from our institute. These experiments and also the HERA-B experiment at DESY (Hamburg, Germany), the fixed target heavy ion experiments at CERN and the D0 project at Fermilab (Batavia, USA) will provide excellent opportunities for research at the forefront of high energy physics while the LHC programme is prepared. In 2001 the Chorus programme was concluded; a number of interesting publications will, however, still follow as is the case for the AmPS programme concluded earlier. The Antares project in the emerging new field of astro-particle physics made important steps towards the launch of the first detector string in the Mediterranean Sea, now planned for late 2002. The NIKHEF participation in Antares represents the only activity in the Netherlands in this rapidly growing field.

During the first six months of the period covered by this annual report the NIKHEF programme was carried out under the responsibility of my predecessor professor Ger van Middelkoop. It was a rewarding task to consolidate this ambitious and well balanced programme in a well organised institute with an excellent infrastructure. I hope that the fruitful collaboration in NIKHEF between FOM and the universities KUN, UU, UvA and VU will continue to proof an excellent basis for research at the frontier of one of the most exciting fields in physics - a field in which imaginative attempts to look beyond the horizon of the LHC already appear on the agenda; NIKHEF certainly has the ambition to also participate in the definition of this agenda and with our priorities clearly reflected in this Annual Report 2001 I hope we will have a lively scientific debate even beyond these priorities.

Jos Engelen

A Experimental Programmes

1 AmPS

1.1 Introduction

The analysis of the experiments performed with AmPS reaches its final stage. While the analysis of all experiments carried out in EMIN is finished, there remain the analyses of a few experiments performed in the Internal-Target Facility (ITF). These pertain to scattering of polarised electrons off polarised ^{1}H, ^{2}H and ^{3}He targets.

The electron-scattering programme with AmPS has been concluded with a report *Results of the AmPS Program* submitted early 2001 to the funding agency FOM. In this report an overview is given of the physics program carried out at the electron-scattering facility AmPS at NIKHEF in the period 1992-1998. The report describes the instrumentation built for this program, and the results obtained with the extracted beam in the EMIN hall and with the stored (polarised) beam in the internal target facility. The scientific program at AmPS was subjected to continuous review by an international Program Advisory Committee (PAC) that met five times between 1991 and 1997. In this period the PAC has considered about 50 proposals, of which 25 were approved for running. The total amount of beam time spent on data taking for these proposals was 4900 hours in EMIN and 3400 hrs in ITF. About 40 groups from abroad have participated in the research program with the beams from AmPS. Part of this work took place within the framework of European network collaborations. The AmPS program has yielded about 60 publications in refereed journals and 35 theses.

1.2 Experiments at EMIN

Spin-Momentum Correlations in Quasi-Elastic Electron Scattering from Deuterium
(Prop. 97-01; with *ETH, Virginia, Arizona, TJNAF, MIT, Hampton, Novosibirsk*)

The deuteron serves as a benchmark for testing nuclear theory. Its simple structure allows reliable calculations to be performed in both non-relativistic and relativistic frameworks. Such calculations are based upon state-of-the-art nucleon-nucleon (*NN*) potentials and the resulting ground-state wave function is dominated by the *S*-state, especially at low relative proton-neutron momentum $\mathbf{p}$ in the centre-of-mass system. Due to the tensor part of the *NN* interaction a *D*-state component is generated. Models predict that the *S*- and *D*-state components strongly depend on $\mathbf{p}$ and are sensitive to the repulsive core of the *NN* interaction at short distances. To obtain sensitivity to the spin structure of the deuteron, spin-dependent observables in quasi-elastic scattering can be used. In the ^{2}H$(e,e'p)n$ reaction, an energy ω and a three-momentum $\mathbf{q}$ are transferred to the nucleus and the nuclear response can be mapped as a function of missing momentum $\mathbf{p}_m$ and missing energy. In the plane-wave impulse approximation (PWIA) the neutron is only a spectator during the scattering process, and $\mathbf{p}_m$ is equal to the initial proton momentum in the deuteron, while the missing energy equals the binding energy.

The polarisation of a proton P_z^p inside a deuteron with a vector polarisation P_1^d, is given by

$$P_z^p = \sqrt{\frac{2}{3}} P_1^d \left(P_S - \frac{1}{2} P_D \right), \qquad (1.1)$$

where P_S and P_D represent the *S*- and *D*-state probability densities of the ground-state wave function, respectively. Note that the polarisation of a nucleon in the *D*-state is opposite to that of a nucleon in the *S*-state.

The cross section for the $^2\vec{\mathrm{H}}(\vec{e},e'p)n$ reaction, in which longitudinally polarised electrons are scattered from a polarised deuterium target, can be written as

$$\begin{aligned} S &= S_0 \{ 1 + P_1^d A_d^V + P_2^d A_d^T \\ &+ h (A_e + P_1^d A_{ed}^V + P_2^d A_{ed}^T) \}, \end{aligned} \qquad (1.2)$$

where S_0 represents the unpolarised cross section, h the polarisation of the electrons, and P_1^d (P_2^d) the vector (tensor) polarisation of the target. The beam analysing power is denoted by A_e, with $A_d^{V/T}$ and $A_{ed}^{V/T}$ the vector and tensor analysing powers and spin-correlation parameters, respectively. We report on the first measurement of A_{ed}^V in the $^2\vec{\mathrm{H}}(\vec{e},e'p)n$ reaction.

Fig. 1.1 shows the experimental results in comparison to various predictions. The short-dashed and dot-dot-dashed curves are PWIA predictions for the Argonne v_{18} *NN* potential with and without inclusion of the *D*-state, respectively. The figure shows that inclusion of the *D*-state is essential to obtain a fair description of the data for the higher missing momenta. The other curves are

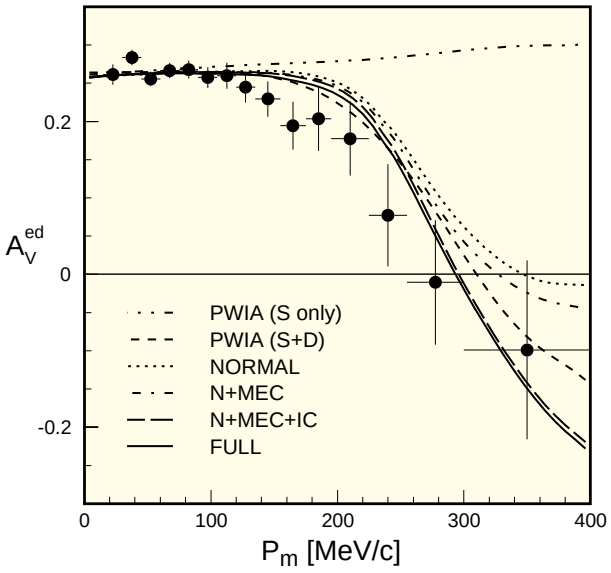

Figure 1.1: *Spin correlation parameter $A_{ed}^V(90^\circ, 0^\circ)$ as a function of missing momentum for the $^2\vec{\mathrm{H}}(\vec{e}, e'p)n$ reaction at $Q^2 = 0.21$ (GeV/c)^2. The short-dashed and dot-dot-dashed curves are PWIA predictions for the Argonne v_{18} NN potential with and without inclusion of the D-wave, respectively. The other curves are predictions of the model of Arenhövel et al., for PWBA+FSI (dotted), PWBA+FSI+MEC (dashed-dotted), PWBA+FSI+MEC+IC (long-dashed) and FULL calculations which include relativistic corrections (solid). The predictions are folded over the detector acceptance by using a Monte-Carlo method.*

predictions of the model of Arenhövel *et al.* for the Bonn *NN* potential and with different descriptions for the spin-dependent reaction mechanism.

At $p_m < 100$ MeV/c, the theoretical results for A_{ed}^V neither depend on the choice of the *NN* potentials, nor on the models for the reaction mechanism. This shows that in this specific kinematic region the deuteron can be used as an effective neutron target. For increasing missing momenta, both the data and predictions for the asymmetry reverse sign. This is expected from Eq. (1.1) for an increasing contribution from the *D*-state component in the ground-state wave function of the deuteron. It can also be observed that inclusion of reaction-mechanism effects, mainly isobar configurations, are required for a better description of the data.

In the region of p_m around 200 MeV/c where the *S*- and *D*-states strongly interfere, the data suggest that all models underestimate A_{ed}^V. This may be attributed to an underestimate of the *D*-state contribution or to a lack in our understanding of the effects of Δ-excitation. This observation may be related to the deficiency in the prediction of the deuteron quadrupole moment by modern *NN* potentials.

The present data comprise the first-time results for the spin correlation parameter $A_{ed}^V(90^\circ, 0^\circ)$ in quasi-elastic electron-proton knock-out from the deuteron. The data are sensitive to the effects of the spin-dependent momentum distribution of the nucleons inside the deuteron. The experiment reveals in a most direct manner the effects of the *D*-state in the deuteron ground-state wave function and shows the importance of isobar configurations for the $^2\vec{\mathrm{H}}(\vec{e}, e'p)n$ reaction.

Spin-Dependent Electron-Proton Scattering in the Δ-Excitation Region
(Prop. 97-01; with *ETH, Virginia, Arizona, TJNAF, MIT, Hampton, Novosibirsk*)

Pion production in the Δ-resonance region is dominated by the magnetic dipole transition form factor ($M1$). Polarisation experiments have established the presence of small but non-zero quadrupole components ($E2$ and $C2$). In the present $^1\vec{\mathrm{H}}(\vec{e}, e')$ experiment, we have measured for the first time both longitudinal and transverse spin correlation parameters in the Δ-region, which are sensitive to the $E2$ and $C2$ form factors, respectively. In order to reliably associate the data with this subtle feature of baryon structure, models, such as the MAID model and the model of Sato and Lee, are required that can accurately describe the reaction mechanism of $\gamma^* p \rightarrow \pi N$ and that are able to disentangle resonant from non-resonant contributions.

The experiment was performed with polarised electrons, accelerated to 720 MeV and stacked in the AmPS storage ring in which a polarised gas target was positioned. The scattered electrons were detected in a large-acceptance magnetic spectrometer. The polarisation axis of the target was oriented, by means of a magnetic holding field, parallel or perpendicular to the direction of the central momentum transfer for $W = 1232$ MeV.

To compare the theoretical results to the data, we developed a Monte-Carlo (MC) code that folded the model predictions over the acceptance. Radiative effects were taken into account by incorporating the fully spin-dependent code POLRAD. Figure 1.2 shows the event distribution as a function of invariant mass in comparison with the MC simulation using the MAID

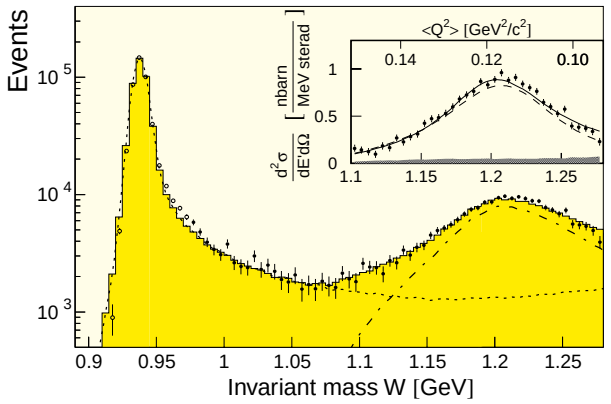

Figure 1.2: *Event distribution as a function of W (see text for explanation).*

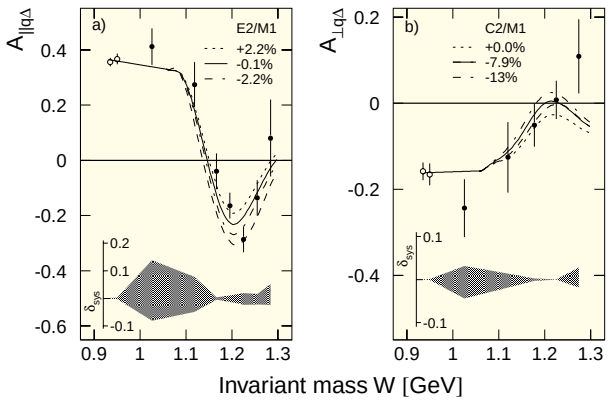

Figure 1.3: *Preliminary results for the spin correlation parameters for longitudinal (a) and transverse (b) spin kinematics as a function of invariant mass W. The dashed curves represent the Sato and Lee model predictions. The other curves indicate predictions of the MAID model for different quadrupole strengths (see text for explanation).*

model. The target density was determined by normalising the MC results to the data in the region of the elastic peak (open circles). The dotted and dot-dashed curves show the contributions from elastic and pion-production processes (including radiative effects). The insert shows the cross section extracted from our measured rates after subtracting the elastic radiation tail and correcting for radiative effects. On top the average Q^2 for each W bin is shown. The shaded area represents the size of the systematic uncertainty. The results are consistent with the cross section of the MAID model (solid curve) and Sato and Lee model (dashed curve).

The two spin correlation parameters are shown as a function of the invariant mass W in Fig. 1.3. The asymmetry data were normalised to the predicted value in the elastic region (open circles). The systematic errors δ_{sys} are indicated by the shaded area. The models describe reasonably well the global behaviour of the present spin correlation data.

The agreement between the models and the data may be improved by adjusting the quadrupole strengths, which are relatively unconstrained model parameters. The solid curves indicate the best fits for $E2/M1$ and $C2/M1$ using the MAID model ($E2/M1 = -0.1\%$ and $C2/M1 = -7.9\%$). The predictions of the Sato and Lee model ($E2/M1 = -2.0\%$ and $C2/M1 = -4.2\%$) are indicated by the dashed curves.

Polarisation observables in $^3\vec{\text{He}}(\vec{e}, e'n)$
(Prop. 94-05; with *ETH, Virginia, Arizona, TJNAF, MIT, Hampton, Novosibirsk*)

In the Internal Target Hall of the MEA/AmPS electron accelerator facility we performed an electron-scattering experiment with polarised electrons and polarised ^{3}He. As the two protons are in a relative S state for 90% of the ^{3}He ground state wave function, polarised ^{3}He can be used as an effective polarised neutron target. The A'_x asymmetry in the $(e, e'n)$ reaction channel is of order 0.1 and sensitive to G_E^n, the electric form factor of the neutron. The A'_z asymmetry is of order 0.5 and mainly used as a benchmark for the theoretical models and for possible systematic errors in the experiment.

In 2001 the background contributions were reanalysed and found to be significantly larger than previously estimated. A remaining unexplained correlation of the A'_z asymmetry with the beam current has been translated into a systematic error, which turned out to be of the same order of magnitude as the statistical error.

For the kinematics in our experiment ($Q^2 \approx 0.2\,\text{GeV}^2/c^2$) Final-State Interactions (FSI) are expected to play an important role. Calculations were carried out by the Bochum theory group of J. Golak and by S. Nagorny, using fundamentally different formalisms. Golak's calculations are based on a non-relativistic formalism which takes FSI into account to all orders by solving a set of Faddeev equations. Nagorny's Lorentz covariant calculations include rescattering terms up to second order. Both methods use G_E^n as a free parameter.

The final results of the Monte-Carlo simulations based on these calculations became available in 2001 (see Fig.

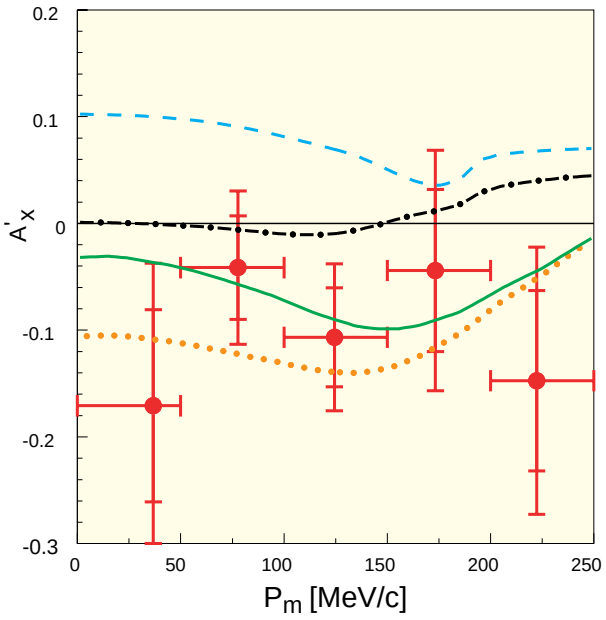

Figure 1.4: *The A'_x asymmetry versus missing momentum. The curves are results of Monte-Carlo simulations based on Faddeev calculations with $G_E^n = 0$ (dotted) or equal to the Galster parameterisation $G_{E,Galster}^n$ (solid), and on the calculations by Nagorny, with $G_E^n = 0$ (dash-dotted) or $G_E^n = G_{E,Galster}^n$ (dashed).*

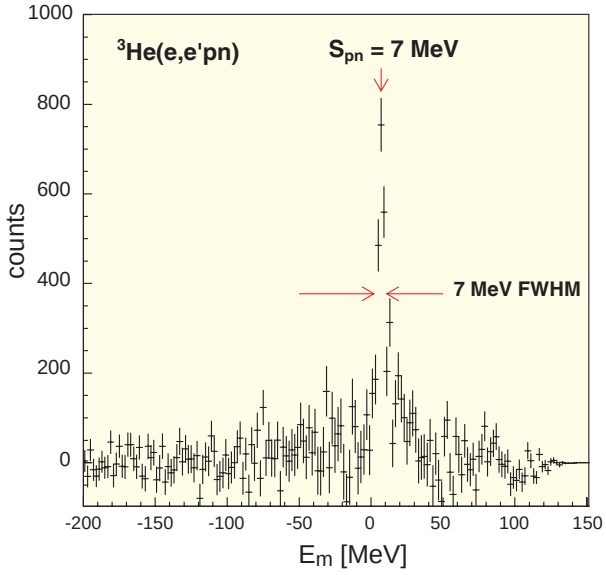

Figure 1.5: *Missing energy spectrum of the $^3He(e, e'pn)$ reaction. The peak corresponds to the transition in which the residual system is left in its ground state.*

1.4). The MC results based on Nagorny's calculations do not show a large deviation from the lowest-order calculation (plane-wave impulse approximation), whereas the Faddeev calculations exhibit a large negative offset due to FSI. This negative offset is compatible with our experimental A'_x data for a G_E^n value of $+0.031 \pm 0.034$ (the purely statistical error is 0.023). Using Nagorny's calculations one would extract a negative value for G_E^n which is inconsistent with the world data set by four standard deviations.

1.3 Experiments abroad

Study of the ^{3}He$(e, e'pn)$ Reaction
(Prop. A1/4-98; with *the Universities of Mainz, Tübingen and Glasgow*)

Nucleon-nucleon correlations and two-body currents in the three-nucleon system are under investigation by means of a ^{3}He$(e, e'pn)$ experiment in the A1 hall at MAMI, Mainz. This nucleus has been chosen because continuum-wave Faddeev calculations with realistic *NN* interactions are presently available. The interpretation of these data will be done in combination with the existing data of the complementary ^{3}He$(e, e'pp)$ reaction, obtained at AmPS. This approach offers the unique possibility to directly compare the relative importance of pp and pn correlations, as well as the contribution of isobar and meson-exchange currents, in the three-nucleon system.

During a first beam time period data were taken at a momentum transfer $q = 375$ MeV$/c$ and an energy transfer $\omega = 220$ MeV. The scattered electrons were detected in the magnetic Spectrometer B. Proton detection was performed with the highly segmented scintillator array HADRON3, while the neutrons were detected in a time of flight unit (TOF) placed opposite to HADRON3.

After the accomplishment of the single-arm calibrations of the HADRON3 detector, the electronic lifetimes of the front ends have been determined and timing calibrations have been performed. After all corrections are applied on the data, the timing resolution achieved for electron-proton coincidences amounts to 1.1 ns (FWHM).

The implementation of the HADRON3 analysis code in the software package COLA, traditionally used by the A1 collaboration, has been accomplished. A first version of the Monte-Carlo simulation of the detection

volume in phase space has also been implemented in the package for this detector.

Finally, a procedure to evaluate and subtract the contribution of accidental coincidences is under development. The TOF detector provides a wide window for the arrival time of the neutron. Therefore the neutron spectra are dominated by accidental events. In the two-fold time-difference distribution, electron-proton versus electron-neutron time differences, regions are allocated where the various types of accidental coincidences contribute. These contributions must be properly normalised and subtracted during data analysis. After subtraction of accidental coincidences the missing energy spectrum, as shown in Fig. 1.5, is obtained. Here, the peak at E_m=7 MeV with a resolution of 7 MeV (FWHM) corresponds to the transition in which the residual system is left in its ground state, which in the case of ^{3}He$(e, e'pn)$, is the recoiling proton. It represents the first observation of a discrete transition in the reaction $(e, e'pn)$.

The combination of the results provided by the simulation and the data analysis is in progress in order to obtain the experimental cross section corresponding to the ^{3}He$(e, e'p)$ and ^{3}He$(e, e'pn)$ reactions.

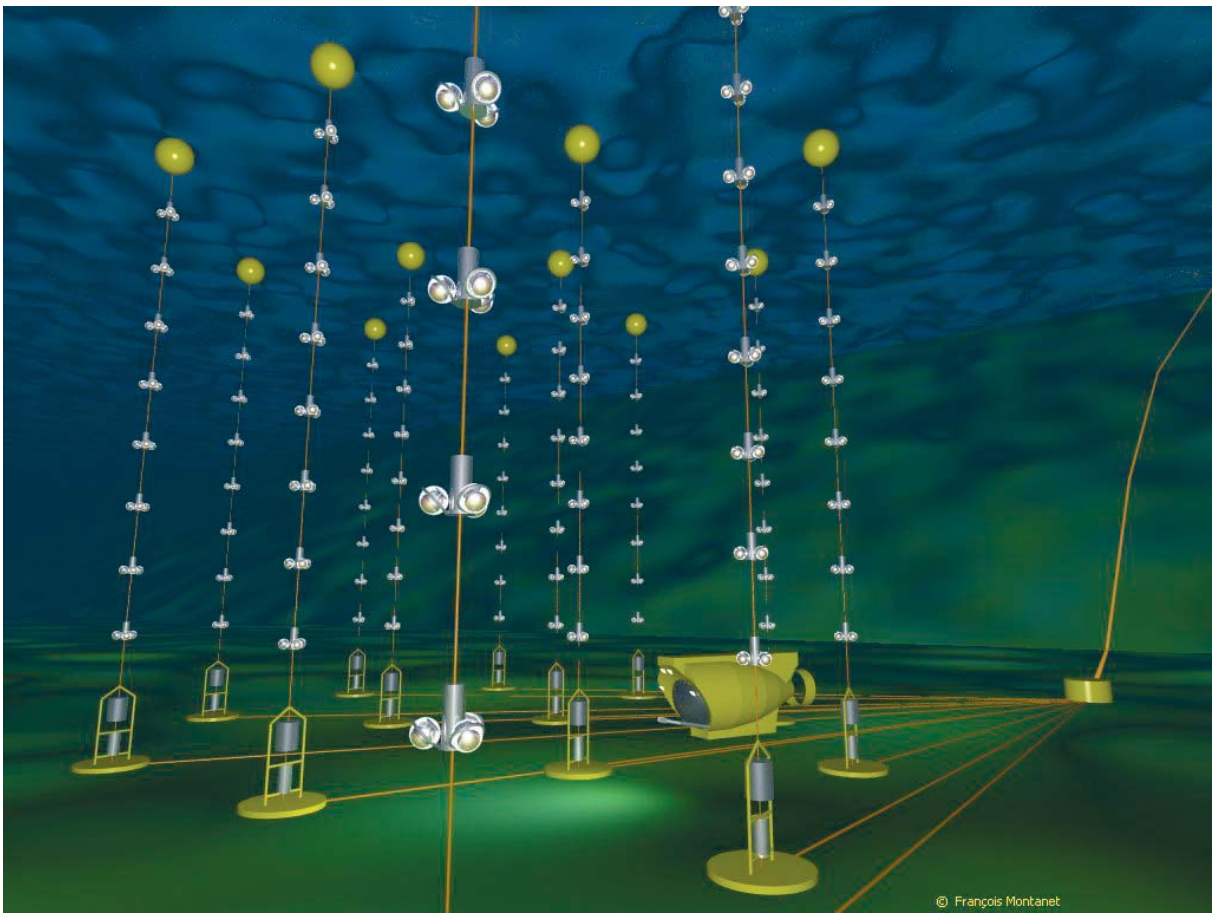

Antares, a neutrino telescope at the bottom of the Mediterranean Sea (Artist impresssion).

2 The Antares Project

2.1 Introduction

The current Antares detector is designed to comprise 1000 photo-multipliers (PMs) protected from the ambient water pressure of 250 atm by spherical glass containers. The PMs are arranged in triplets, attached at 12 m vertical inter-triplet distance to strings with a length of about 500 m. These strings, anchored on the sea bed and kept vertical by a buoy, will be positioned at a depth of 2500 m in the Mediterranean sea, 40 km off the coast near Toulon. The Čerenkov light associated with muons originating from charged-current neutrino interactions in or near the active volume of the detector (0.1 km$^2\times$0.5 km) is detected by the PMs. The arrival times of the photons are measured with better than 1 ns accuracy with the help of synchronous offshore (slave) clocks driven from shore by a master clock that is coupled to the Global Positioning System. Timing accuracy combined with position information of the PMs to better than 20 cm yields an angular resolution of the reconstructed muon track (and hence the neutrino track) of 0.2°.

Whilst the cosmic neutrino spectrum above a few tens of MeV (below this energy range there are e.g. the solar neutrinos) is unknown, the existence of charged-particles in cosmic rays with energies from 10^9 eV up to 10^{21} eV suggests the existence of high-energy cosmic neutrinos of similar energies. Angular resolution is a crucial parameter for the detection of cosmic neutrino point sources, such as gamma-ray burst sources and galactic micro quasars: looking for a neutrino signal in a given direction and time interval implies a background free observation. In general, due to the light-propagation characteristics of water, underwater neutrino detectors are expected to feature a better angular resolution than that of an ice-based detector. The current Antares demonstrator experiment entails a scientific and technical research and development project that has the objective to optimise the performance of underwater neutrino detectors. In addition, first observations of cosmic neutrino events are foreseen with a lower-energy bound of a few tens of GeV. In view of the exploratory nature of cosmic neutrino research, a data sample as unbiased as possible is desirable. At NIKHEF, we therefore developed the 'All Data to Shore' concept: timing, amplitude and in some cases waveform information of the light pulse will be sent to the data-acquisition station on shore (40 km away from the detector) for *all* photo-multiplier hits. This will allow maximum flexibility in devising optimal algorithms for data filtering. Data buffering allows us to correlate events with (delayed) information from another observatory (e.g. a Gamma-Ray-Burst warning).

2.2 Progress in 2001

In May 2001 the Antares collaboration completed a Technical Design Report, stipulating the choices for the technical implementation of the detector (optical modules, front-end electronics, timing and position calibration and monitoring, readout and optical fibre communication, electrical power generation and distribution, geometrical layout of the detector, infrastructure, launching and deployment procedures). The objective of the next major milestone of the Antares project is to launch a prototype sector line consisting of 5 PM triplets and comprising all of the essential prototype technologies of the detector. This prototype corresponds to $\frac{1}{6}$ of a completely equipped line.

In 2001 progress has been achieved by the Collaboration in the following areas :

- The master-slave clock system with a realistic layout of the optical fibre network was measured to have a time jitter of better than 500 ps FWHM, well within specifications. Long-term stability appears to be adequate.
- Installation of the acoustic positioning system offshore and validation of acoustic positioning accuracy *in situ*.
- Submarine target-site validation. Adequate flatness of sea bed and absence of major obstacles at the selected site was assessed.
- A mechanical test-line deployment has validated launching procedures and assessed the Fourier spectrum of accelerations and line movements during launching, landing and recovery.
- The Main Electro Optical Cable (40 km long), providing electrical power and the optical fibre links between detector and shore station, has been laid.

Responsibilities of NIKHEF in Antares comprise :

- Optical–fibre data communication with Dense Wavelength Division Multiplexing (DWDM).

- On–shore data router and PC farm (typically 100 PCs) for data filtering and data archiving.
- Run Control and Graphical User Interface.
- Track Reconstruction.

In addition, the NIKHEF–Antares programme leader coordinates the Readout subproject, comprising Data Acquisition, trigger, Slow Control and database.

DWDM optical fibre communication

The counting rate of the 10" photo-multipliers is entirely dominated by beta decay of ^{40}K in the sea water and by bursts of bioluminescence. The average counting rate of about 70 kHz leads to a total data rate of about 1 GByte/sec. The technology of choice for transporting the data is dense wavelength division multiplexing. The NIKHEF group has designed a read-out system based on this modern optical fibre communication technology. A proof of concept of the DWDM electronic design has been established in summer 2001. Special care has been invested to assure the reliability of the design by optimising the mean time between failure (mtbf) of components and improving other relevant design features, such as a minimal temperature in the Local Control Module (LCM). The latter feature was implemented by a complete redesign of the LCM cooling system, resulting in a 10° reduction of the working temperature. The series production will start April 2002.

On-shore data acquisition system

The NIKHEF group is designing the on-shore data processing system which will consist of a medium sized PC farm. A fast algorithm has been developed, in collaboration with the Centre de Physique des Particules de Marseille (CPPM), that can filter the physics signals from the background at the foreseen maximum data rate. This data-reduction algorithm will reduce the speed of the data writer to $\leq$10 MByte/s. It has been shown that with a real time simulation of the sector line, the data processing requirements can be met. A run-control system is being developed that enables remote operation of the detector, including on-line monitoring and data storage.

Track reconstruction

Our contribution to the off-line reconstruction software developments has resulted in a substantial improvement of the muon reconstruction efficiency and track angular resolution. The angular resolution, obtained with a set of simulated data, equals 0.2° and the effective detection volume of the detector has improved with a factor of about 2, as is illustrated in Fig. 2.1.

2.3 Recent developments

Recently, NIKHEF has adopted supplementary tasks in the construction of the Antares detector by taking responsibility for two key features of the electrical off-shore power system – String Power Module (SPM) and local Power Box (PB).

The SPM provides electrical power (1 kW) to the Local Control Modules and the Optical Modules (OM) of a detector line by converting 500 V/AC to 380 V/DC on 6 independent outputs, each output feeding one sector of a line. The requirements of optimal reliability (design goal: 50 years mtbf) and a lifetime of 10 years implies the use of military-specs components and production standards. The project has been outsourced to industry. A prototype has been delivered in December 2001.

Functionality of the Power Box comprises DC/DC conversion of the 380 V input voltage to the various DC voltages that provide power for the LCM– and OM electronics. A prototype with a power conversion efficiency of better than 85% is being designed by industry in collaboration with the NIKHEF Electronics–Technology Department. Series production of Power Boxes is foreseen to start in March 2002.

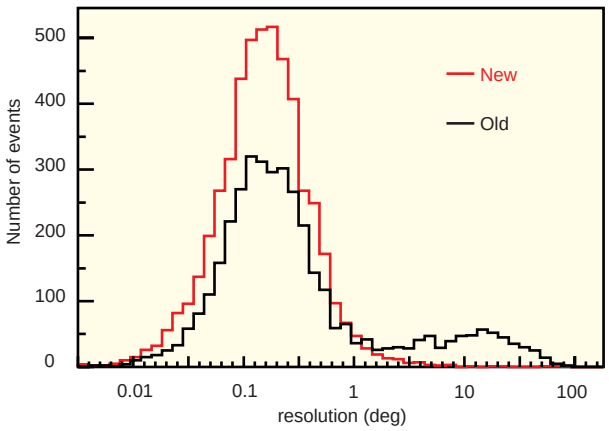

Figure 2.1: *Number of reconstructed Monte-Carlo events as a function of the angular resolution for two different track-reconstruction algorithms. The curve labelled "new" corresponds to an algorithm recently developed at NIKHEF; the curve labelled "old" is obtained with the standard Antares reconstruction software.*

3 The ATLAS Experiment

3.1 Introduction

An important event in 2001 for the ATLAS/D0 group was the registration of the first Tevatron Run 2 $p\bar{p}$ interaction by the D0 experiment on April 3, 2001.

Regarding the ATLAS experiment at CERN, we finished a period of intensive preparation for the assembly of muon (MDT) chambers. Since the summer of 2001, the MDT chambers are produced at NIKHEF at a speed of about two chambers per week.

3.2 D0 experiment

The Tevatron Run 2 is aimed at collecting an integrated luminosity of at least 2 fb^{-1}. During most of 2001 the Tevatron collider and the D0 detector were being commissioned. By the end of 2001 both the collider and the experiment seem to have reached a stable mode of operation.

A Fermilab staff member who supervises some of the Dutch students has become a "bijzonder hoogleraar" at the University of Amsterdam and held his inaugural speech about the D0 detector and its physics in 2001. Three PhD students have returned from a nearly two year stay at Fermilab to the Netherlands. This, together with the staff members that joined the D0 collaboration in 2000 and 2001 and actively pursue local computing at NIKHEF, has caused the groups in the Netherlands to become important analysis groups within D0.

3.2.1 D0 detector status (NIKHEF-responsibilities)

Radiation monitor and beam abort system

This system consists of two parts: beam loss monitors, argon filled proportional tubes that have been purchased from the Fermilab beams division and for which mounting supports were made in Nijmegen; and silicon diode sensors which are an integral part of the D0 Silicon Microvertex Tracker design. The radiation monitoring system has been commissioned and functions as expected. Several beam aborts have been triggered by the system in cases where radiation damage threatened the detector. A student from the University of Twente has cross calibrated the different measurement channels in a three month internship at Fermilab.

Silicon Track Trigger

The design of the Silicon Track Trigger has been established and the system is in production now. A Dutch PhD student is working on using this refined tracking information in the second level trigger. This work is conceptually advanced and implementation is about to start, in time to be ready when the hardware is commissioned. A Nijmegen electronics engineer is spending part of his time on implementing the VHDL code for the Field Programmable Gate Arrays that interface the first level track trigger to the second level track trigger.

Inner tracker magnetic field sensors

The Hall probe magnetic field sensor system was already succesfully installed in 2000. The system has been used in the final detector configuration to check the magnetic field predictions from a theoretical calculation. The readings of the system are stored in a data base, to enable the analysis of the magnetic field, when this is required for the analysis.

Forward proton detectors

Engineering support has been given to the design of the roman pot system. The vacuum pots and the positioning mechanism for the castles in which these are mounted have been made by NIKHEF Amsterdam. At the end of 2001, ten stations of the Forward proton detectors were installed and commissioning and calibration has started using colliding beams.

3.2.2 D0 software progress

Reconstruction software and offline analysis

With the arrival of the first data, in 2001 there has been a shift from a concentrated effort in the reconstruction software to data analyses. One of the NIKHEF PhD students won the prize for finding the first reconstructed muon in the D0 data. Another nice event found by a NIKHEF PhD student is the inclusive $Z \rightarrow \mu^+\mu^-$ event candidate shown in Fig. 3.1. Analyses of data and Monte Carlo studies are being performed for b-quark tagging using semi-leptonic decay in muons and using track impact parameters. The first J/ψ's have been reconstructed using their decay in muon pairs. Reconstruction of tau-leptons in the data has started, while also the analysis of single top quark events and top-pair decays into all jets has started. At a reduced level the group is still contributing to the offline reconstruction software, notably for muon tracking.

Monte Carlo event production

NIKHEF is the second biggest production center for D0 Monte Carlo events. A 50 node dual processor farm is in full operation. Many contributions were made by

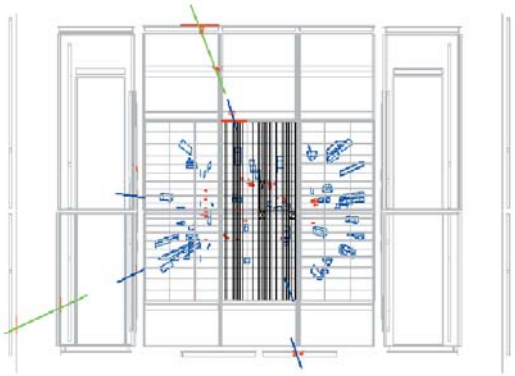

Figure 3.1: *D0 inclusive $Z \rightarrow \mu^+\mu^-$ event candidate. The two muons are the tracks indicated in green extending to the muon spectrometer. The other activity in the detector stems from the (anti-) proton remnants.*

the NIKHEF group to the organisation of the Monte Carlo simulation and to the data transfer between the Netherlands and Fermilab. This effort is integrated in the more general GRID effort that NIKHEF participates in. At the end of 2001 a processor farm at Nijmegen University was also started, in first instance with the aim of doing offline analysis on the D0 data, but with the prospect of also producing Monte Carlo events in otherwise empty CPU cycles.

3.3 ATLAS experiment

3.3.1 Muon Spectrometer

MDT chamber construction

In the summer of 2001 NIKHEF started the serial production of the 96 large muon chambers to be installed in the Barrel Outer Layer (BOL) of the ATLAS muon spectrometer. A BOL chamber consists of 432 aluminium drift tubes of approximately 5 m length and 30 mm diameter with a tungsten wire held at the tube centre by precision endplugs. These drift tubes are wired using a semi-automatic robot which produces typically 80 drift tubes per day. The rejection rate after stringent quality control tests on wire location, wire tension, gas leak rate and high voltage characteristics is about 2%. In 2001 about 5,000 drift tubes were produced. The drift tubes are glued in 2×3 layers on either side of a support structure, leading to a drift chamber dimension of $5 \times 2.1 \times 0.6$ m. In total 8 chambers were produced in 2001. For four of these the mechanical precision of the wire positions was measured through X-ray scans with the ATLAS tomograph at CERN. The analysis software was written in C++ by a Dutch PhD student. The root mean square of the position deviations from the a-priori fixed grid was found to be about 15 μm for both chambers, thus amply fulfilling the 20 μm requirement for this parameter. Moreover the individual small deviations of the wires were found to be very well correlated with the values found with the various RASNIK and planarity laser checks which are part of the quality control and assurance procedures during chamber construction. This shows that handling of the precision mechanics is well under control during the gluing of the tube layers.

Several modifications of the jigging tools were made to facilitate and speed up the production. The total mechanical assembly time of one complete chamber went from 20 to approximately 9 working days in the course of the year. In 2002 we aim to reduce this further to 7 working days per chamber in order to finish the production and start the installation of the chambers in the ATLAS experiment in 2004.

MDT chamber test stand

With the mechanical aspects of the MDT chamber production under control, we started to work on an MDT chamber test stand. This stand uses cosmic ray muons (triggered by a scintillator counter array) to evaluate the performance of MDT chambers as a charged particle trajectory tracker. The setup at NIKHEF Amsterdam houses a maximum of five MDT chambers and will be operational throughout the MDT chamber production period. In addition to MDT chamber studies the same setup will be used to develop the muon spectrometer reconstruction and simulation software for ATLAS; to evaluate the performance of the high level data acquisition electronics and the detector control system. Finally, this setup serves as an ideal on site laboratory to familiarize physics students and beginning PhD students with the many hard- and software related aspects of a particle physics experiment. Starting in the spring of 2002 it will be an integral part of the UvA physics curriculum.

3.3.2 End Cap Toroids

The ATLAS End Cap Toroids (ECTs) are an in kind contribution of NIKHEF to the ATLAS collaboration. Their basic design was made by the Rutherford Appleton Laboratory. Dutch Industry is responsible for the manufacturing. Contracts for the manufacturing were signed in February 1999. NIKHEF's supply for the ECTs consists of three major parts:

1. A 1:5 scale model of the vacuum vessels, completed and tested in 1998.

2. Two aluminium vacuum vessels of 10.7 m diameter and 5 m axial length and a weight of 80 ton each. Each vessel houses a cold mass.

3. Two cold masses each consisting of eight superconducting coils of 4×4.5 m^2 and eight keystone boxes. The keystone boxes are used as reinforcement of the whole structure and form a major part of the cold "buffer". The coils are indirectly cooled. The weight of a cold mass is 160 ton.

Vacuum Vessel

The two vacuum vessels are made by Schelde Exotech in Vlissingen. Manufacturing started mid 1999. All welding was done by Exotech and the final machining was performed by Machinefabriek Amersfoort in IJsselstein. The vessels are first fully assembled and vacuum tested at works and then transported in two halves to an assembly hall at CERN. The first vessel was assembled at CERN just before Christmas 2001 (see Fig.3.2). No vacuum leaks were found and within a few days a pressure of 10^{-3} Pa was achieved. The second vessel is presently being assembled at works and is scheduled to be tested at CERN before Summer 2002, almost in time.

Cold Mass

HMA Power Systems in Ridderkerk manufactures the two cold masses. In 2000 the company became part of the Brush Generator division of FKI (UK). The fabrication problems encountered by one of the two suppliers of the superconducting conductor have now been resolved so the supply of conductor is no longer endangered. In 2001 the vacuum impregnation of the coils was thoroughly tested. The qualification of both the vacuum mould and the resin mixing machine gave problems that have not been solved yet. Proper cleaning of all material that has to be impregnated is essential for the bonding. Qualification of the cleaning is close to acceptance. The impregnation procedure will be tested through the impregnation of the dummy coil, which was succesfully produced at the end of 2000.

This will allow the assembly of the 16 aluminium coil formers and the start of the winding.

3.3.3 Semi-Conductor Tracker

Early in 2001 we constructed three silicon-detector-module prototypes; one of these is shown in figure 3.3.

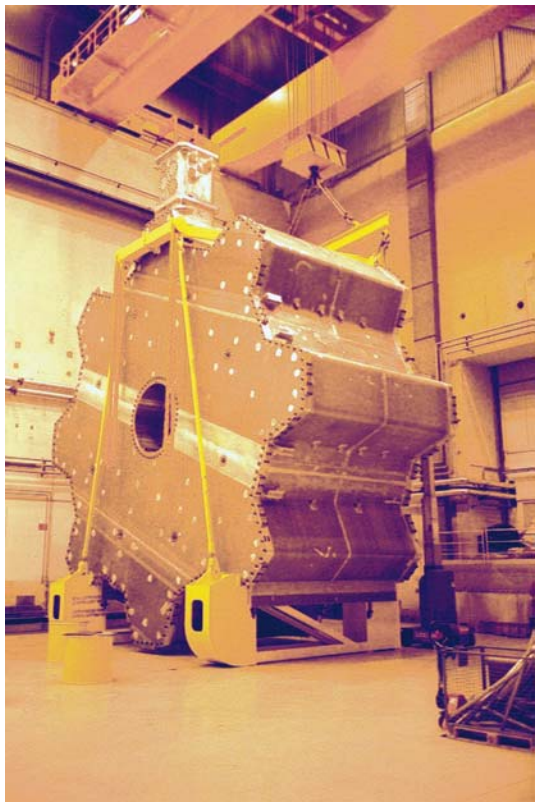

Figure 3.2: *The first vacuum vessel assembled at CERN.*

The two silicon wafers in each module were succesfully aligned to an excellent precision of 1 micrometer. The modules also functioned well electrically. However the circuit board used (known as "K4") has some excess feedback from its power supplies to the sensitive amplifiers. This problem was investigated at NIKHEF and a solution with extra power-supply filters was found which worked well for our short modules. However, this solution did not cure the problem on modules made elsewhere which have longer silicon detectors. Instead a new circuit, K5 has been developed by the collaboration, as well as a back-up solution using a circuit adapted from another part of the detector. Both these solutions work and one will be chosen in February 2002, allowing us to proceed to module production in 2003.

Engineering work progressed very well with the completion of tests on prototypes of carbon fibre support discs. This culminated in the Final Design Review in October 2001, which was successfully passed. Now the search is on for a manufacturer to make the 20 discs needed. We have also developed a compliant joint to hold the

Figure 3.3: *Silicon module.*

discs in the support cylinder. The discs must be held firmly in place without vibrating, but the fixation must also allow for differences in expansion of the disc and support cylinder, without excessive force. Prototypes of the fixing have been made and tested with excellent success. Major progress has been made in developing a gas-tight transport and storage box for the discs. This must protect the discs, which when complete will be worth about 250,000 EUR each.

The Semi-Conductor Tracker (SCT) detectors must be kept cold and dry in an inert atmosphere, requiring a flush of nitrogen gas. The group's experience in wire-chamber gas-systems has allowed us to take on the design of this system, which must keep the pressure in the enclosures to 1 mbar above atmospheric pressure at all times, despite atmospheric pressure variations of up to 200 mbar.

3.3.4 Trigger, Data-Acquisition & Detector Control

In 2001 activities on the ATLAS trigger, DAQ and Detector Control (DCS) system were focused on design and implementation work and on studies needed for preparing the Technical Design Report, to be submitted at the end of 2002. NIKHEF contributed in the following areas:

1. Studies relevant for the design of the Read-Out System (ROS) and utilising the ROB hardware developed earlier.

2. Paper and computer modelling of the trigger and DAQ system, including a Monte-Carlo study of event fragment size distributions for the inner detector and of possible lossless data compression algorithms for data from the Transition Radiation Tracker (TRT).

3. The "On-Line Software", in particular with respect to the information exchange with the DCS and to general support for test software.

4. The software for the ELMB, a dual processor CAN node to be used for control of the ATLAS detectors.

Directly related to these contributions is the development of the MROD, a Read-Out Driver for the muon chambers. The new prototype MROD-1 design was completed. This consists of a 9U VME board to which up to 6 chambers can be connected. One board and two associated daughter boards have been produced, most of the functional testing has been successfully completed in 2001.

In October 2001 NIKHEF has been the host of a workshop on the DCS, while in November 2001 the annual trigger/DAQ workshop took place at NIKHEF.

3.3.5 Reconstruction & Simulation Software

The time-line for the year 2001 for the computing model had the following important issues: migration to object-oriented framework, validation of the Geant4 toolkit and a first order continuity check of the new software (Data Challenge Zero). For the year 2002 the ATLAS computing challenge includes a "large scale reconstruction and analysis" (Data Challenge One), a processing farm being able to produce around 10% of ATLAS' needs (including GRID model) and to produce some 100 TB of Monte Carlo data. At ATLAS a control framework for simulation issues ("Goofy") is being developed separately from a frame for the digitization, reconstruction and analysis programmes ("Athena"). Both have their advantages and are currently supported within ATLAS. The simulation control framework "Goofy", is build on top of the Geant4 simulation toolkit. This toolkit, the C++ follow-up of Geant3, is developed at CERN. The programme was validated last year by several ATLAS sub-detector groups to increase thrust in Geant4 simulation so that it can be used for data production. The status of Geant4 can be compared to

the status of Geant3 just before the turn-on of LEP. "Athena" is a control framework that represents a concrete description of the abstractions or components and how they interact with each other. The architecture underlying Athena is the GAUDI architecture originally developed by LHCb. This architecture has been extended through collaboration with ATLAS. Athena is the sum of this kernel framework, together with ATLAS-specific enhancements. The latter include the event data model and event generator framework.

Detector Description

NIKHEF plays an important role in the detector description of ATLAS. The description of the detector geometry is isolated from all 'client' programmes, i.e. simulation, reconstruction and visualisation packages. To describe the detector geometry, including logical structure, readout tree and a material database. A syntax in XML was developed and adopted by the ATLAS collaboration. The syntax utilises the symmetries as present in the geometry of the ATLAS detector. By using the XML industry standard many utility tools like inspection, validation and visualisation tools are facilitated. The extreme complexity of the ATLAS geometry necessitates the introduction of algorithmic descriptions. We have extended the syntax in XML to allow, besides a very explicit internal geometry description, connection to external algorithms in C++. One can build these complex, optimised geometries starting from the parameters stored in XML, We have created an automatic tool to convert the geometry as described in XML to Geant4 objects. As an example, we show in Fig. 3.4 the geometry of the muon chambers in the cosmic ray test stand. This geometry is described by XML and automatically converted to Geant4 in order to simulate the passing of a cosmic muon.

Inner Detector

We developed the code for the new transient representation of the pixel and SCT event data. The main improvement with respect to the previous code is, apart from the extensive use of object oriented techniques, to have a description of the data much closer to the data format which will come out of the detector in the future. Although the code is dedicated to the pixel and SCT detectors, the overall infra-structure (event containers) has been inherited from the common ATLAS code. For the pixel and SCT detectors all the necessary information about the segmentation into diodes of the modules and the connection scheme between these diodes and the readout electronics are provided. This information is interfaced with the XML files. A central

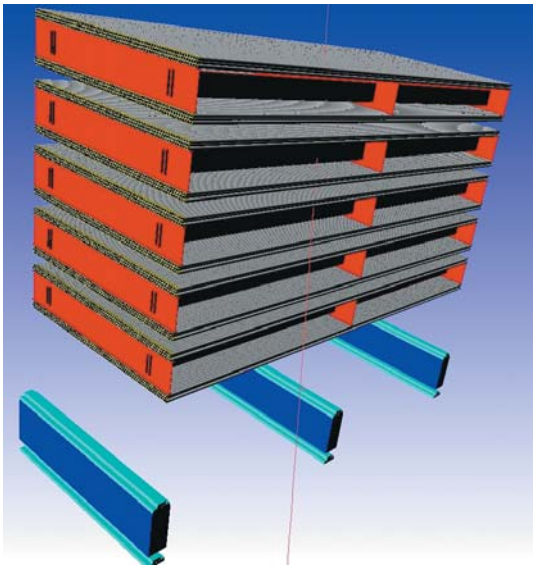

Figure 3.4: *Simulation of a cosmic ray muon traversing the MDT chamber test stand in NIKHEF Amsterdam.*

logical entity in the description corresponds to the detector element (a pixel module or a SCT module side). It contains information about its own local geometry, its global orientation in ATLAS and has a unique logical identifier. The detector element will further be used by reconstruction algorithms as starting point for track determination. For the SCT detector a software package is being written to build the detector elements directly from the parametric description of the SCT. This code can easily be extended to the pixel detector.

3.4 ATLAS detector R&D spin-off

3.4.1 Medipix: Lowering the radiation dose for X-ray imaging

Over 65 thousand of microscopically small X-ray detectors have been integrated on an area of 2 square centimeters in the Medipix-2 detector, a chip that is able to count individual photons and convert them into images. The principle of the detector is illustrated in Fig. 3.5.

In collaboration with the Circuit-Design group of prof. B. Nauta at the MESA+ Research Institute in Twente, of CERN in Geneva, and of the Medical Physics group of the University Federico II of Naples, the Medipix team at NIKHEF has adapted the semiconductor pixel detector technology of the LHC experiments at CERN for X-ray imaging, the main difference being the inclusion in every pixel of a digital counter. The new

imaging method is up to 50 times more sensitive than current methods based on scintillators and CCD's or photographic films. This implies that patients, but also dentists and other medical staff using X-rays during diagnostics and therapy, will be exposed to a lower dose of ionising radiation.

The Medipix-2 detector consists of a sensor chip with 65k semi conducting sensor diodes, an electronic chip with 65k amplifiers, comparators, and digital counters, and an interface unit connecting the detector to a standard PC. Every pixel constitutes a complete X-ray counter, and thanks to the modern deep-submicron technologies, the size of such a pixel has been reduced to only 55 x 55 μm^2. The digital to analog converters of the chip have been designed by NIKHEF and MESA+, while the pixel matrix was done at the microelectronics department at CERN. Production of the electronics chip is done by IBM in the United States, the sensor chip is produced by Canberra Semiconductors in Belgium. The two chips are soldered together

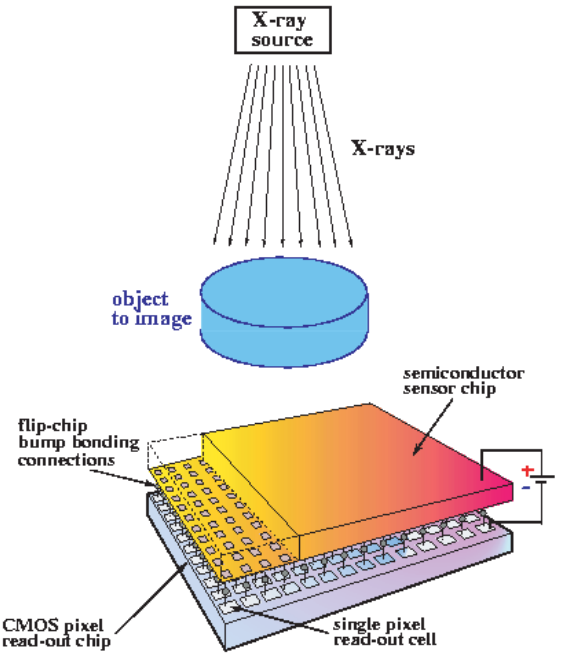

Figure 3.5: *Schematic representation of the Medipix-2 detector. Incoming quanta of X-ray radiation cause small electrical pulses in the semiconducting sensor, that are then counted in the deep submicron CMOS chip.*

with 65k lead/tin solder balls, in a photolithographic process called 'bump-bonding' by VTT, a company in Finland.

SAF/NIKHEF has designed and built the interface unit, based on a Field Programmable Logic Array. This circuit does the parallel to serial conversion at speeds up to 200 MHz, and the signal level conversions. The University of Naples has contributed the software.

The next goal is to combine eight Medipix-2 chips on a single sensor matrix, to obtain a larger imaging area of 28 x 56 mm^2 and a total of 0.5 million pixels.

Industry has shown interest. A contract has been signed with Philips, giving them a license for commercial application of the chip, the interface and the software. This money will be used to further improve the technology, e.g. to move from current 0.25 to 0.13 micron technology, allowing still more and still smaller pixels on the chip. Also ESRF in Grenoble has shown interest to use our detectors at synchrotron experiments.

Activities at NIKHEF in 2001 included the design of 8-bit Digital to Analog converters for the MEDIPIX-2 chip in 0.25 micron technology. These circuits are now also used as design blocks in other chips for the ALICE and the LHC−b detectors. In addition, several different 4-bit pixel-level Analog to Digital Converter designs have been submitted in two Multi Project Wafer runs in 0.25 micron technology, via CERN-MIC. Ten Medipix-1 CMOS readout wafers have been probed at the NIKHEF semi-automatic probe station.

In collaboration with our Electronics Technology (ET) department, a 2 by 4 Multi-chip carrier was designed, to carry a tiled array of 8 MEDIPIX-2 chips, allowing an X-ray imager with 28 x 56 mm^2 sensitive area. It uses cutting edge high-density interconnect technology, with a nine-layer printed wire board in stacked microvia buildup technology. The board is now in production at a special workshop at CERN.

Also in collaboration with the ET department, an interface unit was designed and built, to control and readout this multichip board via a standard commercial Digital I/O PCIbus card mounted in a PC. The communication is based on a high bandwidth serial token ring protocol, using Low Voltage Differential Signaling (LVDS). The serialisation, de-serialization and all other functionalities are performed in a high-speed programmable logic chip (Altera FPGA EP20K100EQC240-1X). A serial loop speed of 200 Mhz has already been demonstrated. Production of 25 of these interface units has been outsourced to an external Dutch company. Af-

ter testing they will be made available to the members of the MEDIPIX Collaboration, and to our industrial partner.

Finally, preparations have been made for the 4th International Workshop on Radiation Imaging Detectors (IWORID2002), which will be hosted by NIKHEF in September 8-12, 2002.

3.4.2 Diamond Detector Research

The use of diamond as a medium for detecting high energetic particles is investigated at NIKHEF in the framework of the RD42 collaboration. Diamond has the advantage over silicon of a better radiation tolerance. However, it suffers from limited charge collection efficiency due to charge traps in the bulk. The material under investigation is made using the CVD process allowing substrates of at least 100 mm diameter. In the report year six recently produced samples were characterised using the test set-up at NIKHEF. The average charge signal of four of them ranged from 8100 to 10000 electrons indicating a charge collection efficiency of 48 to 59%. The charge signal distribution had a Landau shape with a width (FWHM/mip) of 1.05, a value caused by the polycrystalline nature of CVD diamond. These results indicate that the recently produced material has sufficient qualities for use as a tracker in high-energy physics. During an invited stay at the University of Florence the NIKHEF routines for DAQ and analysis were installed and a contribution was given to the improvement of the characterisation set-up. For 2002 a radiation tolerance test for 1 MeV neutrons is planned at Debrecen (Hungary) in collaboration with the University of Florence.

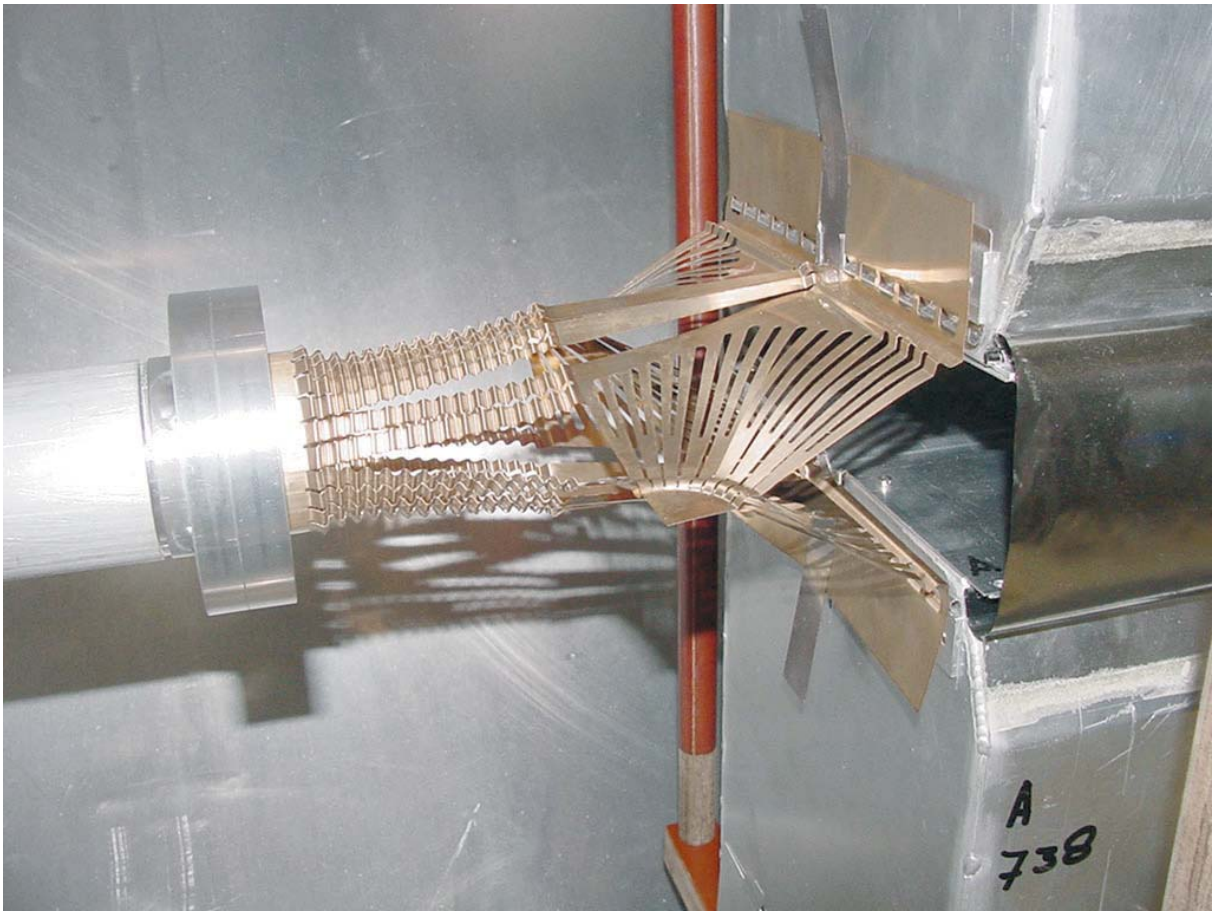

Experimental wakefieldsupressor for the LHCB-Vertex Detector. The Wake Field Suppressor is made of two 0.075 mm thin CuBe foils.

4 B-physics

4.1 Introduction

Field theories constitute the basis of present-day physics. Three discrete operations are possible symmetries of the Lagrangian. Two of them, *parity* $\mathcal{P}$ and *time reversal* $\mathcal{T}$, are spacetime symmetries. The third, a non-spacetime symmetry, concerns *charge conjugation* denoted by $\mathcal{C}$, which operation interchanges particles and antiparticles. In 1964 it was shown for the first time that matter and antimatter behave differently. The undisputed proof was delivered by a delicate experiment that revealed a small difference between the decay of neutral kaons and their antiparticles. Since then, for nearly forty years, the violation of $\mathcal{CP}$ and the violation of time reversal has only been observed in kaon decay. The kaon data constrain the parameters of the mixing matrix (CKM matrix) of the Standard Model, but do not constitute a test of it. However, the Standard Model gives precise predictions for a series of $\mathcal{CP}$ violating effects in the decay of B-mesons. A large number of independent measurements can be carried out in the B system; thus, it becomes possible to submit the present theories to stringent tests. The year 2001 presented a milestone in this line of research: thanks to the experiments BaBar at the Stanford Linear Accelerator Center in the U.S.A. and Belle at KEK in Japan the existence of $\mathcal{CP}$ violation in the B-meson system has been firmly established.

The LHC proton-proton accelerator at CERN will produce an abundance of B-mesons. Starting in 2006, the LHCb experiment, in which NIKHEF participates, will investigate the origin of $\mathcal{CP}$ violation and study whether radically new and different laws of physics will be needed for the description of this phenomenon. With a production of 10^{12} $b\bar{b}$ pairs per year a wide range of B decay modes can be studied. In this way it is possible to over-constrain and extract all four parameters of the CKM matrix even in the presence of new physics. In 2001 significant progress was achieved in the preparation of LHCb. The technical designs for both the vertex detector and the large drift chambers have been finished and documented. Both designs have been evaluated by the LHCC (a CERN review committee) and brought up for approval to the CERN management. The production of both detectors can commence in 2002, allowing a timely start of the LHCb experiment.

In order to gather experience in $\mathcal{CP}$-violation physics, NIKHEF is presently participating in the HERA-B experiment at DESY.

4.2 HERA-B

During the past year, much work was accomplished on the hardware of the detector, as well on the analysis of the data taken during the commissioning period in summer 2000.

Trigger Linkboards and Optical Links

The Trigger Linkboards (TLink) serialise the TDC-information of part of the inner and outer tracker detectors and send it at GHz rate via optical fibres to the First Level Trigger (FLT). As this is part of the trigger that performs tracking on-line, it must be highly efficient. The year 2000 run, however, showed that a major part of the connections was not working reliably. During the shut-down of HERA, since September 2000, the Linkboards and connections, including the drivers and receivers, were thoroughly tested, corrected and adjusted.

The data transmission was tested in order to check for missing bits and bad solder connections on the TLink. This has been done with a code that reads out the content of the Wire Memory (WM) of the Track-Finding Units TFUs and checks that all data bits are recorded correctly.

A bit-error test was conducted by measuring the bit-error rate of the transmission line. By checking for repeating Bunch-Crossing numbers in the Wire Memory, up to 10^8 bits per second can be checked. In general, the test was done for 1200 seconds corresponding to a bit-error rate of 10^{-11}. These tests were done for all links in the Trigger, Pattern-recognition and MUON chambers. In January 2002, not more than two problematic links per chamber persist, which corresponds to less than 1% of all links.

In order to implement the Inner Tracker into the First Level Trigger, the required geometry files were prepared to fill the wire memories in the FLT simulation code.

In order to verify that all connections between the TDCs and FLT indeed correspond to the required geometry, and that all data are transmitted correctly, an event-by-event comparison between Outer-Tracker hits and Wire Memory has been started. Until now, this was done on a statistical basis only.

J/ψ-production

The formation of quarkonium states, and specifically of J/ψ's, is at the centre of lively debate for several rea-

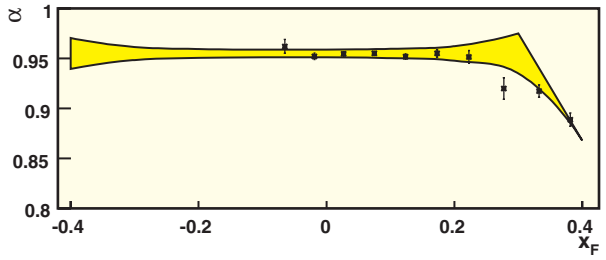

Figure 4.1: *Estimated uncertainty (hatched) in α versus $X_{Feynman}$ for J/ψ-production at Hera-B.*

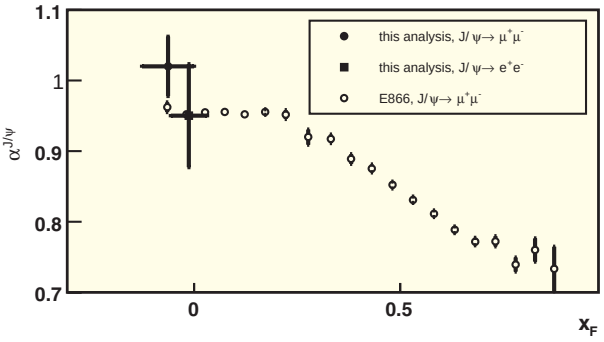

Figure 4.2: *Two preliminary data points for the factor $\alpha^{J/\psi}$ (summer 2000 - commissioning data) compared to data from the Fermilab experiment E866.*

sons. On the one hand, suppression of J/ψ-production in the interaction between energetic heavy ions, characterised by $\sigma_{pA}^{J/\psi} = \sigma_{pN}^{J/\psi} A^{\alpha}$, is believed to be the clearest indication of the formation of a Quark-Gluon Plasma. On the other hand, the formation process itself is highly interesting, since it yields information on perturbative as well as nonperturbative QCD aspects. Since the trigger of Hera-B is geared towards the leptonic decay of J/ψ's, and the target station of Hera-B contains different materials, a study of the dependence of J/ψ-production on the nuclear mass can be performed with small systematic uncertainty. Because of its large acceptance for both charged and neutral particles, Hera-B offers the unique possibility to study charmonium formation at negative values of the Feynman scaling variable X_F, to study the correlation between the charmonia and other particles in the event (co-mover scenarios, double pomeron exchange) and to study the formation of P-wave χ_c states via their decay $\chi_c \rightarrow J/\psi + \gamma$.

Fig. 4.1 shows the estimated accuracy in α for J/ψ-production versus X_F at Hera-B. The data points represent published values for α from Fermilab experiments and indicate that the acceptance in previous experiments does not extend to negative values of X_F.

Fig. 4.2 compares two preliminary data points of Hera-B (run summer 2000) with the results of the Fermilab experiment E866.

B-meson production cross section

In spite of the very small fraction of interactions that contain B-mesons decaying via $B \rightarrow J/\psi + X$, $J/\psi \rightarrow$ *two leptons*, and the very limited trigger possibilities in the year 2000, Hera-B succeeded in isolating the first spectrum of B-mesons. For this, use has been made of the different decay lengths of a J/ψ, which decays virtually at the spot of production, and of a B-meson, which has a typical decay length of 1.1 cm. Fig. 4.3 shows a mass spectrum of electron pairs after several cuts, the most important being the condition that the common vertex of the two electron tracks does not coincide with one of the wire targets of a primary vertex, and that the two-electron vertex is at least 0.5 cm downstream of the target wire. The background has been estimated from detached vertices at the wrong (upstream) side of the wire and has been subtracted from the spectrum shown here. An enhancement at the correct J/ψ mass is observed. Extraction of the cross section is under way.

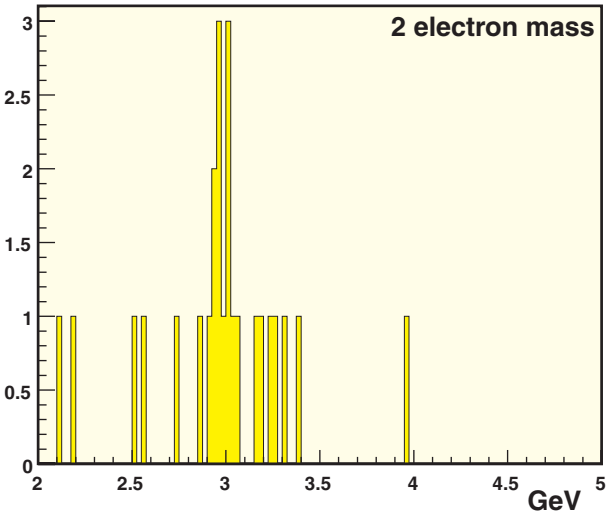

Figure 4.3: *Mass spectrum of detached J/ψ vertices indicative of B-meson decay (preliminary).*

4.3 LHCb Outer Tracker

The Research and Development (R&D) carried out by the Outer Tracker group led, in the course of 2001, to the production of prototype detector modules, which were then tested in the pion beam (T7) of the PS accelerator at CERN. The analysis of the test-beam data (See Fig. 4.4) showed that these prototypes attained the desired space resolution ($\sim$200 μm) and efficiency ($\sim$97%).

From the R&D and the test-beam results a set of baseline solutions emerged for the technical design of the Outer Tracker, which were summarized in the Technical Design Report (TDR). The approval of the Outer Tracker TDR by the LHCC has therefore marked an important milestone for the project. The principal baseline solutions presented in the TDR are:

- Detector configuration

  Each station will consist of 4 detector planes (XUVX), with wires running vertically (X) and under $\pm 5^o$ from the vertical (U and V).

  Each plane will consists of basic detector units ('modules') mounted on aluminum frames, as shown in Fig. 4.5.

  The cross section of a module, containing two staggered layers of straw tubes inside a gas-tight box, is shown in Fig. 4.6.

  Each of the two sandwich panels has a 10 mm thick core material and two 0.1 mm thick carbon-fiber composite facings, plus an aluminum foil on the inner side to ensure electrical shielding and ground connection.

- Gas mixture

  An $Ar/CF_4/CO_2$ gas mixture will be used as drift gas: the presence of CF_4 takes care of the requirement for fast drift-times, necessary to minimize the overlap of signals from different LHC bunches.

- Cathode material

  To minimize the effects of the gas contamination due to the decomposition of CF_4 molecules, the straw-tube material will be Kapton with a volume doping of carbon (Kapton XC-160).

- Electrical configuration

  In the course of the R&D, we carried out very detailed studies of the detector electrical configuration, that led to the following conclusions: leaving open the end of the anode wire far from the preamplifier will compensate (thanks to the reflected signal component) the signal attentuation caused by the high resistance of these long wires; an outer winding of aluminum foil (25 μm) will greatly reduce the analog cross-talk between neighbouring straws; the outer aluminum winding will be contacted to the ground plane at least every 20 cm to prevent oscillatory behaviour.

- Front-end electronics

  For the front-end electronics, we will adopt the ASDBLR chip (orginally developed for the ATLAS Transition Radition Tracker), containing 8 channels of preamplifier, shaper, discriminator and baseline restorer circuitry, implemented in DMILL technology, which offers excellent radia-

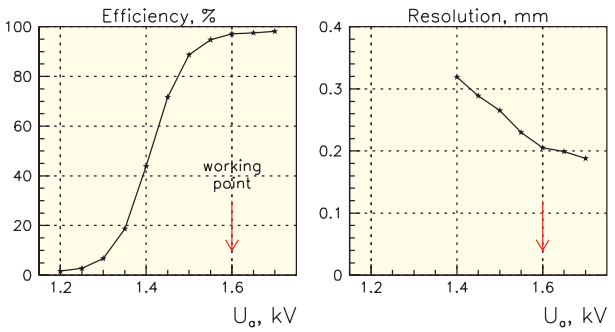

Figure 4.4: *Efficiency and resolution of a test-prototype detector module as a 4function of the operating voltage.*

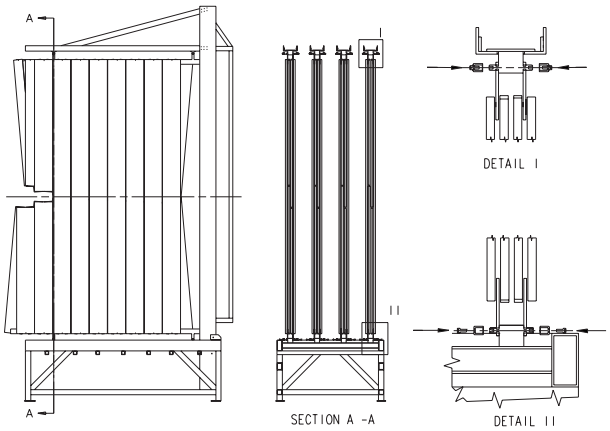

Figure 4.5: *View of the mounting of a station half and its subdivision into modules.*

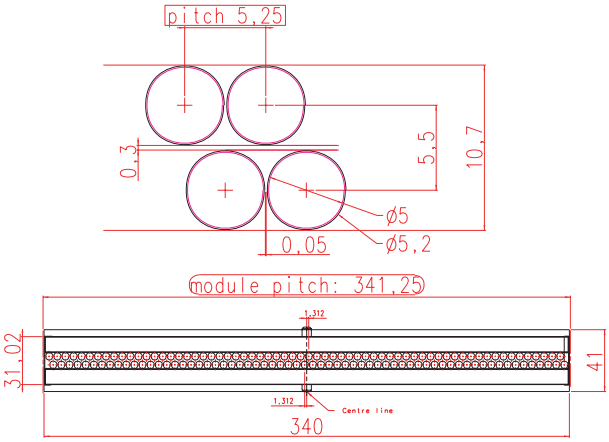

Figure 4.6: *Cross section of a straw tube module.*

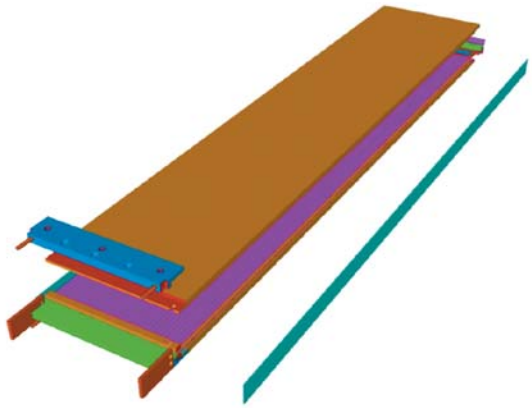

Figure 4.7: *Exploded view of an OTR module assembly.*

tion hardness and thus allows on-detector mounting.

- Drift-time measurement electronics

  The Outer-Tracker Time Information System (OTIS) TDC, with a clock-driven architecture especially developed for the LHCb Outer Tracker in the ASIC laboratory in Heidelberg, will be the baseline solution. It will be implemented in a radiation-hardness process to allow on-detector mounting.

Preparation of Detector Production and Quality Control

Since the approval of the TDR, the focus of our work has shifted from R&D towards production and quality tests. All designs presented in the TDR are translated into detailed technical solutions that can be implemented in the production scheme outlined in the TDR.

The construction of an assembly facility, including cleanrooms, suitable to mass production of the longest ($\sim$5 m) detector modules is under way at NIKHEF.

The key elements for the production of detector modules are the sandwich panels (see Fig. 4.7). Our strict mechanical requirements, combined with the requirement of a minimum material budget, render the production of these panels as standard industrial laminates difficult and expensive. The Cracow Institute, having substantial experience in producing carbon-fiber composite structures, has produced in a low-temperature process test panels that have given excellent results and thus provide a viable solution for this production issue.

While Kapton XC has been selected as the basic straw-tube material, the details of the production technique will have an influence on the mechanical properties of the straws (See Fig. 4.8). In particular, the number of windings and the glueing procedure will strongly influence the mechanical resistance and the gas tightness of the straws themselves. In collaboration with LAMINA Dielectrics Ltd., several test batches of straw

Figure 4.8: *View of a straw tube with Kapton XC (inner) and aluminum (outer) windings.*

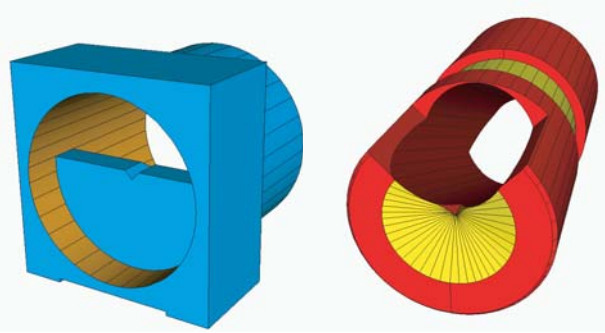

Figure 4.9: *End-piece block (left) and wire locator (right)*

tubes with different combinations of windings and glueing procedures were produced and tested. Our quality tests showed that a loss of pressure well below 10^{-7} s^{-1} per individual straw (thus sufficient to assure the desired gas tightness) can be attained with double Kapton XC windings.

At the end of each straw tube, wire-support elements and gas-distribution blocks are necessary. These two functionalities have been combined in a single 'end-piece'. Additionally, due to their length, wires have to be supported at intermediate positions by so called 'wire locators'. The desing solutions offered by the TDR have been translated into elements suitable for industrial series production, shown in Fig. 4.9.

Essential tests of the quality of the detector modules produced include the accurate determination of the wire tensions and of the wire positions. For the wire-tension measurement, we designed and built a device to determine the main eigenmode of a wire vibrating in a magnetic field with an accuracy of approximately 0.5 Hz.

For the measurement of the wire positions, we developed a method based on scanning modules with a ^{90}Sr source and recording the cathode current as a function of the source position (See Fig. 4.10). A dedicated current meter was built, with a precision of 100 pA, which allows current determination with an accuracy of less than 1% at low currents, and thus an accurate determination ($\pm 100\,\mu$m) of the position of the wire with respect to the cathode straw.

This experimental apparatus will also allow the determination of the I-V characteristic curve of the detector modules.

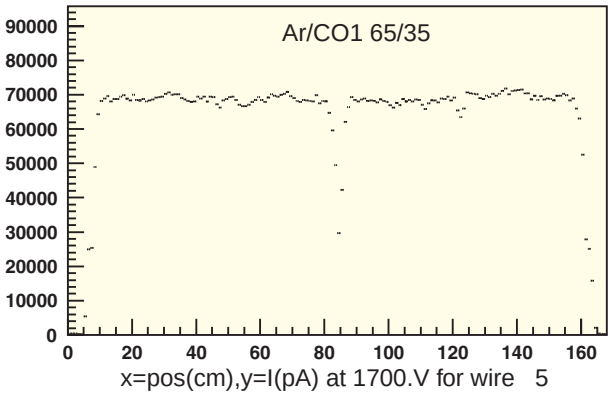

Figure 4.10: *Current measured in a source scan of a test wire as a function of the source position: the sudden current drops are due to the presence of the wire locators.*

4.4 LHCb Vertex detector

The required performance of the LHCb Vertex Locator (VELO) demands positioning of the sensitive area of the detectors as close as possible to the beams and with a minimum amount of material in the detector acceptance. This is best accomplished by operating the silicon sensors in vacuum. However, the need for shielding against RF pickup from the LHC beams, and the need to protect the LHC vacuum from outgasing of the detector modules, requires a protection to be placed around the detector modules. Furthermore, during injection, the aperture required by the LHC machine increases, necessitating the retraction of the two detector halves by 3 cm. Finally, to allow for a replacement of the sensors in case of radiation damage, access has to be rather simple. As a consequence, integration into the LHC machine is a central issue in the design of the VELO.

A complete system design was carried out. This includes a design of the vacuum vessel, motion and positioning mechanics, thin-walled structures for RF screening, systems for cooling, vacuum, monitoring and control. The VELO vacuum vessel is a 1 m diameter stainless steel vessel of about 1.8 m length which is evacuated by two powerful ion pumps (combined with Ti-sublimation pumps). The vacuum vessel and associated vacuum pumps rest on a concrete stand. Finite element analysis (FEA) was performed for the vessel and other components (exit window, cooling capillaries, thin-walled detector encapsulation). Extensive prototyping was carried out on critical items, such as the

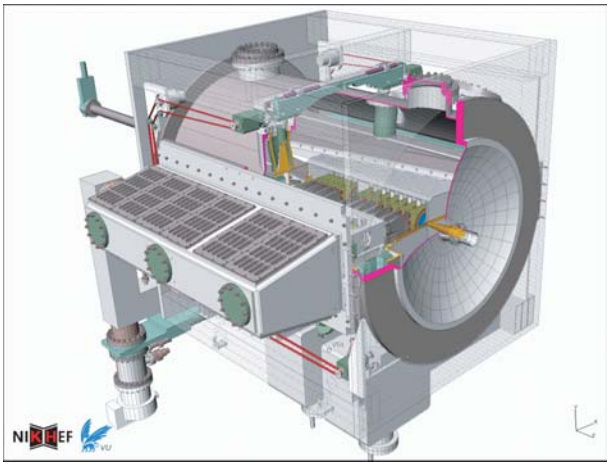

Figure 4.11: *3D-view of the vacuum vessel of the vertex detector. The silicon detectors are placed in a secondary vacuum vessel. For illustrative reasons part of this secondary vacuum vessel has been removed from the front box. Each detector halve is connected to the tank through a large rectangular bellow. During injection the two secondary vacuum vessels will be moved apart.*

thin-walled structures, vacuum protection devices, large rectangular bellows and the cooling system. The new design allows baking out of the primary vacuum surfaces and provides easy access to the silicon sensors.

A 3D-view of the mechanical design of the VELO is shown in Fig. 4.11. Large rectangular bellows allow precise movement (in the transverse directions) of the detectors during data taking as well as complete retraction of the detector elements prior to filling and dumping the beam. These large rectangular bellows decouple the complete VELO detector system from the primary vacuum vessel. The detector halves are attached to a frame which can be moved in the two transverse directions relative to the concrete stand. All motors, bearings, gear boxes and chains of the positioning system are outside the vacuum. Coupling to the frame is done via bellows.

The secondary vacuum container represents one of the most critical parts of the VELO structure. The container must be radiation resistant and act as a wakefield suppressor (electrical properties). In addition, the container provides a separation between primary and secondary vacuum (ultra-high vacuum compatibility). The container walls located within the LHCb acceptance must be manufactured from low-mass material.

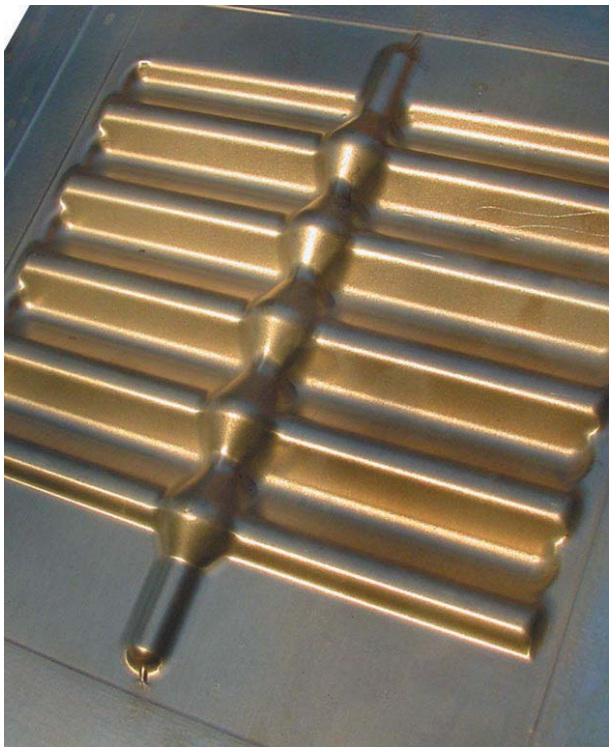

Figure 4.12: *Sample of a* 0.25 *mm thick encapsulated aluminium foil.*

Further, this thin-walled structure must allow for a small overlap between the silicon sensors of the two opposite halves, implying the use of a complex corrugated structure, and it must accommodate the motion of the detector halves. The fabrication of such complex thin-walled encapsulations is delicate and time-consuming. An extensive prototyping programme is ongoing, in which various techniques are being studied to realise the desired shape. Fig. 4.12 shows the current status of these developments. The corrugated foil was manufactured from a 0.25 mm aluminium-magnesium alloy AlMg3.

The large rectangular bellows (36 cm width $\times$ 126 cm length) separating the two vacua must accommodate the 30 mm displacement in the horizontal plane (compression of the bellows) as well as for a $\pm$6 mm lateral displacement in the vertical plane. For the latter reason, a pair of bellows separated by a flat section is used (see Fig. 4.13).

These bellows do not need to sustain a differential pressure of 1 bar, hence a dedicated production method was developed that starts from preformed 0.15 mm thick

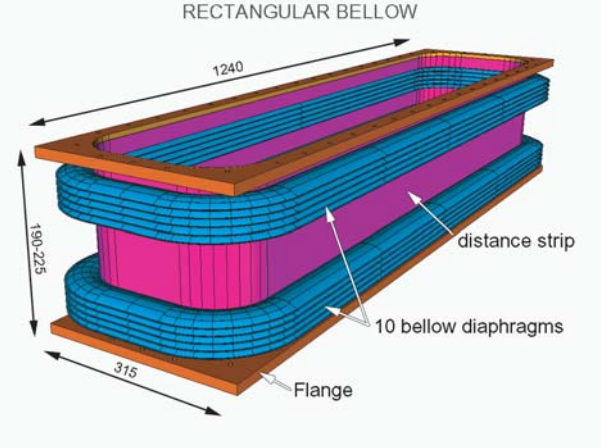

Figure 4.13: *The rectangular bellow.*

stainless steel sheets: in a first step the sheets are spot-welded around the edges with a Nickel-alloy (brazing) foil pinched between the two surfaces; in a second step, the Nickel-alloy foil is molten in a vacuum oven. This results in a smooth solder joint.

Beam bunches passing through the VELO structures will generate wake fields as a consequence of the geometrical changes and/or of the finite resistivity of the wall materials. The generated wake fields can affect both the VELO system (RF pick-up, heat dissipation) and LHC beams (instabilities). Hence, the design must take into account minimisation of heat dissipation, of the coupling impedance, and of the electro-magnetic fields inside the detector housing. The aluminium envelope of the silicon stations must be electrically connected to the exit window to guarantee appropriate wake-field suppression and to prevent possible sparking in this transition region. This constitutes a delicate design issue. The segmented half tapers of these wake-field suppressors are fabricated from 70 μm thick corrugated copper-beryllium strips. The corrugations are needed to allow for mechanical motion of the detector housings relative to the vacuum vessel and exit window. The performance of the system has been measured in a one-to-one scale model of the VELO, shown in Fig. 4.14. Realistic wake-field suppressors and detector encapsulations are implemented in this vessel. Several loop antennas are used to monitor the components of the (oscillating) magnetic fields tangent to the wall surface. Measurements of the resonant modes and coupling impedance of the mock-up have been performed by using network analysers.

Figure 4.14: *The full size mock-up of the vertex vessel for RF tests.*

Two kinds of safety valves are used to protect the thin separation foil (detector housing) from an irreversible deformation, or rupture, in case of a pressure increase on either side of the foil. A differential pressure switch is used to open an electrically activated valve whenever the pressure difference between the primary and secondary vacua rises above a value $\simeq 1$ mbar. If the pressure difference exceeds the value $\simeq 5$ mbar, then a gravity-controlled valve opens under the direct effect of the pressure independently of any electrical power or pressurised air supply. The principle of this valve consists essentially of a light aluminium disc resting on the end of a tube under the action of gravity. In case of an increase of pressure in one of the vacuum sections, the disc moves up directly under the effect of the pressure difference and equalises the pressures in the two volumes. To reduce the residual valve conductance between the two vacua in normal operation, the valve can be pumped differentially by an auxiliary pump. The purpose of these safety valves is to maintain the pres-

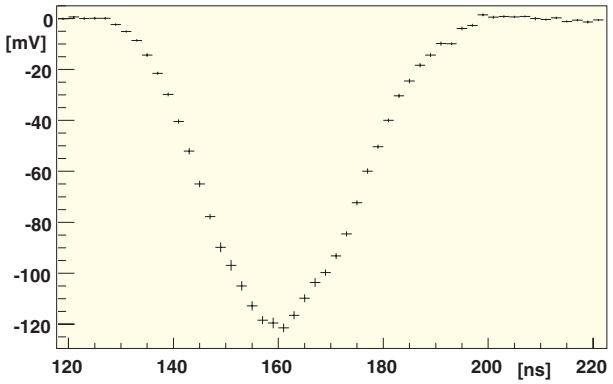

Figure 4.15: *Pulse shape measured with the BEETLE1.1 chip at the X7 test beam of CERN. The values found for the rise time and overspill amount to 20 ns and 19%, respectively.*

sure difference below $\simeq$ 17 mbar, the value above which the thin-walled detector housing is expected to deform irreversibly. At this pressure, the largest (permanent) displacement on the encapsulation has been calculated to be about 0.3 mm. The actual rupture pressure of the encapsulation is expected to be several hundred mbar.

The complete vacuum system will be controlled by a PLC unit backed with an uninterruptable power supply and interfaced to the LHC and LHCb Supervisory Control and Data-Acquisition (SCADA) systems (via e.g. ethernet). In addition to this software interface, hard-wired interlocks between LHC and LHCb will be implemented, for example for operation of the sector valves.

Preliminary studies have shown that electron cloud build-up may occur when the VELO is in the open position. The effects on the gas pressure may be tolerable due to the large pumping speed. However, the emittance increase due to electron space charge has yet to be assessed. A coating with low secondary electron yield on the detector encapsulation might be necessary.

Cooling of the detector modules is required since the sensors are operated in a high radiation environment. This is achieved by using a mixed-phase CO_2 cooling system. Besides being an adequate coolant for applications in high radiation environments, CO_2 exhibits excellent cooling properties.

In the proposed cooling circuit, CO_2 is supplied as a liquid and expanded into a number of stainless steel capillaries (one line per detector module) via flow restrictions. The capillaries and flow restrictions are vacuum-brazed to a manifold. The connection to the detector modules is achieved via an aluminium coupler and a soft metal indium joint. A carbon-fibre substrate provides a mechanical and thermal link to the sensors. The temperature of the coolant in the capillaries is set by controlling the pressure on the return line (typically 15 bar). In this way, a temperature in the range of -25 to $+10$ °C can be maintained with a total cooling capacity of about 2.5 kW ($\approx$ 50 W per cooling capillary).

A risk analysis was carried out for the VELO to first identify critical parts of the system and their possible failure scenarios, then to estimate the associated damage (essentially, the downtime for LHC) and finally to define a number of requirements (tests and precautions) to be fulfilled in order to bring the system to a level of acceptability compatible with LHC standards. The main conclusion from the risk analysis is that, even in the worst scenario (rupturing of the exit window or LHCb beam pipe), the downtime for LHC is not expected to exceed two weeks.

An important highlight this year was the submission of the Technical Design Report for the Vertex Locator VELO on May 31, 2001. The TDR has been approved by the CERN Research Board in its meeting of November 15. In view of the discussions on a reduction in the material budget ('LHCb-light') the Board made the restriction that *any change in this design have to be communicated to the LHCC and approved before construction commences.* Finally a mini-preview meeting took place on December 4 at CERN where the status of the mechanical issues (RF-foil, bellows and vacuum) and RF-issues were discussed.

4.5 LHCb front-end chip

The development of a radiation-hard front-end chip in 0.25 μm CMOS technology for the vertex detector of LHCb is in full progress. In a collaboration between the ASIC-lab in Heidelberg, Oxford University and NIKHEF an improved design of a 128 channel 40 MHz chip has been submitted. Two of these BEETLE1.1 chips have been bonded to a 300 μm VELO prototype Phi-detector. This configuration has been implemented in a setup that subsequently was used for performance tests at the X7 test beam of CERN. Data have been collected in coincidence with the VELO beam telescope and in stand-alone mode. Preliminary pulse shape results are shown in Fig. 4.15.

The values found for the rise time and overspill are

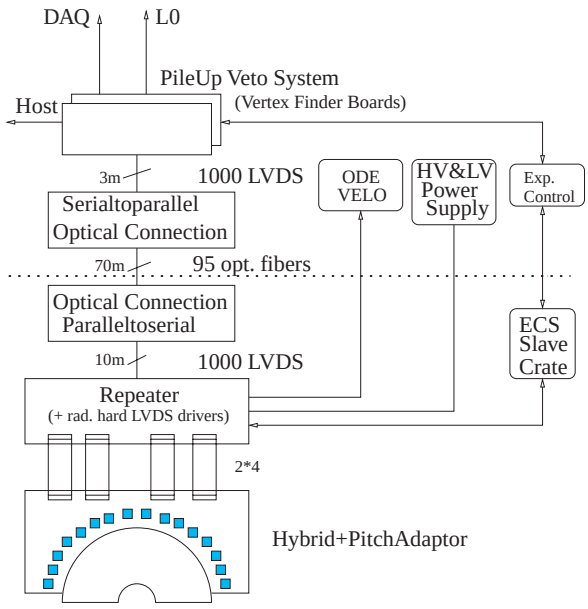

Figure 4.16: *Schematic overview of the Pile-Up VETO system.*

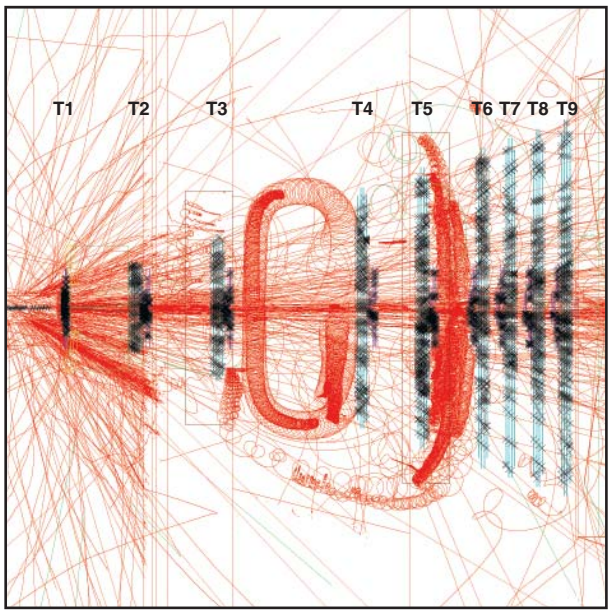

Figure 4.17: *A simulated $B \to \pi^+\pi^-$ event in the LHCb detector. The curves are the particle trajectories, the crosses ('x') represent the tracking detector hits.*

within LHCB specs. In the mean time new shaper and pre-amplifier circuits, featuring better characteristics from the point of view of saturation, have been designed, submitted and measured in the lab.

The technology used for the design of the chip promises excellent radiation hardness thanks to special layout techniques, like enclosed transistors and guard rings. Irradiation tests performed on BEETLE1.1 chips did not show any significant performance degradation up to a total dose of 300 kGy (SiO_2), which is equivalent to 15 years of LHCb running.

4.6 L0 Pile Up Veto System

In Fig. 4.16 an overview is given of the system. The digital signals from the comparators of 16 BEETLE chips on the hybrid are amplified in the Repeater Station on the vertex tank (if necessary) and led to an LVDS-bus-to-Optical-Transceiver Station. Behind the shielding wall the receiver ends of the optical links are located. There, the serialised data will be fanned out again. The other output paths of the BEETLE and ECS connections are as described in the VELO TDR in 2001. The decision to locate the processor part behind the shielding wall is governed by the fear for radiation effects (dose effects, SEUs and SELs) that could occur when the system would be located near the vertex tank.

The Pile-Up VETO system is either part of the VELO partition or a partition on its own. It is envisaged to use as much as possible standard components of the VELO or of the central DAQ system. An ODE Digitizer board will be used for the BEETLE output, either in selectable binary or analog readout mode. The data to be included in the LHCb data stream flow via the L1 Buffer. Network Processor modules combine the data. For the Pile-Up VETO system output a dedicated FIFO will be provided on the Output Board. The use of the system as luminosity monitor requires an additional output as well. The design for the Pile-Up VETO hybrid closely follows that of the VELO system. A prototype of the VELO BEETLE hybrid is being designed. It will be used in tests for the Pile-Up VETO system. Compared to the VELO system the number of signal paths of the VETO hybrid is significantly higher because of the additional LVDS signal pairs from the comparators. The additional connections add complexity to the design.

The output lines of the Beetle chip are LVDS conform. Perhaps no Repeater Station modules are needed for transmitting the digital output, provided the optical transmission boards can be placed nearby in a more or less radiation free environment (estimated rate at 10 m: < 1Gy/y). Otherwise the Repeater Station will house modules with radiation hard LVDS drivers (estimated

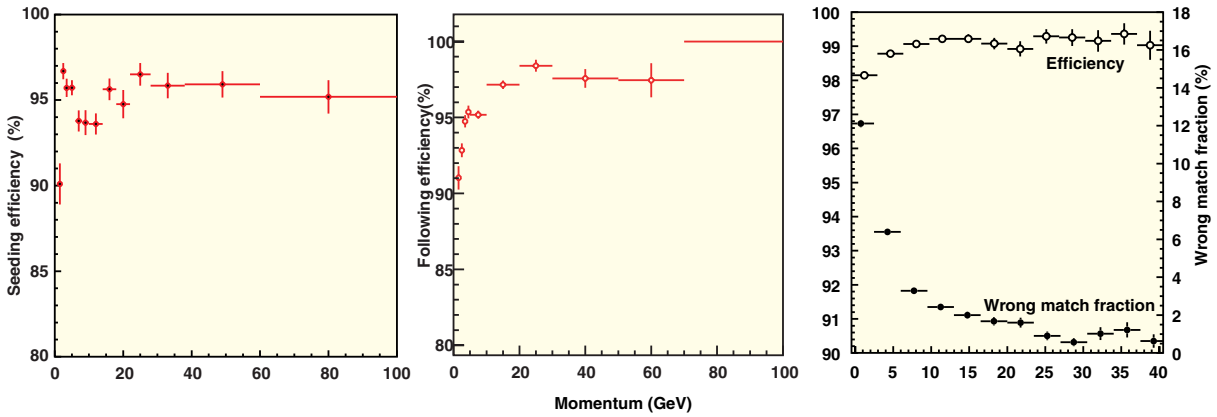

Figure 4.18: *Efficiency versus particle momentum for track seeding (left plot), track following (centre plot) and track matching (right plot).*

rate: ∼200 Gy/y) to bridge additional distance. Since using LVDS for distances over 70 m is not feasible at a rate of 80 MHz, optical transmission has been chosen as the baseline solution for transporting the signals to the VETO-system. For the L0-Mu trigger prototypes tests of such a system have been performed.

The heart of VETO system is formed by the Vertex Finder Boards. In total 5 Vertex Finder Boards are planned to be used. Four of them handle subsequent events. The fifth one is a spare processor board that can be used for checking the results of the others, provided that the data can be routed into it. Algorithms for different configurations will be pre-programmed. For a prototype Vertex Finder VME-board the algorithm has been translated in VHDL and translated into code for 3 large XILINX FPGA's. The prototype board will be tested with test patterns.

4.7 Track Reconstruction

The main tracking system, consisting of a series of stations with Inner Tracker and Outer Tracker components, must perform the following tasks:

- Find charged particle tracks in the region between the vertex detector and the calorimeters and measure the particle momenta. The momentum precision is an important ingredient of the mass resolution of the reconstructed B-mesons.
- Provide precise measurements of the direction of track segments in the two RICH detectors, to be used as input to the particle-identification algorithms
- Link the measurements in the vertex detector with the calorimeters and the muon detector.

An example of a $B \to \pi\pi$ event is shown in Fig. 4.17. In addition to the B decay particles, on average hundred background trajectories are observed in the event. The track reconstruction program aims to reconstruct all trajectories that traverse the full spectrometer. With the above tasks in mind the layout of the LHCb tracking detector systems is being optimised for optimal performance. The NIKHEF group plays a leading role in the track reconstruction as well as in the detector optimisation studies.

Pattern Recognition

The layout of the tracking system is optimised for upstream tracking, where one searches for track segments in stations farthest away from the interaction point and traces particle trajectories backwards through the magnet towards the vertex region. More specific, the pattern recognition task of assigning series of detector hits to particle trajectories is executed in three consecutive steps:

1. Search of track segments in the downstream seeding stations T6 - T9, located in a low-field region.
2. Track propagation through the dipole magnetic field towards the vertex detector. At each station track continuations are searched making use of a Kalman filter procedure.
3. Matching of tracks of the main tracker with independently found track segments in the vertex detector.

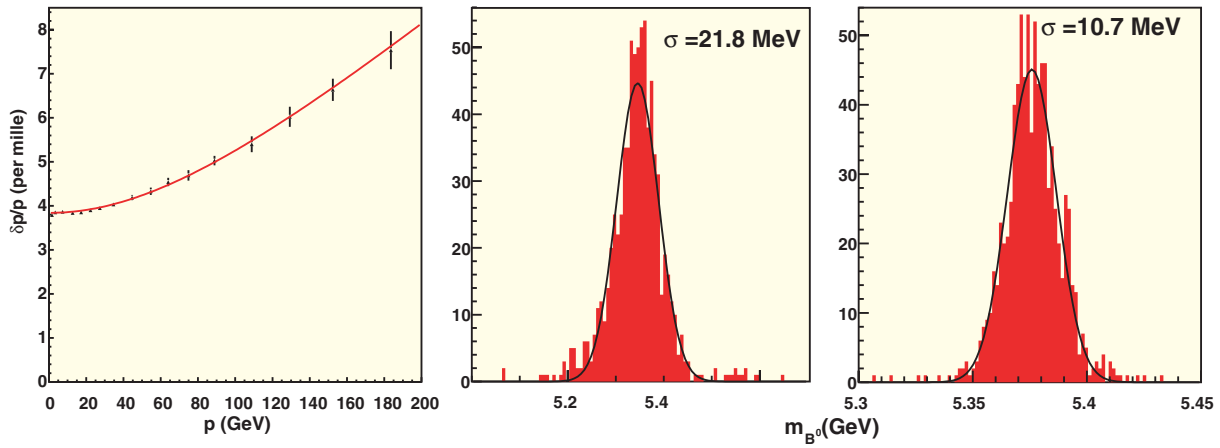

Figure 4.19: left: *Reconstructed momentum resolution as a function of track momentum,* center: *Mass resolution of reconstructed $B \to \pi\pi$ events,* right: *Mass resolution of reconstructed $B \to D_s K$ events.*

The efficiency of each of these algorithms is shown in Fig. 4.18. Combining the three efficiencies the average efficiency for a track in the event is 90%, the efficiency for a typical B-decay track is 95%.

Momentum Fit and Mass Resolution

The found tracks are fitted with a Kalman fit procedure that takes into account kinks in the trajectories due to multiple scattering in the detector materials. The resolution of the reconstructed momentum is shown in Fig. 4.19. It is parametrised by: $\delta p/p = A_{ms}^2 + (B_{res} \times p)^2$ with $A_{ms} = 3.8 \times 10^{-3}$, (the multiple scattering term) and $B_{res} = 3.6 \times 10^{-5}$ (the resolution term).

The momentum resolution is of crucial importance for the mass resolution of reconstructed B and D mesons. The expected mass resolutions of the reconstructed B-meson, in the case of a high multiplicity ($B \to \pi^+\pi^-$) and a low multiplicity ($B \to D_s K$) benchmark decay are 21.8 MeV and 10.7 MeV, respectively (see Fig. 4.19).

Detector Optimisation

The technical design of most LHCb subdetectors is finished and presented in the corresponding TDR documents. However, the layout of LHCb is currently subjected to final optimisation studies. These studies serve to reach an optimal physics performance using detectors as designed in the subdetector TDR reports. NIKHEF plays a prominent role in these final design studies.

The main aspect in these optimisation studies is to minimise the amount of detector material in the acceptance of the experiment. The effects of material are event losses due to either hadronic interactions of final-state particles (pions, kaons, governed by the interaction length λ_I) or by electromagnetic interactions (electrons, photons, governed by the radiation length X_0). In addition, dead material leads to secondary particle tracks and multiple scattering, which distort the measurement of the B decay tracks.

The following results in the optimisation have been obtained:

- Modification of the beam-pipe design from an aluminium based pipe to a beryllium-aluminium alloy based design, with less flanges, reduces the number of hits in the tracking detectors by a factor of two.
- The presence of a tracking station just downstream of the vertex detector is not crucial for the pattern recognition task of connecting tracks in the VELO with tracks in the main tracker.
- The presence of a tracking station at the center of the LHCb dipole magnet, where background conditions are severe, is not crucial for the pattern recognition task of track propagation.
- The presence of a tracking station just downstream of RICH-2 is not crucial for the efficiency and mis-tag rate of particle identification.

Additional optimisation studies are ongoing that aim to further reduce the amount of material in LHCb, without

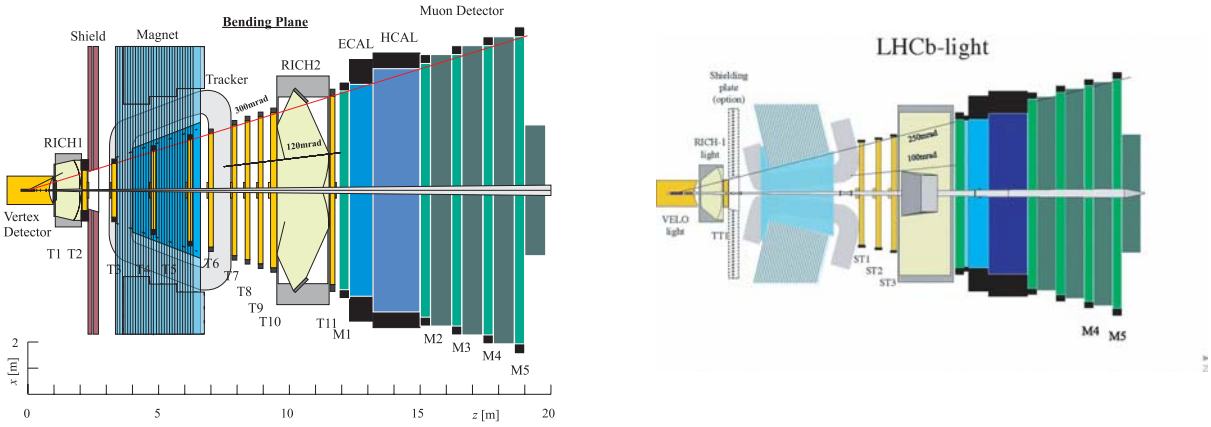

Figure 4.20: left: *Baseline LHCb detector design,* right: *'LHCb-light' design.*

compromising the performance of the experiment. The following subjects are presently being investigated:

- Use of lighter materials and thinner detectors can reduce the integrated amount of material in the VELO and RICH-1 detector from 0.33 X_0 to 0.19 X_0.
- Removal of the tracking stations just downstream of the VELO (T1) and in the magnet region (T3-T6) can reduce the amount of material in the tracking system from 0.27 X_0 to 0.12 X_0 without losses in efficiency for tracks that traverse the complete spectrometer.

The layout of the proposed LHCb light detector is compared to baseline geometry in Fig. 4.20.

4.8 LHCb Physics Performance

In the physics performance studies NIKHEF focused on the decays of the B_s meson. One of the main challenges of physics with the B_s meson is to resolve the oscillation frequency of the B_s - $\bar{B_s}$ oscillations, for which the lower limit currently is $\Delta m_s > 14$ ps^{-1}. The expected decay-time resolution for reconstructed B_s mesons in LHCb is 3% (see Fig. 4.21).

The topics studied by NIKHEF are:

- Measurement of the B_s oscillation frequency, using a flavour-specific decay channel, *i.e.* the decay determines the flavour of the B_s mesons at decay. The most promising decay-channel is $B_s \rightarrow D_s^{\mp}\pi^{\pm}$. Current studies indicate a sensitivity up to $\Delta m_s = 60$ ps^{-1}.
- Measurement of the unitarity angle γ using the decay $B_s \rightarrow D_s^{\mp}K^{\pm}$. Contrary to the previous channel, in this decay each charge configuration of the final state can be reached by both flavour B-mesons, allowing for $\mathcal{CP}$ violation to occur. The reconstruction of this channel is similar to the previous channel, the main experimental challenge is the suppression of backgrounds.
- Looking for $\mathcal{CP}$ violation caused by physics beyond the standard model with the decay $B_s \rightarrow J/\psi\phi$. The Standard Model predicts no $\mathcal{CP}$ asymmetry, so any observed $\mathcal{CP}$ violation in this decay indicates the existence of physics beyond the Standard Model. A particularly interesting aspect of the decay is that the final state can be produced by decays of the $\mathcal{CP}$ eigenstates of the B_s meson: B_{heavy} and B_{light}. An angular analysis of the final-state particles also allows a precise measurement of the difference of the decay rate of the B_{heavy} and B_{light} mesons.

4.9 Grid Activities

Computer 'Grids' consist of many machines, perhaps distributed over a large geographical area, that can collaborate on task execution and/or data storage and distribution. The LHC collaborations at CERN plan to use Grid computing to supply the computing resources needed for analysis of the LHC data. About five petabytes per year of LHC data are expected to be stored, and the total CERN-related analysis effort will require on the order of 50,000 high-end PCs in 2007.

The LHCb group at NIKHEF has begun preparations for the use of DataGrid in its computing efforts. A

cluster of ten machines (each with two GHz-class processors) has been installed on the Grid segment of the NIKHEF network. The LHCb simulation framework has been installed, along with the PBS job manager and a web interface to the job-submission program. This cluster is participating in Monte-Carlo production, directed remotely from CERN.

When the DataGrid software has been fully installed on the current DataGrid cluster, we plan to add the ten-node LHCb cluster as Grid computational 'worker nodes'. At this point, the Grid cluster will become available for the collaboration.

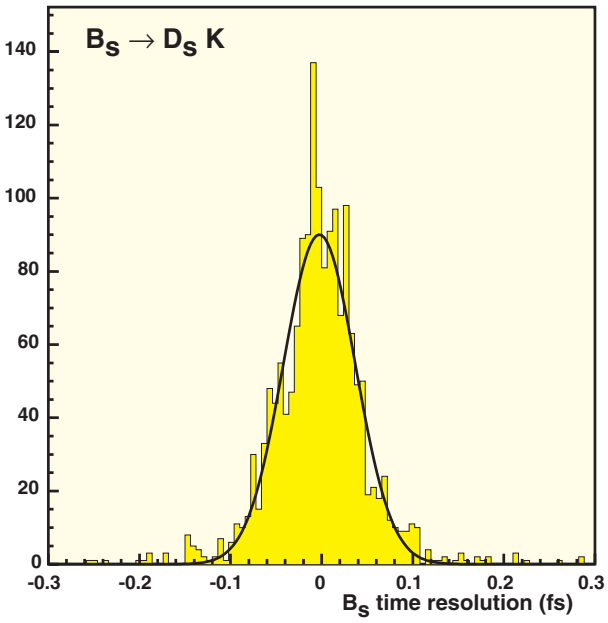

Figure 4.21: *Reconstructed decay time resolution for simulated $B_s \rightarrow D_s K$ events. The time resolution is 40 fs, corresponding to 3% of the B_s lifetime.*

First full length 15 metres prototype high field superconducting magnet for the Large Hadron Collider (LHC).

5 CHORUS

The CHORUS experiment at CERN (WA95) has been designed to discover or exclude $\nu_\mu \leftrightarrow \nu_\tau$ oscillations with high sensitivity in the parameter region of small mixing ($< 10^{-3}$) and 'large' Δm^2 (> 10 eV^2). Data were taken during 5 years, from 1994–1998. NIKHEF participates in the CHORUS collaboration since 1992.

The characteristic of the CHORUS detector is that –apart from electronic tracking– it allows high-precision tracking in the massive nuclear emulsion [1] used as neutrino target. This 'hybrid' detection provides a powerful method to find unambiguous signatures for secondary vertices, not only for $\nu_\tau \rightarrow \tau$ charged-current (CC) interactions for the $\nu_\mu \leftrightarrow \nu_\tau$ oscillation search [2], but also for ν_μ CC interactions producing short-lived charmed hadrons with track lengths of order 100 μm. In the emulsion target, charged particles produce –after development– silver grains with an average size of 1 μm and a density of 300 per mm. A τ-lepton or charmed hadron can be recognized by the topology of the decay into charged particles. In parallel with the oscillation search this latter possibility has opened up top-of-the-line charm-physics studies.

Upon any event trigger in the electronic detector, kinematic measurements are carried out using the muon and the hadron spectrometer, and the 118 t compensating lead 'spaghetti' calorimeter. Precise positions and directions of trajectories are deduced from fibre tracker planes and special emulsion sheets. For events of interest these trajectories are followed backward in the analysis, pointing –with increasing accuracy– the way towards the corresponding neutrino interaction vertices inside the emulsion target. Using automatic scanning techniques first developed in Nagoya (Japan) and originally mostly hardware controlled, the vertex and emerging tracks are then located with μm precision.

After years of hardware and software developments to speed-up and to increase efficiency of the automated track and vertex finding a powerful method (NETSCAN, see Fig. 5.1) has been developed, which allows essentially full reconstruction of events for which the vertex has been located. The emulsion scanning, still to a major extent being performed in Japan, is supplemented by essential contributions from several European laboratories. CERN and NIKHEF together operate an automatic scanning facility (three microscope systems with mega-pixel digital cameras) that is fully software controlled. A camera (resolution) upgrade of the earliest built system is in progress. Scanning of four

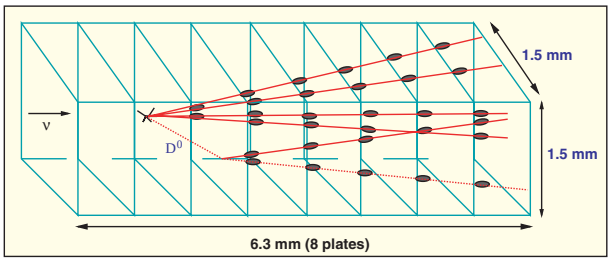

Figure 5.1: *The NETSCAN [1] volume with a sketch (not to scale) of D^0 decay. The ellipses represent track segments in 100 μm emulsion layers in which automatic scanning is performed.*

outer emulsion sheets has been recently completed and scanning inner ('bulk') emulsion sheets is being started.

Last year at NIKHEF a pioneering physics study [3] has been completed, based on 132 charm production –with muon decay– events. From this sample the ratio of neutral-to-charged charm production has been determined as a function of neutrino energy. In the mean time a sample of already 283 neutral charm D^0 events with different decay topologies has been collected and analysed [4]. The D^0 production cross section as a fraction of the total CC cross section as a function of the neutrino energy is shown in Fig. 5.2 together with results from an earlier emulsion experiment E531 at Fermilab (USA).

After a CC charm-production study based on di-muon events from neutrino interactions in the (lead) calorimeter, an analysis of the same data provided the observation of weak neutral-current neutrino production of J/Ψ's [5].

Up to now only massive counter experiments could provide high statistics measurements in the field of charm physics, while emulsion experiments had the advantage of very low background but the statistics that could be reached was limited by the scanning load required.

The development of NETSCAN has opened to CHORUS the possibility to become the first high-statistics emulsion experiment in charm physics thanks to the fact that the full decay-vertex topology can be automatically reconstructed for a very large number of events in a relatively short time.

At the moment about 130,000 events have been analysed with NETSCAN. High purity selections were developed to isolate charm events, and a sample of about

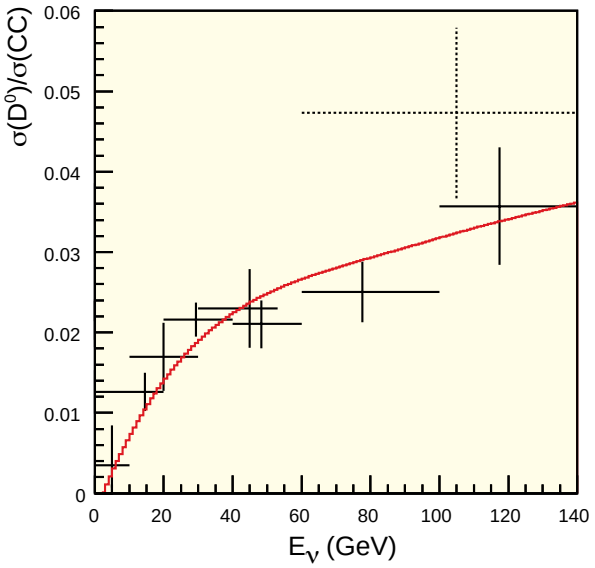

Figure 5.2: *The CHORUS results for the measured ratio of D^0 versus total CC cross section as a function of the neutrino energy, shown as solid crosses and compared with those of the E351 experiment (dashed). The curve is based on the slow rescaling model fitted to NOMAD charm data scaled by the measured (by CHORUS) D^0/(total charm) ratio.*

1000 events was manually checked in order to confirm the presence of a charmed particle and to refine the measurement of the parameters of tracks and vertices.

This sample was used for the D^0 production study [4] and for a first attempt to determine the production fractions of charged charmed hadrons [7].

Many other studies are in progress which aim to determine e.g. the charm production by $\bar{\nu}_\mu$ (from the antineutrino component of the beam), the charm production via mechanisms other than deep inelastic interactions and Λ_c production. Recently, a measurement of the total branching fraction of charm into muon has been completed without the need of a manual check [8].

A high statistics data sample with the CHORUS calorimeter as active target was obtained during a dedicated run in 1998 after the emulsion data taking was terminated. The analysis of these data provided a measurement of neutrino-induced deep-inelastic differential cross-sections on lead, from which $F_2(x, Q^2)$ and $xF_3(x, Q^2)$ structure functions can be extracted with a precision comparable to earlier results for iron targets. Neutrinos with an energy between 10 and 200 GeV were selected for the analysis. After cuts the data sample comprises about 1.1M ν-events and 230K $\bar{\nu}$-events. Using a fast dedicated Monte-Carlo simulation corrections for acceptance and experimental resolution are applied. The underlying cross-section model is based on the GRV94LO [6] parton distributions with modifications to allow for a non-zero longitudinal cross section and nuclear effects. A phenomenological correction improves the description of the data at low Q^2. Some final checks and minor improvements on the analysis are in progress to prepare the data for publication.

Simultaneous measurements on four targets of widely different nuclear composition (polyethylene, marble, iron and lead) to measure ratios of neutrino-nucleus total cross sections for different nuclear targets have been analysed in detail. Some systematic studies are underway to prepare also these data for publication.

References

[1] S. Aoki *et al.*, Nucl. Instr. Meth. **A473** (2001) 192.

[2] E. Eskut *et al.*, Phys. Lett. **B497** (2001) 8.

[3] O. Melzer, PhD Thesis, University of Amsterdam, 2001.

[4] A. Kayis-Topaksu *et al.*, Phys. Lett. **B527** (2002) 173.

[5] E. Eskut *et al.*, Phys. Lett. **B503** (2001) 1.

[6] M. Gluck *et al.*, Z. Phys. **C67** (1995) 433.

[7] F.R. Spada, PhD-thesis University 'La Sapienza', Rome, 2002.

[8] B.L.F. van de Vyver, PhD-thesis in preparation.

6 Heavy Ion Physics

6.1 Introduction

The heavy ion group at NIKHEF participates in the current CERN heavy ion programme. The NIKHEF contribution to the data analysis of the WA98 experiment, publishing its final conclusions, is described below. Both the NA57 experiment and the NA49 experiment are considering additional data taking during the next two years to further investigate the tantalising hints of the production of a quark-gluon plasma seen in the SPS experiments.

In addition to the analysis of the SPS data, NIKHEF contributes strongly to the preparation of the ALICE experiment. The NIKHEF group concentrates on the design and construction of the ALICE silicon tracker. This work is now in transition between the design phase and the production phase.

6.2 Direct photons in WA98

To investigate Quark-Gluon plasma (QGP) formation in a direct way, one needs penetrating probes which reflect the hot early stage of the interaction.

The thermal radiation of a deconfined system is a source of direct photons, i.e. photons not originating from hadron decays. Direct photons are thought to provide an excellent means for studying the state of nuclear matter at the various stages of the interaction, since photons decouple from the nuclear system immediately after their production and are essentially uninfluenced by the hadronisation process.

Within WA98 [1] the background problem of the hadronic decay photons has been overcome by reconstruction of the parent π^0 and η mesons by means of a two-photon invariant mass analysis. The thus obtained π^0 and η momentum spectra provide the basis for a prediction of the hadronic decay photon spectrum. This calculated spectrum is then subtracted from the actually observed photon spectrum. WA98 showed [2] that indeed a direct photon signal is present in the data. However, due to the limitations imposed by the reconstruction of the parent mesons, only the relatively high $p_\perp$ region could be investigated with sufficient accuracy. Since in this region direct photons from hard initial scattering processes are expected to dominate, no conclusion can be drawn concerning direct photons originating from thermal radiation.

In order to investigate the thermal regime, an alternative analysis based on inclusive photon spectra [3] is currently in progress. Application of this method on the WA98 lead-lead data reveals indeed a possible direct photon signal due to thermal radiation as shown in Fig. 6.1.

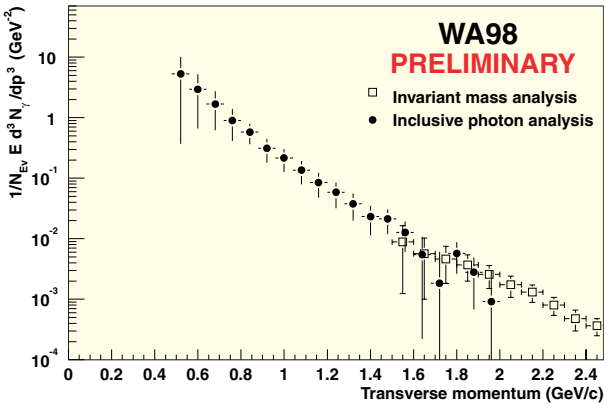

Figure 6.1: *Invariant direct photon yield as observed in central 158 AGeV Pb+Pb collisions by the WA98 experiment.*

Theoretical models [4, 5] indicate that the temperature of the system that is created, determines the shape of the direct photon spectrum, whereas the absolute photon yield reflects the space-time evolution of the radiating system. Consequently, observations of direct photon spectra in the thermal regime are expected to reveal the temperature profile and space-time history of the interaction process.

The data of WA98 can be compared with theoretical calculations based on various values for the temperatures corresponding to the start of the QGP phase (T_0), the phase transition (T_c) and the hadronic freeze-out (T_f) [6, 7].

In Fig. 6.2 the invariant yield of Fig. 6.1 is shown as a function of the photon energy in the cms of the nucleus-nucleus collision, together with the calculated yield for the values $T_0 = 300$ MeV, $T_c = 180$ MeV and $T_f = 100$ MeV.

An overal good agreement of the calculated yields with the data is observed. It should be noted that the various temperatures in the model have not been obtained from minimisation procedures, but have been 'eye-fitted' and put in by hand. However, these values provide agree-

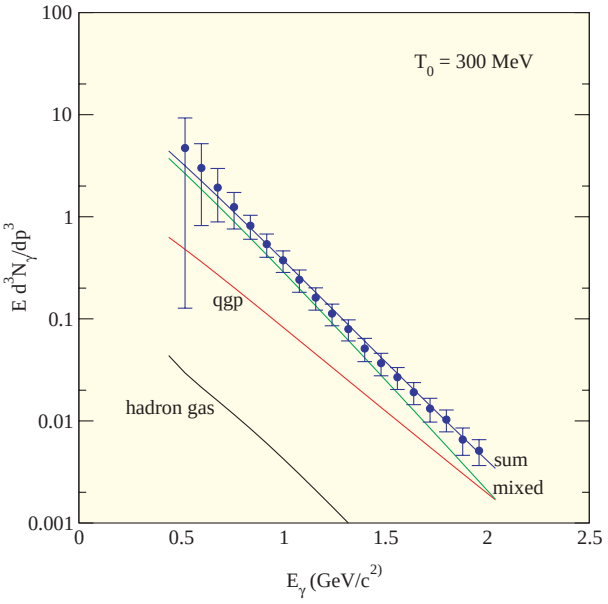

Figure 6.2: *Data with calculated thermal yields (curves) within the framework of a hydrodynamical evolution model [6, 7].*

ment with the data. Furthermore, it was observed that the dependence on T_f was only very weak.

Based on an analysis as the one described above, one can make a link between the observations in heavy ion collision experiments and the physics of the early universe. It is generally believed that the latter underwent also the phase transition from a deconfined quark-gluon plasma to normal nuclear matter. The temperatures mentioned above indicate that, within the framework of the standard Big Bang model, such a phase transition has occurred about 10^{-5} s after the Big Bang corresponding to a temperature of about 10^{12} K.

6.3 Strange baryon production in NA57

The NA57 experiment has been designed to study the production of strange baryons and anti-baryons in p-Be and Pb-Pb collisions at the CERN SPS. It intends to extend the scope of its predecessor, the WA97 experiment, which observed an enhanced production of strange particles in Pb-Pb collisions with respect to p-A collisions at 158 *A*GeV beam energy [8]. This enhanced production is more pronounced for particles with a larger strangeness content, yielding a maximum of a factor 15 for $\Omega + \bar{\Omega}$. This behaviour is in accordance with predictions, where the strangeness enhancement is a sensitive signature for the existence of a QGP phase [9].

	Pb-Pb	
	40 *A*GeV (NA57)	160 *A*GeV (WA97)
$\Lambda/\bar{\Lambda}$	0.023 ± 0.001	0.133 ± 0.007
$\Xi/\bar{\Xi}$	0.080 ± 0.025	0.249 ± 0.019
	p-Be	
	40 *A*GeV (NA57)	160 *A*GeV (WA97)
$\Lambda/\bar{\Lambda}$	0.059 ± 0.007	0.332 ± 0.008
$\Xi/\bar{\Xi}$	—	0.45 ± 0.07

Table 6.1: *Particle anti-particle ratios for the Λ and Ξ. The values at 40 AGeV are measured by NA57, the values at 160 AGeV by WA97.*

In order to study the evolution of strangeness enhancement as a function of the beam energy and as a function of the centrality of the collision, NA57 has measured strangeness production at both 40 *A*GeV and 158 *A*GeV. In the most central events the number of nucleons undergoing at least one primary inelastic collision (the wounded nucleons) is large. For the more peripheral events the number of wounded nucleons and therefore the size of the produced system is much smaller. The number of charged particles detected at mid-rapidity can be related to the number of wounded nucleons by the Glauber model [10]. The NA57 experiment can detect collisions corresponding to a number of wounded nucleons between 60 and 250.

Strangeness production at lower beam energy.

In 1999 NA57 has taken data at 40 *A*GeV for both Pb-Pb and p-Be collisions. For the Pb-Pb data the Λ, $\bar{\Lambda}$, Ξ and $\bar{\Xi}$ signals could be extracted and the $\Lambda/\bar{\Lambda}$ and $\Xi/\bar{\Xi}$ ratios were calculated [11]. Table 6.1 shows the values found by NA57 together with the ratios published by WA97 for the 158 *A*GeV data [12]. For the lower beam energy the $\Lambda/\bar{\Lambda}$ and the $\Xi/\bar{\Xi}$ ratios are smaller than for the higher beam energy by factors $\sim$6 and $\sim$3 respectively. An increase of the anti-hyperon over hyperon ratios with increasing beam energy is expected if the baryon density of the state formed in the collision is reduced. However, the values from NA57 are not yet corrected for acceptance and efficiency. The final result will be produced in 2002. The comparison to proton induced reactions will be made soon, using the data collected in the summer of 2001. The combined statistics of the WA97 and NA57 experiments will improve the errors significantly.

Enhancement versus centrality

The production yields for hyperons in proton-nucleus collisions can be extrapolated to the yield for nucleus-nucleus collisions by scaling with the number of wounded nucleons in the system. Dividing the measured hyperon yields by the scaled p-Be yields shows that the simple scaling law does not predict the measured hyperon yields. The obtained ratios, separated in five centrality classes, are shown in figure A6 for the Λ, Ξ and their anti-particles. For comparison the results from the WA97 are also shown. The dashed lines in the figure are predictions by a recently published canonical statistical model [14] for the strangeness enhancement, which reproduces the WA97 results. This model predicts a saturation of the yield down to $N_{wound} = 20$. It can be noted that the preliminary NA57 yields for the Ξ and $\bar{\Xi}$ are larger than the yields measured by WA97 [11]. This systematic difference is currently under investigation. Furthermore the Λ yields are increasing as a function of the number of wounded nucleons, while the WA97 results are constant in the four most central collision classes [13]. Therefore it is too early to draw conclusions from the data. However, if the NA57 results are confirmed then the striking drop in the $\bar{\Xi}$ yield (3.5 σ) possibly indicates a change in the production mechanisms, in contradiction with the predictions of the model. This could indicate that in smaller collision systems not enough energy is available for the creation of a QGP, whilst it could have been created in larger systems.

6.4 Strangeness and Charm Production in NA49

The aim of the NA49 experiment at the CERN SPS is a comprehensive study of hadronic reactions ranging from elementary proton-proton ($p-p$) via proton-nucleus ($p-A$) to heavy ion ($A-A$) interactions. One of the main motivations for this study is a critical investigation of the hypothesis that a quark-gluon plasma (QGP) state of matter is created in the early stage of central Pb-Pb collisions at the highest SPS energy of 158 *A*GeV. The data collected thus far by the various experiments at the CERN SPS are indeed consistent with this hypothesis. This immediately raises the question if a transition point can be experimentally observed by varying the collision energy or the size of the interacting nuclei. For this purpose NA49 has taken central Pb-Pb data at different beam energies of 40, 80 and 158 *A*GeV. Also recorded were 158 *A*GeV data with different colliding systems ($p-p$, C-C, Pb-Pb) at various centralities.

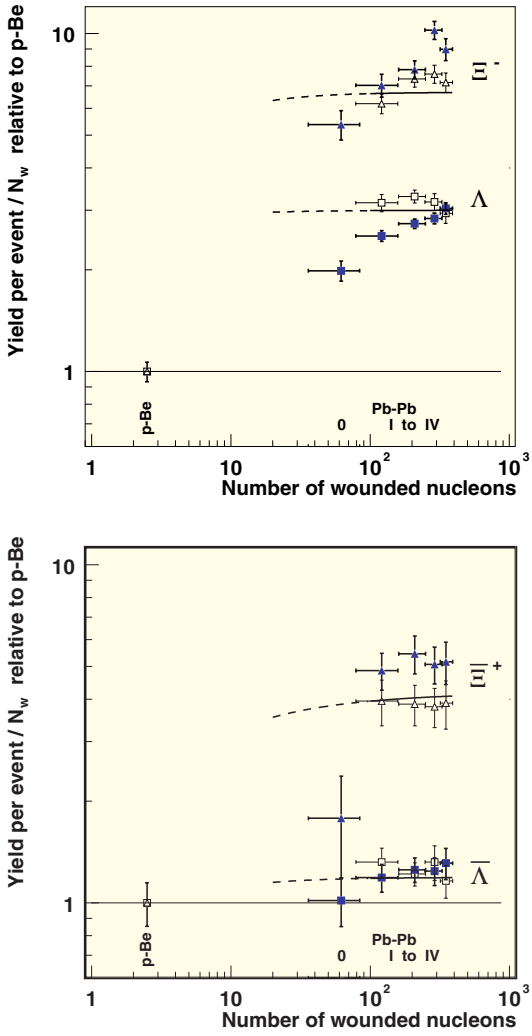

Figure 6.3: *Strange particle yield per wounded nucleon in Pb-Pb relative to p-Be as a function of the number of wounded nucleons. The open symbols depict the WA97 results, the closed are from NA57. The lines show the predicition of a statistical model (see text).*

The NA49 detector [15] consists of four Large Volume Time Projection Chambers (VTPCs). Two of these VTPCs are placed behind each other downstream of the target in a magnetic field. This allows for a separation of positively and negatively charged tracks and for an accurate measurement of their momenta; about a 1000 charged tracks are routinely reconstructed in a 158 *A*GeV central Pb-Pb event. The other two TPCs are placed behind the magnet left and right of the beam line. These MTPCs increase the lever arm of the track reconstruction and are optimised to provide particle

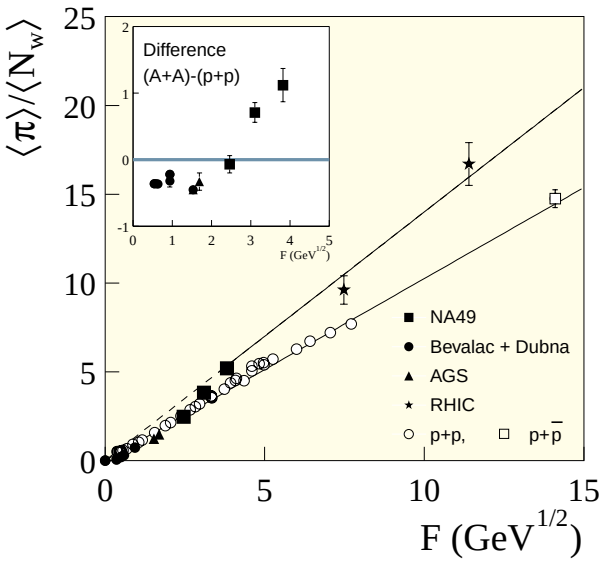

Figure 6.4: *The pion multiplicity per wounded nucleon versus the Fermi energy measure (F) for central A-A collisions (full symbols) and inelastic p-p interactions (open symbols).*

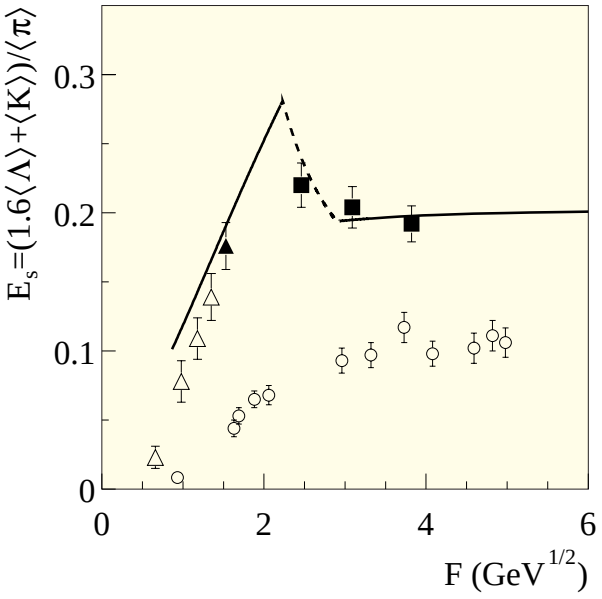

Figure 6.5: *The ratio of strangeness to pion yields versus the Fermi energy measure (F) for central A-A collisions measured at the AGS (triangles) and by NA49 (squares). Also shown are the results from inelastic p-p interactions (open circles). The curve corresponds to a prediction of a statistical model assuming a crossing of the threshold for QGP formation at* $\sqrt{s} \approx 9$ *AGeV.*

identification through a measurement of the specific energy loss (dE/dx). At central rapidity the particle identification is further improved by a measurement of the time-of-flight with 60 ps resolution. The centrality of $A-A$ collisions is measured by the energy deposition of spectator nucleons in a downstream calorimeter.

Within the large and diverse physics programme of NA49, NIKHEF participates in the analysis of the energy dependence of strangeness production in central Pb-Pb collisions as well as in a search for open charm production in Pb-Pb events at the highest SPS energy.

Figure 6.4 shows the pion yield per wounded nucleon versus the collision energy (expressed by Fermi's measure $F \propto s^{1/4}$) measured in heavy ion collisions (full symbols) and p-p interactions (open symbols). It can be seen that in the SPS energy range the pion multiplicity starts to increase faster in nucleus-nucleus than in nucleon-nucleon collisions. The strangeness to pion ratio measured in $A-A$ and $p-p$ collisions is plotted as a function of F in Fig. 6.5. One observes that this ratio increases at the lower AGS energies followed by a decreasing trend at the SPS. This non-monotonic energy dependence is not seen in elementary $p-p$ collisions. Both the steepening of the increase of pion production and the saturation of the strangeness to pion ratio at large energies can be understood in a statistical model [16] of the early stage of the reaction assuming the transition to a phase of deconfined matter at SPS energies (curves in Fig. 6.4). However, statistical hadron gas models [17] can also qualitatively explain the trend observed in the data. It is foreseen to complete the energy scan in 2002 with Pb-Pb runs at 20 and 30 *A*GeV incident energy.

The study of open charm production in heavy ion collisions is of considerable interest because the yield expected from statistical production of charm in equilibrium with a hot QGP [16] is more than an order of magnitude larger than that predicted from perturbative QCD based calculations (see Fig. 6.6). To date, no measurement of open charm yields (D^0 and $\bar{D}^0$ in the present analysis) in heavy ion collisions exists. To search for an open charm signal in central Pb-Pb collisions at 158 *A*GeV, NA49 has taken a large statistics sample of 3M events in the year 2000. The analysis of the total sample of 4M events is currently being finalised. Because NA49 has no capability to detect the secondary vertices of the $D^0 \rightarrow \mathrm{K}\pi$ decay, the search proceeds through an analysis of the invariant

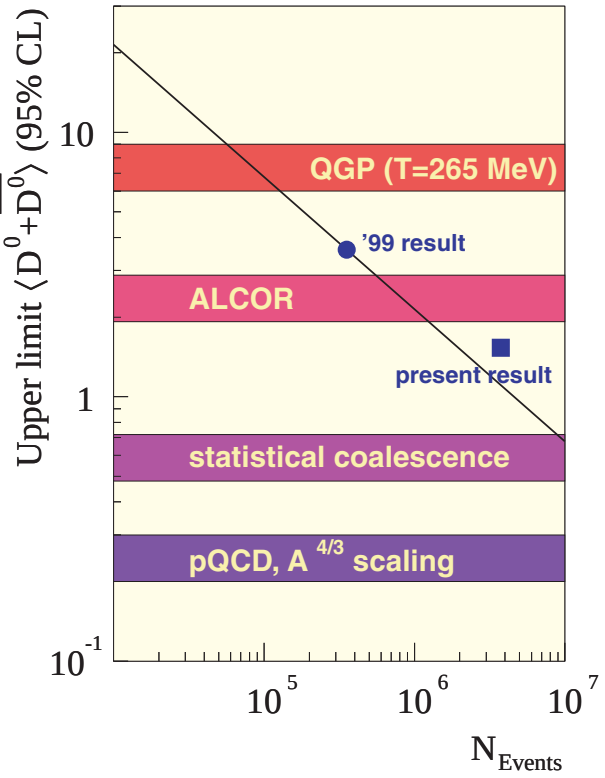

Figure 6.6: *Preliminary upper limit of the $D^0 + \bar{D}^0$ production yield per central Pb-Pb event at 158 AGeV incident energy (full square) compared to the predictions from various models (horizontal bands). Also shown is the upper limit obtained from the 1999 data (full circle) and the sensitivity as function of the number of events analyzed (full line).*

mass spectra of all pairs of positively and negatively charged tracks in the event using, of course, the particle identification capabilities of the detector to suppress as much as possible the large combinatorial background. Presently no signal is observed in the D^0 mass window resulting in an upper limit of at most 1.5 produced D^0 and $\bar{D}^0$ per event, see Fig. 6.6. This result, although still preliminary, clearly excludes statistical charm production in equilibrium with a QGP, in contrast to strangeness production. Indeed, the equilibration time of charm is expected to be much longer than that of strangeness due the larger mass.

6.5 The Alice experiment

In 2001 the design of the silicon strip module, based upon the the newly designed front-end ASIC (HAL25), was completed. In this design the mechanical decoupling of front-end electronics and silicon detector was retained thanks to the aluminium microcables, at the cost of a more complicated module assembly procedure. The module can be cooled by either water or fluorcarbon monophase coolants, without net dissipation in the air. the overall electronics design (HAL25, hybrid, cables and EndCap) was optimised to reduce the number of additional discrete components. The fully differential output will improve the signal-to-noise ratio, even at reduced voltages due to the IBM25 technology. Prototypes of various types of microcable were produced and assembly methods were worked out to the extent that industry could start producing a test series of hybrids.

Another important event was the tendering procedure for the detectors. Three companies were selected and production will start early 2002, with delivery continuing into 2003. Testing procedures for both detectors and modules are being worked out. In Utrecht a microscanning (3 μm) set-up using infra-red light was realised. This set-up can measure the charge collection both between neighbouring strips on both sides of the detector and between P- and N- sides as a function of the particle position. This knowledge can be used to improve the spatial resolution and to spot malfunctioning strips.

The EndCap modules take care of buffering the front-end signals, the power regulation and the front-end control. Moreover, the front-end electronics being at two different voltage levels (corresponding to the P and N strips), the EndCap also translates the signals to the same reference. Two ASICs (ALABUF and ALCAPONE) are foreseen in the same IBM 0.25 μm technology as the HAL25 front-end ASIC. Both were fully designed and partly submitted in two engeneering runs. Excessive power consumption, due to the use of standard libraries, necessitates additional engeneering runs in 2002, as is the case with the HAL25. Test set-ups for all these are being realised.

For the assembly of the detector modules on the carbon fibre frames a robot was designed. The main purpose of this robot is to automate the fine positioning of the 2000 detectors. The development of the motion control software and the calibration of the complete system are done by a commercial company. Design work on some details, like handling of the detector modules, will continue in 2002.

The production of the carbon fibre frames in St. Petersburg is approximately half-way. A set-up to measure the mechanical properties of these frames was tested.

These properties, like rigidities in all axes, are needed to predict the sagging of the detector ladders: once mounted inside the ITS this sag cannot be measured.

References

[1] WA98 collaboration, CERN/SPSLC 91-17 (1991).

[2] WA98 collaboration, Phys. Rev. Lett. **85** (2000) 3595.
WA98 collaboration, nucl-ex/0006007.

[3] N. van Eijndhoven, Nucl. Phys. **A618** (1997) 330.

[4] J. Kapusta, *et al.*, Phys. Rev. **D44** (1991) 2774.
R. Baier, *et al.*, Z. Phys. **C53** (1992) 433.
P.V. Ruuskanen, Nucl. Phys. **A544** (1992) 169c.

[5] D. Steffen and M. Thoma, Phys. Lett. **B510** (2001) 98.

[6] J. Cleymans, private communication.

[7] J.B. Bjorken, Phys. Rev. **D27** (1983) 140.

[8] E.Andersen *et al.*, CERN-EP/98-64.

[9] P.Koch, B.Müller and J.Rafelski, Phys. Rep. 142 (1986) 167.

[10] F. Antinori *et al.*, Eur. Phys. J. C 18 (2000) 57-63.

[11] N. Carrer for the NA57 collaboration, *Quark Matter 2001*, Long Island (2001).

[12] R.Caliandro *et al.*, J. Phys. G: Nucl. Part. Phys. 25 (1999) 171.

[13] Peter van de Ven, Ph.D.thesis, Utrecht University, The Netherlands (2001).

[14] S.Hamieh, K.Redlich and A.Tounsi, Phys. Lett. B486(2000) 61-66.

[15] NA49 Collab., S.Afanasiev *et al.*, Nucl. Instr. Meth. **A430** (1999) 210.

[16] M. Gazdzicki and M. Gorenstein, Acta Phys. Pol. **B30** (1999) 2705.

[17] J. Cleymans and K. Redlich, Phys. Rev. **C60** (1999) 054908.

[18] P. Lévai *et al.*, nucl-th/0011023.

[19] M. Gorenstein *et al.*, Phys. Lett. **B509** (2001) 277.

7 HERMES

7.1 Introduction

The HERMES experiment at DESY studies the spin structure of the nucleon with polarised targets that are internal to the HERA electron/positron ring.

In the year 2001 no data were collected by the HERMES experiment, because of an upgrade of the HERA collider. As a result the emphasis of the activities of the HERMES collaboration was on data analysis and detector development. This change in emphasis as compared to previous years was reflected in the work carried out by the NIKHEF/VUA group in Amsterdam.

The year 2001 also marked the completion of the construction of the Lambda Wheels, a wheel-shaped array of silicon detectors, which was largely developed and built at NIKHEF. In the spring the entire instrument was successfully installed in the HERMES experimental set-up at DESY. Afterwards, the silicon modules were taken out again in order to avoid the large radiation load to which the modules would be exposed during the commissioning of the upgraded HERA collider. A large radiation load will lead to a dramatic increase of the leakage currents and a corresponding reduction of the life time of the silicon detectors. In order to reduce the radiation load during normal operations a dedicated Beam-Loss Monitor (BLM) was developed and constructed by the HERMES group in 2001. This monitor will provide a trigger signal if the HERA beam starts to diverge from the desired orbit. The trigger signal will be sent to a kicker magnet that was installed in the HERA ring in 2001. The BLM was installed and successfully tested at HERMES in the fall of this year.

The analysis of HERMES data that were obtained in the period 1995 to 2000 yielded several prominent results. Two publications should be mentioned in this respect: (i) the first observation on a polarised hydrogen target of Compton scattering at the quark level (known as Deeply-Virtual Compton scattering or DVCS); and (ii) the first observation of single-spin azimuthal asymmetries in the production of neutral and charged pions. The former result is important as data of this type give access to the recently introduced generalised parton distributions, which contain information on dynamic correlations between different partons. The latter result implies that the only unmeasured leading-order structure function, i.e. the transversity distribution $h_1(x)$, is non-zero. Both publications represent a proof-of-principle, which will be followed by more precise measurements of this kind in the future.

Several guests were hosted by the NIKHEF/VUA group in the year 2001. In the first half of the year Dr. Moskov Amarian (Rome and Yerevan) shared his extensive knowledge on charm production with us. In the months July and August, a foreign undergraduate, Michiel Demey, worked as a summer student in our group. In the fall our group participated in a project on 'arbeidsorientatie' for high-school students. All these projects were successfully concluded.

Near the end of the year the upgraded HERA collider was commissioned. During these commissioning runs the HERMES experiment was checked out, demonstrating that the entire experiment is operational again. Unfortunately, the HERA commissioning has not yet resulted in stable high-intensity lepton beams, which are required for experimentation at HERMES. It is expected that data taking at HERMES will be resumed in the first half of the year 2002.

7.2 Physics analysis

In this section several preliminary analysis results are presented that have been obtained by the HERMES collaboration in the year 2001. The subjects were taken from analyses with a large NIKHEF/VUA involvement.

The spin structure of the nucleon

From measurements of the proton spin structure function $g_1^p(x, Q^2)$ it has been learned that the spin carried by the quarks can only partly account for the total spin of the nucleon. Consequently, it is expected that gluons and possibly even the orbital angular momentum of quarks and gluons also contribute to the spin of the nucleon. For that reason it has been tried to obtain information on the gluon polarisation in the proton. At HERMES a first (somewhat model-dependent) result was obtained from data collected on a longitudinally polarised hydrogen target in 1996 and 1997. A negative asymmetry was observed for events containing a pair of oppositely charged high-p_T hadrons if a sufficiently large value of the transverse momentum p_T of each hadron is required. The negative asymmetry could be interpreted in terms of a positive gluon polarisation $\Delta G/G = 0.41 \pm 0.18$, if it is assumed that the two hadrons are produced by photon-gluon fusion (PGF).

The analysis has been repeated using the new data collected in the years 1998, 1999 and 2000, on a longitudinally polarised deuterium target. Unfortunately, the expected asymmetry is smaller for this isoscalar target since the requirement of an oppositely charged

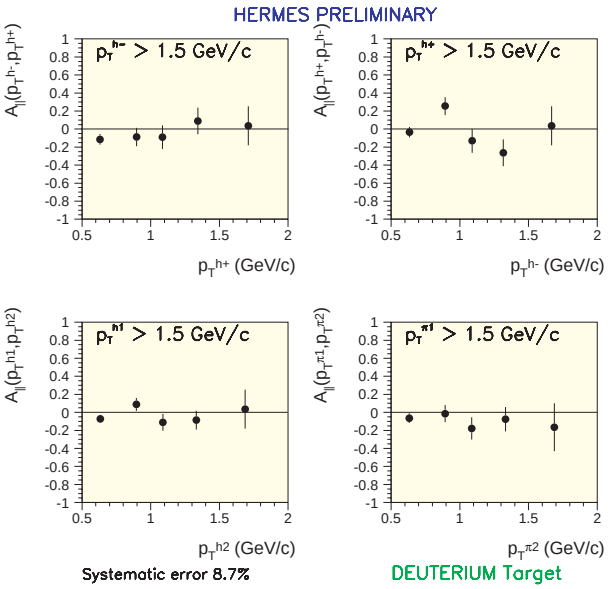

Figure 7.1: *Measured target-spin asymmetry $A_{\parallel}$ for the production of two high-momentum hadrons from a longitudinally polarised deuterium target. In the upper left (right) panel the asymmetry is shown as a function of the transverse momentum p_T of the positive (negative) hadron while the momentum of the negative (positive) is larger than 1.5 (GeV/c)^2. In the lower left panel the same is plotted for a leading hadron ('h1') versus the p_T of the next-to-leading hadron ('h2'), and in the lower right panel the same asymmetry is shown for identified pions.*

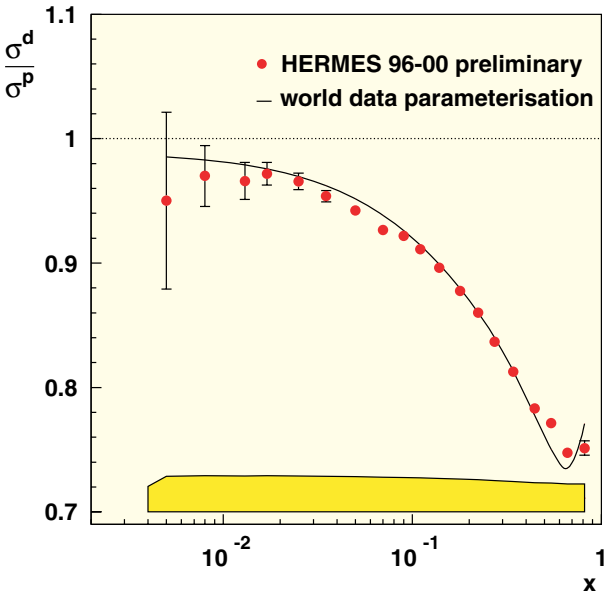

Figure 7.2: *Ratio of inclusive deep-inelastic scattering cross sections on deuterium over hydrogen versus the Bjorken scaling variable x. The curve corresponds to a parameterisation of existing data, mainly those reported by NMC. The band at the bottom part of the plot represents the systematic uncertainty of the data.*

hadron pair is less effective on deuterium. This can be understood from the positive charge of the proton, which enhances the probability of detecting two equally charged (positive) hadrons stemming from the competing QCD Compton process. Hence, by requiring oppositely charged hadrons the QCD Compton contribution is suppressed on the proton as compared to the PGF process. However, since the neutron is uncharged, this requirement is much less effective when trying to identify the PGF process on a deuteron target. As a result the expected asymmetry is less. This is confirmed by the data shown in Fig. 7.1. Detailed Monte-Carlo studies are needed to compare the proton and deuteron results in a more quantitative fashion.

The structure-function ratio F_2^n/F_2^p

The data collected for studies of the spin structure of the nucleon can also be used to obtain information on the spin-independent structure function $F_2(x, Q^2)$ by adding the data for the two different spin orientations. Of particular interest is the ratio of neutron and proton structure functions F_2^n/F_2^p, for which very precise data have been published by NMC. As the HERMES data were obtained at a much lower incident lepton energy, the comparison of the two data sets can be used to extract information on $R = \sigma_L/\sigma_T$ (at small x) and on higher-twist effects (at large x). These data extend the (x, Q^2)-range of existing measurements of $\Delta R = R^p - R^n$, which is very important as the value of R^p and R^n enters in many analyses. Possible higher-twist effects at large x are of considerable interest as well, since it has always been very difficult to identify unambiguous evidence for such effects. At large x both the HERMES and the NMC data are largely dominated by the $F_2(x)$ contribution (rather than the R-contribution, which is more important at small x), thus enabling such a study.

The preliminary data for the Deep-Inelastic Scattering (DIS) cross-section ratio σ^d/σ^p are shown in Fig. 7.2. Under the assumption that $\Delta R = R^p - R^n = 0$, the cross-section ratio equals the structure-function ratio. The data are in reasonable agreement with a parameterisation of the existing data, in particular in the mid-x

range. At small x the data are somewhat below the parameterisation, but the deviation is smaller than the preliminary estimate of the statistical and systematic uncertainty. A similar situation occurs at large x, where the deviation is also smaller than the presently estimated systematic uncertainty. It is clear from these preliminary data that neither the deviation from $\Delta R = 0$ nor the higher-twist effects can be very large. This is remarkable since the present data correspond to Q^2-values which are on average about a factor of 5 below those covered by the NMC data.

Photoproduction of Ξ and Λ_C baryons.

In an effort to obtain complementary information on the spin structure of the nucleon, it could be very interesting to search for Ξ and Λ_C baryons. The Ξ hyperon contains two strange quarks, and can thus be used as a probe of the strange sea, while the charmed Λ_C baryon –if produced by photon-gluon fusion– provides information on the gluon polarisation. For those reasons it has been tried to identify Ξ and Λ_C baryons in photoproduction data that were collected at HERMES in the years 1998, 1999 and 2000 on a polarised deuterium target.

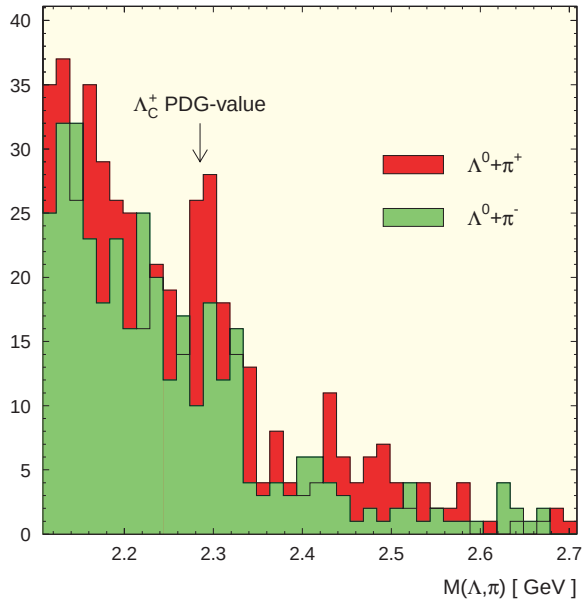

Figure 7.3: *Mass spectrum for photo-produced Λ-π pairs. The upper (lower) histogram corresponds to the use of positive (negative) pions in the analysis. In both cases the transverse momentum p_T of the Λ hyperon with respect to the Λ_C^+ direction is required to be between 0.6 and 0.88 GeV/c.*

Combining all data obtained in those three years (corresponding to roughly 8 million DIS events), a search for Λ_C baryons was undertaken. The search was based on the $\Lambda_C \rightarrow \Lambda + \pi^+$ decay, which has a branching ratio of only 0.9%. In the analysis the events are required to contain at least three hadrons. Using the particle identification capabilities of the HERMES Ring Imaging Čerenkov (RICH) detector, the hadrons must be identified as a proton and (at least) two pions. By combining the four-momenta of the proton and the pion a Λ^0-peak is easily found in the $p\pi$-invariant mass spectrum. The reconstructed four-momentum of the Λ^0 hyperon is used to evaluate the invariant mass of $\Lambda^0 - \pi$ pairs. By also requiring that the transverse momentum p_T^Λ of the Λ^0 hyperon with respect to the propagation direction of the assumed Λ_C baryon is large ($0.6\ \mathrm{GeV}/c < p_T^\Lambda < 0.88\ \mathrm{GeV}/c$), the spectra shown in Fig. 7.3 are obtained. While no structures are observed in the $\Lambda^0\pi^-$-spectrum, a clear peak is seen in the $\Lambda^0\pi^+$-spectrum at the location of the known Λ_C mass.

Although this result represents the first observation of a Λ_C baryon in a *polarised* deep-inelastic scattering experiment, the number of observed events is insufficient to evaluate a the asymmetry of the yield with respect to the orientation of the target spin. In order to increase the number of events containing a Λ_C baryon, it has also been tried to consider partially reconstructed Λ_C events. Since the branching ratio $\Lambda_C \rightarrow \Lambda^0 + \pi^+ + X$ is about 10%, an analysis of the $\Lambda^0\pi^+$-spectrum at lower invariant mass will yield considerably more events. This analysis is in progress.

As a by-product of the Λ_C search, very clear evidence for the production of Ξ hyperons was obtained. The results are shown in Fig. 7.4. The Ξ hyperon has a branching ratio of close to 100% into a $\Lambda\pi$-pair. Hence, its observation is considerably favoured as compared to the observation of a Λ_C^+ baryon. In fact, both the Ξ^- and its anti-particle the $\bar{\Xi}^+$ hyperon are observed. The latter particle, which has a $(\bar{d}\bar{s}\bar{s})$ structure, is an 'all-sea' object. Its production in an experiment with both beam and target polarised, will make it possible to obtain information on the sea-quark polarisation. The determination of the target-spin asymmetry for the Ξ hyperons is underway. Furthermore, Monte-Carlo simulations were begun to study the importance of competing production mechanisms.

Nuclear effects

During selected (brief) periods the HERMES experiment has been operated with unpolarised nuclear tar-

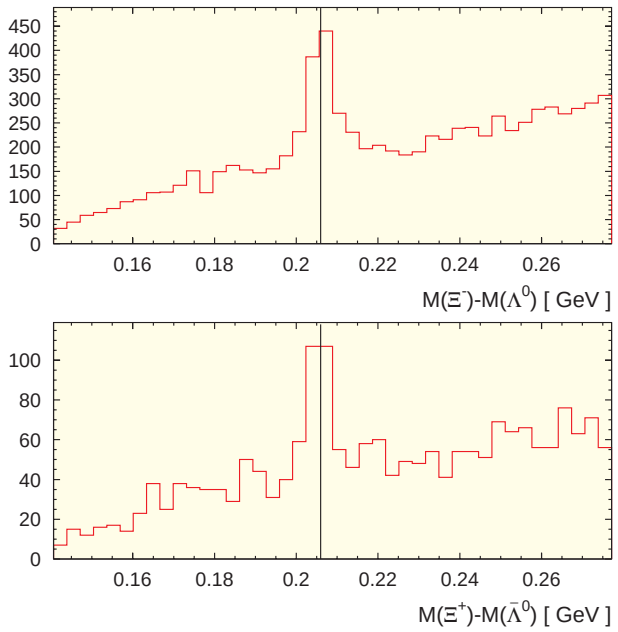

Figure 7.4: *Yield of photo-produced $\Lambda\pi$-pairs as a function of the invariant mass of the pair. The reconstructed mass of the Λ hyperon has been subtracted from the invariant mass. In the upper panel the results are shown for $\Lambda^0\pi^+$-pairs, while the lower panel shows $\bar{\Lambda}^0\pi^-$-data. In both cases a clear peak corresponding to the production of a Ξ hyperon is observed.*

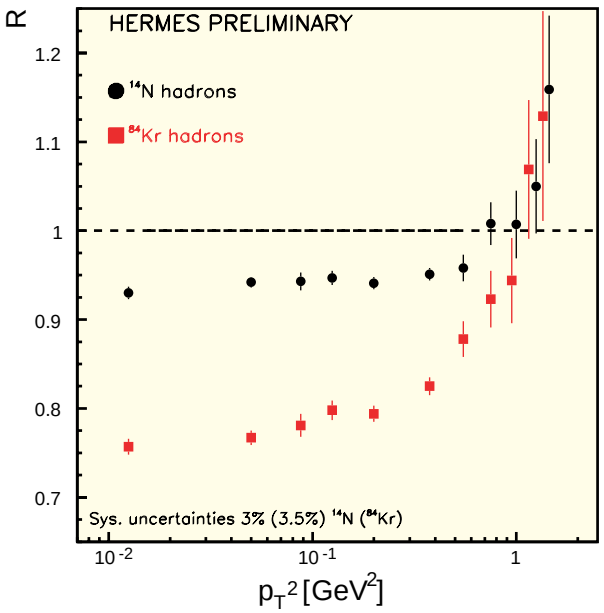

Figure 7.5: *Ratio of semi-inclusively produced hadrons on a heavy nucleus with respect to deuterium as a function of the transverse momentum squared of the emitted hadron. The closed circles represent the nitrogen over deuterium data and the closed squares the krypton over deuterium data.*

gets. These measurements have been used to study the effect of the nuclear environment on the formation of hadrons, resulting in (indirect) determinations of the formation length of hadrons and the coherence length of $(q\bar{q})$-fluctuations of the virtual photon.

Unexpectedly, these data also showed a difference between the ratio of inclusive DIS cross sections obtained on nitrogen and deuterium as compared to similar nuclear ratios obtained elsewhere at higher lepton energies. This difference has been attributed to a possible mass dependence of the ratio $R = \sigma_L/\sigma_T$ of longitudinal over transverse photo-absorption cross sections. In order to study this effect in more detail additional data on an even heavier nucleus, krypton, were collected. While analysing these data a serious experimental problem was discovered. Bremsstrahlung photons radiated in elastic *nuclear* scattering may cause large showers in the frames of some of the tracking detectors, leading to large local inefficiencies. When corrected for these inefficiencies the previously reported differences between nuclear ratios obtained at HERMES and other experiments largely disappeared.

Fortunately, the inefficiencies caused by the photon showers do not affect the semi-inclusive data quoted at the beginning of this section since the observation of an additional hadron in the final states excludes contributions from radiation produced in elastic scattering. In fact, the additional data collected on krypton enabled us to extend our studies on the influence of the nuclear environment on the hadronisation process to a heavier nucleus. Part of these results are shown in Fig. 7.5, where the hadron yields in a semi-inclusive reaction on a heavy nucleus relative to those on deuterium are shown. It is observed that the ratio is more or less constant up to $p_T^2 \approx 0.6$ (GeV/c)^2. For larger values of p_T^2, the data show a steep rise.

The relative rise of the p_T^2-distributions in nuclei beyond $p_T^2 \approx 1$ (GeV/c)^2 has also been seen in proton-nucleus and nucleus-nucleus collisions, where it is known as the Cronin effect. This effect has now also been observed for the first time in deep-inelastic scattering. The effect is assumed to arise from multiple scattering of the

struck quark (and/or the produced hadron) on its way out of the nucleus.

Other nuclear effects (such as possibly different formation times for pions and protons) are presently under study using the new krypton data. This data set has two advantages as compared to the (already published) nitrogen data: the effects are larger, and the data were collected with the new RICH detector enabling the determination of the attenuation ratio for different hadron species.

7.3 The JLab experiment

In order to investigate the nuclear dependence of inclusive deep-inelastic scattering in a different domain, a dedicated experiment was carried out at the Jefferson Laboratory (JLab) in Newport News, Virginia. The experiment (E99-118) was performed in Hall C in the summer of the year 2000 using electron beams of 2.301, 3.419 and 5.648 GeV, and an average electron current of 25 μA. The scattered electrons were detected with the High-Momentum Spectrometer. Data were taken at electron scattering angles between 10 and 60 degrees using six different targets: LH_2, LD_2, C, Al, Cu and Au.

Cross sections for deep-inelastic electron-nucleon and electron-nucleus scattering were measured at small values of x and Q^2, i.e. $0.007 < x < 0.55$ and $0.03 < Q^2 < 2.8$ $(\mathrm{GeV}/c)^2$. The data will be used to determine the cross-section ratio σ^A/σ^D. As data have been collected at different beam energies it is possible to perform a Rosenbluth separation, which will yield the ratio of longitudinal over transverse cross sections, $R = \sigma_L/\sigma_T$.

The analysis is in progress. Various efficiencies (tracking, Čerenkov, Calorimeter) have been determined. The density of the cryogenic targets has been corrected for the effect of local boiling under the influence of the beam. The charge-symmetric background has been determined for all targets by measuring positron cross sections, obtained by reversing the polarity of the spectrometer. Pion rejection was implemented in the hardware trigger, and the remaining pion background was cut by using the information from the Čerenkov and Calorimeter detectors.

An example of the measured cross section with and without radiative corrections applied is shown in Fig. 7.6. As can been seen, the radiative corrections at low scattered energy E' are very large, which is largely due to the radiation tail of elastically scattered electrons. Therefore, special attention must be paid to an accurate description of all radiative corrections, both internal and external ones.

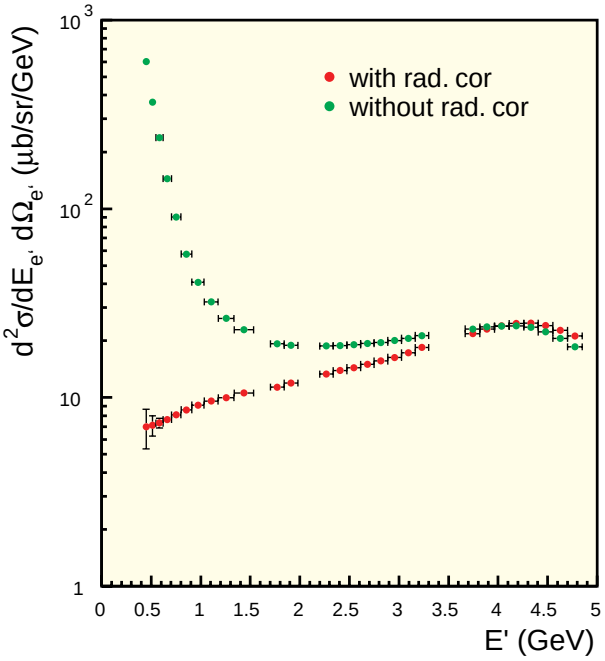

Figure 7.6: *Spectrum for inelastic electron scattering off a Cu target as obtained in Hall C at JLab. The incident electron energy was 5.648 GeV, and the spectrometer was located at an angle of 10.6°. The data are shown both with and without radiative corrections.*

7.4 The Lambda Wheel project

In the last couple of years a new wheel-shaped silicon detector, known as the Lambda Wheels, has been developed. The purpose of this detector is to increase the acceptance of the HERMES spectrometer for Λ^0 hyperons and charmed particles, such that the polarisation of strange quarks and gluons can be measured with improved precision. Most of the development work related to the construction of the Lambda Wheels was carried out at NIKHEF.

Near the beginning of 2001 the construction of the Lambda Wheels was completed. A few months later the entire system was installed at HERMES, where it is located just downstream of the (polarised) internal target. The installation was fully successful, as illustrated in Fig. 7.7 showing the front view of the installed Lambda Wheels. After the installation the individual detector modules were taken out again, in order to avoid radiation damage which usually occurs during

Figure 7.7: *Photograph of the new wheel-shaped silicon detector at HERMES. The instrument is known under the name Lambda Wheels. The picture was taken after the test installation during the HERA shut down. Each of the 12 individual silicon modules can be seen.*

extensive beam-tuning efforts that are needed to commission the upgraded HERA collider. It has been decided to wait until the commissioning of HERA is (more or less) finished before the Lambda Wheel modules will be reinstalled.

It has been shown during tests of a prototype Lambda Wheel module (in 2000) that unexpected beam losses, may cause a significant increase in the leakage current of the silicon detectors. In order to avoid such damage to accumulate, it was decided to build a dedicated Beam Loss Monitor (BLM) that will create a trigger signal if excessive radiation levels are observed. The trigger signal will fire a newly installed HERA kicker magnet in order to dump the beam in a controlled fashion.

The BLM consists of two sets of 3 ionisation chambers (see Fig. 7.8) and one dummy detector of the same size. A trigger is generated if 2 of the 3 chambers generate a signal (above threshold) while the dummy gives no signal. In this way the dummy prevents false triggers due to electromagnetic interference. After construction the BLM was calibrated at an intense X-ray source in

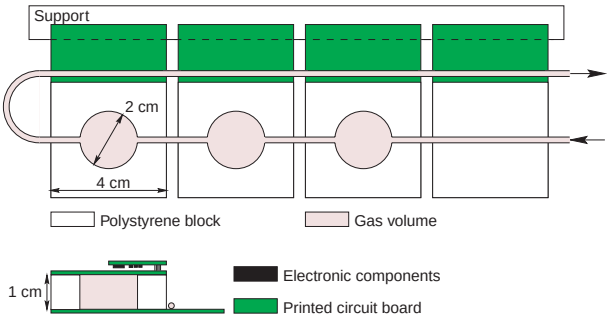

Figure 7.8: *One side of the Beam Loss Monitor that was installed at HERMES in 2001. The other side is similar to the side shown. The BLM consists of 3 polystyrene ionisation chambers, and one dummy. The dummy chamber is shown on the far right of the figure. Both the gas flow, the support structure and a cross sectional view are shown.*

Mons (Belgium). As a result the output of the BLM can now be specified in units of Gy/s.

As the BLM is equipped with fast electronics, which are connected to the dump kicker by means of an 5 km long optical fibre, it is possible to dump the HERA beam within a few milliseconds. The BLM is the fastest beam-dump system of all HERA experiments.

The BLM was installed in the summer of 2001, and is fully operational since October. During the last months of the year it has operated stably. The trigger has not yet been connected to the fast kicker magnet in order to avoid interference with the HERA commissioning effort. Using the BLM three types of beam loss events have been observed: (i) fast losses (within one HERA revolution) causing very little radiation; (ii) losses spread out over many hundreds of revolutions, which cause a fair amount of radiation; and (iii) slow losses, causing a significant amount of excess radiation. The BLM is able to dump the beam for the last two event classes.

7.5 Longitudinal Polarimeter

Since early 2001 our group is in part responsible for the operation and maintenance of the HERMES longitudinal polarimeter (LPOL). The polarimeter measures the polarisation of the HERA lepton beam making use of the asymmetry in the Compton cross section for scattering circularly polarised (laser) photons off polarised leptons. The intersection point of the laser is located 39 m downstream of the HERMES target. The back scattered photons are detected in a calorimeter that measures the total energy of the photons. Due to the

very large boost of the photons, almost all photons are scattered into a very small cone around 180° in the laboratory frame and travel along the lepton beam. In order to separate the photons from the beam a dipole magnet bends the beam by 0.54 mrad, which is enough to extract the photons from the beam line 16 m downstream of this bend. The intensity of the laser beam and the lepton beam is such that the polarisation can be measured for separate electron bunches.

In 2001 a new second calorimeter has been built, tested and installed. This calorimeter consists of scintillation plates sandwiched between tungsten plates with a total depth of 20.6 radiation length. This new calorimeter was tested at the DESY test beam facility with electrons from 1 to 6 GeV and at CERN with electrons between 10 and 30 GeV. The analysis of the data is in progress and preliminary results show that the response is linear with energy.

Since the new calorimeter is not segmented an additional detector is needed to measure the distribution of the back scattered photons. For this purpose a scintillating fibre detector is needed, which will be located in front of the calorimeter. An improved scintillating fibre detector is presently under construction.

7.6 Outlook

Following the HERA commissioning the Lambda Wheel modules will be installed at HERMES, and the trigger generated by the Beam Loss Monitor will be connected to the HERA dump kicker. Thereafter, the measurements at HERMES can be resumed. For the NIKHEF/VUA group initially the emphasis will be on the final commissioning of both the Lambda Wheels and the Beam Loss Monitor, while we also carry a shared responsibility for the operation of the longitudinal (beam) polarimeter.

Data taking in the year 2002 will employ a polarised hydrogen target with its spin axis polarised perpendicularly (or transversely) to the beam. Such data will give access to the sofar unmeasured leading order structure function $h_1(x)$. It is of considerable interest to obtain data on $h_1(x)$, as its scaling violations (or Q^2-dependence) are predicted to be dramatically different from those of the other leading-order structure functions. Moreover the integral over $h_1(x)$ will make it possible to determine the tensor charge of the nucleon, a quantity for which predictions exist based on lattice gauge theory.

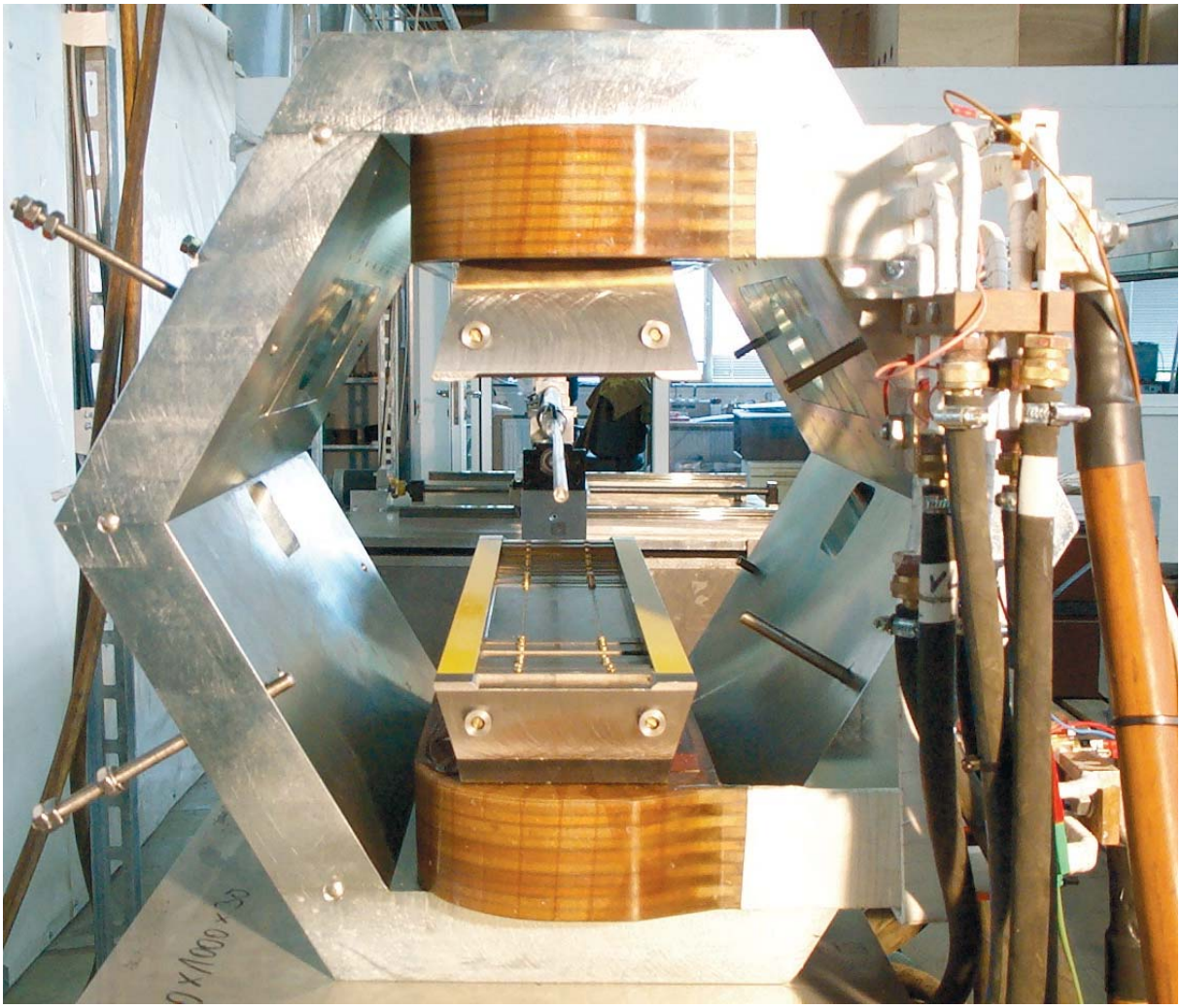

End view of the Hermes transverse target magnet.

8 ZEUS

8.1 Introduction

This year HERA accumulated no luminosity. Due to the work on the luminosity upgrade the accelerator was shut down until September. The upgrade entailed a complete rework of the H1 and ZEUS intersection regions, where completely new final focus quadrupoles were installed significantly closer to the intersection points of the electron and proton beams. This means for ZEUS that these magnets are now *inside* the ZEUS detector. In the forward region the quadrupole magnet now protrudes to inside the forward tracker and in the rear it is installed inside the rear calorimeter.

The placing of these magnets gives a significant increase in the produced synchrotron radiation near the detector in the horizontal plane (due to early separation of the beams). In order to allow the unhindered passage of this radiation the beam-pipe needed to be redesigned. It now has an elliptical shape. At the same time the material from which this was manufactured was chosen to be an Al-Be alloy, which will significantly reduce the amount of material particles need to traverse before being measured in the new micro-vertex detector.

At startup in September the installed radiation monitors in the ZEUS interaction region showed an intolerable background, presumably from synchrotron radiation. Significant machine studies in the last months of the year pinned down the source of this radiation to a bending magnet in the electron ring some ninety metres from the intersection region. To reduce the flux of radiation two new collimators have been designed and ordered. They will be ready for installation in the machine at the beginning of 2002.

It was also determined that a collimator that is placed downstream of the detector was dimensioned too small, so that this could be a source of backscattered synchrotron radiation in the detector. This has in the meantime been enlarged. Several other modifications in other parts of the accelerator will also be performed at the beginning of 2002. With these modifications there is good hope that the machine will start producing high luminosity running towards March 2002.

8.2 Structure Function F_2

The work of the NIKHEF group in ZEUS continued on the extraction of the structure function F_2 of the proton. It culminated in a publication. The present results surpass the previously published results in both systematic and statistical accuracy. Much work was invested in the correct description of correlated systematic errors. These are of significant importance when interpreting the data in terms of QCD evolution of parton densities in the proton. The analysis of the data in terms of the QCD DGLAP evolution equations provided confirmation of the previous results that the structure of the proton can be described by perturbative QCD down to four-momentum transfer squared, Q^2, values of about 1 GeV^2.

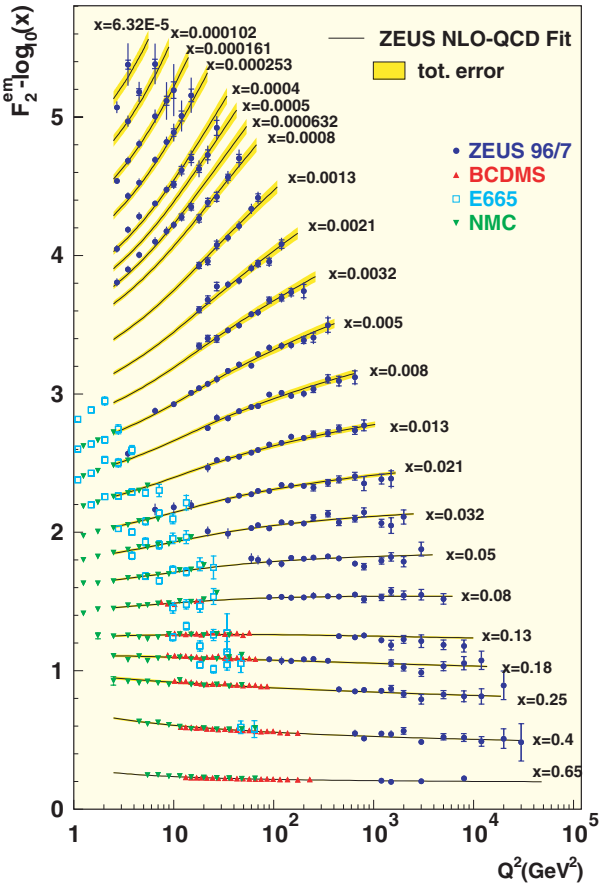

Figure 8.1: *The F_2 structure function as a function of Q^2 for various values of x.*

The precision with which the parton densities can be extracted from the data has followed the data precision. Figure 8.1 shows the structure function F_2 as a function of Q^2 for several values of x, the fraction of the proton four-momentum carried by the struck quark. A fit to the data in terms of the DGLAP evolution equations is also shown. Especially noteworthy is the precision

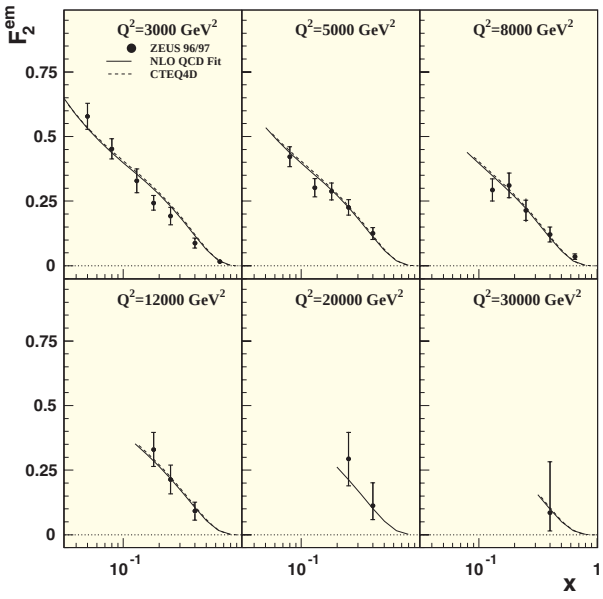

Figure 8.2: *The F_2 structure function as a function of x at high Q^2.*

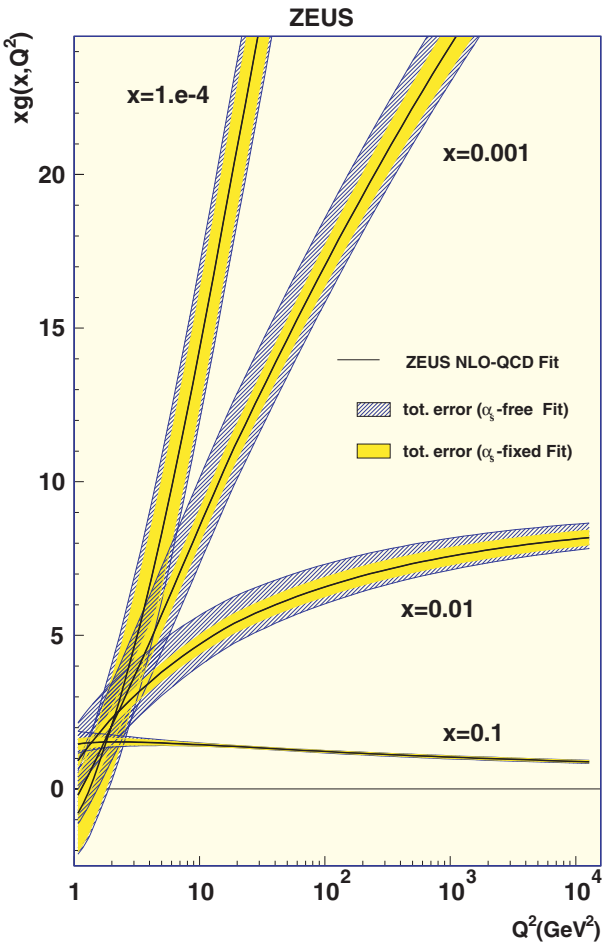

Figure 8.3: *The gluon density in the proton as extracted from a NLO QCD fit to the data on the F_2 structure function.*

obtained for very large Q^2 values (Fig. 8.2). Figure 8.3 shows the gluon density extracted from the fit as a function of Q^2 for several values of x.

Especially the evolution of the gluon density at $x = 10^{-4}$ is striking. Both the extremely steep rise and the fact that the density drops below zero for $Q^2 < 1$ GeV^2 has been the subject of much controversy. Although the fit to the data provides an excellent description of the structure function over a very wide range in x and Q^2 the present precision of the data indicates that the extension of the fits to include the very low Q^2 data is no longer possible as it leads to a very large increase in the χ^2 of the fit.

Figure 8.4 shows a comparison of the fit, performed on data with $Q^2 > 2.5$ GeV^2, to the ZEUS data for $Q^2 < 1$ GeV^2. Increasingly large deviations from the fits are observed as Q^2 decreases, indicating the breakdown of the description of the structure of the proton in terms of parton densities evolving according to perturbative QCD. This is of course not surprising. It is the fact that the data deviates from this perturbative description *only* at such low values of Q^2 that is the real surprise.

8.3 Micro-Vertex Detector

Apart from the ongoing physics analyses the major effort of the NIKHEF group was this year concentrated on the finalisation of the micro-vertex detector. This has been a major responsibility of the group, not only in hardware but also in the tracking software. The construction of the detector was finalised at NIKHEF and the detector was shipped in two halves to DESY for a full system test in March. Prior to the installation in the ZEUS detector, the two vertex detector halves were build together around the new beampipe. Then it was fully equipped and several weeks of cosmic ray data were taken.

From this system test it could be concluded that, in all, more than 99 percent of the 207360 channels performed according to specification. After completion of the cosmic ray test run the vertex detector was inserted in the ZEUS detector. The system has again been tested after installation using cosmic rays. This time the ZEUS cen-

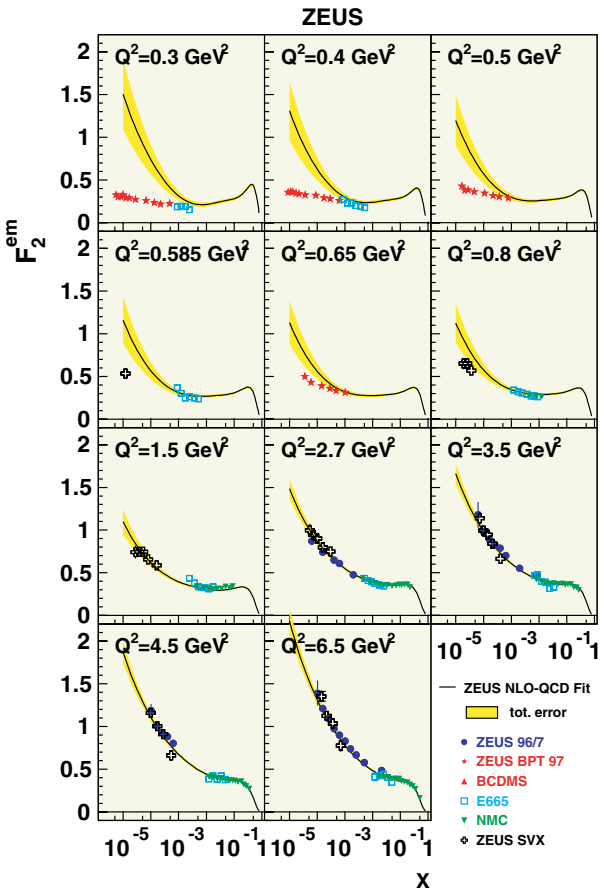

Figure 8.4: *The prediction from the fit performed at $Q^2 > 2.5$ GeV ^{2} of the F_2 structure function at very low Q^2 compared to ZEUS data.*

tral tracker which surrounds the micro-vertex detector was also activated and the magnetic field was turned on. This allowed a first test of the Kalman Filter track-fitting software which has been developed at NIKHEF (see Fig. 8.5a).

This package written in the object oriented language C++ performed without problems even when incorporated in the standard ZEUS software environment, that is predominantly written in FORTRAN. The cosmic ray test showed that the micro-vertex detector was positioned within 1 mm of the nominal position. Further alignment of the detector with respect to the central tracker is ongoing.

Finally the Monte-Carlo description of the micro vertex has been completed and after tests with single particles now many neutral current deep inelastic scattering events are available for testing the track-fitting package. Figure 8.5b shows a typical example of the performance of the fitting package. With this new detector and the foreseen increase of luminosity we look forward to several years of exciting physics.

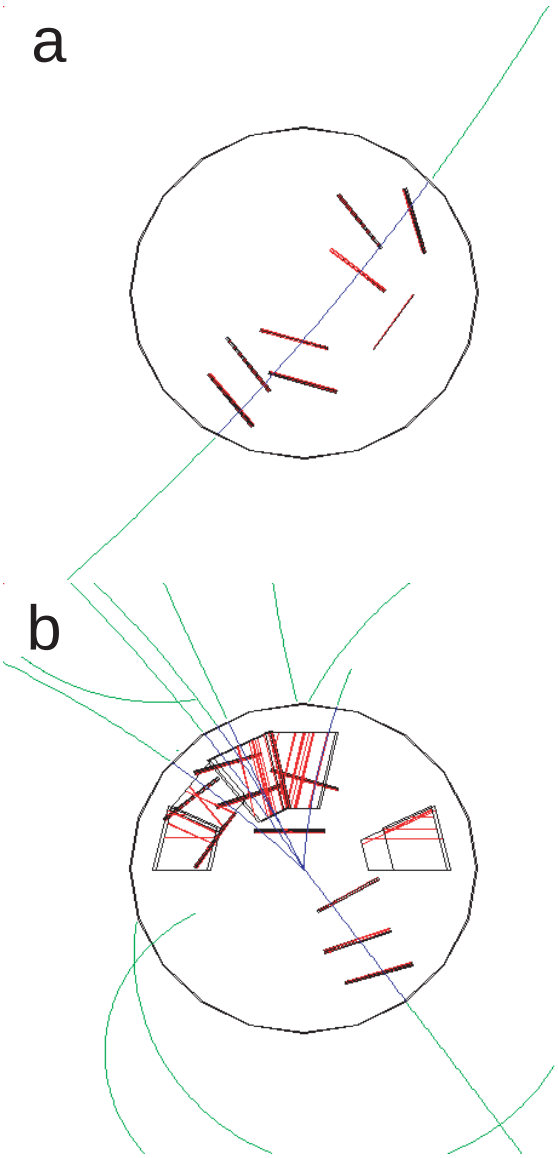

Figure 8.5: *(a) A cosmic ray muon reconstructed in the micro-vertex detector.(b) A typical Monte Carlo neutral current deep inelastic scattering event.*

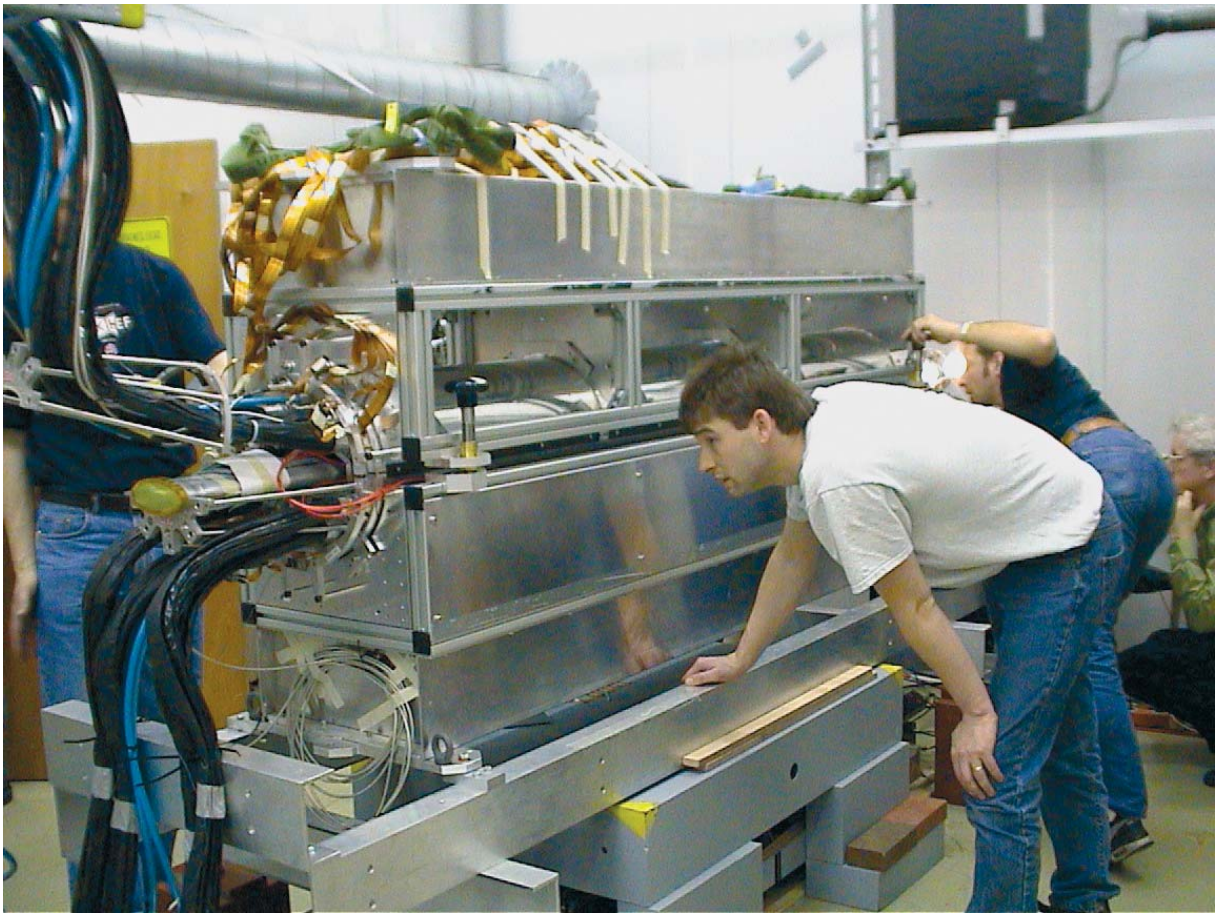

The two detector halves of the ZEUS vertex detector are 'mated' for the very first time.

B LEP in 2001

1 DELPHI

1.1 End of data taking and reprocessing

The DELPHI detector stopped data taking on the 2^{nd} of November 2000. The dismantling of the two end-caps and a large fraction of the Barrel Muon Chambers started the end of that month and was completed end of May 2001. The other part of the detector and some of its muon chambers remain in pit 8 and serve as a permanent exhibition for visitors.

The final reprocessing of all LEP2 data taken in 1997-2000, using the latest detector calibrations, alignments and the final version of the reconstruction software, was started on June 1^{st} and continued until September 21^{st}. The reprocessing of the much smaller sample of 1996 data was done during the first week of November. In addition, about 170 million Monte-Carlo events have been generated in 2001.

1.2 Selected research topics

A total of 18 papers were published in physics journals by the DELPHI Collaboration in 2001. Fifty papers were submitted to the EPS Conference in Budapest and to Lepton Photon 2001 in Rome, of which 12 contributions were based exclusively on LEP1 data and 38 on LEP2 data.

The NIKHEF group contributed to B and τ physics, W physics and Triple Gauge Couplings (TGC's), measurement of the ZZ cross section and to the Higgs search. Two PhD theses were completed: one on kaon production in τ decays and one on the measurement of the W boson mass.

Four studies by our NIKHEF group, will be discussed here.

1.3 $B^0_d - \overline{B^0_d}$ oscillations

Neutral B meson oscillations were studied using a total sample of about 4.0 million hadronic Z decays registrated by the DELPHI detector between 1992 and 2000.

In the Standard Model, $B^0_d - \overline{B^0_d}$ mixing is a direct consequence of second order weak interactions. Starting with a B^0_d meson produced at time t=0, the probability, $\mathcal{P}$, to observe a $\overline{B^0_d}$ decaying at the proper time t can be written, neglecting effects from $\mathcal{CP}$ violation:

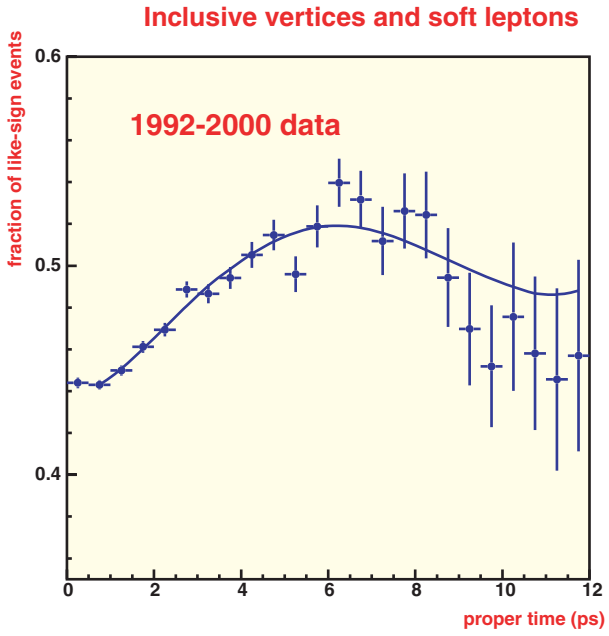

Figure 1.1: *Fraction of like sign events as a function of the reconstructed proper time. The points with error bars correspond to the data, the continuous line to the fit result.*

$$\mathcal{P}(B^0_d \to \overline{B^0_d}) = \frac{\Gamma_d}{2} e^{-\Gamma_d t}[\cosh(\frac{\Delta\Gamma_d}{2}t) + \cos(\Delta m_d t)].$$

Here $\Gamma_d = \frac{\Gamma^H_d + \Gamma^L_d}{2}$, $\Delta\Gamma_d = \Gamma^H_d - \Gamma^L_d$, and $\Delta m_d = m^H_d - m^L_d$, where H and L denote respectively the heavy and light physical states.

The width difference $|\Delta\Gamma_d|/\Gamma_d$ is expected to be much smaller than 0.01. The mass difference Δm_d is proportional to CKM matrix element $|V_{td}|^2$.

In the analysis a sample of 155k soft leptons, i.e. identified electrons and muons with a transverse momentum of less than 1.2 GeV/c, and a sample of 615k inclusively reconstructed secondary vertices were selected.

From the flight distance and the estimated momentum, the reconstructed proper time was determined. At the Z pole $b\bar{b}$ quark pairs are produced back to back. The event is separated into two hemispheres where the b or $\bar{b}$ charge was estimated from several discriminating

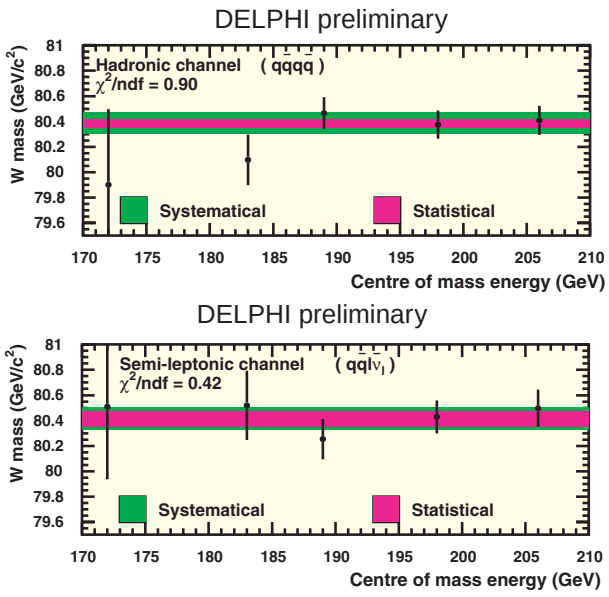

Figure 1.2: *Fitted W mass as a function of the centre-of-mass energy in the fully-hadronic (top) and semi-leptonic (bottom) WW decay channels. The statistical and systematic components of the combined W mass uncertainty are shown, where the shaded areas are proportional to the ratio of the squares of the two component errors.*

variables. Events that mix will lead to a like-sign ($++$ or $--$), while unmixed events give an unlike-sign ($+-$ or $-+$) charge combination.

The mass difference between the two physical states in the $B_d^0 - \overline{B_d^0}$ system was determined by fitting the fraction of like-sign tagged events as a function of the reconstructed proper time t as shown in Fig. 1.1. The preliminary result is:

$$\Delta m_d = (0.531 \pm 0.025\ (\text{stat}) \pm 0.007\ (\text{syst.}))\ \text{ps}^{-1}.$$

In the fit also the width difference between the heavy and light state was a free parameter. Using the measured B_d lifetime $\tau_{B_d} = (1.55 \pm 0.03)$ ps, $|\Delta\Gamma_{B_d}|/\Gamma_{B_d} = 0.00 \pm 0.09\,(tot)$. The following preliminary upper limit was derived:

$$|\Delta\Gamma_{B_d}|/\Gamma_{B_d} < 0.15 \text{ at } 90\% \text{ CL}.$$

The measurement of Δm_d is the single most precise measurement of this quantity at LEP. It is compatible with the present world average of $\Delta m_d = 0.496 \pm 0.007\ \text{ps}^{-1}$. It provides a precise estimate of the fundamental CKM matrix element $|V_{td}|$ and a test of the Standard Model. The measurement of the width difference is currently the best in the world. It will take some time before the B factories will measure this quantity more precisely. This measurement is an important test of our understanding of the B_d meson, as Heavy Quark Effective Theory predicts the relative width difference to be less than 0.01.

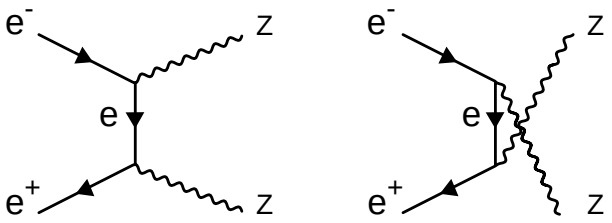

Figure 1.3: *The NC02 diagrams describing ZZ boson pair production.*

1.4 W mass and width

Preliminary values for the mass and width of the W boson using all data collected in 1996-2000 were obtained:

$$\begin{aligned} M_W &= 80.401 \pm 0.045\ (\text{stat}) \pm 0.034\ (\text{syst}) \\ &\pm 0.029\ (\text{FSI}) \pm 0.017\ (\text{LEP})\ \ \text{GeV}/c^2 \end{aligned}$$

$$\begin{aligned} \Gamma_W &= 2.109 \pm 0.099\ (\text{stat}) \pm 0.057\ (\text{syst}) \pm \\ &0.042\ (\text{FSI})\ \ \text{GeV}/c^2 \end{aligned}$$

where FSI represents the uncertainty due to final state interactions. The W mass results for each of the WW decay channels obtained at the different centre-of-mass energies are fully compatible, as can be seen in Fig. 1.2. Work is in progress to improve on the understanding of the systematics.

1.5 ZZ cross section

At centre-of-mass energies above 182.3 GeV two Z bosons can be produced according to the NC02 processes shown in Fig. 1.3. Because the Z can decay into quark-antiquark (q) or lepton-antilepton (l or ν) pairs five main final states can be analysed: $q\bar{q}q\bar{q}$, $l^+l^-q\bar{q}$, $\nu\bar{\nu}q\bar{q}$, $\nu\bar{\nu}l^+l^-$ and $l^+l^-l^+l^-$ where $l = e, \mu, \tau$. The NIKHEF group contributes to the analysis of the more abundant four quark final state. By using a probabilistic technique to combine several discriminating variables, the large background in the four quark channel

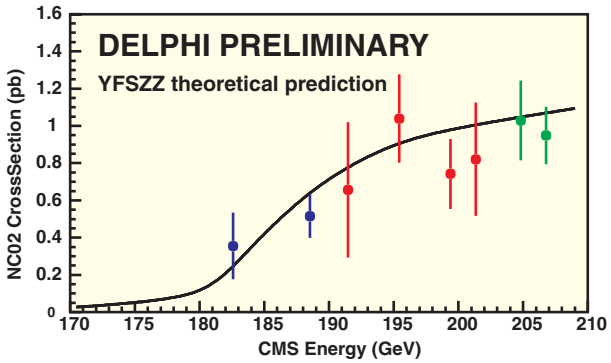

Figure 1.4: *The ZZ cross section as a function of the centre-of-mass energy. The points with error bars correspond to the data, the solid line to the Standard Model prediction.*

- from WW and $q\bar{q}\gamma$) events - can be suppressed and an average signal purity of about 50% is reached. The selection efficiency is about 34%. The preliminary results for the NC02 ZZ cross section as a function of the centre-of-mass energy using all the channels is shown in Fig. 1.4. The Standard Model prediction using the YFSZZ generator is shown as a solid line. The results are compatible with the Standard Model prediction and limits on non-Standard Model γZZ and ZZZ couplings will be derived.

1.6 Flavour blind Higgs search

The results of the search for the Standard Model Higgs were published in 2001 and a lower limit on the mass of the Standard Model Higgs boson of 114.3 GeV/c^2 was set.

An analysis was started to search for a Higgs decaying hadronically but not necessarily into $b\bar{b}$ quarks. In the so-called flavour blind search, one is looking for a Higgs decaying into a quark-antiquark pair or gluons. It was assumed that the Higgs is produced as in the Standard Model, i.e. through Higgsstrahlung with an associated Z. The search is motivated by Supersymmetric Theories where the Higgs decay into $b\bar{b}$ quarks can be strongly suppressed and the Higgs decays e.g. predominantly into gluons.

Final states with the Z decaying into quarks or leptons were selected. By applying a mass constraint on the Z decay products and the H decay products, the probability of an event to be compatible with a ZH decay is calculated. By combining this information with other discriminating variables a combined variable was constructed. Using simulation, the efficiency of the analysis for Higgs decays into different quark pairs or gluons was estimated as a function of the Higgs mass.

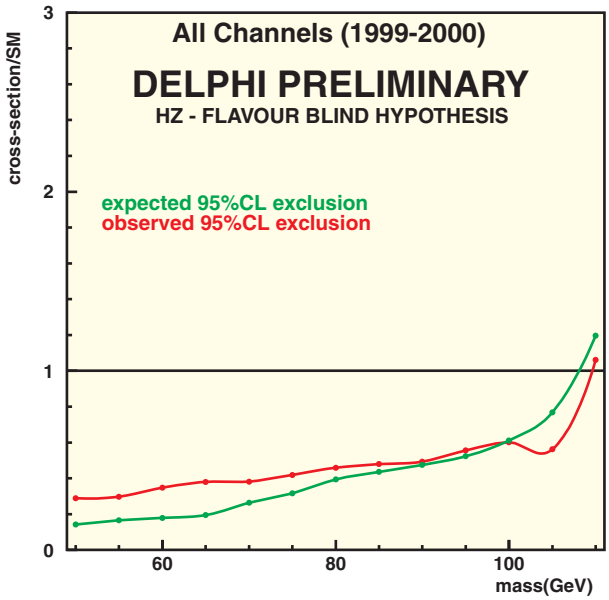

Figure 1.5: *Expected and observed upper limits on the production cross section of a flavour blind Higgs as a function of the Higgs mass.*

The combined results are summarised in Fig. 1.5. The observed and expected upper limit at 95% CL on the production cross section divided by the Standard Model Higgs cross section are shown as a function of the Higgs mass. A more model independent - preliminary - lower limit on the Higgs mass was put at 109.9 GeV/c^2.

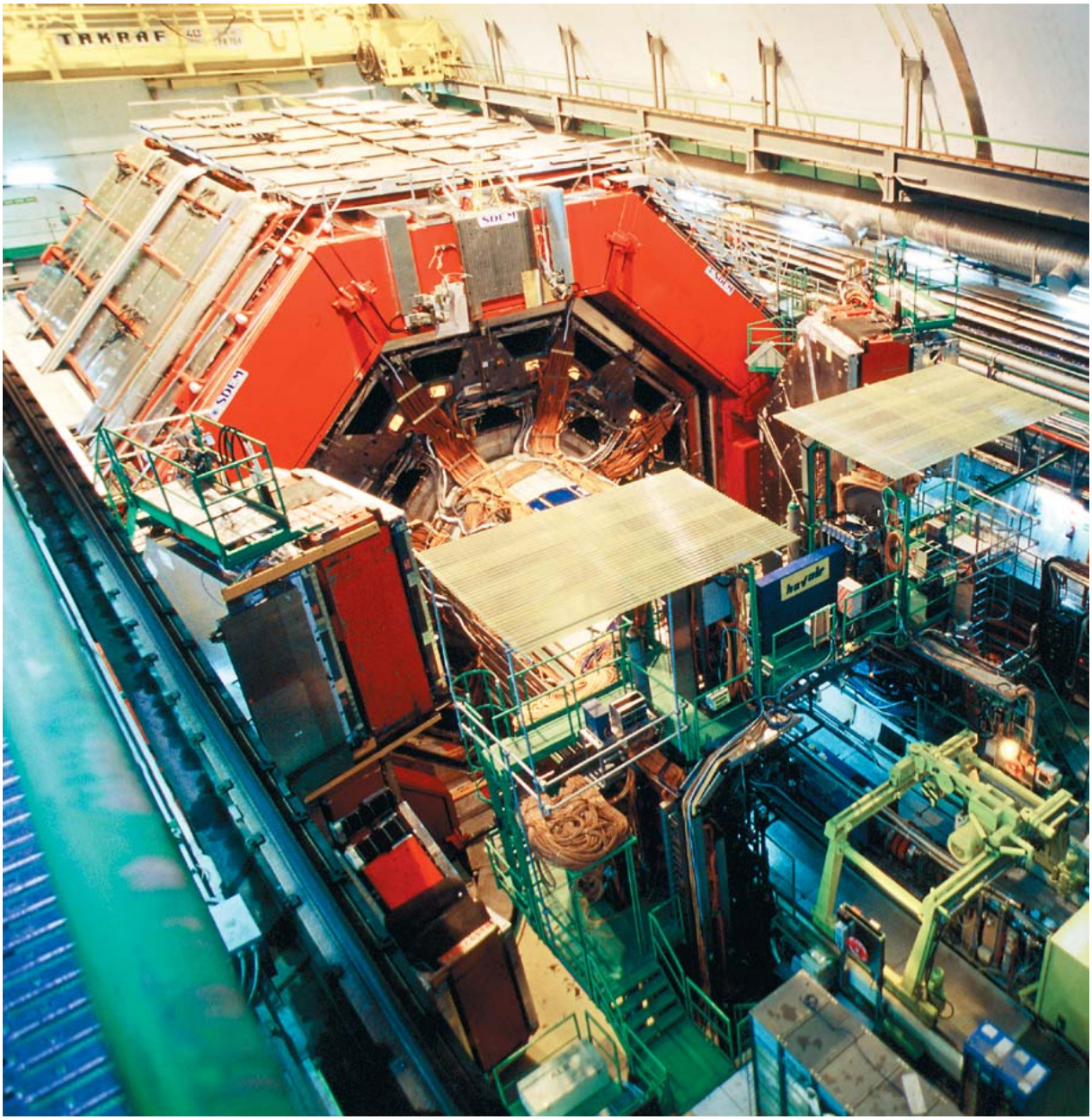

The L3 detector at the 'old LEP' accelerator.

2 L3

2.1 Introduction

L3 was a general purpose detector designed with good spatial and energy resolution to measure electrons, photons, muons and jets produced in e^+e^- reactions.

After the decision to close LEP, the L3 detector was dismantled at the beginning of 2001, ending the period of yearly data-taking which began in 1989. This also meant the end of its detection of cosmic ray muons. However, the air shower array above L3 continued to take data.

With no possibility of more data, the collaboration's publication policy shifted toward final rather than interim publications. As a result only 15 papers were published in 2001, compared to 27 in 2000. There were, as usual, a large number of contributions to conferences, e.g., 46 to the EPS Conference on High Energy Physics in Budapest, Hungary. The collaboration expects the analysis of the L3 data sample to last at least until the end of 2003.

At the end of 2000, 11 Ph.D. students in the Netherlands were analysing L3 data. NIKHEF physicists (including those from NIKHEF partners universities of Amsterdam and Nijmegen) contribute primarily to analyses of the mass and couplings of the W-boson; QCD, in particular multiplicity correlations and Bose-Einstein correlations (BEC); two-fermion production, in particular τ pairs; searches for the Standard Model Higgs; ZZ production; charm and bottom production in two-photon collisions; and studies of the cosmic ray muon flux. Three Ph.D. theses were defended in 2001 on the subjects of τ-pair production, resonance production in two-photon collisions, and the cosmic ray muon spectrum.

As in previous years, the computer farm in Nijmegen contributed a large fraction of the L3 Monte Carlo event production, accounting for more than 40 million events.

2.2 Searches

In the Fall of 2000, the LEP experiments, in very preliminary analyses seemed to have a small excess of events, suggesting the Higgs boson with a mass of around 115 GeV. The final analysis of the data was therefore eagerly awaited. The final L3 analysis was published in 2001 and gave a lower limit on the Higgs mass: $m_H > 112\,\text{GeV}$ at 95% confidence level. The confidence levels as function of Higgs mass hypothesis are shown in Fig. 2.1.

Apart from the Higgs, the only particle of the Standard Model not yet discovered, searches were performed for particles which occur in various extensions of the Stan-

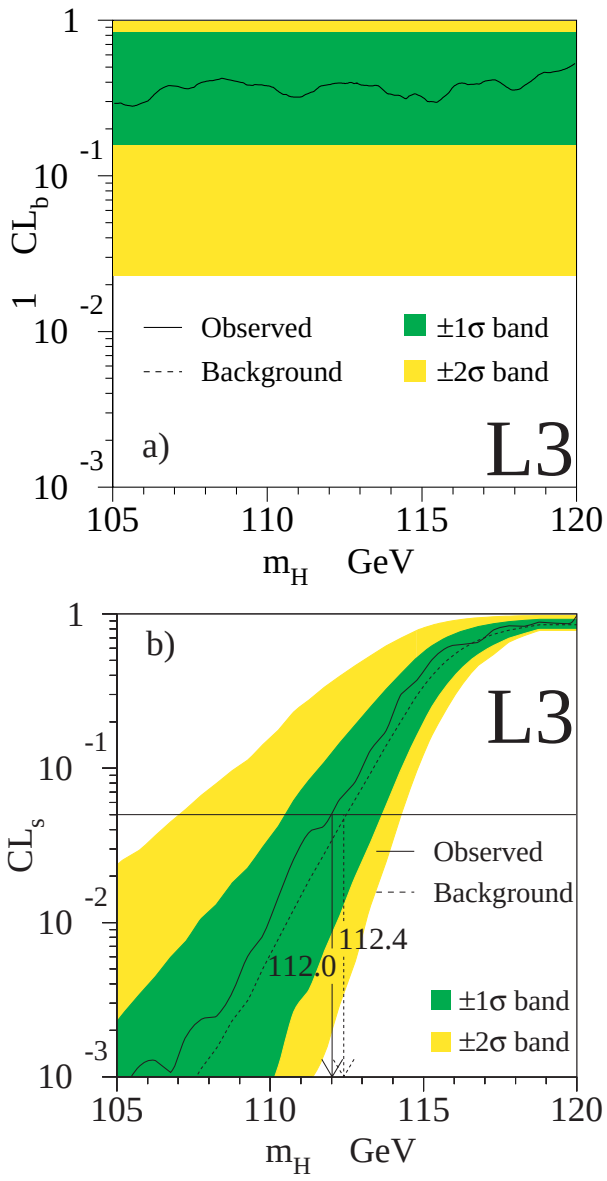

Figure 2.1: *(a) The background confidence level $1-CL_b$ and (b) the signal confidence level CL_s, as a function of the Higgs mass hypothesis, m_H, for all channels combined. The solid line shows the observed value. The dashed line shows the median expected value in a large number of simulated "background only" experiments.*

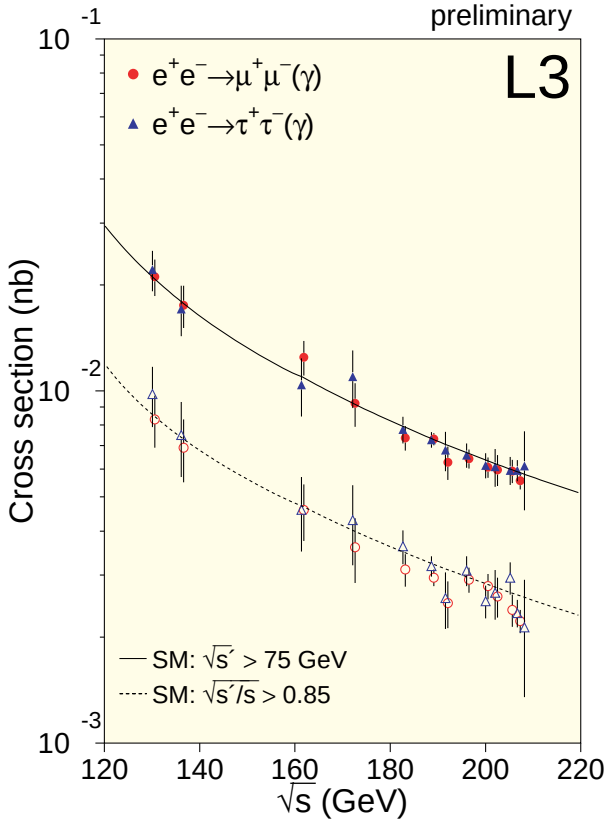

Figure 2.2: *Cross section as a function of centre-of-mass energy for μ- and τ-pair production compared with the predictions of the Standard Model.*

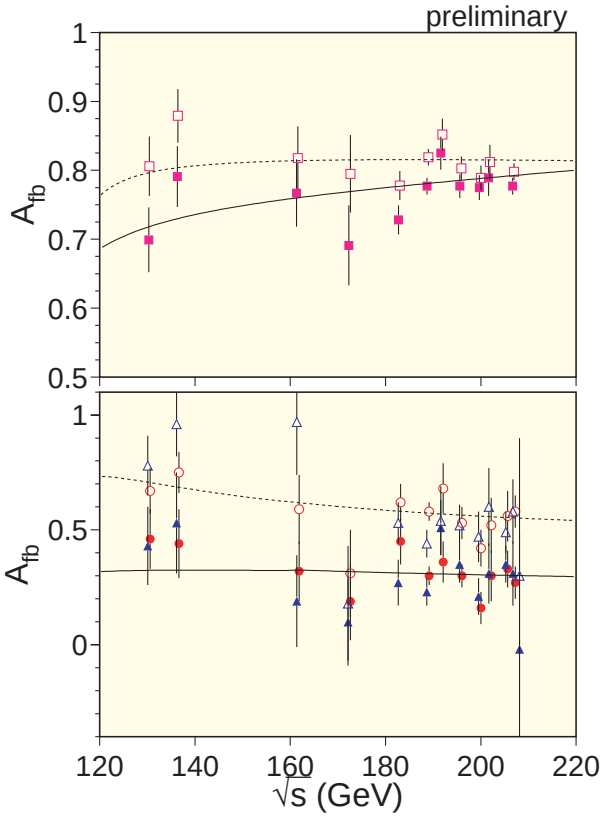

Figure 2.3: *Forward-backward asymmetries as a function of centre-of-mass energy for* e- *μ- and τ-pair production compared with the predictions of the Standard Model.*

dard Model. Supersymmetric particles were searched for in many different channels and kinematic regions. No signal was observed and in many channels limits corresponding to the allowed kinematic phase space were established. Besides supersymmetric particles, searches were performed for "exotic" leptons, e.g., "sequential," vector, and "mirror" leptons and heavy isosinglet neutrinos. In all cases limits were set on their existence.

2.3 Fermion pairs

Apart from the lack of the Higgs boson, the Standard Model continues to agree well with the results from LEP. An example is fermion pair production, where cross sections and forward-backward asymmetries agree well, as shown in Figures 2.2 and 2.3. These results are used to place limits on several scenarios for "new physics." For example, the scale of quantum gravity in theories with extra dimensions must be above about 1 TeV.

2.4 W physics

One of the main goals of the LEP programme is the measurement of the properties of the W-boson. In total some 10000 $e^+e^- \to W^+W^-$ candidate events have been selected.

The measured cross section for $e^+e^- \to W^+W^-$ as a function of $\sqrt{s}$ is found to agree well with the Standard Model, as do the branching fractions of the W.

The differential production and decay cross sections of W-bosons, as well as their total production cross section, are used in fits to determine the WWZ and $WW\gamma$ couplings. These results are combined with information on W couplings obtained from analyses of single W production, $ee \to We\nu$, and single photon production, $ee \to \nu\nu\gamma$. The self-coupling between the electroweak vector bosons in the WWZ and $WW\gamma$ vertices plays a crucial role in the gauge structure of the Standard

Model. Experimental tests of these couplings are sensitive to new physics beyond the Standard Model. Preliminary results find these couplings in agreement with the Standard Model predictions and limits have been set on anomalous contributions.

The cross section for the process $e^+e^- \to W^+W^-\gamma$ has been measured for isolated, energetic photons in the detector. This channel is sensitive to quartic gauge couplings of the type $WWZ\gamma$ or $WW\gamma\gamma$. The measured cross section agrees with the Standard Model prediction, and limits have been set on anomalous contributions to these quartic couplings.

From the joint decay angular distributions of W-pairs, the fractions of the different helicity states and their correlations are measured.

CP conservation demands that the fraction of W^- bosons in a given helicity state be equal to the fraction of W^+ bosons in the opposite helicity state. This has been verified experimentally and constitutes another test of the Standard Model.

In addition, correlations between the helicity of the W^- and the W^+ in a given event have been measured to agree with the Standard Model prediction.

The W mass and width are measured using a fit to the invariant mass spectrum of W decay products. Events are reconstructed into four jets ($q\bar{q}q\bar{q}$ events), or two jets, a lepton (or τ "jet") and a missing momentum vector identified with an undetected neutrino ($q\bar{q}\ell\nu$ events). A kinematic fit is applied to the measured event, demanding energy- and momentum-conservation. The combined invariant mass spectrum is shown in Fig. 2.4. The W mass and width are extracted using an unbinned maximum likelihood fit by reweighting a fully reconstructed Monte Carlo sample. These measurements are compared in Fig. 2.5 with the SM expectation calculated using the world-average value of M_W. Good agreement is observed.

The dominant systematic uncertainty on the measurement of the W mass and width in the four-quark channel arises from theoretical uncertainty on two QCD effects. One is the amount and nature of colour flow between gluons arising in the hadronisation of the $q\bar{q}$ from one W, *e.g.*, $W^- \to d\bar{u}$, and those from the

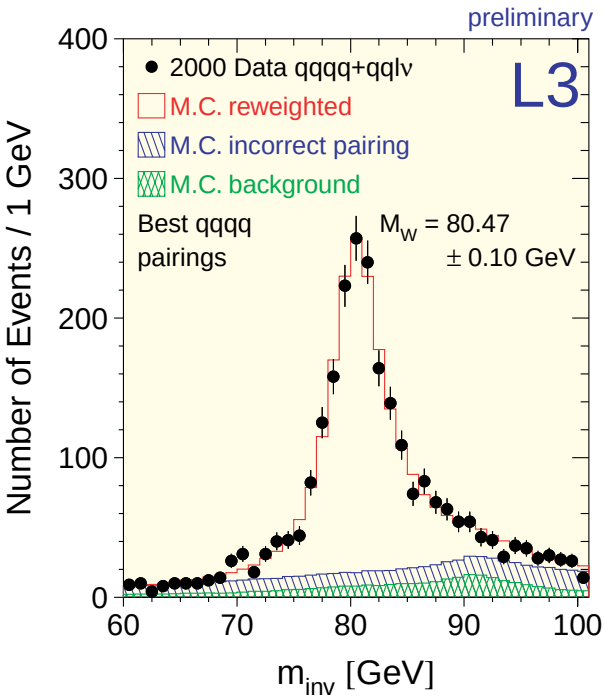

Figure 2.4: *The W-mass distribution, from which the mass and width of the W boson are extracted.*

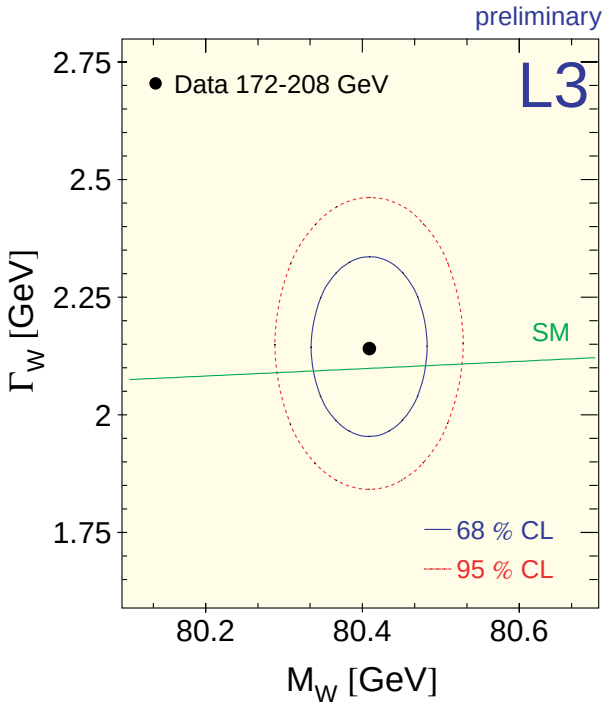

Figure 2.5: *The measured value of the mass and width of the W boson compared to the Standard Model expectation.*

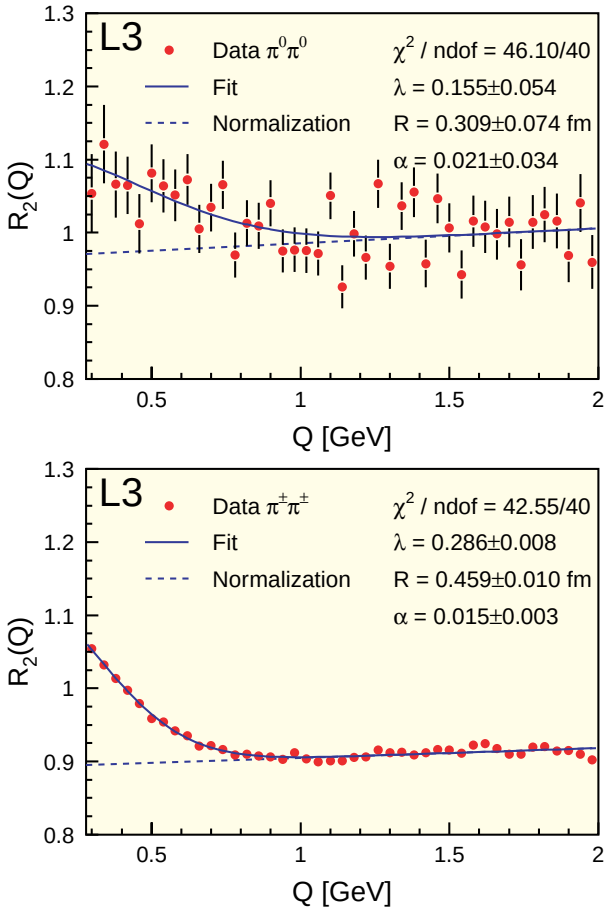

Figure 2.6: *The BEC correlation function R_2 as function of the four-momentum difference between the pions for neutral and like-sign charged pions. The data are fitted to a Gaussian parametrisation.*

other W, *e.g.*, $W^+ \to \bar{s}c$. This is usually referred to as colour reconnection. The other effect is BEC between identical bosons from different W bosons.

Both of these effects have been intensely studied. Preliminary results have ruled out the most extreme models of these effects, indicating that the systematic uncertainties on the W measurements will be smaller than feared. Work is ongoing to reduce these uncertainties to the minimum.

Another source of systematic uncertainty is the modelling of hadronisation in the Monte Carlo programmes, both in the hadronisation of $W \to q\bar{q}$ and in $e^+e^- \to q\bar{q}$, which forms an important background to $e^+e^- \to W^+W^-$.

2.5 QCD

Stimulated by the need for better understanding of various QCD effects in order to reduce systematic uncertainties on W-boson results, several investigations were pursued using the very high statistics Z-decay data previously (1989–1995) collected.

For the first time in e^+e^- interactions, the BEC of neutral pions were compared to those of like-sign charged pions. It was found (see Fig. 2.6) that the size of the source of neutral pions is somewhat smaller than that of charged pions: $R_0/R_{\pm\pm} = 0.67 \pm 0.16 \pm 0.15$.

Also, the BEC among three identical charged pions is being investigated. From the correlation functions for genuine three-particle BEC and for two-particle BEC one can investigate the degree of incoherence of the pion emission. Preliminary results found the data consistent with completely incoherent production of the pions. Further, work continued on the investigation of various parametrisations of BEC and on their implementation in Monte Carlo programmes.

2.6 L3+Cosmics

Understanding of the systematic uncertainties on the measurement of the cosmic ray muon spectrum and on the charge ratio of this spectrum has increased considerably. The final measurement is expected in 2002.

The analysis of the data from the air shower array on top of the L3 building is maturing. Combination of the air shower array information with the number of muons observed in the L3 detector yields, through use of an air shower simulation programme (CORSIKA), information on the primary cosmic ray composition. Very preliminary results suggest a larger amount of iron than previously thought.

A search is being performed for an excess of muons in the L3 detector which are correlated in time and direction with gamma ray bursts observed by the BATSE satellite. Preliminary results show no excess of muons.

C Theoretical Physics

1 Theoretical Physics Group

1.1 Particles, fields and symmetries

Theoretical physics provides the mathematical description of the properties and interactions of subatomic particles. These include quarks and leptons (e.g. electrons and neutrinos), as well as field quanta like photons for the electro-magnetic field, and gluons for the colour field of the strong interactions. The electric forces bind electrons to nuclei, whilst the colour forces are responsible for keeping together the quarks inside the nucleon. Furthermore the weak forces, mediated by heavy field quanta known as massive vector bosons (W and Z), induce radioactive transmutations, notably the β-decay of the neutron and the muon.

The general framework for the description of the subatomic particles and their interactions is quantum field theory. It provides a universal scheme for computations of particle scattering and decay, for determining the properties of multi-particle and bound states, as well as for studying collective phenomena such as symmetry breaking and phase transitions; an example of the latter is the transition from a hadron gas to a quark-gluon plasma expected to take place at extremely high temperatures.

Present developments in quantum field theory relate to increased understanding of the mathematical structures involved, as well as to their application to the analysis and prediction of experimental results. In addition to experiments at particle accelerators, the applications of quantum field theory and particle physics to cosmology and high-energy astrophysics is of increasing importance.

1.2 Research program

The research program of the NIKHEF Theoretical Physics Group covers several aspects of quantum field theory, string theory and their applications to the physics of subatomic particles.

QCD

The strong forces acting on particles with colour-charges, notably quarks and gluons, determine the structure of hadrons. All of their interactions, including the electroweak interactions, are affected by the hadronic environment in which they live. To estimate reliably the cross sections for production of particles like top quarks or Higgs scalars in proton-proton collisions, a good understanding of this hadronic structure is a prerequisite. The precision of the experimental data requires QCD-effects to be evaluated to a very high accuracy. Powerful techniques for computing QCD-effects to third order in the coupling constant α_s have been developed at NIKHEF by Dr. J.A.M. Vermaseren and co-workers. Estimating the cross sections and rates for the production of top-quarks and Higgs particles is part of the research program of Prof. E. Laenen. These studies include analytic methods, like the resummation of large logarithmic contributions, as well as numerical simulations of certain types of events using Monte-Carlo methods.

A new initiative has been taken to develop a set of parton-distribution functions accurate to order α_s^3 in perturbation theory, in which Prof. E. Laenen en Dr. J.A.M. Vermaseren cooperate with Dr. A. Vogt and colleagues from experimental groups.

Quarks and gluons at finite temperature

In the collisions of heavy ions, such as lead on lead, at very high energies, the large number of particles involved in the process allows for a thermodynamic treatment. There is good reason to believe that the energy distribution over the different particles involved is of a thermal nature. The reaction times are very short compared to the duration of the ion-collision itself, allowing equilibrium to be established. Therefore, one can assign a well-defined temperature to the gas of hadrons, or possibly the plasma of quarks and gluons, which is formed in the collision. Prof. J.H. Koch and co-workers study the effects of finite temperatures on the structure of hadrons. As a first step they have undertaken to determine the temperature dependence of the form factor of the pion and the rho-meson. As also input from lattice gauge theory is required, they have initiated a collaboration with the university of Bielefeld (Germany), where the necessary expertise is available.

Supersymmetry

Supersymmetry relates the properties of bosons with those of fermions. In field theories with an exact supersymmetry the masses and charges of bosons and fermions are equal. If supersymmetry is broken in a self-consistent way, the masses of these particles may be-

come different although their charges remain the same. Supersymmetric versions of the standard model exist, but depend on a large number of free parameters. This number can be greatly reduced in the context of unification of the electro-weak and strong interactions.

Non-standard scenarios for superunification are developed at NIKHEF by Prof. J.W. van Holten and co-workers. Consistency conditions from quantum field theory have been incorporated, and allow for models with interesting phenomenological properties, including an explanation of charge quantisation.

Superstring theory

In string theory the point-like nature of elementary objects and field quanta is abandoned in favour of an extended object of finite length in one dimension. Point particles may be associated with such strings as viewed on scales much larger than the string length. However, more recently it has also become clear that one may associate point particles in a D-dimensional space with the endpoints of strings living in additional dimensions. These dimensions are not visible from the restricted D-dimensional space-time in which the end point of the string can move, although they may be probed by gravitational effects. This development has resulted in a theory of D-branes, D-dimensional objects in which the end points of open strings can live. The notion of D-branes has become an important tool in elucidating non-perturbative effects in string theories. At NIKHEF Prof. A. Schellekens studies the interplay between such non-perturbative string dynamics and the perturbative dynamical behaviour of strings described by conformal field theories on their two-dimensional world surface.

Gravity

Gravity and cosmology have become intimately linked with particle physics. The behaviour of particles in strong gravitational backgrounds, such as black-hole or gravitational wave fields, is part of the research program of Prof. J.W. van Holten and co-workers. A recent new line of investigation in relativistic hydrodynamics and its supersymmetric generalisation has been opened up.

1.3 Teaching

In addition to the research described above, the Theoretical Physics Group is also involved in teaching, both in house and at the partner universities, and in the organisation of schools and conferences. In 2001 Dr. E. Laenen was appointed ordinary professor of theoretical physics at the university of Utrecht. Prof. J.W. van Holten was responsible for the organisation of the winterschool in theoretical high-energy physics of the Dutch Research School of Theoretical Physics (DRSTP) in Nijmegen (January 2001). Prof. J.H. Koch participated in the organisation of the international Belgian-Dutch-German summerschool on experimental high-energy physics in October 2001.

D Technical Departments

1 Computer Technology

1.1 Introduction

NIKHEF invested a total amount of 3.5 million NLG in the computer- and network infrastructure in the years 2000 and 2001. A global idea on how this money was spent is presented in figure 1.1. Apart from the upgrades of the server and network infrastructure and the replacement program for desktops, a major upgrade was performed of the hardware and software for the CAD workstations of the engineering groups of the electronic and mechanical departments. Compute nodes and server systems were installed to increase the capacity of farm resources for the LHC experiments.

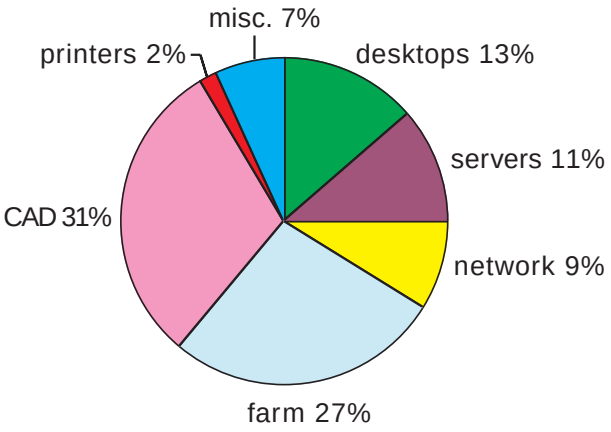

Figure 1.1: *Computer investments 2001-2002*

Some examples of contributions from the CT engineering group will be presented below.

1.2 Central services

In the course of the year 2001 essential services were migrated from the two Sun SPARCserver 1000 systems *gandalf* and *park* to the new server *ajax*. This Sun Enterprise server 3500 is linked with a gigabit adapter to the network backbone and is configured with three RAID disk arrays with a total gross storage capacity of 1.2 TB. High quality file services are available for home and project directories. This file service provides NFS version-3 protocol to serve the Unix clients and CIFS protocol to serve Microsoft Windows clients. Miscellaneous networks services, such as DNS, NIS, DHCP, RARP and Radius authentication for the dial-in server were migrated to the *ajax* server.

The backup for the home and project directories on the Unix server *ajax* and the Windows-NT server *paling* has been outsourced to the SARA ADMS backup services. During the nocturnal hours the data of the incremental backups is transported through the WTCW campus network to the tape robot at SARA. By the end of the year 2001 the total amount of file storage on the robot contained 1 TB of data.

In the fourth quarter of 2001 a Xerox 2135 laser printer was installed.

1.3 Network infrastructure

In the first quarter of this year an upgrade of the internal local area network was realised. Stackable switches with a port capacity of 100 Mb/sec and a gigabit uplink replaced switches with a port capacity of 10 Mb/sec. All desktop systems (with the exception of systems connected to the *guestnet*) are connected to the gigabit backbone with a 100 Mb/sec link. Most of the server systems are connected directly to the backbone through a link with a capacity of 1 Gb/sec. For this reason an additional blade with eight gigabit ports was installed in the backbone switch. This switch is the very same device as the *hefrouter* that connects the NIKHEF local area network to the outside world by means of a 2 Gb/sec link to the WTCW campus network and a 1 Gb/sec link to our internet service provider SURFnet. SURFnet-5 became operational in October 2001. SURFnet-5 offers a high-capacity connection to

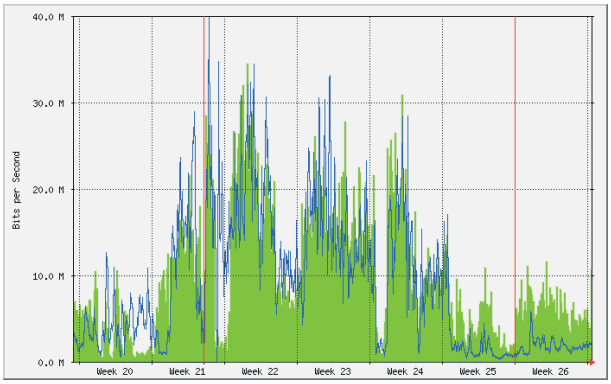

Figure 1.2: *The network traffic between NIKHEF and SURFnet during a typical period.*

desktop system	number	remark
Windows (98/NT/2000)	175	including instrumentation systems
Linux	150	excluding farm systems
Other Unix (Sun, HP, SGI)	40	

Table 1.1: *Overview of the number of desktop systems for several operating systems.*

its users in the Netherlands and it operates a backbone with a capacity of 80 Gb/sec, a state of the art infrastructure. Figure 1.2 presents the amount of network traffic between NIKHEF and SURFnet for a typical period.

To be able to offer more flexibility in case of meetings and workshops and to overcome a shortage of fixed network connections on certain places in the NIKHEF buildings, the basic components for a wireless network infrastructure were installed. This service will be limited to connect laptops to the *guestnet* segment of the local area network.

1.4 Security

Special attention was given this year to the protection of the NIKHEF computers and services against hazardous attacks from the internet. Given the facts that the number of users and systems on the internet are increasing rapidly and that our connectivity to the internet is very good, it was not surprisingly to notice that the number of attempts from non-authorised users to enter our network increased significantly. Measures were taken to prevent these attacks as much as possible.

1.5 Desktop systems

Table 1.1 presents a summary of the number of desktop systems for each platform (no server systems included). New systems installed run in most cases Microsoft Windows-NT / -2000 or Linux Red Hat version 6. Almost all new systems are commodity PC's. A total of 110 new desktop systems were installed this year. Note that this is an average of more than two systems per week (excluding server and farm systems!). Remarkable is that about 40% of these systems concerned new network connections, without trading in the obsolete systems.

Procedures were simplified as much as possible, to minimise the time spent on system installations. E.g. for the installation of Windows-2000 one can install a *ghost image* which includes not only the system itself, but also some standard applications, such as Microsoft Office. The aim is to develop scripts for the automation of system upgrades of Windows and Linux systems to decrease the effort spend on the maintenance of a large number of systems.

As a result of a market survey and extensive benchmarking, the Sun Blade workstations were selected to replace the SGI and HP workstations of the engineering groups of respectively the mechanical and electronic departments.

1.6 Farm configurations

There is an increasing interest of our scientific users to use stacks of standard PC's, running some Linux version and interconnected in a private segment of the network. Such a 'farm' consists of regular compute nodes and server systems for management and file server purposes. A farm consisting of 50 dual-processor DELL PC's was setup in the year 2000 to generate Monte-Carlo events for the D0 experiment. This year more farms were installed to solve the computing needs of the LHC experiments LHCb and ALICE and as a prototype for the ANTARES DAQ system. For a more sophisticated use of this kind of compute and data storage resources, the European DataGrid project was started this year. In the second half of this year a number of farm nodes and associated server systems were integrated into the DataGrid testbed-1 prototype. Other sets of nodes and servers were exported to the LHCb group at the VU in Amsterdam and the D0 group at the KUN in Nijmegen.

For the new farms, we decided to configure and assemble rack-mountable PC's ourselves. For this purpose we selected the company JMS, specialised in building rack-mounted PCs for industrial purposes. Once the requirements were established, the components were ordered and built into a '2-Units' high chassis. A photograph of the result is shown in Figure 1.3. Each node contains a dual-processor Pentium III processor with a clock speed of 933 MHz, a gigabyte RAM, a 45 GB hard disk and a 100 Mb/sec ethernet adapter. 3-Com switches with 24 ports each and a gigabit back plane interconnect the nodes.

1.7 Amsterdam Internet Exchange (AMS-IX)

NIKHEF is one of the four locations of the Amsterdam Internet Exchange AMS-IX. This exchange is one

Figure 1.3: *Rack-mountable farm node*

of the largest exchanges in Europe in terms of number of customers (120) and the amount of network traffic (4 Gb/sec). The CT group is, in close collaboration with the technical facilities and financial departments at NIKHEF, responsible for the infrastructure at the AMS-IX location. In spite of the decreasing investments in telecom market, we decided that an extension of the location with another 60 racks could be justified. This implied a major upgrade of the power and cooling infrastructure as well. The extension of the AMS-IX location with 60 racks was ready to use for our customers in September 2001.

1.8 Software engineering

The software engineering group participates in the DataGrid project and in the ATLAS and ANTARES instrumentation projects. A selection of the software engineering contributions to the instrumentation projects is presented in the following sections.

1.9 ANTARES

In the ANTARES project standard industrial ethernet components and network protocols were selected for the transport of the event data from the front-end systems near the detector in the water to the on-line compute farms and data storage devices located in the shore station. A prototype of this data acquisition system was setup at NIKHEF for software development and system integration tests. To understand the behaviour of the flow in the detector network, we performed a simulation study of the data traffic pattern. The results predict a high level of packet loss due to repeated transmissions from many sources to one destination. In response, we

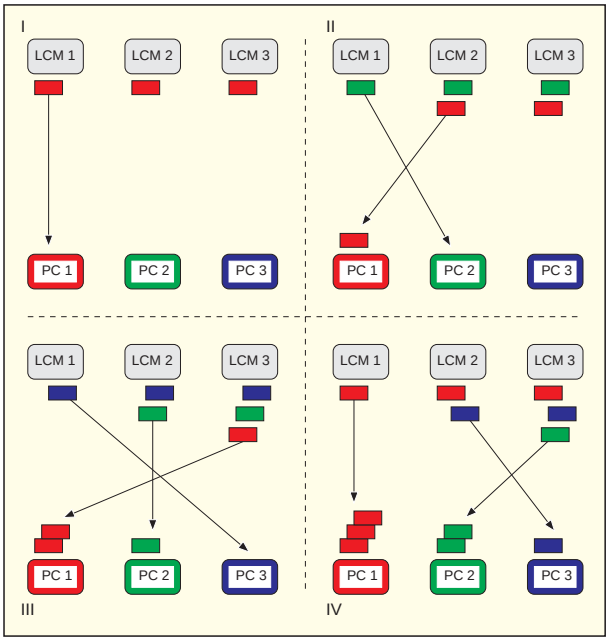

Figure 1.4: *Delayed transmission concept*

developed a delayed transmission method, which avoids packet loss by balancing the traffic more evenly through the network (Figure 1.4).

1.10 Embedded software for ATLAS hardware modules

In collaboration between hardware engineers from CERN and software engineers from NIKHEF a low-cost, low-power general-purpose microcontroller-based I/O-module has been developed for the ATLAS experiment, called ELMB (Embedded Local Monitor Board), see Figure 1.5. As the name suggests it is a *plug-on* board that can be embedded in other electronics systems. The ELMB has 64 analog inputs and 30 digital inputs/outputs and communicates to the outside world via a CAN field-bus. Two on-board 8-bit microcontrollers provide the local intelligence. Components have been selected and tested for better radiation-tolerance of the ELMB as a whole.

In the ATLAS experiment a few thousand ELMBs will be used for monitoring and control tasks throughout the detector. NIKHEF is one of the major users of the ELMB (ca. 1200 modules) because it has developed a monitoring subsystem for the ATLAS muon chambers based on the ELMB, so it took up the task of developing embedded software for the muon system as well as a more general application.

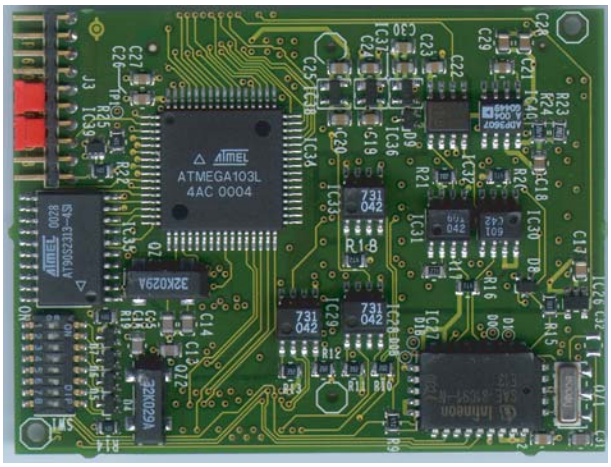

Figure 1.5: *A picture of the Embedded Local Monitor Board (ELMB). An I/O module developed for the ATLAS experiment.*

Although the various users of the ELMB often have different requirements, many aspects in the embedded software of the ELMB are in common, such as the communication functions for the CAN-bus using the *CANopen* protocol, the *in-system-programmability* (the ELMB can be reprogrammed in-situ via the CAN-bus), the automatic health-checks, configuration storage, etc. Special precautions have been built into the software to better withstand radiation effects (memory *bit-flips*), which otherwise easily crash a running program. The second onboard microcontroller has the important task of detecting such events (they still happen) and taking appropriate action.

NIKHEF has provided a fully operational general-purpose application program for the ELMB (for both microcontrollers) which can be used as-is, but users are free to change and add to this software, since the source code has been provided, as well as documentation. A few hundred ELMBs have produced so far and they are in use by several people in different test set-ups, not only by ATLAS, but also by several other experiments and CERN groups. A production series of 7000 is currently being prepared. The embedded software for the ELMB is being refined and extended.

1.11 Communication between Trigger/ DAQ and DCS in ATLAS

Within the ATLAS experiment, the Trigger/DAQ and DCS (Detector Control System) are both logically and physically separated. Nevertheless there is a need to communicate. The Trigger/DAQ DCS Communication (DDC) project should support the ability to:

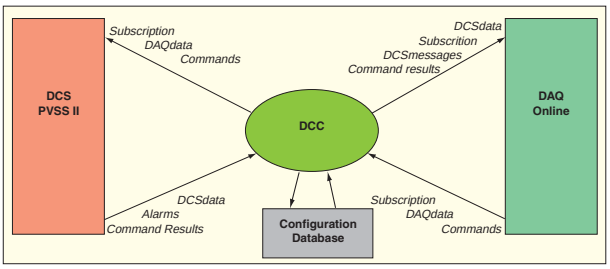

Figure 1.6: *DDC context diagram*

- exchange data between Trigger/DAQ and DCS;
- send alarm messages from DCS to Trigger/DAQ;
- issue commands to DCS from Trigger/DAQ.

Each subsystem is developed and implemented independently using a common software infrastructure. Among the various subsystems of the ATLAS Trigger/DAQ the Online is responsible for the control and configuration. It is the glue connecting the different systems such as data flow, level 1 and high-level triggers. The DDC uses the various Online components as an interface point on the Trigger/DAQ side with the PVSS II SCADA system on the DCS side and addresses issues such as partitioning, time stamps, event numbers, hierarchy, authorization and security. PVSS II is a commercial product chosen by CERN to be the SCADA system for all LHC experiments. Its API provides full access to its database, which is sufficient to implement the 3 subsystems of the DDC software. The DDC project adopted the Online Software Process, which recommends a basic software life-cycle: problem statement, analysis, design, implementation and testing. Each phase results in a corresponding document or in the case of the implementation and testing, a piece of code. Inspection and review take a major role in the Online software process. The DDC documents have been inspected to detect flaws and resulted in a improved quality. A first prototype of the DDC was ready and used in a test-beam set-up during summer 2001. Figure 1.6 shows the basic context diagram of the DDC package.

1.12 Applications for the production of ATLAS muon chambers

During the production of drift tubes for the muon chambers, many checks are performed to guarantee

high mechanical precision. These checks, involving quantities such as temperature and wire tension, are automated and implemented as LABVIEW applications using the CAN field bus as hardware interface. Also, a setup to measure, for 80 drift tubes simultaneously, the gas leak tighthness and the High Voltage behaviour over a period of several hours, was completely automated.

Most notably is the LABVIEW application that steers the gluing 'robot'. This machine is used to glue layers of 72 tubes laying on a granite table (2.5m $\times$ 5m) to a tube layer already on the muon chamber. The programme controls the various step-motors that move the machine and its gluing units and distribute the glue. After the operator has selected the appropriate operation via a graphical user interface, the process is started automatically and is continuously monitored by the software.

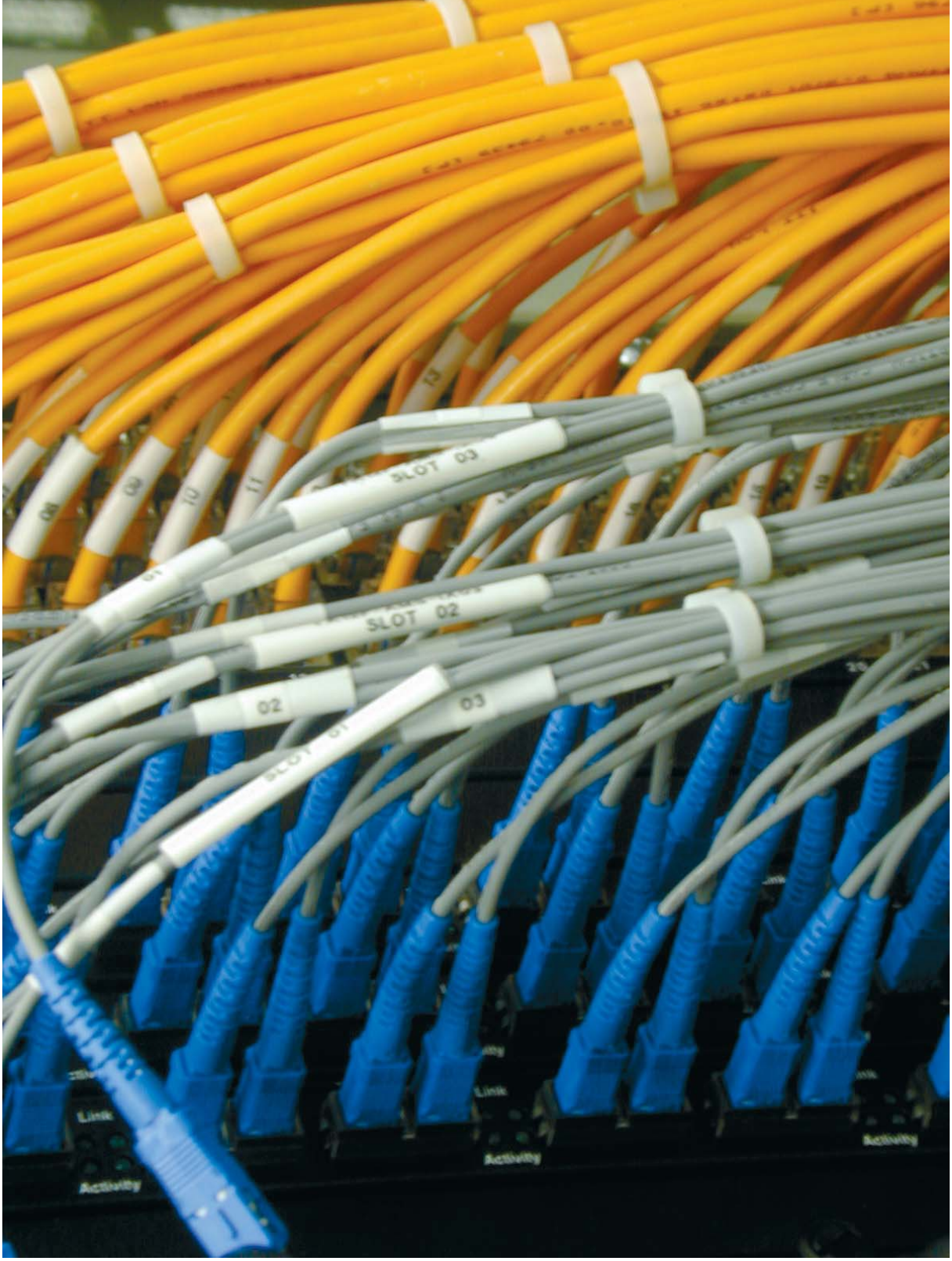

Cabling at the Amsterdam Internet Exchange.

2 Electronics Technology

2.1 Introduction

The work carried out by the Electronics Technology Group in 2001 was focused on three main subjects:

- Finalizing the components for and the installation of the Zeus microvector detector and the Hermes lambda-wheel detector. These detectors will become operational in 2002.
- Designing components and start prototype production for the LHC detectors at the Atlas, LHCb and Alice projects. For this prototyping the group provides support with high standard instrumentation like signal analysers, oscilloscopes, power meters, SMD (Surface Mounting Devices), handling tools, etc.
- Components for other non-accelerator based projects like Antares and Medipix.

Because of this large number of projects there is a permanent high claim on the manpower (staff of 35 fte) and expertise of the group. In Fig. 2.1 the projects are listed that consumed $\geq$ 0.5 fte.

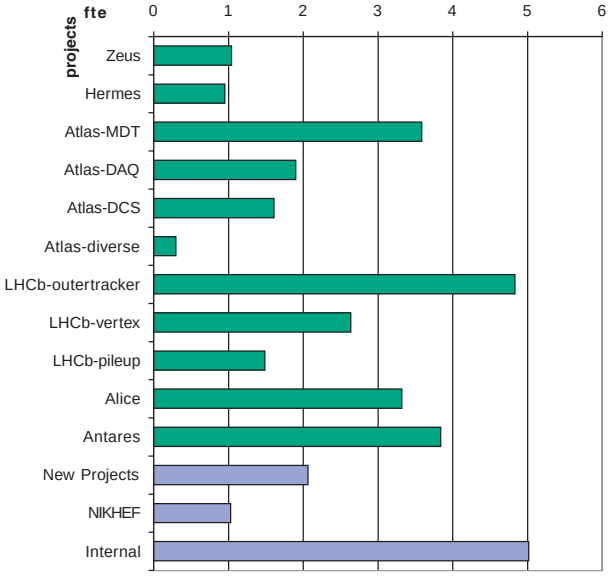

Figure 2.1: *ET manpower distribution in 2001*

2.2 Projects

2.2.1 HERMES

To protect the Lambda Wheels against unnecessary radiation damage caused by unstable beam conditions, a Beam Loss Monitor (BLM) was developed, tested and installed in the shutdown period of the HERA beam. The BLM consists of two sets of four ionization chambers, placed at a distance of 20 cm from the beam in the horizontal plane.

In case of too high radiation levels, the BLM generates a trigger signal, which is sent to the dump kicker. Each ionization chamber is equipped with a charge sensitive preamplifier with a shaping time of 5 μs, and a line driver. Three of the four chambers monitor the radiation level, while the fourth dummy chamber supplies a veto signal in case of electromagnetic pickup. A discriminator unit that filters spurious signals picked up during transmission handles the analog signals from the front ends. The major trigger decision is built in standard NIM logic. For diagnostic purposes, a PC-based ADC card records the front-end signals in a time window around the trigger.

2.2.2 ATLAS

Monitored Drift Tubes (MDT)

On the MDT production site the department provides support by optimizing the controls and installing several extra test features. This site has to produce 96 of the largest muon chambers of the ATLAS detector.

For the MDT chamber tests a cosmic-ray setup has been realised. A signal-delay line of $\approx$11 ns has been developed that is made of a four-layer PCB with a high voltage isolation of 4 kV.

With this delay line it becomes possible to measure the z-coordinate with higher accuracy. The advantages of this delay-line construction are a low price by mass production, a high reproducibility, and the absence of magnetic parts.

Semi-Conductor Tracker (SCT)

Prototype SCT silicon detector modules have been extensively tested. The modules are functional, but under certain conditions they show instabilities. Due to the small size of the components and sophisticated functionality, debugging is a real challenge. Different groups within the ATLAS collaboration are working on the sta-

Figure 2.2: *Delay line for MDT test purposes. Dimensions in mm are 51×26×3.5, weight is 9.1 g.*

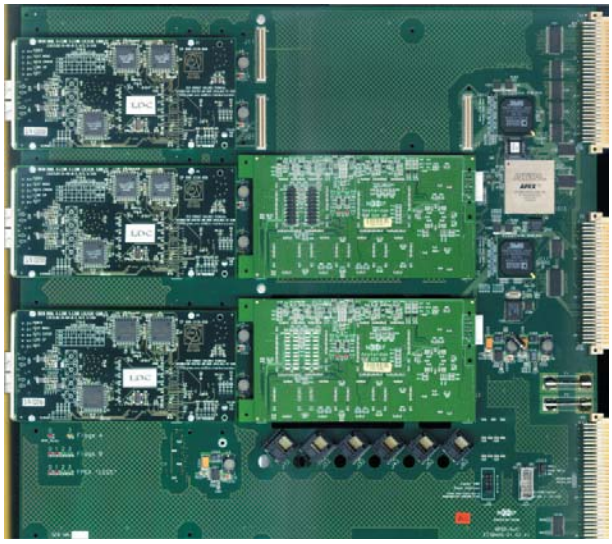

Figure 2.3: *The MROD-1 module with at the left three S-link daughter boards and in the centre two of three MROD-in boards. On the right are the three VME64x connectors.*

bility problem. At NIKHEF it has been shown that noise entering the power distribution from the digital logic was a source of the instability. Better decoupling of the power distribution was required. The biggest problem was finding space for the surface mount components. There was no space on the kapton hybrid, and designing a new four-layer kapton circuit would be too time consuming and expensive. To test some proposed improvements we used a small (5 mm x 6 mm) kapton circuit that was glued directly on the active part of the ABCD Integrated Circuit. The mini-kapton has a single copper layer with electrical connections to the chip made by wire bonding. Modification of a module with short silicon wafers at NIKHEF was very successful, resulting in the first stable short-wafer module. The same recipe was tried on a long silicon-wafer module. It considerably reduced the instabilities but, unfortunately, failed to cure them. More work is needed to solve this problem, including the development of a new six-layer hybrid.

RasNik Alignment system

The full series production of 5700 RasCaM's (sensor) and 6300 RasLeD's (light source) modules was finished. A pre-production of RasMuX (multiplexer) modules was carried out. Here, the mechanical envelope was optimised such that it will fit on (almost) all chambers. Radiation hardness tests were continued, resulting in the conclusion that some replacement of components is needed. Temporary interface boxes (MiniMaster) between CPU, grabber and four Rasmuxes were built for the chamber production sites.

The specifications for the cable types, lengths and connectors for all chamber components were finalised.

With the low-cost RasNik components a test setup for LHC magnet alignment was installed at CERN.

Muon Readout Driver (MROD)

The design and simulations of the MROD-1 prototype were finished. This prototype will support six input links, from a Chamber Service Module (CSM) on the Muon-chamber. The CSM converts serial data-bits from at maximum 18 TDC's of one layer of the Muon-chamber into 32-bits data words. The MROD groups these data words for each TDC and checks whether the data from all TDC's belonging to the same event number have arrived. The data from this event are formated and sent via an output link to the Read Out Buffer (ROB) for further processing by the central Data Acquisition (DAQ) system. The use of Digital Signal Processors (DSP's) makes extensive error checking, recovering and self-testing possible.

The MROD-1 consists of a 9U x 400mm VME64x board, called MROD-out, on which three daughter boards, called MROD-in, are mounted. Furthermore six S-Link Destination Cards (LDC) and one S-Link Source

Card (LSC) are also mounted on the MROD-out. All S-Links operate at a speed of 160 MBytes/s. Each MROD-in accepts and organises the data from two S-Link inputs. The MROD-out collects and formats the data from the three MROD-in boards and sends its data to the Read Out Buffer via the S-Link output. Furthermore the MROD-out communicates with the rest of the system via a Timing, Trigger and Control (TTC) interface and via a VME64x interface.

Two MROD-in boards and one MROD-out board are produced at the moment and tests were started. The test-setup is built up with a prototype of the standard ATLAS 9U-VME64x crate.

During testing minor were problems discovered in the design of the MROD-1 which were easy to fix by re-programming the Field-Programmable Gate Arrays (FPGA). However, a serious problem with the SHARC Digital Signal Processors (DSP) showed up. Depending on the skew between the power-on sequence of the 3V3 and 2V5 power inputs of the SHARC DSP's, the internal Phase-Lock Loop (PLL) circuit can get locked in an error state, preventing any further use of the DSP. A (difficult to implement) hardware patch of the power distribution in the MROD-1 will have to be realised to solve this problem. The MROD-1 interfaces to the TTC system via a TTC Interface Module (TIM) that is developed by the University College London in the UK. The TIM needs a special P3 backplane in the VME64x crate. This backplane is developed by the Royal Holloway University of London, also in the UK. A prototype of the TIM module and a backplane are integrated in the test-setup of the MROD-1. After a few start-up problems, the TIM was working correctly with the MROD-1.

Besides functioning as a Muon Read-Out Driver, the hardware of the MROD can also be used to build a Read-Out Buffer. Exactly the same hardware that forms the MROD-1 can be transformed into a ROB, only by re-programming the functionality in the FPGA's. During the design of the MROD-1, the possibility for the transformation to a ROB was taken into account. The re-programming of the FPGA's and testing of the ROB functionality is planned for the near future.

2.2.3 B-Physics

LHCb Outer Tracker

Most of the work done was focused on the Technical Design Report, published in September 2001. Assistance was given in the form of specifications and pre-designs of the electronics. The work also resulted in two public LHCb notes.

Assistance was given with the further development of the straw chamber in the area of chamber boards, grounding and shielding and beam tests at CERN.

A prototype board for measurement of very low currents in the high-voltage lead of a straw has been developed; it is able to measure currents down to 100 pA.

Together with our colleagues from Krakow we have successfully tested a digital front-end prototype for the Outer Tracker in November as a proof of concept. After further developments it can serve as a backup solution. The next step will be the development of a special Time to Digital Converter (TDC) chip at Heidelberg and the matching front-end electronics by NIKHEF. Additionally we have provided a Timing and Trigger Control (TTC) generator and receiver to trigger our present and future front ends in a CERN-compatible way (on glass fibre).

LHCb Vertex

In order to design reliable mechanics for the Vertex detector investigations were done to characterise its high-frequency behaviour.

To measure the longitudinal coupling impedance of the Vertex mechanical setup under realistic conditions a measurement tank (mockup tank) has been constructed. This tank has been built up according to the latest design review in which all parts like silicon detector boxes and bellows are simulated by aluminium and stainless steel parts. In the final design the silicon detector boxes have to be movable from closed position to a maximum opening of 60 mm, which is desired for the beam-injection cycle.

The connection of the LHC standard beam pipe of 54 mm to the 12 mm inside dimension of the boxes is provided by the so called 'Wakefield suppressors' (see Fig. 2.4), mounted at both sides of the boxes. The goal is an 'ideal situation' (beam pipe with right dimensions and the change by means of closed tapers), with no coupling to the tank and where the real part of the impedance is $\approx$100 Ω. The measurement results are still $< 100\ \Omega$ for the boxes closed or at a distance of 20 mm of each other. At silicon box distances from 20 to 60 mm the opening in the wake field suppressors produces an increase in RF coupling to the tank resonances and the real part of the coupling impedance increases to 400 Ω. To minimise this RF coupling a modified wake field suppressor will be constructed.

A measurement was performed close to the shielding of the silicon detector boxes. EM field penetration

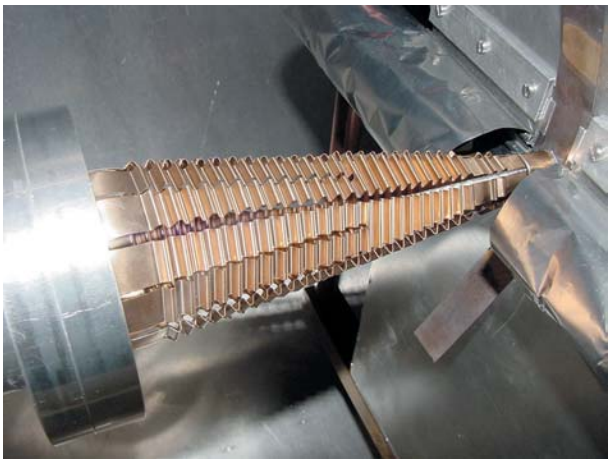

Figure 2.4: *RF suppressors at the detector box of the LHCb Vertex detector tank.*

through the thin aluminium shielding of the boxes possibly increases the noise level of the output signal.

A coaxial line of 50 Ω has been made of which the outer conductor consists of aluminium foil, the thickness of which can be chosen. The power level in this coaxial line over the frequency band of interest, in our case with an upper limit of 150 MHz, can be increased to 15 W maximum. In this way the EM field level at the outside of the foil can be controlled to the expected level introduced by the beam in the desired frequency domain.

At 0.5 mm distance of the aluminium foil a prototype silicon detector with a BEETLE front end will be mounted.

LHCb Pile-up Veto system

For the Pile-up Veto project a full-scale prototype of the vertex processor was designed and currently the printed circuit board is being developed. The central part of this board consists of two large FPGA's with 3.2M logic gates each. These FPGA's contain the correlation matrices that produce the trigger decision as input for the level0 trigger logic.

The Pile-up Veto system supplies a trigger decision to the level0 trigger of LHCb. Therefore, digital data are required prior to level0 buffering. The only readout chip for strip detectors that can deliver these discriminated signals is the 'BEETLE' chip. It was therefore decided to increase the effort in the development and test of this chip. In a collaboration between the ASIC-lab in Heidelberg, Oxford University and NIKHEF various components of the front-end chip have been submitted in the 0.25 μm CMOS technology and tested. During this year we characterised a prototype front-end and discriminator chip before and after irradiation. Also two complete BEETLE 1.1 chips were connected to a silicon strip detector and successfully operated in a test beam at CERN.

A point of concern is the cabling inside the vacuum tank of the vertex locator. Apart from the radiation and out-gassing requirements, it should be able to withstand 10000 movements during its lifetime. The basic solution is a fine-pitch strip line on a kapton backing.

2.2.4 ALICE

For the ALICE programme NIKHEF designs the electronics that handles the signals between the front-end hybrids in the Silicon Strip Detector (SSD) and the data acquisition outside the detector. This electronics is placed at both ends of each detector ladder and is called an EndCap module. The development of the electronics was presented at the *7th Workshop on Electronics for LHC Experiments*, held in Stockholm.

The electronics must be radiation tolerant and therefore application specific IC's (ASICs) are being developed using 0.25 μm CMOS technology. Two types of ASICs are necessary, a control and buffer ASIC for all signals that are needed for the front-end chip on the detectors (ALCAPONE) and an analog buffer to send the analog data from the detector to the data-acquisition (ALABUF). In the design of the EndCap module, power consumption, mass and space are important issues. Low power ASICs reduce the amount of space and power in comparison with several commercial IC's that would be needed instead.

Three prototypes of parts of the complete ASICs have been designed (see Fig. 2.5), produced and (two) tested in 2001. One of the tested circuits is a radiation-tolerant power-supply regulator and the other is an analog buffer with multiplexer for the handling of the analog detector data. After the tests these parts will be integrated in the complete control chip which will be produced early 2002.

The control chip has functions for buffering digital (LVDS and CMOS) signals, for the control of configuration data of the front-end chip and the chip itself, for power regulation of the power in the EndCap and the front-end Hybrid. This makes this ASIC a 'mixed-signal' design with analog and digital functions. Both the analogue- and digital parts are verified with sim-

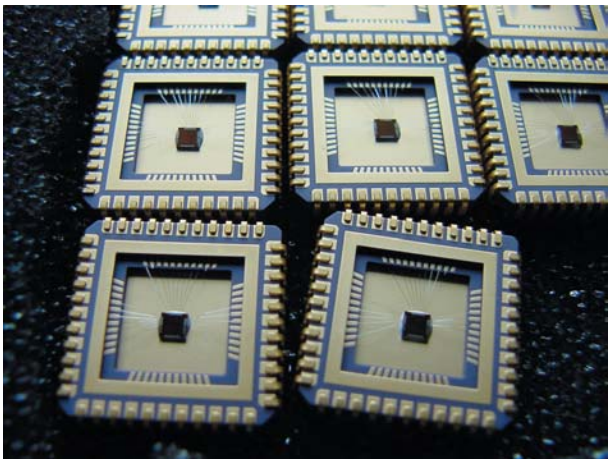

Figure 2.5: *Prototype ASIC in test package.*

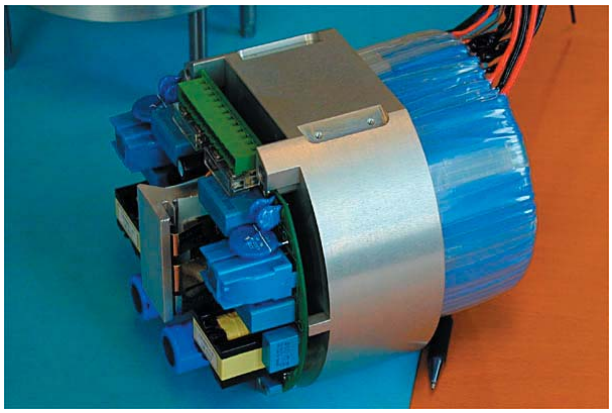

Figure 2.6: *Power supply part to feed two of the six sectors (2×180W-400V) in a string.*

ulations. The digital part is designed using Verilog as the description language. The layout is generated automatically, whereas for the analog part everything must be done by hand.

2.2.5 ANTARES

During the year 2001 the final Technical Design Report has been completed and construction of the first string components has been started. Deployment of one sector, a modular unit corresponding to $\frac{1}{6}$ of a string, is foreseen for 2002. NIKHEF contributes to several parts of this project.

Optical network

For the communication between shore and detector parts an optical network will be applied. This system will be based on dense wavelength division multiplexing (DWDM) at 1500 nm - 8 wavelengths on ITU-grid at 400 GHz separation.

The final optical DWDM network design for Antares was concluded with the continued cooperation of the fibre optics engineering firm Coenecoop. DWDM lasers, DWDM receivers and DWDM multiplexer-filters were selected, with emphasis on extreme long-term stability for unattended underwater operation for over 10 years. Details in fibre handling, connecting and routing inside the electronic crates and titanium cylinders were fixed.

NIKHEF has investigated lay-out issues, such as high-frequency constraints, ground loops, shielding and temperature behaviour of the DWDM board. Especially the 2.5 GHz transmit laser and laser driver circuit, with its high current 80 ps rise-time edges and the V sensitivity of the Avalanche Photo Diode (APD) circuit of the optical receiver asked for expertise in the field of high frequency and cooling.

In order to increase the NIKHEF expertise on optical networks several industrial courses were attended by ET personnel.

Power distribution

Based on the proposed power distribution from the conceptual design report the string power distribution topology has been designed. It will exist of two parts; a string power module and a local power box. The string power module will convert the power from shore to a dc power such as to minimise noise and optimise efficiency (see Fig. 2.6). This power will be converted by the local power box in each module into all voltage levels needed by the different electronic boards. A prototype of the SPM has been realised by the firm Power Concept, specialised in power supplies and reliability.

Module mechanics

The original module crate setup designed by the project partner in Marseille has been evaluated. The temperature behaviour of all boards has been taken into account to produce a concept that can dissipate all power in a reliable way. An improved design, which was presented to and accepted by the collaboration, served as a basis for a prototype (see Fig. 2.7), which will be tested at the beginning of 2002. A grounding and shielding philosophy was also included in this design.

Test system setups

Special equipment to test the parameters of optical net-

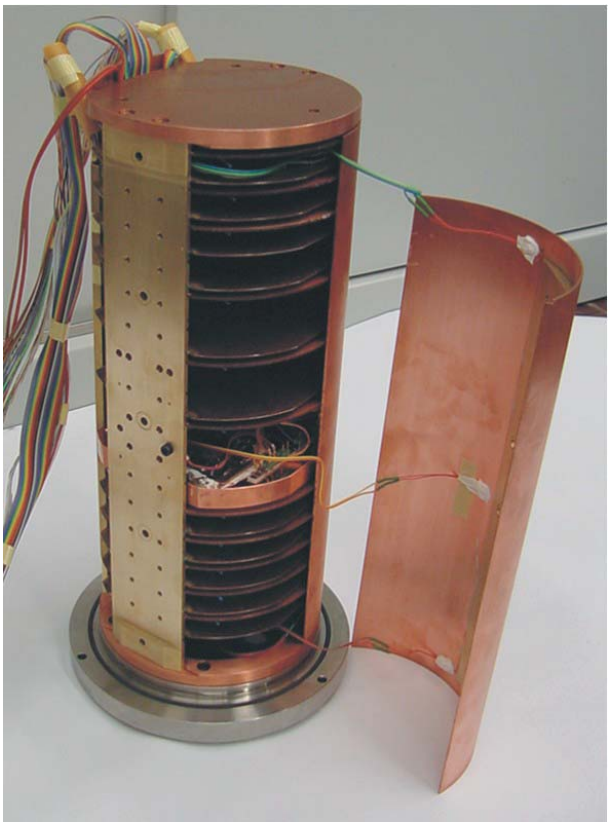

Figure 2.7: *Test system for temperature behaviour of the electronics. Diameter 155 mm, height 420 mm, weight 9 kg.*

work systems was required. Wavelength precision and stability, damping and reflection, and bit-error rate detection are important items to check before installation of the network. Crucial instruments were selected and acquired, such as an Optical Spectrum Analyser, a Tunable 1550 nm Laser Source, an Optical/Electrical converter, etc. Also, a real-time oscilloscope with high analog bandwidth ($>$ 2.5 GHz), high sampling rate (20 GHz) and matching 4 GHz active probes has been selected for electrical test probing and verification of the DWDM circuit designs.

Several tests on optical connections were performed as a proof of concept. A 50 km optical-link test was carried out. To interface the commercial single-mode transmitter and receiver to the Gigabit Ethernet cards, two 1000base-SX to electrical signal converters with retimer where built. Without optimalisation a Bit Error Rate $< 3 \times 10^{11}$ was measured. The optical fibres of the Interconnecting cable, between Junction Box and SCM, have been tested to a pressure of 300 bar at the IFREMER Brest high-pressure test facility. A delay variation of -10 ps/bar/km and a negligible attenuation as function of pressure have been measured.

Optical loss measurements have been made at the tension tests of the vertical string cable in Marseilles. Without tension, the cable showed a larger loss than specified and the loss increased dramatically at higher tension.

2.2.6 Medipix

An interface was developed and tested successfully in 2000. This year new designs for interfacing electronics and pixel carriers have been provided for the new larger and faster Medipix chips. NIKHEF contributed to two challenging aspects: to realise a 200 MHz read-out system for the chips and to realise a printed circuit board with a very high resolution as carrier for the pixel chips. Early 2002 the test phase will start.

2.3 Department development

As the Electronic Technology Group is involved in a wide variety of projects, a broad field of expertise and high-quality tools are a prerequisite. To keep the expertise on the required level and to increase the deployability of the members of the electronic department various courses were attended by members of the group. For instance, knowledge about electromagnetic compatibility is very important for the high-frequency designs of communication electronics and electronics in a noisy environment, especially for near-beam experiments and when switching power is close to the electronic circuits. Other fields in which expertise is required are VLSI-design, PCB-design and optical networks.

Due to the specific electronic constraints on printed circuit boards, the layout of most of the boards is done in house. This means a high claim on expertise and tools. Presently two layout systems are in use. The software of the Ultiboard system has been upgraded. Many special features have been realised in intensive contacts with the supplier. For the Mentor Graphic system new workstations and software with new features, like a state-of-the-art autorouter, have been installed.

The ergonomic aspects of the office furniture and the workshop furniture are being evaluated on a continuous basis. Half of the almost 40 years old furniture has been replaced with modern parts. The new desks are in accordance with the latest ergonomic (e.g. RSI) and safety (ESD) regulations.

3 Mechanical Workshop

3.1 Introduction

The mechanical workshop has contributed to several projects. The work varied from constructing prototypes to the serial production of muon chambers, which is presently the largest project.

Below the contributions are described in more detail, ordered by invested manpower.

3.2 Projects

3.2.1 ATLAS Muon chambers (7.4 Fte)

After a period of preparation, the serial production of 96 ATLAS muon drift tube (MDT) chambers started in June 2001. An MDT chamber consists of 2x3 tube layers glued on a support structure with high precision (aim: < 20 μm). Each layer consists of 72 drift tubes.

The production line starts with the assembly of precision end-plugs, which hold the wire in the centre of the drift tubes. The drift tubes are then finalised with a semi-automated wiring machine, which successfully wired about 4000 tubes. During the production process, experience was acquired by the operator, which allowed to make improvements to this machine.

As part of the standard Quality Control procedure, all produced tubes are checked by measuring the wire tension, leak rate and High Voltage behaviour. About 10% of the tubes are also checked by measuring the wire position which is determined by two precision end-plugs. The final rejection rate is about 2%.

The first step in the chamber assembly is the construction of the support structure (spacer), which takes in the present set-up at least 2 days. Then, in six subsequent days, the tube layers are glued to the spacer. Each gluing step is prepared carefully to ensure that only good quality tubes are used and that each tube is placed in the gluing jigs to high accuracy. The gluing machine, used for gluing the tube layers, is now operating with disposable glue-cylinders, reducing cleaning time. In addition a glue mixing and dispensing machine has been bought to avoid hand mixing. A total of eight chambers were produced in 2001. The first chamber took 18 days to build, for the last one in this year we needed 8 days.

Some chambers are equipped with gas systems. The production of the required parts has started and in the future we foresee to equip all chambers with gas systems directly after assembly.

Figure 3.1: *Some of the ATLAS Muon chambers and storage racks produced in 2001. In the background the MDT (cosmic Ray) test station.*

Four chambers, which were produced in 2001 were sent to CERN to undergo an X-tomography scan to determine the position of each of the 432 wires. The results are excellent: all four chambers have their wires positioned to typically 15 μm RMS.

In the fall of 2001 we have set up a test station for MDT chambers using cosmic muons, see Fig. 3.1. This station allows testing all the chambers before they are stored (to be installed in 2004 in ATLAS).

For the coming years the production of muon chambers will continue; we are studying production schemes that allow us to produce chambers in a 7 working day cycle.

3.2.2 ATLAS Semi-Conductor tracker (2.5 Fte)

We tried several techniques to find the best way to machine the carbon fibre discs, used as support structures of the tracker. During these studies we obtained experience and found that it is necessary to use a mould to retain the disc while milling. The first tests for serial production were made with a 1/3 pie piece of a full size disc, see Fig. 3.2. We adopted the following procedure. First, the holes are machined. Then, the mounting blocks, inserts and pads are bonded onto the disc. Finally, it is machined to the required height and flatness.

A Carbon fibre (Korex) core, which will probably be used in the future, is very sensitive to moisture. For this

Figure 3.2: *Prototype piece for a full size disc with mounting blocks and other inserts.*

reason we made a prototype storage- and transport box, which can be flushed with a dry gas. The electronic design of the silicon modules (K4) has not yet been finalised, which prevents the further development of the mechanics concerning these modules. However, various precision prototypes for cooling- and module support are already being made.

3.2.3 LHCb Vertex detector (2.6 Fte)

We constructed a prototype thin-walled foil, which is used to separate the silicon modules from the primary vacuum. The foil can be produced 'cold' with a pressure of approximately 65 bar or 'warm' (500 Celsius) with a pressure of approximately 15 bar. Initially, the thickness of the foil is 250 μm. At places where the foil needs to be bent to follow the shapes of the silicon modules its thickness is reduced to only 70 μm, which has led to several leaks. We are confident that these leaks can be avoided in the future.

The silicon modules are placed in a secondary vacuum vessel, which is connected to a safety-valve to protect the thin separation foil against high pressure differences (limitation at 3 mbar.). This valve was designed and made at NIKHEF. Figure 3.3 shows the parts of the valve before welding. The valve was tested and the results are promising.

During data taking the detectors have to be positioned at 8 mm from the beam, but until stable beam conditions are reached, they have to be retracted over 3 cm. For this movement, a bellow on each side of the beampipe will be used. The first prototypes of these

Figure 3.3: *The stainless steel parts of the safety valve before welding.*

bellows are being made. The movements have to be followed by the Wakefield suppressor. A few models of Wakefield suppressors were made this year. The best design was chosen and fatigue tests will follow in 2002.

3.2.4 LHCb Outer Tracker (on average 2.2 Fte's)

We performed much prototype work for the wire locators and the tools needed for production of the straw chambers, see Fig. 3.4. The way of putting a wire in a tube is to suck it through using an air pump and/or to blow it through with compressed air. Despite several attempts to automate the wiring of the tubes and putting the locators in place, the wiring by 'hand' seems to be the best option to get the 50.000 tubes wired. At NIKHEF we decided to wire the tube by using the suction method, in combination with soldering a little

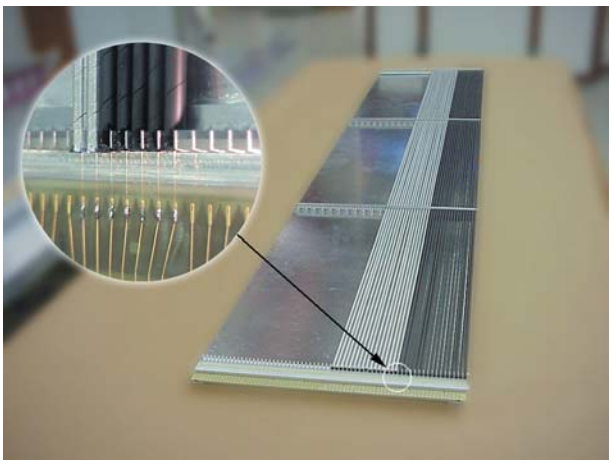

Figure 3.4: *Prototype of a LHCb Outer Tracker chamber.*

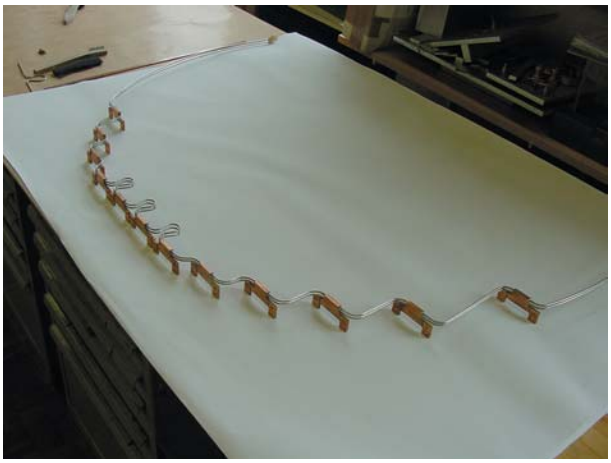

Figure 3.5: *CO_2 evaporator cooling circuit AMS.*

bullet of tin at the end of the wire, to be cut off at the end of the wiring.

Another issue to work out was the electrical contact between the straw and the honeycomb material covered with conductive foil. The latest suggestion is to make a lip at the end of the straw and clamp it with a metal plate to the contact.

3.2.5 ZEUS micro vertex detector (on average 1 Fte)

In February the pre-assembly and tests of the two detector halves took place at DESY. In May, the detector was successfully installed in the ZEUS experiment.

3.2.6 HERMES (on average 0.8 Fte)

All silicon modules were bonded and tested. A system to mount the modules in a precise way on the 'lamba wheels' was constructed. The mounting scheme was successfully tested at DESY. The final assembly will be, after some delay, realised in March 2002.

3.2.7 ANTARES (on average 0.5 Fte)

For Antares we made prototypes of the crates that will hold and cool the p.c. boards. Some crates were made for testing in a water container, some for the test string in the sea.

3.2.8 AMS (on average 0.4 Fte)

The first prototype of an AMS cooling ring (Fig 3.5), including mounting pieces, has been made.

3.2.9 DUBBLE (on average 0.4 Fte)

The group took care of service aspects of the equipment delivered in the past to ESRF in Grenoble. A new prototype slit has been successfully constructed and the green light was given to produce twelve final slits.

3.2.10 ALICE (on average 0.2 Fte)

In collaboration with the University of Utrecht we contributed to prototype work for the ALICE detector.

The cosmic ray test stand at NIKHEF with four BOL chambers installed.

4 Mechanical Engineering

4.1 Introduction

The Engineering Group has been involved in many projects in the development phase in the year 2001 as shown in Fig. 4.1. Moreover the group invested manpower in projects in the running phase, projects for third parties and the internal operation of the group.

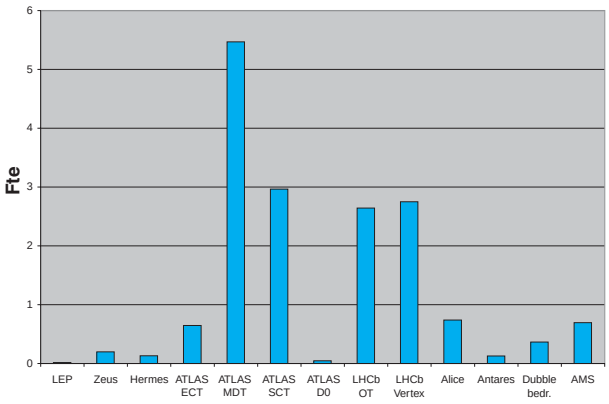

Figure 4.1: *Distribution of manpower of the Engineering Group in 2001 over the projects.*

4.2 Running Experiments

4.2.1 HERMES

A final test installation of the silicon detectors and their cooling system has been performed. The final integration on the lambda wheels is waiting for the test runs of HERA in order not to risk damaging the detectors.

4.2.2 ZEUS

In a fruitful collaboration with colleagues from Oxford University the micro vertex detector has been installed in the beginning of 2000 in ZEUS (Fig. 4.2). All precautions with respect to damaging the silicon wafers have been effective. The preliminary tests with cosmic rays show a perfect behavior of the detector.

4.3 Projects in development

4.3.1 ATLAS muon chambers

Major progress has been made in finalizing the production drawings of the muon chambers of the ATLAS detector. The leak tightness of the tubes has been checked in an automated test setup. Diffusion of the helium test gas through the sealing complicates the procedure considerably, as the diffusion rate for the chosen

Figure 4.2: *Installation of the Zeus micro vertex detector*

construction materials appeared to be 10^{-9} mbarl/sec. The development of the tooling in order to optimise the production site was a major investment for our group.

4.3.2 ATLAS SCT

The final design of the discs is depending on many parameters like cooling, minimal mass, and stiffness and alignment aspects. The fixation of the disc in the cylinder with respect to the vibration modes, resulted into the design of a flexible fixation. The optimization of the number of fixations with respect to the resonance frequency of the assembled disc has resulted in a feasible solution, see Fig. 4.3. A lot of effort was put into the final specifications for the outsourcing of the disc manufacturing where a balance between quality control and costs was found.

A storage box for discs equipped with silicon modules, cooling systems and electronics in a protective atmosphere has been designed and built such that a protective gas atmosphere could be created.

A finite element study has been performed in order to predict the influences of temperature changes of the cooling circuit on the stability of the disc.

4.3.3 LHCb Outer tracker

The final prototypes have been designed and tested at CERN and at DESY. Discussions with the Heidelberg group are still ongoing with respect to the electrical properties of the assembly. Grounding problems in combination with conductivity of the straws have been

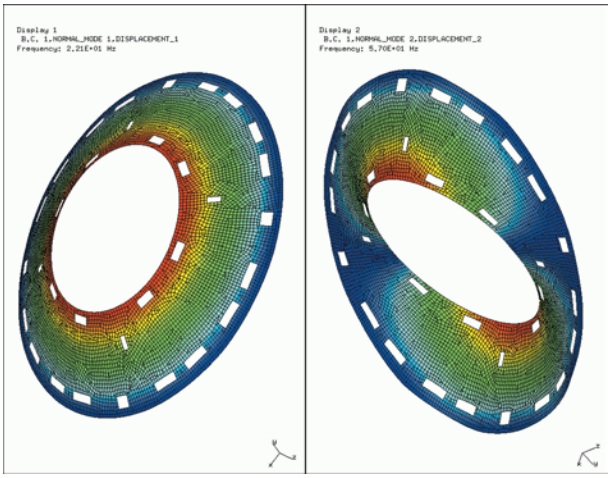

Figure 4.3: *The figures show the relative deformation as an effect of the vibration in the first and second resonance frequency respectively.*

solved in the design. The test setup for this construction will lead to the final decision.

The design of the production site has evolved to a final setup. The tooling design is in full progress.

A finite element study has been carried out in order to determine the stiffness of the modules, which consists of an assembly of the detection straws and their supporting panels.

Different types of wire locators were made by rapid prototyping to test their performance in the wire insertion process. This evolution of prototypes resulted in a final version made by injection molding suitable for mass production.

4.3.4 LHCb Vertex detector

The prototyping of the various challenging items in the construction of the equipment in the vertex region has evolved, e.g. the so-called gravity valve. The protection of the primary vacuum against back streaming from the secondary housing can by this mechanism be guaranteed to a level of less than 10^{-9} mbarl/sec. Progress has been made on the manufacturing of the 'toblerone' shaped 250 μm aluminum foil. The adjustment mechanism for the alignment to the beam centerline and the cable routing have been finalised in the design. Many presentations of NIKHEF experts at CERN gave the LHC committees the confidence in the present design.

The parts for the realization of the large bellows have been designed and constructed. Integration and testing of this crucial construction still is ongoing.

4.3.5 ALICE

The design of the silicon strip modules for the Inner Tracker Silicon detector (ITS) was finalised. Special tools for its construction and handling are being designed in collaboration with Utrecht University. For the mounting of these modules on the carbon fiber ladders we designed an innovative, high precision, assembly robot, see Fig. 4.4. The construction is partly performed at Utrecht University and partly in industry, under supervision of NIKHEF. Possible corrosion in the thin (40 μm) walled cooling tubes for the modules requires a thorough study by the engineering group. Many integration issues are still to be decided upon by the collaboration. We play an important role in the ongoing discussions.

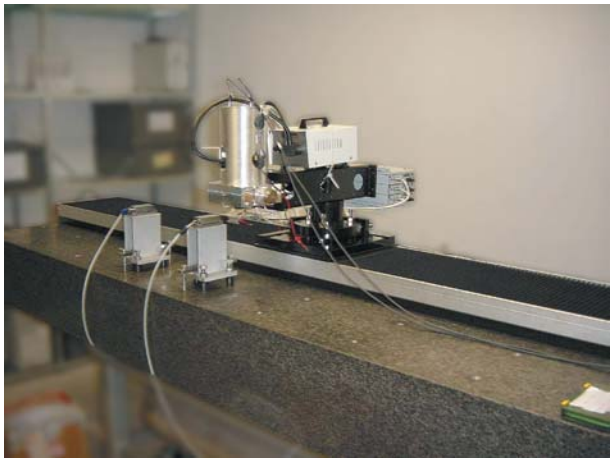

Figure 4.4: *Positioning mechanism for the ALICE silicon detectors.*

4.3.6 ANTARES

Thermal simulation studies of the MLCM[1] and SCM[2] electronics crates were performed to come up with a crate design with a good thermal contact between the DWDM[3] laser board and the 14 ^{o}C seawater. This good thermal contact is necessary to minimise the power consumption of the Peltier element, which is used to control the temperature of the DWDM Laser. A prototype crate was made and tested successfully in

1. MLCM: Master Local Control Module
2. SCM: String Control Module
3. DWDM: Dense Wavelength Division Multiplexing

a water container simulating the deep sea water conditions, see Fig. 2.7 in Chapter D2 on page 74.

4.3.7 ATLAS end cap

The first vacuum vessel has been leak checked at Exotech in Vlissingen. We assisted in doing this quality control. After transportation the vessel had to be integrated and tested again at CERN. Just before Christmas this job was successfully finished.

4.3.8 AMS

Our group also contributes to the thermal study of the tracker in the Alpha Magnetic Spectrometer. A prototype of an innovative space compatible cooling system based on CO2 cooling liquid has shown an almost ideal behavior. The specifications of the total system are fixed and we will start building the final circuit in collaboration with the Dutch Aerospace Laboratory (NLR).

4.3.9 DUBBLE

A redesign of the slit construction in the beam line has been performed. The parts are under construction. Several set ups for the experimental stations have been produced.

4.3.10 COLDEX

Measurements of ion desorption effects in a temperature trajectory of 2K to 30 K are ongoing. The apparatus that we have designed, built and tested is at present being implemented in the SPS machine at CERN, producing data with which the conditions in the future accelerator can be simulated. The quality of the LHC vacuum is among other effects depending on these figures.

The D0-farm at NIKHEF.

5 Grid Projects

5.1 Introduction

The unprecedented increase in network bandwidth over the last decade has enabled novel ways of solving the simulation and analysis problems for the LHC era. Traditionally, the amount of computational power one could buy for the same price has doubled every 18 months, a phenomenon known as Moore's Law. But the increase in wide-area network bandwidth has been much faster, doubling every 9-12 months.

The 'Grid' exploits this almost unlimited international bandwidth to interconnect compute clusters, large disk caches, and tape robots scattered over a large geographical area. This Grid can be used simultaneously by many communities (also called Virtual Organisations), like Alice, Atlas, D0 and LHCb. At the startup of LHC, the expected data rate after the level-3 trigger is approximately five petabytes per year for all the LHC experiments, and the total CERN-related analysis effort will require on the order of 50,000 high-end PCs in 2007. This effort will be distributed over all collaborators, since no single institution will be able to support such a large-scale infrastructure.

NIKHEF personnel are involved in several Grid-related projects.

5.2 DataGrid

The European DataGrid (EDG) is a project funded by the European Union with the aim of setting up a computational and data-intensive grid of resources for the analysis of data coming from scientific exploration. It started in January 2001 and is partially based on the successful Globus meta-computing toolkit, which provides basic 'Grid' services. The EDG project has been extending this basic set with the required functions for LHC computing: a resource broker, data replication and management, fabric management, grid-wide monitoring and networking.

All these tools will be available for the three data-intensive applications that drive DataGrid: the LHC experiments, whole-earth ozone profiling using earth-observation satellite data (in collaboration with colleagues from the KNMI (The Netherlands)), and biomedical analysis. The first working test bed was deployed in November 2001, and NIKHEF was one of the first institutes with an operational system (alongside CERN, IN2P3, INFN and RAL). This 'EDG Test bed 1' will supplement the pre-existing Grid test beds at NIKHEF that originate from the ICES-KIS WTCW Virtual Laboratory project.

NIKHEF contributes in the EDG project in half of the work packages (WP): Fabric Management (WP4), Test bed Integration (WP6), Authorisation (WP6/WP7), Networking (WP7), High-Energy Physics Applications (WP8), and Project Management (WP12).

Fabric Management

NIKHEF used the installation system provided by the EDG Fabric Management work package to install and configure its Testbed1 computers. We were able to produce an excellent evaluation of the Local Configuration (LCFG) system after this exercise, since none of the group knew anything about LCFG beforehand.

Another part of Fabric Management is the 'front end' of the compute cluster. All interaction between the Grid and the local centre will be through a single logical gateway. This allows for sophisticated scheduling techniques to be used inside a fabric to optimise computer use. It will also protect the centre against cracking attempts and will support pluggable authorisation and dynamic account creation and mapping.

Inside the fabric, monitoring and correlation tools will make a farm of thousands of nodes manageable and provide metrics on utilisation. For the current set of farms, load measurements have indicated large variations per experiment and per user; something that can be balanced once the various farms are combined into one (see Fig. 5.1).

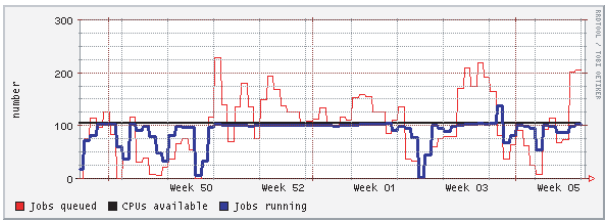

Figure 5.1: *Farm load (# jobs running, blue line) and queue length (# jobs waiting, red line) for the 104-CPU NIKHEF D0 Farm.*

Testbed Integration

The NIKHEF Testbed1 site currently comprises ten machines. One of these is an installation server. Configuration instructions for the other machines are archived

Figure 5.2: *The NIKHEF DataGrid Testbed. Each of the boxes contains a complete dual-CPU machine with 40 GB hard disk and 896 MB RAM. The network switches are located in the centre.*

here, as are all the software packages which must be installed. This machine broadcasts update or reconfiguration notices to the other machines. Another machine runs a directory service (Lightweight Directory Access Protocol (LDAP)) that contains the mapping of Grid users onto communities called Virtual Organisations (VOs). VOs are analogous to Unix 'groups'; for example, a large storage area could be declared as writable by the LHCb VO. When this storage service receives a write request from a grid user, it consults the NIKHEF VO server to verify that the user belongs to the LHCb VO, and accepts or denies the request based on the answer. The NIKHEF VO server is authoritative for the entire EDG project.

The other eight machines are high-end computers, each with two GHz-class Pentium processors. Some of them are visible in Fig. 5.2. One of them hosts the Grid storage service (Storage Element), and another provides network monitoring services. The other six have yet to be configured. Ten more high-end dual-processor machines are marked for inclusion in the Testbed once its configuration is complete.

Security services

When interconnecting a multitude of systems worldwide with high-speed connectivity, such a system will instantly become a valuable target for abuse. It is therefore important to do strong authentication of the users of such a system, and to make sure that authorisation reflects usage policies.

The user authentication in the Grid is based on public-key cryptography and an associated Public Key Infrastructure (PKI) to distribute the keys. This system is well known from its role in e-commerce transactions, where sensitive financial data (credit card numbers) are encrypted such that only the intended recipient (the web trader) can read it. The Grid takes this technique one step further, and has also the individual end-users authenticate in this way. Using limited-lifetime 'proxies', it has been successfully leveraged to provide 'single sign-on' for all users on the Grid: you only need to type your pass phrase once at the beginning of the day, and all grid resources can be used without further hassle.

NIKHEF provides trusted third-party services (the Certification Authority) for all Grid users in the Netherlands, and is recognised as the authoritative Dutch Grid-CA in Europe.

Networking

Aside from the network monitoring machine on the Testbed, Grid networking activities at NIKHEF are common across projects. They will be described in the DataTAG section below.

HEP Applications

This work package (WP8) has been responsible for key projects in the past year. The first was the generation of a requirements document. This document provides essential direction for the project, as it defines the goal: *What should the Grid be able to do for High-Energy Physics?* The second project was making the first evaluation of Testbed1. NIKHEF appointed a full-time staff physicist to (WP8) in 2001, who participated fully in both these projects.

Since Testbed1 roll out was behind schedule, for two months all full-time WP8 personnel were temporarily reassigned to WP6 to provide deployment support. NIKHEF's decision to appoint a full-time WP8 person

has therefore been generously rewarded; the full-time WP8 people are among the best-informed in the project because of this dual WP6/WP8 role.

5.3 AliEn

AliEn is a grid prototype constructed by members of the Alice Collaboration at CERN. NIKHEF was the first site (outside of CERN) on which AliEn was successfully installed and this experience contributed valuable corrections to the AliEn design. NIKHEF allocated seven CPUs to the first AliEn production run in December, and they delivered about 43 CPU days of computing power. Grid techniques were used extensively, as the job execution commands were issued remotely from CERN and job output was stored on mass storage at CERN.

5.4 D0 Grid

The 104-CPU D0 farm has been running efficiently for the past year; details of the Monte-Carlo production done with the farm can be found in the D0 section of this annual report. Besides D0, the farm has also been used to run Monte-Carlo production for Antares and L3.

Trials with running the D0 Monte-Carlo production chain under the control of the Condor batch system were made this summer. Initial tests were successful, but it was not possible to run the production in full Grid fashion due to a limitation in the way the D0 software is constructed. Developers at Fermilab are currently trying to correct this situation and expect to have compatible software sometime in early 2002.

5.5 DataTAG

The DataTag is a new project that will start in 2002. The fundamental objective of the DataTAG project is to create a large-scale intercontinental Grid test bed involving the DataGrid project, several national projects in Europe, and related Grid projects in the USA. This will allow to explore advanced networking technologies and interoperability issues between different Grid domains.

The project will address the issues that arise in the sector of high performance inter-Grid networking, including sustained and reliable high performance data replication, end-to-end advanced network services, and novel monitoring techniques. The project will have its own dedicated Trans-Atlantic optical link of capacity 2.5Gbps between CERN and Starlight(Chicago).

The project will also directly address the issues which arise in the sector of interoperability between the Grid middle ware layers such as information and security services. The advance made will be disseminated into each of the associated Grid projects.

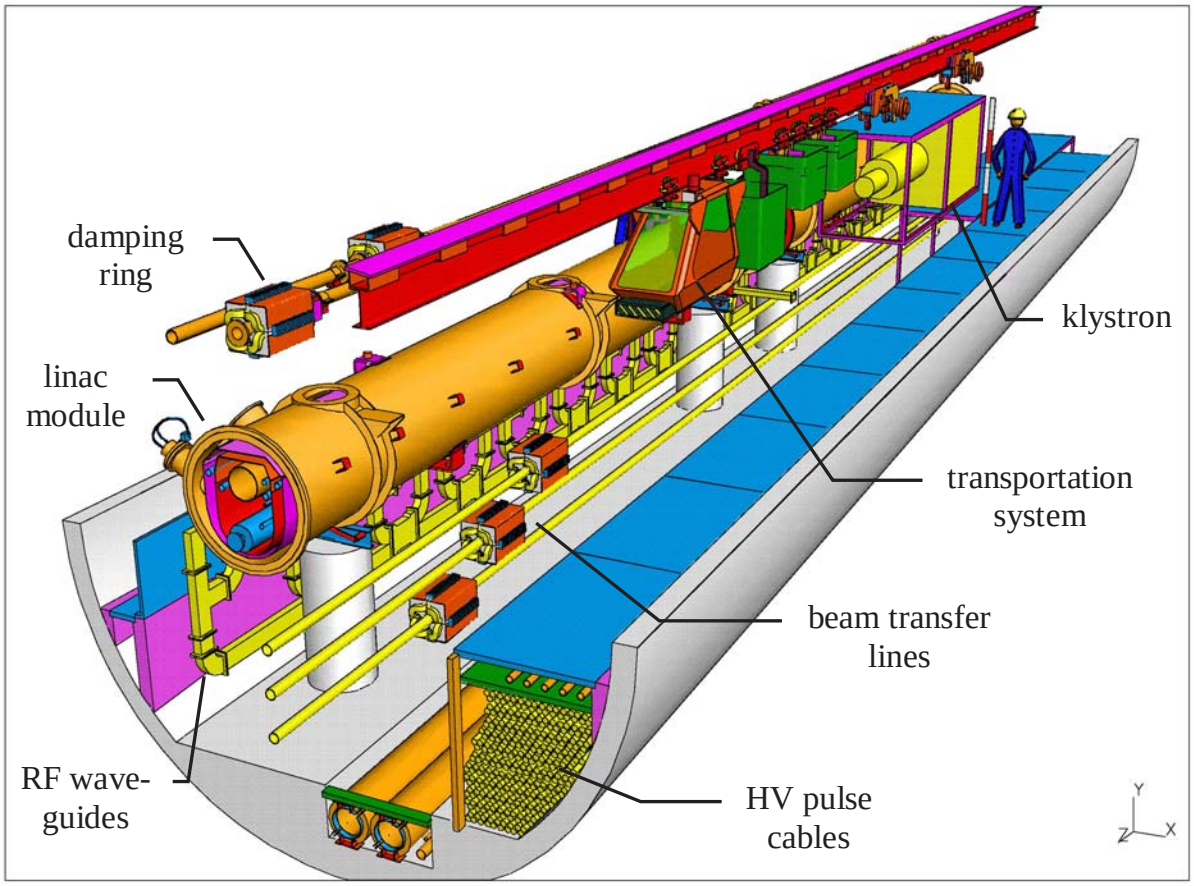

TESLA Tunnel Layout

6 Future Projects: TESLA

6.1 Introduction

There is now worldwide consensus in the particle physics community that the next major accelerator after the LHC should be a linear e^+e^- collider.

TESLA is one of the three projects under study. It is a superconducting e^+e^- collider of 500 GeV total energy, extendable to 800 GeV. The project includes an X-ray Free Electron Laser facility. A schematic view of the layout is given in figure 6.1. The total length of the collider is approximately 33 km and it is proposed to be built adjacent to the DESY laboratory in Hamburg. The basic accelerating elements of TESLA are 9-cell superconducting Niobium cavities. More than 60 of them have been routinely produced by industry, reaching now an accelerating gradient well above the 23.4 MV/m needed for operation at the total collision energy of 500 GeV. A first 9-cell electro-polished cavity has reached a gradient of 35 MV/m, needed for 800 GeV operation. The design luminosity is $3.4 \cdot 10^{34}$ cm^{-2}s^{-1}, almost 1000 times more than that reached at LEP2. This is in part due to the extremely small sizes of the electron and positron beams at the interaction point of 553 nm and 5 nm in the horizontal and vertical plane respectively. TESLA can also be operated as an e^-e^-, $e\gamma$ or $\gamma\gamma$ collider with (effective) luminosities 15-20% of the e^+e^- luminosity.

6.2 Physics Motivation

The Higgs particle is expected to play a central role in the experimental programme of TESLA. At 500 GeV collision energy a Standard Model (SM) Higgs boson of mass up to 400 GeV/c^2 can be observed. This is well above the upper limit of about 200 GeV/c^2 obtained from precision measurements at LEP. If (SM) Higgs(es) exist in this mass range they will be discovered at the Large Hadron Collider under construction at CERN (and possibly already at the Fermilab Tevatron collider). However, previous experience has shown that proton-(anti)proton colliders and e^+e^- colliders are complementary. The W and Z bosons were discovered at the $Sp\bar{p}S$ collider of CERN in the early eighties. But precision measurements at LEP of the properties of the Z and W bosons really established the Standard Model, allowing a precise prediction of the top quark mass and to constrain the Higgs boson mass. Even if the Higgs is discovered before at the LHC, the clean experimental conditions of the e^+e^- collider allow precise determination of its properties like mass, width, spin, decay branching fractions. In addition, TESLA offers the unique possibility to establish the coupling of the Higgs boson to itself. The precision of the measurements will be vital for the full understanding of the origin of mass.

Further powerful tests of the Standard Model can be made by comparing the top quark mass, precisely measured from a threshold scan, with much better measurements of the electroweak mixing angle $sin^2\theta_W$ and of the W boson mass, by lowering the energy of TESLA to 91 GeV (Giga-Z factory) and to around 161 GeV (WW threshold scan), delivering 100 times more data at these energies than collected at LEP.

Supersymmetry (SUSY) predicts many new particles, partners of the matter and force particles that we know today, and more than one Higgs boson. Although there is a large spectrum of masses for these supersymmetric particles, depending on the values of the parameters of the theory, again TESLA is complementary to the LHC in the sense that precision measurements of the masses and other properties of the particles accessible in the energy range of TESLA, will allow an accurate determination of the parameters of the theory and therefore its consistency and completeness over a large energy range.

The physics case for TESLA and a possible detector have been worked out in a series of workshops and are reported in the TESLA Technical Design Report. NIKHEF was involved in the study of the measurement of the branching ratio of the Higgs boson decaying into two photons. This is an important decay mode to measure, as it proceeds through (heavy) particle loops and is therefore very sensitive to new physics. It was shown that a relative uncertainty on this branching ratio of between 10% and 16% could be obtained for a Higgs mass of 120 GeV/c^2. Together with a measurement of the total width of the Higgs boson, possible in the $\gamma\gamma$ mode of operation of TESLA, a precision of 10% on the partial width of the Higgs boson decaying into $\gamma\gamma$ is feasible.

6.3 Detector R&D

The ECFA-DESY workshop is continuing with special emphasis on higher energies up to 1 TeV, on $\gamma\gamma$, $e\gamma$ and e^-e^- options, and on the detector design following further detector R&D. Important aspects of the detector design are related to track momentum resolution, vertexing, energy flow and hermiticity. The proposed TESLA detector therefore consists of a very high pre-

cision vertex detector, surrounded and complemented in the forward directions by several additional layers of Silicon detectors, a large tracking volume covered by a Time Projection Chamber (TPC), and a high granularity calorimeter, all embedded in a 4 Tesla solenoidal magnetic field.

NIKHEF just started with investigating the feasibility of a highly segmented readout of the TPC by means of pixel detectors. The studies by NIKHEF of a beam protection system are discussed in the next section.

6.4 Investigation into a beam protection system for TESLA

Special about the high-energy high luminosity beam are the intense (4 nC) electron bunch and a small (less than 100 μm) beam diameter. The long response time (more than 50 μs) precludes swift action in case of miss-steering. An off-axis electron beam, hitting a surface, will cause irreversible mechanical damage by impulse heating. The radiation induced heat load for the cryogenic beam-line components due to a beam 'halo' should be many orders of magnitude lower than for a room temperature accelerating structure. NIKHEF proposed to apply its MEA Protective Collimator Compton Battery system (PCCB system) for TESLA. This sensitive system consisted of maintenance free radiation hard components. The success of its performance has been demonstrated by the complete absence of radiation activation of beam-line components after more than 15 years of MEA operation. The proposed PCCB system consists of many protection collimators located at strategic places along the beam line. A 'scraping' electron beam generates a photon shower. The shower is converted in a thin aluminium sheet into Compton-electrons. The Compton-electrons are collected by a lead absorber and converted into an external electrical current. A full beam pulse may produce more than 100 V pulses into a 50-ohm load. The minimum pulse output is limited by external electrical noise, typically 1 mV. The sensitivity for a sustained miss-steered beam is several orders better. Our design was tested at the Tesla Test Facility and the results are promising. The results were presented to the TESLA collaboration.

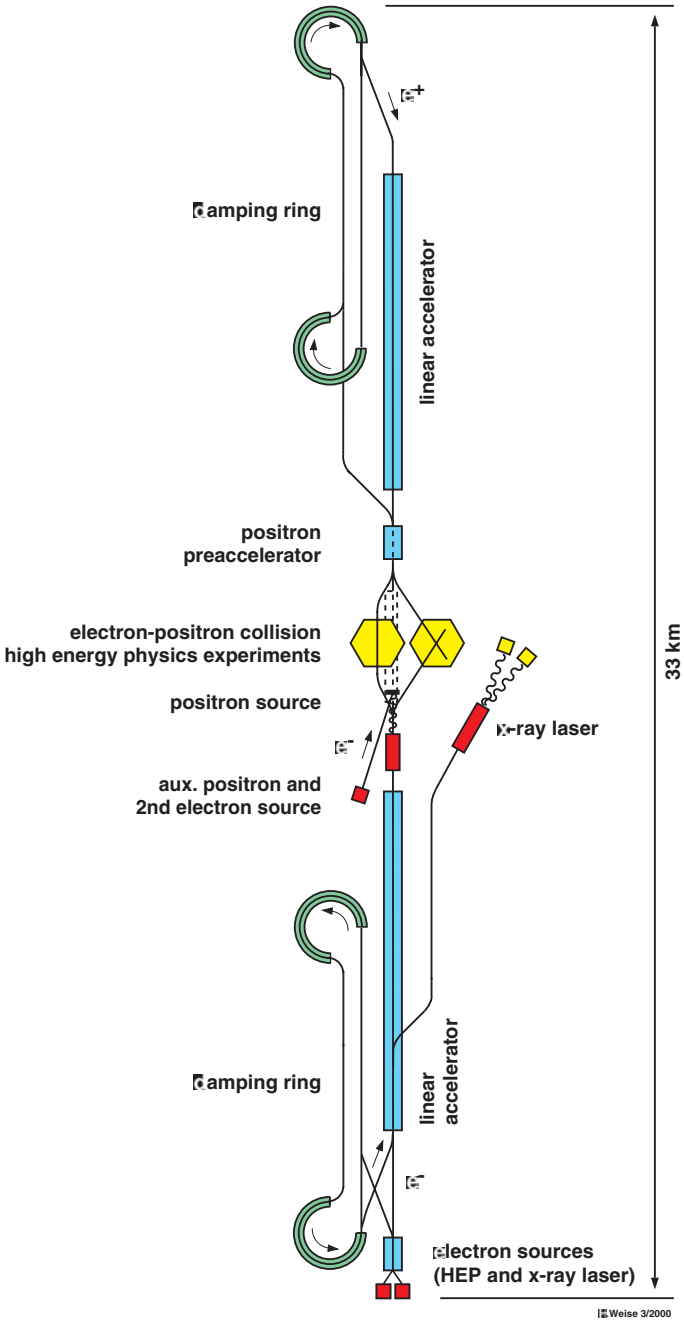

Figure 6.1: *Sketch of the overall layout of TESLA (the second interaction region with crossing angle is optional and not part of the baseline design).*

E Publications, Theses and Talks

1 Publications

[1] Abazov, V.M. *(et al.)*; Balm, P.W.; Bos, K.; Peters, O.; Ahmed, S.N.; Duensing, S.; Filhaut, F.; Wijngaarden, D.A.; D0 collaboration
Differential cross section for W boson production as a function of transverse momentum in $p\bar{p}$ collisions at $\sqrt{s}$ =1.8 TeV
Phys. Lett. **B 513** (2001) 292-300

[2] Abazov, V.M. *(et al.)*; Balm, P.W.; Bos, K.; Peters, O.; Ahmed, S.N.; Jong, S.J. de; Duensing, S.; Filhaut, F.; Wijngaarden, D.A.; D0 collaboration
Search for heavy particles decaying into electron-positron pairs in $p\bar{p}$ collisions
Phys. Rev. Lett. **87** (2001) 061802

[3] Abazov, V.M. *(et al.)*; Balm, P.W.; Bos, K.; Peters, O.; Ahmed, S.N.; Jong, S.J. de; Duensing, S.; Filhaut, F.; Wijngaarden, D.A.; D0 collaboration
High-p_T Jets in $p\overline{p}$ Collisions at $\sqrt{s}$ =630 and 1800 GeV
Phys. Rev. **D 64** (2001) 032003

[4] Abazov, V.M. *(et al.)*; Balm, P.W.; Bos, K.; Peters, O.; Ahmed, S.N.; Jong, S.J. de; Duensing, S.; Filhaut, F.; Wijngaarden, D.A.; D0 collaboration
Measurement of the ratio of differential cross sections for W and Z boson production as a function of transverse momentum in $p\overline{p}$ collisions at $\sqrt{s}$ =1.8 TeV
Phys. Lett. **B 517** (2001) 299-308

[5] Abazov, V.M. *(et al.)*; Balm, P.W.; Bos, K.; Peters, O.; Ahmed, S.N.; Jong, S.J. de; Duensing, S.; Filhaut, F.; Wijngaarden, D.A.; D0 collaboration
Search for single top quark production at D0 using neural networks
Phys. Lett. **B 517** (2001) 282-294

[6] Abazov, V.M. *(et al.)*; Balm, P.W.; Bos, K.; Peters, O.; Ahmed, S.N.; Jong, S.J. de; Duensing, S.; Filhaut, F.; Wijngaarden, D.A.; D0 collaboration
Search for first-generation scalar and vector leptoquarks
Phys. Rev. **D 64** (2001) 092004

[7] Abazov, V.M. *(et al.)*; Balm, P.W.; Bos, K.; Peters, O.; Ahmed, S.N.; Jong, S.J. de; Duensing, S.; Filhaut, F.; Wijngaarden, D.A.; D0 collaboration
Search for new physics using QUAERO: a general interface to D0 event data
Phys. Rev. Lett. **87** (2001) 231801

[8] Abazov, V.M. *(et al.)*; Balm, P.W.; Bos, K.; Peters, O.; Ahmed, S.N.; Jong, S.J. de; Duensing, S.; Filhaut, F.; Wijngaarden, D.A.; D0 collaboration
Ratio of isolated photon cross sections in $p\bar{p}$ collisions at $\sqrt{s}$ =630 and 1800 GeV
Phys. Rev. Lett. **87** (2001) 251805

[9] Abbott B. *(et al.)*; Balm, P.W.; Peters, O.; Duensing, S.; Wijngaarden, D.A.; D0 collaboration
Search for electroweak production of single top quarks in $\overline{p}p$ collisions
Phys. Rev. **D 63** (2001) 031101

[10] Abbott B. *(et al.)*; Balm, P.W.; Peters, O.; Duensing, S.; Wijngaarden, D.A.; D0 collaboration
Search for large extra dimensions in dielectron and diphoton production
Phys. Rev. Lett. **86** (2001) 1156-1161

[11] Abbott B. *(et al.)*; Balm, P.W.; Peters, O.; Duensing, S.; Wijngaarden, D.A.; D0 collaboration
Inclusive jet production in $\overline{p}p$ collisions
Phys. Rev. Lett. **86** (2001) 1707-1712

[12] Abbott B. *(et al.)*; Balm, P.W.; Peters, O.; Duensing, S.; Wijngaarden, D.A.; D0 collaboration
Measurement of the angular distribution of electrons from $W \to e\nu$ decays observed in $p\bar{p}$ collisions at $\sqrt{s}$ =1.8 TeV
Phys. Rev. **D 63** (2001) 072001

[13] Abbott, B. *(et al.)*; Balm, P.W.; Bos, K.; Peters, O.; Duensing, S.; Filhaut, F.; Wijngaarden, D.A.; D0 collaboration
A Quasi-Model-Independent Search for New High p_T Physics at D0
Phys. Rev. Lett. **86** (2001) 3712-3717

[14] Abbott, B. *(et al.)*; Duensing, S.; Wijngaarden, D.A.; D0 Collaboration
Ratios of multijet cross-sections in $p\bar{p}$ collisions at $\sqrt{s}$ =1.8 TeV
Phys. Rev. Lett. **86** (2001) 1955

[15] Abbott, B. *(et al.)*; Duensing, S.; Wijngaarden, D.A.; D0 Collaboration
The ratio of jet cross-sections at $\sqrt{s}$ =630 GeV and 1800 GeV
Phys. Rev. Lett. **86** (2001) 2523

[16] Abbot, B; *(et al.)*; Balm, P.W.; Bos, K.; Peters, O.; Duensing, S.; Filhaut, F.; Wijngaarden, D.A.; D0 collaboration
Quasi-model-independent search for new physics at large transverse momentum
Phys. Rev. **D 64** (2001) 012004

[17] Abdallah, J. *(et al.)*; Blom, H.M.; Ferreira-Montenegro, J.; Kluit, P.; Mulders, M.; Reid, D.; Timmermans, J.; Dam, P. van; Eldik, J. van; Vulpen, I. van; DELPHI Collaboration
Search for technicolor with DELPHI
Eur. Phys. J. **C 22** (2001) 17-29

[18] Abele, A. *(et al.)*; Hessey, N.; The Crystal Barrel Collaboration
Measurement of the radiative decay omega to eta gamma in proton-antiproton annihilation at rest
Phys. Rev. **D 61** (2000) 032002

[19] Abele, A *(et al.)*: Hessey, N.; The Crystal Barrel Collaboration
Test of NN potential models: Isospin relations in antiproton deuterium annihilations at rest and the search for quasinuclear bound states
Eur. Phys. J. **C 17** (2000) 583

[20] Abele, A. *(et al.)*; Hessey, N.; The Crystal Barrel Collaboration
Study of f_0 Decays into Four Neutral Pions
Eur. Phys. J. **C 19** (2001) 667

[21] Abele, A. *(et al.)*; Hessey, N.; The Crystal Barrel Collaboration
High resolution search for the tensor glueball candidate $\xi(2230)$
Phys. Lett. **B 520** (2001) 175

[22] Abele, A. *(et al.)*; Hessey, N.; The Crystal Barrel Collaboration
Branching ratios for $p\bar{p}$ annihilation at rest into two-body final states
Nucl. Phys. **A 679** (2001) 563

[23] Abreu, P. *(et al.)*; Blom, H.M.; Boudinov, E.; Kluit, P.; Mulders, M.; Reid, D.; Timmermans, J.; Dam, P. van; Eldik, J. van; Vulpen, I. van; DELPHI Collaboration
Search for a fermiophobic Higgs at LEP2
Phys. Lett. **B 507** (2001) 89-103

[24] Abreu, P. *(et al.)*; Blom, H.M.; Boudinov, E.; Kluit, P.; Mulders, M.; Reid, D.; Timmermans, J.; Dam, P. van; Eldik, J. van; Vulpen, I. van; DELPHI Collaboration
Measurement of the semileptonic b branching fractions and average b mixing parameter in Z decays
Eur. Phys. J. **C 20** (2001) 455-478

[25] Abreu, P. *(et al.)*; Blom, H.M.; Boudinov, E.; Kluit, P.; Mulders, M.; Reid, D.; Timmermans, J.; Dam, P. van; Eldik, J. van; Vulpen, I. van; DELPHI Collaboration
Measurement of V_{cb} from the decay process $\bar{B^0} \to D^{*+}\ell^-\bar{\nu}$
Phys. Lett. **B 510** (2001) 55-74

[26] Abreu, P. *(et al.)*; Blom, H.M.; Boudinov, E.; Kluit, P.; Mulders, M.; Reid, D.; Timmermans, J.; Dam, P. van; Eldik, J. van; Vulpen, I. van; DELPHI Collaboration
Measurement of the Mass and Width of the W Boson in e+e- Collisions at $\sqrt{s}$ =189 GeV
Phys. Lett. **B 511** (2001) 159-177

[27] Abreu, P. *(et al.)*; Blom, H.M.; Boudinov, E.; Kluit, P.; Mulders, M.; Reid, D.; Timmermans, J.; Dam, P. van; Eldik, J. van; Vulpen, I. van; DELPHI Collaboration
A measurement of the tau topological branching ratios
Eur. Phys. J. **C 20** (2001) 617-637

[28] Abreu, P. *(et al.)*; Blom, H.M.; Boudinov, E.; Kluit, P.; Mulders, M.; Reid, D.; Timmermans, J.; Dam, P. van; Eldik, J. van; Vulpen, I. van; DELPHI Collaboration
Measurement of Trilinear Gauge Boson Couplings WWV, $(V \equiv Z, \gamma)$ in e^+e^- Collisions at 189 GeV
Phys. Lett. **B 502** (2001) 9-23

[29] Abreu, P. *(et al.)*; Blom, H.M.; Boudinov, E.; Kluit, P.; Mulders, M.; Reid, D.; Timmermans, J.; Dam, P. van; Eldik, J. van; Vulpen, I. van; DELPHI Collaboration
Single Intermediate Vector Boson Production in e^+e^- collisions at $\sqrt{s}$ =183 and 189 GeV
Phys. Lett. **B 515** (2001) 238-254

[30] Abreu, P. *(et al.)*; Blom, H.M.; Boudinov, E.; Kluit, P.; Mulders, M.; Reid, D.; Timmermans, J.; Dam, P. van; Eldik, J. van; Vulpen, I. van; DELPHI Collaboration
Search for the Standard Model Higgs boson at LEP in the year 2000
Phys. Lett. **B 499** (2001) 23-37

[31] Abreu, P. *(et al.)*; Blom, H.M.; Boudinov, E.; Kluit, P.; Mulders, M.; Reid, D.; Timmermans, J.; Dam, P. van; Eldik, J. van; Vulpen, I. van; DELPHI Collaboration
Search for R-parity violation with a $\overline{UDD}$ coupling at $\sqrt{s}$ =189 GeV
Phys. Lett. **B 500** (2001) 22-36

[32] Abreu, P. *(et al.)*; Blom, H.M.; Boudinov, E.; Kluit, P.; Mulders, M.; Reid, D.; Timmermans, J.; Dam, P. van; Eldik, J. van; Vulpen, I. van; DELPHI Collaboration
Update of the search for supersymmetric particles in scenarios with gravitino LSP and sleptons NLSP
Phys. Lett. **B 503** (2001) 34-48

[33] Abreu, P. *(et al.)*; Blom, H.M.; Boudinov, E.; Kluit, P.; Mulders, M.; Reid, D.; Timmermans, J.; Dam, P. van; Eldik, J. van; Vulpen, I. van; DELPHI Collaboration
Study of dimuon production in photon-photon collisions and measurement of QED photon structure functions at LEP
Eur. Phys. J. **C 19** (2001) 15-28

[34] Abreu, P. *(et al.)*; Blom, H.M.; Boudinov, E.; Kluit, P.; Mulders, M.; Reid, D.; Timmermans, J.; Dam, P. van; Eldik, J. van; Vulpen, I. van; DELPHI Collaboration
Measurement of the ZZ cross-section in e^+e^- interactions at 183-189 GeV
Phys. Lett. **B 497** (2001) 199-213

[35] Abreu, P. *(et al.)*; Blom, H.M.; Boudinov, E.; Kluit, P.; Mulders, M.; Reid, D.; Timmermans, J.; Dam, P. van; Eldik, J. van; Vulpen, I. van; DELPHI Collaboration
Search for sleptons in e^+e^- collisions at $\sqrt{s}$ =183 to 189 GeV
Eur. Phys. J. **C 19** (2001) 29-42

[36] Abreu, P. *(et al.)*; Blom, H.M.; Boudinov, E.; Kluit, P.; Mulders, M.; Reid, D.; Timmermans, J.; Dam, P. van; Eldik, J. van; Vulpen, I. van; DELPHI Collaboration
Search for neutralino pair production at $\sqrt{s}$ =189 GeV
Eur. Phys. J. **C19** (2001) 201

[37] Abreu, P. *(et al.)*; Blom, H.M.; Boudinov, E.; Kluit, P.; Mulders, M.; Reid, D.; Timmermans, J.; Dam, P. van; Eldik, J. van; Vulpen, I. van; DELPHI Collaboration
Search for Spontaneous R-parity violation at $\sqrt{s}$ =183 GeV and 189 GeV
Phys. Lett. **B 502** (2001) 24

[38] Acciarri, M. *(et al.)*; Baldew, S.V.; Bobbink, G.J.; Dierckxsens, M.; Dierendonck, D.N. van; Duinker, P.; Erne, F.C.; Gulik, R. van; Jong, P. de; Linde, F.L.; Muijs, A.J.M.; Dalen, J.A. van; Hu, Y.; Kittel, W.; König, A.C.; Mangeol, D.; Metzger, W.J.; Petersen, B.; Roux, B.; Sanders, M.P.; Schotanus, D.J.; Timmermans, C.; Wilkens, H.; Buijs, A.; L3 collaboration
Measurement of the tau branching fractions into leptons
Phys. Lett. **B 507** (2001) 47-60

[39] Acciarri, M. *(et al.)*; Baldew, S.V.; Bobbink, G.J.; Dierckxsens, M.; Dierendonck, D.N. van; Duinker, P.; Erne, F.C.; Gulik, R. van; Jong, P. de; Linde, F.L.; Muijs, A.J.M.; Dalen, J.A. van; Hu, Y.; Kittel, W.; König, A.C.; Mangeol, D.; Metzger, W.J.; Petersen, B.; Sanders, M.P.; Schotanus, D.J.; Timmermans, C.; Wilkens, H.; Buijs, A.; L3 collaboration
Study of Z Boson Pair Production in e^+e^- Interactions at $\sqrt{s}$ =192-202 GeV
Phys. Lett. **B 497** (2001) 23-38

[40] Acciarri, M. *(et al.)*; Baldew, S.V.; Bobbink, G.J.; Dierckxsens, M.; Dierendonck, D.N. van; Duinker, P.; Erne, F.C.; Gulik, R. van; Jong, P. de; Linde, F.L.; Muijs,

A.J.M.; Dalen, J.A. van; Hu, Y.; Kittel, W.; König, A.C.; Mangeol, D.; Metzger, W.J.; Petersen, B.; Roux, B.; Sanders, M.P.; Schotanus, D.J.; Timmermans, C.; Wilkens, H.; Buijs, A.; L3 collaboration
Measurement of the charm production cross section in $\gamma\gamma$ collisions at LEP
Phys. Lett. **B 514** (2001) 19-28

[41] Acciarri, M. *(et al.)*; Baldew, S.V.; Bobbink, G.J.; Dierckxsens, M.; Dierendonck, D.N. van; Duinker, P.; Erne, F.C.; Gulik, R. van; Jong, P. de; Linde, F.L.; Muijs, A.J.M.; Dalen, J.A. van; Hu, Y.; Kittel, W.; König, A.C.; Mangeol, D.; Metzger, W.J.; Petersen, B.; Sanders, M.P.; Schotanus, D.J.; Timmermans, C.; Wilkens, H.; Buijs, A.; L3 collaboration
Search for heavy isosinglet neutrino in e^+e^- annihilation at LEP
Phys. Lett. **B 517** (2001) 67-74

[42] Acciarri, M. *(et al.)*; Baldew, S.V.; Bobbink, G.J.; Dierckxsens, M.; Dierendonck, D.N. van; Duinker, P.; Erne, F.C.; Filthaut, F.; Gulik, R. van; Jong, P. de; Linde, F.L.; Muijs, A.J.M.; Dalen, J.A. van; Hu, Y.; Kittel, W.; König, A.C.; Mangeol, D.; Metzger, W.J.; Petersen, B.; Roux, B.; Sanders, M.P.; Schotanus, D.J.; Timmermans, C.; Van de Walle, R.T.; Wilkens, H.; Buijs, A.; L3 collaboration
Search for heavy neutral and charged leptons in e^+e^- annihilation at LEP
Phys. Lett. **B 517** (2001) 75-85

[43] Acciarri, M. *(et al.)*; Baldew, S.V.; Bobbink, G.J.; Dierckxsens, M.; Dierendonck, D.N. van; Duinker, P.; Erne, F.C.; Filthaut, F.; Gulik, R. van; Jong, P. de; Linde, F.L.; Muijs, A.J.M.; Dalen, J.A. van; Hu, Y.; Kittel, W.; König, A.C.; Mangeol, D.; Metzger, W.J.; Petersen, B.; Roux, B.; Sanders, M.P.; Schotanus, D.J.; Timmermans, C.; Van de Walle, R.T.; Wilkens, H.; Buijs, A.; L3 collaboration
Standard model Higgs boson with the L3 experiment at LEP
Phys. Lett. **B 517** (2001) 319-331

[44] Acciarri, M. *(et al.)*; Baldew, S.V.; Bobbink, G.J.; Dierckxsens, M.; Dierendonck, D.N. van; Duinker, P.; Erne, F.C.; Gulik, R. van; Jong, P. de; Linde, F.L.; Muijs, A.J.M.; Dalen, J.A. van; Hu, Y.; Kittel, W.; König, A.C.; Mangeol, D.; Metzger, W.J.; Petersen, B.; Roux, B.; Sanders, M.P.; Schotanus, D.J.; Timmermans, C.; Wilkens, H.; Buijs, A.; L3 collaboration
Study of the $e^+e^- \to Z\gamma\gamma \to q\bar{q}\gamma\gamma$ Process at LEP
Phys. Lett. **B 505** (2001) 47-58

[45] Acciarri, M. *(et al.)*; Baldew, S.V.; Bobbink, G.J.; Dierckxsens, M.; Dierendonck, D.N. van; Duinker, P.; Erne, F.C.; Gulik, R. van; Jong, P. de; Linde, F.L.; Muijs, A.J.M.; Dalen, J.A. van; Hu, Y.; Kittel, W.; König, A.C.; Mangeol, D.; Metzger, W.J.; Petersen, B.; Roux, B.; Sanders, M.P.; Schotanus, D.J.; Timmermans, C.; Wilkens, H.; Buijs, A.; L3 collaboration
Total cross section in $\gamma\gamma$ collisions at LEP
Phys. Lett. **B 519** (2001) 33-45

[46] Acciarri, M. *(et al.)*; Baldew, S.V.; Bobbink, G.J.; Dierckxsens, M.; Dierendonck, D.N. van; Duinker, P.; Erne, F.C.; Filthaut, F.; Gulik, R. van; Jong, P. de; Linde, F.L.; Muijs, A.J.M.; Dalen, J.A. van; Hu, Y.; Kittel, W.; König, A.C.; Mangeol, D.; Metzger, W.J.; Petersen, B.; Roux, B.; Sanders, M.P.; Schotanus, D.J.; Timmermans, C.; Van de Walle, R.T.; Wilkens, H.; Buijs, A.; L3 collaboration
Measurement of the topological branching fractions of the τ lepton at LEP
Phys. Lett. **B 519** (2001) 189-198

[47] Acciarri, M. *(et al.)*; Baldew, S.V.; Bobbink, G.J.; Dierckxsens, M.; Dierendonck, D.N. van; Duinker, P.; Erne, F.C.; Gulik, R. van; Jong, P. de; Linde, F.L.; Muijs, A.J.M.; Dalen, J.A. van; Hu, Y.; Kittel, W.; König, A.C.; Mangeol, D.; Metzger, W.J.; Petersen, B.; Sanders, M.P.; Schotanus, D.J.; Timmermans, C.; Wilkens, H.; Buijs, A.; L3 collaboration
Measurements of the cross sections for open charm and beauty production in $\gamma\gamma$ collisions at $\sqrt{s}$ =189-202 GeV
Phys. Lett. **B 503** (2001) 10-20

[48] Acciarri, M. *(et al.)*; Baldew, S.V.; Bobbink, G.J.; Dierckxsens, M.; Dierendonck, D.N. van; Duinker, P.; Erne, F.C.; Gulik, R. van; Jong, P. de; Linde, F.L.; Muijs, A.J.M.; Dalen, J.A. van; Hu, Y.; Kittel, W.; König, A.C.; Mangeol, D.; Metzger, W.J.; Petersen, B.; Roux, B.; Sanders, M.P.; Schotanus, D.J.; Timmermans, C.; Wilkens, H.; Buijs, A.; L3 collaboration
Search for neutral Higgs bosons of the minimal supersymmetric standard model in e^+e^- Interactions at $\sqrt{s}$ =192-202 GeV
Phys. Lett. **B 503** (2001) 21-33

[49] Acciarri, M. *(et al.)*; Baldew, S.V.; Bobbink, G.J.; Dierckxsens, M.; Dierendonck, D.N. van; Duinker, P.; Erne, F.C.; Gulik, R. van; Jong, P. de; Linde, F.L.; Muijs, A.J.M.; Dalen, J.A. van; Hu, Y.; Kittel, W.; König, A.C.; Mangeol, D.; Metzger, W.J.; Petersen, B.; Roux, B.; Sanders, M.P.; Schotanus, D.J.; Timmermans, C.; Wilkens, H.; Buijs, A.; L3 collaboration
Light resonances in $K^0_s K^\pm \pi^\mp$ and $\eta\pi^+\pi^-$ final states in $\gamma\gamma$ collisions at LEP
Phys. Lett. **B 501** (2001) 1-11

[50] Acciarri, M. *(et al.)*; Baldew, S.V.; Bobbink, G.J.; Dierckxsens, M.; Dierendonck, D.N. van; Duinker, P.; Erne, F.C.; Gulik, R. van; Jong, P. de; Linde, F.L.; Muijs, A.J.M.; Dalen, J.A. van; Hu, Y.; Kittel, W.; König, A.C.; Mangeol, D.; Metzger, W.J.; Petersen, B.; Roux, B.; Sanders, M.P.; Schotanus, D.J.; Timmermans, C.; Wilkens, H.; Buijs, A.; L3 collaboration
$K^0_s K^0_s$ Final state in two photon collisions and implications for glueballs
Phys. Lett. **B 501** (2001) 173-182

[51] Acciarri, M. *(et al.)*; Baldew, S.V.; Bobbink, G.J.; Dierckxsens, M.; Dierendonck, D.N. van; Duinker, P.; Erne, F.C.; Gulik, R. van; Jong, P. de; Linde, F.L.; Muijs, A.J.M.; Dalen, J.A. van; Hu, Y.; Kittel, W.; König, A.C.; Mangeol, D.; Metzger, W.J.; Petersen, B.; Roux, B.; Sanders, M.P.; Schotanus, D.J.; Timmermans, C.; Wilkens, H.; Buijs, A.; L3 collaboration
Search for excited leptons in e^+e^- interactions at $\sqrt{s}$ =192-202 GeV
Phys. Lett. **B 502** (2001) 37-50

[52] Acciarri, M. *(et al.)*; Baldew, S.V.; Bobbink, G.J.; Dierckxsens, M.; Dierendonck, D.N. van; Duinker, P.; Erne, F.C.; Gulik, R. van; Jong, P. de; Linde, F.L.; Muijs,

A.J.M.; Dalen, J.A. van; Hu, Y.; Kittel, W.; König, A.C.; Mangeol, D.; Metzger, W.J.; Petersen, B.; Roux, B.; Sanders, M.P.; Schotanus, D.J.; Timmermans, C.; Wilkens, H.; Buijs, A.; L3 collaboration
Search for the standard model Higgs boson in e^+e^- collisions at $\sqrt{s}$ up to 202 GeV
Phys. Lett. **B 508** (2001) 225-236

[53] Acciarri, M. *(et al.)*; Baldew, S.V.; Bobbink, G.J.; Dierckxsens, M.; Dierendonck, D.N. van; Duinker, P.; Erne, F.C.; Gulik, R. van; Jong, P. de; Linde, F.L.; Muijs, A.J.M.; Dalen, J.A. van; Hu, Y.; Kittel, W.; König, A.C.; Mangeol, D.; Metzger, W.J.; Petersen, B.; Roux, B.; Sanders, M.P.; Schotanus, D.J.; Timmermans, C.; Wilkens, H.; Buijs, A.; L3 collaboration
Search for R-parity violating decays of supersymmetric particles in e^+e^- collisions at $\sqrt{s}$ =189 GeV
Eur. Phys. J. **C 19** (2001) 397-414

[54] Adam, W. *(et al.)*; Eijk, B. van; Hartjes, F.
Diamond pixel detectors
Nucl. Instr. Meth. **A 465** (2001) 88-91

[55] Afanasev, S.V. *(et al.)*; Leeuwen, M. van; NA49 collaboration
Event-by-event fluctuations of the kaon to pion ratio in central Pb+Pb collisions at 158-GeV per nucleon.
Phys. Rev. Lett. **86** (2001) 1965-1969.

[56] Aggarwal, M.M. *(et al.)*; Buijs, A.; Eijndhoven, N.J.A.M. van; Geurts, F.J.M.; Kamermans, R.; Pijll, E. van der; WA98 Collaboration
Localized charged-neutral fluctuations in 158 A GeV Pb plus Pb collisions
Phys. Rev. **C 64** (2001) 011901

[57] Aggarwal, M.M. *(et al.)*; Eijndhoven, N.J.A.M. van; Kamermans, R.; Pijll, E.C. van der; WA98 collaboration
Scaling of Particle and Transverse Energy Production in Pb+Pb Collisions at 158 A GeV
Eur. Phys. J. **C 18** (2001) 651

[58] Airapetian, A. *(et al.)*; Amarian, M.; Aschenauer, E.C.; Bulten, H.J.; Witt Huberts, P.K.A. de; Ferro-Luzzi, M.; Garutti, E.; Heesbeen, D.; Hesselink, W.H.A.; Hoffmann-Rothe, P.; Ihssen, H.; Kolstein, M.; Kolster, H.; Laziev, A.; Simani, C.; Steijger, J.J.M.; Brand, J.F.J. van den; Steenhoven, G. van der; Hunen, J.J. van; Visser, J.; HERMES collaboration
Hadron formation in deep-inelastic positron scattering in a nuclear environment
Eur. Phys. J. **C 20** (2001) 479-486

[59] Airapetian, A. *(et al.)*; Amarian, M.; Aschenauer, E.C.; Bulten, H.J.; Witt Huberts, P.K.A. de; Ferro-Luzzi, M.; Garutti, E.; Heesbeen, D.; Hesselink, W.H.A.; Kolster, H.; Laziev, A.; Simani, C.; Steijger, J.J.M.; Brand, J.F.J. van den; Steenhoven, G. van der; Hunen, J.J. van; Visser, J.; HERMES collaboration
Double-spin asymmetry in the cross section for exclusive ρ^0 production in lepton-proton scattering
Phys. Lett. **B 513** (2001) 301-310

[60] Airapetian, A. *(et al.)*; Amarian, M.; Aschenauer, E.C.; Bulten, H.J.; Witt Huberts, P.K.A. de; Ferro-Luzzi, M.; Garutti, E.; Heesbeen, D.; Hesselink, W.H.A.; Kolster, H.; Laziev, A.; Simani, C.; Steijger, J.J.M.; Brand, J.F.J. van den; Steenhoven, G. van der; Hunen, J.J. van; Visser, J.; HERMES collaboration
Single spin azimuthal asymmetries in electroproduction of neutral pions in semiinclusive deep inelastic scattering
Phys. Rev. **D 64** (2001) 097101

[61] Airapetian, A. *(et al.)*; Amarian, M.; Aschenauer, E.C.; Bulten, H.J.; Witt Huberts, P.K.A. de; Ferro-Luzzi, M.; Garutti, E.; Heesbeen, D.; Hesselink, W.H.A.; Hoffmann-Rothe, P.; Ihssen, H.; Kolster, H.; Laziev, A.; Simani, C.; Steijger, J.J.M.; Brand, J.F.J. van den; Steenhoven, G. van der; Hunen, J.J. van; Visser, J.; HERMES collaboration
Multiplicity of charged and neutral pions in deep-inelastic scattering of 27.5 GeV positrons on hydrogen
Eur. Phys. J. **C 21** (2001) 599-606

[62] Airapetian, A. *(et al.)*; Amarian, M.; Aschenauer, E.C.; Bulten, H.J.; Witt Huberts, P.K.A. de; Ferro-Luzzi, M.; Garutti, E.; Heesbeen, D.; Hesselink, W.H.A.; Kolster, H.; Laziev, A.; Simani, C.; Steijger, J.J.M.; Brand, J.F.J. van den; Steenhoven, G. van der; Hunen, J.J. van; Visser, J.; HERMES collaboration
Measurement of the beam-spin azimuthal asymmetry associated with deeply-virtual Compton scattering
Phys. Rev. Lett. **87** (2001) 182001

[63] Airapetian, A. *(et al.)*; Amarian, M.; Aschenauer, E.C.; Bulten, H.J.; Witt Huberts, P.K.A. de; Ferro-Luzzi, M.; Garutti, E.; Heesbeen, D.; Hesselink, W.H.A.; Kolster, H.; Laziev, A.; Simani, C.; Steijger, J.J.M.; Brand, J.F.J. van den; Steenhoven, G. van der; Hunen, J.J. van; Visser, J.; HERMES collaboration
Measurement of longitudinal spin transfer to Lambda hyperons in deep-inelastic lepton scattering
Phys. Rev. **D 64** (2001) 112005

[64] Akhmedov, E.K.; Silva-Marcos, J.I.
Neutrino masses and mixing with seesaw mechanism and universal breaking of extended democracy
Phys. Lett. **B 498** (2001) 237-250

[65] Arkhipov V.A. *(et al.)* ; Boer-Rookhuizen, H.; Heine, E.; Heubers, W.P.J.; Kaan, A.P.; Kroes, F.B.; Kuijer, L.H.; Laan, J.B. van der; Langelaar, J.; Louwrier, P.W.F.; Luijckx, G.; Maas, R.; Middelkoop, G. van; Noomen, J.G.; Spelt, J.B.
Project of the Dubna Electron Synchrotron
Nucl. Instr. Meth. **A 467-468** (2001) 59-62 Part 1

[66] Arkhipov V.A. *(et al.)* ; Boer-Rookhuizen, H.; Heine, E.; Heubers, W.P.J.; Kaan, A.P.; Kroes, F.B.; Kuijer, L.H.; Laan, J.B. van der; Langelaar, J.; Louwrier, P.W.F.; Luijckx, G.; Maas, R.; Middelkoop, G. van; Noomen, J.G.; Spelt, J.B.
Project of the Dubna electron synchrotron
Nucl. Instr. Meth. **A 470** (2001) 1-6

[67] Aniol, K.A. *(et al.)*; Templon, J.
New measurement of parity violation in elastic electron-proton scattering and implications for strange form factors
Phys. Lett. **B 509** (2001) 211-216

[68] Antinori, F. *(et al.)*; Kamermans, R.; Kuijer, P.G.; Schillings, E.; Ven, P. van de; NA57 collaboration
Study of the production of Strange and Multi-Strange Particles in Lead-Lead Interactions at the CERN SPS: the NA57 Experiment.
Nucl. Phys. **A 681** (2001) 165-173

[69] Antinori, F. *(et al.)*; Kamermans, R.; Kuijer, P.G.; Schillings, E.; NA57 collaboration
Determination of the event centrality in the WA97 and NA57 experiments
J. Phys. **G 27** (2001) 391-396

[70] Antinori, F. *(et al.)*; Kamermans, R.; Kuijer, P.G.; Schillings, E.; Ven, P. van de; NA57 collaboration
Status of the NA57 experiment at CERN SPS
J. Phys. **G 27** (2001) 383-390

[71] Apeldoorn, G. van *(et al.)*; Bakel, N. van; Bauer, T.S.; Beuzekom, M. van; Boer Rookhuizen, H.; Brand, J.F.J. van den; Bulten, H.J.; Doets, M.; Eijk, R. van den ; Gouz, I.; Groen, P. de; Gromov, V.; Hierck, R.; Hommels, L.; Jans, E.; Jansen, L.; Kaan, A.P.; Ketel, T.J.; Klous, S.; Koene, B.; Kraan, M.; Kroes, F.; Kuijt, J.; Merk, M.; Mul, F.; Needham, M.; Schuijlenburg, H.; Sluijk, T.; Tilburg, J. van; Verkooyen, J.; Vries, H. de; Wiggers, L.; Saitsev, N.; Zupan M.
LHCb VELO Technical Design Report, CERN/LHCC 2001-011
ISBN 92-9083-179-X, 31 May 2001.

[72] Apeldoorn, G. van *(et al.)*; Arink, R.; Bakel, N. van; Bauer, T.S.; Berkien, A.; Born, E. van den; Brand, J.F.J. van den; Bulten, H.J.; Carlogano, C.; Ceelie, L.; Doets, M.; Eijk, R. van den ; Gouz, I.; Groen, P. de; Gromov, V.; Hierck, R.; Hommels, L.; Jans, E.; Ketel, T.J.; Klous, S.; Koene, B.; Kruiper, H.; Merk, M.; Mul, F.; Needham, M.; Petten, O. van; Schuijlenburg, H.; Sluijk, T.; Stolte, J.; Tilburg, J. van; Vries, H. de; Wiggers, L.; Wijk, R. van; Zupan M.; Zwart, A.
LHCb Outer Tracker Technical Design Report, CERN/LHCC 2001-024
ISBN 92-9083-200-2, 14 September 2001.

[73] Atayan, M.R. *(et al.)*; Kittel, W.; EHS-NA22 collaboration
Transverse energy flow in meson-proton and meson-nucleus interactions at 250 GeV/c
Eur. Phys. J. **C 21** (2001) 271-279

[74] Ballaminut A.*(et al.)*; Koeper, D.
WIRED - World Wide Web interactive remote event display
Comput. Phys. Commun. **140** (2001) 266-273

[75] Bardelloni, G. *(et al.)*; Boerkamp, A.L.J.; Calvet, D.; Visschers, J.L.
A new read-out system for an imaging pixel detector
Proc. IEEE Nuclear Science Symposium and Medical Imaging Conf., Lyon, France, 15-20 Oct. 2000. h12.57-60

[76] Barton, R.A.; *(et al.)*; van Leeuwen, M.; Botje, M.; NA49 Collaboration
Production of multi-strange hyperons and strange resonances in the NA49 experiment.
J. Phys. **G 27** (2001) 367-374

[77] Beuzekom, M.G. van; Garutti, E.; Heesbeen, D.; Steijger, J.J.M.; Visser, J.
First experience with the HERMES silicon detector
Nucl. Instr. Meth. **A 461** (2001) 247-250

[78] Boer, F.W.N. de *(et al.)*; Dantzig, R. van
Further search for a neutral boson with a mass around 9 MeV/c^2
J. Phys. **G 27** (2001) L29-L40

[79] Boos, E. *(et al.)*; Reid, D.W.
Measuring the Higgs branching fraction into two photons at future linear e^+e^- colliders
Eur. Phys. J. **C 19** (2001) 455-461

[80] Botje, M.
Error propagation in QCD fits
Proc. DIS 2000, Ed. by J.A. Gracey, T. Greenshaw. 165-167

[81] Branford, D. *(et al.)*; Ireland, D.G.; Jager, C.W. de; Kasdorp, W.J.; Lác, J; Lapikás; Steenhoven, G. van der
Electron- and photon-induced proton knockout from ^{209}Bi
Phys. Rev. **C 63** (2001) 014310

[82] Breitweg, J. *(et al.)*; Bokel, C.; Botje, M.; Bruemmer, N.; Engelen, J.; Grijpink, S.; Koffeman, E.; Kooijman, P.; Schagen, S.; Sighem, A. van; Tiecke, H.; Tuning, W.; Velthuis, J.J.; Vossebeld, J.; Wiggers, L.; Wolf, E. de; ZEUS Collaboration
Measurement of dijet production in neutral current deep inelastic scattering at high Q^2 and determination of α_s
Phys. Lett. **B 507** (2001) 70-88

[83] Breitweg, J. *(et al.)*; Bokel, C.; Botje, M.; Bruemmer, N.; Engelen, J.; Grijpink, S.; Koffeman, E.; Kooijman, P.; Schagen, S.; Sighem, A. van; Tassi. E.; Tiecke, H.; Tuning, W.; Velthuis, J.J.; Vossebeld, J.; Wiggers, L.; Wolf, E. de; ZEUS Collaboration
Measurement of open beauty production in photoproduction at HERA
Eur. Phys. J. **C 18** (2001) 625-637

[84] Breitweg, J. *(et al.)*; Bokel, C.; Botje, M.; Bruemmer, N.; Engelen, J.; Grijpink, S.; Koffeman, E.; Kooijman, P.; Schagen, S.; Sighem, A. van; Tassi. E.; Tiecke, H.; Tuning, W.; Velthuis, J.J.; Vossebeld, J.; Wiggers, L.; Wolf, E. de; ZEUS Collaboration
Measurement of dijet cross sections for events with a leading neutron in photoproduction at HERA
Nucl. Phys. **B 596** (2001) 3-29

[85] Brown, H.N. *(et al.)*; Timmermans, C.; E821 Collaboration
Precise measurement of the positive muon anomalous magnetic moment
Phys. Rev. Lett. **86** (2001) 2227

[86] Buontempo, S. *(et al.)*; Uiterwijk, J.W.E.
The compact emulsion spectrometer
Nucl. Instr. Meth. **A 457** (2001) 464-470

[87] Burckhart, H.; Hart, R.; Jones, V.; Khomoutnikov, V.; Ryabov, Y.
Communication between Trigger/DAQ and DCS in ATLAS
Proc. Int. Conf. on Computing in High Energy and Nuclear Physics, Ed. H.S. Chen, Beijing, China, 3-7 Sept. 2001, p. 109

[88] Buuren, L.D. van; 97-01 collaboration
Measurement of spin parameters in the Δ region for the $^1\vec{H}(\vec{e},e')$ reaction.
Proc. 16^{th} Int. Conf. on Few-Body Problems in Physics (FB 16), Taipei, Taiwan, China, 6-10 Mar. 2000
Nucl. Phys. **A 684** (2001) 324c-326c

[89] Buuren, L.D. van; Szczerba, D.; van den Brand, J.F.J.; Bulten, H.J.; Ferro-Luzzi, M.; Klous, S.; Kolster, H.;

Lang, J.; Mul, F.A.; Poolman, H.R.; Simani, M.C.
Performance of a hydrogen/deuterium polarized gas target in a storage ring
Nucl. Instr. Meth. **A 474** (2001) 209-223

[90] Carloganu, C.
Study of atmospheric neutrino oscillations in ANTARES
Nucl. Phys. **B (Proc. Suppl.) 100** (2001) 145-147

[91] Chekanov, M. *(et al.)*; Bokel, C.; Botje, M.; Engelen, J.; Grijpink, S.; Koffeman, E.; Kooijman, P.; Schagen, S.; Sighem, A. van; Tassi, E.; Tiecke, H.; Tuning, W.; Velthuis, J.J.; Vossebeld, J.; Wiggers, L.; Wolf, E. de; ZEUS Collaboration
Multiplicity moments in deep inelastic scattering at HERA
Phys. Lett. **B 510** (2001) 36-54

[92] Chekanov, M. *(et al.)*; Bokel, C.; Botje, M.; Engelen, J.; Grijpink, S.; Koffeman, E.; Kooijman, P.; Schagen, S.; Sighem, A. van; Tassi, E.; Tiecke, H.; Tuning, W.; Velthuis, J.J.; Vossebeld, J.; Wiggers, L.; Wolf, E. de; ZEUS Collaboration
Study of the effective transverse momentum of partons in the proton using prompt photons in photoproduction at HERA
Phys. Lett. **B 511** (2001) 19-32

[93] Chekanov, M. *(et al.)*; Bokel, C.; Engelen, J.; Grijpink, S.; Maddox, E.; Koffeman, E.; Kooijman, P.; Schagen, S.; Tassi, E.; Tiecke, H.; Tuning, W.; Velthuis, J.J.; Wiggers, L.; Wolf, E. de; ZEUS Collaboration
Three-jet production in diffractive deep inelastic scattering at HERA
Phys. Lett. **B 516** (2001) 273-292

[94] Chekanov, M. *(et al.)*; Bokel, C.; Botje, M.; Bruemmers, N.; Engelen, J.; Grijpink, S.; Koffeman, E.; Kooijman, P.; Schagen, S.; Sighem, A. van; Tassi, E.; Tiecke, H.; Tuning, W.; Velthuis, J.J.; Vossebeld, J.; Wiggers, L.; Wolf, E. de; ZEUS Collaboration
Search for resonance decays to a $\bar{\nu}$ plus jet in e^+p scattering at DESY HERA
Phys. Rev. **D 63** (2001) 052002

[95] Chekanov, S. *(et al.)*; Bokel, C.; Engelen, J.; Grijpink, S.; Maddox, E.; Koffeman, E.; Kooijman, P.; Schagen, S.; Tassi, E.; Tiecke, H.; Tuning, W.; Velthuis, J.J.; Wiggers, L.; Wolf, E. de; ZEUS Collaboration
Measurement of the neutral current cross section and F_2 structure function for deep inelastic e^+p scattering at HERA
Eur. Phys. J. **C 21** (2001) 443-471

[96] Dalen, J.A. van
Bose-Einstein correlations in W-pair production at LEP: results from L3 and OPAL
Proc. IX Int. Workshop on Multiparticle Production "New frontiers in soft physics and correlations on the threshold of the third millennium", Villa Gualino, Torino, Italy,
Nucl. Phys. **B (Proc. Suppl.) 92** (2001) 247

[97] Danby, G.T. *(et al.)*; Timmermans, C.; E821 Collaboration
The Brookhaven muon storage ring magnet
Nucl. Instrum. Meth. **A 457** (2001) 151

[98] Dantzig, R. van; ANTARES collaboration
ANTARES, Physics potential, progress and status
Proc. Europhysics Neutrino Oscillation Workshop (NOW 2000), Conca Specchiulla, Otranto, Lecce, Italy, 9-16 Sep 2000,
Nucl. Phys. **B (Proc. Suppl.) 100** (2001) 341-343

[99] Dinapoli, R. *(et al.)*; San Segundo Bello, D.
A front-end for silicon pixel detectors in ALICE and LHCb
Nucl. Instr. Meth. **A 461** (2001) 492-495

[100] Doerrzapf, M.; Gato-Rivera, B.
Singular dimensions of the N=2 superconformal algebras II: The twisted N=2 algebra
Commun. Math. Phys. **220** (2001) 263-292

[101] Eskut, E. *(et al.)*; Dantzig, R. van; Konijn, J.; Melzer, O.; Oldeman, R.G.D.; Pesen, E.; Poel, C.A.F.J. van der; Uiterwijk, J.W.E.; Visschers, J.L.; CHORUS collaboration
New results from a search for $\nu_\mu \to \nu_\tau$ and $\nu_e \to \nu_\tau$ oscillation
Phys. Lett. **B 497** (2001) 8-22

[102] Eskut, E. *(et al.)*; Dantzig, R. van; Jong, M. de; Konijn, J.; Melzer, O.; Oldeman, R.G.D.; Pesen, E.; Poel, C.A.F.J. van der; Uiterwijk, J.W.E.; Visschers, J.L.; CHORUS collaboration
Observation of weak neutral current neutrino production of J/ψ
Phys. Lett. **B 503** (2001) 1-9

[103] Filthaut, F.
Production and testing of the D0 silicon microstrip tracker
Proc. IEEE Nuclear Science Symposium And Medical Imaging Conf., Lyon, France, 15-20 oktober 2000, Ed. J.D. Valentine, Piscataway, IEEE, 2001,
IEEE Trans. Nucl. Sci. **48** (2001) 1002

[104] Fissum, K.G. *(et al.)*; Templon, J.A.
Vertical drift chambers for the Hall A high-resolution spectrometers at Jefferson Lab
Nucl. Instr. Meth. **A 474** (2001) 108-131

[105] Fornaini, A.; Calvet, D.; Visschers, J.L.
Soft X-ray sensitivity of a photon-counting hybrid pixel detector with a silicon sensor matrix
Nucl. Instr. Meth. **A 466** (2001) 142-145

[106] Gaskell, D. *(et al.)*; Volmer J., Zihlman B.
Longitudinal Electroproduction of Charged Pions from ^1H, ^2H, and ^3He
Phys. Rev. Lett. **87** (2001) 202301

[107] Gaskell, D. *(et al.)*; Volmer J.
Measurement of longitudinal and transverse cross sections in the $^3He(e,e'\pi^+)^3H$ reaction at $W = 1.6$ GeV
Phys. Rev. **C 65** (2001) 011001R

[108] Greene, B.R.; Schalm, K.; Shiu, G.
Dynamical topology change in M theory
J. Math. Phys. **42** (2001) 3171-3187

[109] Groep, D.L.*(et al.)*; Batenburg, M.F. van; Bauer, Th.S.; Blok, H.; Boersma, D.J.; Heimberg, P.; Hesselink, W.H.A.; Jans, E.; Lapikás, L.; Onderwater, C.J.G.; Starink, R.; Steenbakkers, M.F.M.; Vries, H. de
Investigation of the Exclusive $^3He(e,e'pp)$ Reaction
Phys. Rev. **C 63** (2001) 014005

[110] Groot Nibbelink, S.; Nyawelo, T.S.; Holten, J.W. van
Construction and analysis of anomaly-free supersymmetric SO(2N)/U(N) σ-models
Nucl. Phys. **B 594** (2001) 441-476

[111] Hakobyan, R.
Comparison of the pion emission function in hadron-hadron and heavy ion collisions
Proc. 30^{th} Int. Symposium on Multiparticle Dynamics, Ed. R. Csörgő, S. Hegyi and W. Kittel (World Scientific, Singapore, 2001) p.331

[112] Hegyi, S.; Kittel, W.
From e^+e^- to heavy ion collisions
Ed. T. Csörgő, Proc. Multiparticle Dynamics, ISMD 2000, October 9-15, 2000, Published in Singapore World Scientific (2001) 639 p

[113] Hommels, B.
The LHCb outer tracker
Nucl. Instr. Meth. **A 462** (2001) 278-284

[114] Hulsbergen, W.
Status of the HERA-B experiment
Acta Phys. Pol. **B 32** (2001) 1791-1808

[115] Iodice, M. *(et al.)*; Groep, D.L.; Jans, E.; Lapikás, L.; Hesselink, W.H.A. C.J.G. Onderwater, R. Starink
High missing-energy and angular dependence studies of the reaction ^{16}O(e,e'p)
Proc. Fifth workshop on Electromagnetically Induced Two-Hadron Emission, June 13-16, 2001, Lund, Sweden

[116] Jans, E.; Groep, D.L.; Hesselink, W.H.A.
What can one learn from 3He(e,e'pp)n about correlations and currents in the three-nucelon system?
Proc. Fifth Workshop on Electromagnetically Induced Two-Hadron Emission, June 13-16, 2001, Lund, Sweden

[117] Jong, P. de
Colour reconnection in W decays
Proc. 30^{th} Int. Conf. on High Energy Physics, World Scientific, Osaka, Japan, 2000; 2 vol. 694-7 vol.1

[118] Kerner, R. *(et al.)*; Holten, J.W. van
Geodesic deviation in Kaluza-Klein theories
Phys. Rev. **D 63** (2001) 027502

[119] Kerner, R.; Holten, J.W. van; Colistete, R. Jr.
Relativistic epicycles: Another approach to geodesic deviations
Class. Quantum Grav. **18** (2001) 4725-4742

[120] Kidonakis, N. *(et al.)*; Laenen, E.
Sudakov resummation and finite order expansions of heavy quark hadroproduction cross-sections
Phys. Rev. **D 64** (2001) 114001

[121] Kittel, W.
Bose-Einstein correlations in Z fragmentation and other reactions
Proc. XLI Cracow School of Theoretical Physics, Zakopane, Polen, Ed. A. Białas, M.A. Nowak and M. Sadzikowski (Jagellonian University, Cracow, 2001)
Acta Phys. Pol. **B 32** (2001) 3927

[122] Kittel, W.
Interconnection Effects and W^+W^- Decays
Proc. $XXXIV^{th}$ Rencontres de Moriond, '99 QCD and High Energy Hadronic Interactions, Ed. J. Tran Thanh Van (The Gioi Publishers, Vietnam, 2001) p.71

[123] Kjaer, N; Mulders, M
Mixed Lorentz Boosted Z^0's
CERN-OPEN/2001-026 (2001)

[124] Kluit, P.M.
Rare B decays at LEP
Nucl. Instr. Meth. **A 462** (2001) 108-110

[125] Kluit, R; Timmer, P.; Schipper, J.D.; Gromov, V.; Haas, A. de
Design of ladder EndCap electronics for the ALICE ITS SSD
Proc. Seventh workshop on electronics for LHC experiments (2001) 47-51

[126] Koffeman, E.N.
The construction of the ZEUS micro vertex detector
Nucl. Instr. Meth. **A 473** (2001) 26-30

[127] Kozlov, A. *(et al.)*; Templon, J.A.
The longitudinal and transverse response of the ^4He(e,e'p) reaction in the dip region
Nucl. Phys. **A 684** (2001) 460C-463C

[128] Kramer, G.J.; Blok, H.P.; Lapikás, L.;
A consistent analysis of (e,e'p) and (d,^{3}He) experiments
Nucl. Phys. **A 679** (2001) 267-286

[129] Laenen, E. *(et al.)*
Combined recoil and threshold resummation for hard scattering cross sections
Proc. 30^{th} Int. Conf. on High Energy Physics, World Scientific, Osaka, Japan, 2000; 2 vol. 551-3 vol.1

[130] Laenen, E.; Sterman, G.; Vogelsang, W.
Recoil and threshold corrections in short-distance cross-sections
Phys. Rev. **D 63** (2001) 114018

[131] Laenen, E.; Sterman, G.; Vogelsang, W.
Power corrections in eikonal cross-sections
Proc. 30^{th} Int. Conf. on High-Energy Physics, World Scientific, Osaka, Japan, 2000; vol. 2:1411-1413

[132] Leeuwe, J.J. van; Hesselink, W.H.A.; Jans, E.; Kasdorp, W.J.; Onderwater, C.J.G.; Pellegrino, A.R. Templon, J.A.
The ^4He(e, e'p) cross section at high missing energies
Phys. Lett. **B 523** (2001) 6-12

[133] Liyanage, N. *(et al.)*; Templon, J.A.
Dynamics of the ^{16}O(e,e'p) reaction at high missing energies
Phys. Rev. Lett. **86** (2001) 5670-5674

[134] Mangeol, D.J.
Moments of the charged-particle multiplicity distribution in Z decays at LEP
Proc. 30^{th} Int. Symposium on Multiparticle Dynamics, Ed. R. Csörgő, S. Hegyi and W. Kittel (World Scientific, Singapore, 2001) p.312

[135] Matorras, F.; Reid, D.W.
Measurement of the tau topological branching ratios
Nucl. Phys. **B (Proc. Suppl.) 98** (2001) 191-200

[136] De Meyer, G. *(et al.)*; Aschenauer, E.C.; Blok, H.P.; Groep, D.; Hicks, K.; Jans, E.; Lapikás, L.; Nooren, G.J.L.; Onderwater, C.J.G.; Schipper, J.D.; Steijger, J.J.M.; Steenbakkers, M.F.M.; Steenhoven, G. van der; Uden, M.A. van; Volmer, J.
Alpha-cluster knockout in the ^{16}O(e,e'α)^{12}C reaction
Phys. Lett. **B 513** (2001) 258-264

[137] Moch, S.; Vermaseren, J.A.M.; Vogt, A.
Next-to-next-to leading order QCD corrections to the photon's parton structure
Nucl. Phys. **B 621** (2002) 413-458

[138] Nagorny, S.
Comment on "Radiative proton-deuteron capture in a gauge invariant relativistic model"
Phys. Rev. **C 63** (2001) 019801

[139] Nikolenko, D.M. *(et al.)*; Jager, C.W. de; Vries, H. de
Measurement of polarization observables in elastic and inelastic electron deuteron scattering at the VEPP-3 storage ring
Proc. 16^{th} Int. Conf. on Few-Body Problems in Physics (FB 16), Taipei, Taiwan, China, 6-10 Mar. 2000
Nucl. Phys. **A 684** (2001) 525-527

[140] Nyawelo, T.S.; Holten, J.W. van; Groot Nibbelink, S.
Superhydrodynamics
Phys. Rev. **D 64** (2001) 021701

[141] Oldeman, R.G.C.
Measurement of differential neutrino-nucleon cross-sections and structure functions using the CHORUS lead calorimeter
Proc. 30^{th} Int. Conf. on High Energy Physics, World Scientific, Osaka, Japan, 2000; 2 vol. 516-8 vol.1

[142] Phaf, L.; Weinzierl, S.
Dipole formalism with heavy fermions
J. High Energy Phys. **04** (2001) 006

[143] Reid, D.W.
Review of the neutral current
Nucl. Phys. **B (Proc. Suppl.) 98** (2001) 105-114

[144] Reinhold, J. *(et al.)*; Volmer, J.; Zihlman, B.)
Electroproduction of kaons and light hypernuclei
Nucl. Phys. **A 684** (2001) 1

[145] Retey, A.; Vermaseren, J.A.M.
Some higher moments of deep inelastic structure functions at next-to-next-to-leading order of perturbative QCD
Nucl. Phys. **B 604** (2001) 281-311

[146] San Segundo Bello, D.; Visschers, J.
Design of pixel-level ADC's for energy sensitive hybrid pixel detectors
Proc. IEEE Nuclear Science Symposium and Medical Imaging Conf., Lyon, France, 15-20 Oct. 2000. h9.98-100

[147] San Segundo Bello, D.; Nauta, B.; Visschers, J.
Design of analog-to-digital converters for energy-sensitive hybrid pixel detector
Nucl. Instr. Meth. **A 466** (2001) 218-225

[148] Schellekens, A.N.; Sousa, N.
Open descendants of U(2N) orbifolds at rational radii
Int. J. Mod. Phys. **A 16** (2001) 3659-3671

[149] Schellekens, A.N.; Stanev, Ya.S.
Trace formulas for annuli
J. High Energy Phys. (2001) 0112:012

[150] Schulte, E.C. *(et al.)*; Blok, H.P.; Zihlman, B.
Measurement of the High Energy Two-Body Deuteron Photodisintegration Differential Cross Section
Phys. Rev. Lett. **87** (2001) 102302

[151] Snoeys, W. *(et al.)*; San Segundo Bello, D.
Pixel readout chips in deep submicron CMOS for ALICE and LHCb tolerant to 10 Mrad and beyond
Nucl. Instr. Meth. **A 466** (2001) 366-375

[152] Snoeys, W. *(et al.)*; San Segundo Bello, D.
Pixel readout electronics development for the ALICE pixel vertex and LHCb RICH detector
Nucl. Instr. Meth. **A 465** (2001) 176-189

[153] Steenhoven, G. van der; HERMES collaboration
Nuclear effects in $R = \sigma_L/\sigma_T$ in DIS
Proc. DIS 2000 Ed. by J.A. Gracey, T. Greenshaw. 124-125

[154] Steenhoven, G. van der
De nieuwe kernfysica : een spel van quarks en gluonen
Ned. T. Nat. **67** (2001) 322-325

[155] Steenhoven, G. van der; HERMES Collaboration
Hard Exclusive Processes at HERMES
Proc. Eighth Conf. on Mesons and Light Nuclei, Prague, Czech Republic, July 2-6, 2001, Ed. J. Adam, P. Bydzovsky and J. Mares, AIP Conference Proceedings **603** (2001) 161

[156] Steenhoven, G. van der
HERMES: first observation of Compton scattering at the quark level
Nucl. Phys. News Int. **11**, No. 4 (2001) 30

[157] Steenhoven, G. van der
Retirement and policy making at NIKHEF - a symposium
Nucl. Phys. News Int. **11**, No. 4 (2001) 32

[158] Timmermans, C.
Onderzoek naar kosmische muonen met de L3 detector
In jaarboek 2000, Vereniging van Akademie-onderzoekers "Over de grenzen van het weten", Amsterdam, 2001, p.83

[159] Tuning, N.; ZEUS collaboration
Measurement of F_2 and xF_3 structure functions with the ZEUS detector
Proc. DIS 2000, Ed. by J.A. Gracey, T. Greenshaw. 87-89

[160] Virgili, T.; Antinori, F. *(et al.)*; Botje, M.; Haas, A.P. de; Kamermans, R.; Kuijer, P.G.; Schillings, E.; Brink, A. van den; Ven, P. van de; Eijndhoven, N. van
Study of the production of strange and multi-strange particles in lead-lead interactions at the CERN SPS: the NA57 experiment
Nucl. Phys. **A 681** (2001) 165C-173C

[161] Volmer J.; Blok, H.P.
Measurement of the charged pion electromagnetic form factor
Phys. Rev. Lett. **86** (2001) 1713-1716

[162] Weinzierl, S.; Yakovlev, O.
New approach for calculating heavy-to-light form factors with QCD sum rules on the light-cone
J. High Energy Phys. **01** (2001) 005

[163] White, V. *(et al.)*; Bos, K.; Leeuwen, W. van
The D0 Data Handling System
Proc. Int. Conf. on Computing in High Energy and Nuclear Physics, Ed. H.S. Chen, Beijing, China, 3-7 Sept. 2001, p20

2 PhD Theses

[1] Mil, A. van
Cosmic-Ray Muons in the L3 Detector
Katholieke Universiteit Nijmegen, January 2001

[2] Batenburg, Marinus Franciscus van
Deeply-bound protons in ^{208}Pb
Universiteit Utrecht, March 2001

[3] Melzer, Oliver
Study of charm production by neutrinos in nuclear emulsion
Universiteit van Amsterdam, April 2001

[4] Harvey, Mark
Inclusive scattering of electrons from polarized ^{3}He
Hampton University, May 2001

[5] Ven, Peter van de
Centrality Dependence of Λ Production in Pb-Pb Collisions
Universiteit Utrecht, May 2001

[6] Muijs, Alexandra Jantina Monica
Tau pair production above the Z resonance
Katholieke Universiteit Nijmegen, September 2001

[7] Mulders, Martijn Pieter
Direct measurement of the W boson mass in e^+e^- collisions at LEP
Universiteit van Amsterdam, September 2001

[8] Tuning, Niels
Proton structure functions at HERA
Universiteit van Amsterdam, September 2001

[9] Rodrigues, Joao Miguel Pereira Resina
Modelling quark and gluon correlation functions
Vrije Universiteit Amsterdam, October 2001

[10] Sichtermann, Ernst Paul
The nucleon structure fuction g_1 from deep-inelastic muon scattering
Vrije Universiteit Amsterdam, October 2001

[11] Gulik, Robert Christiaan Wilhelmus van
Resonance production in two-photon collisions
Universiteit Leiden, November 2001

[12] Agasi, Erwin
Kaon prodution in τ-decays
Universiteit van Amsterdam, December 2001

3 Invited Talks

[1] M. van den Akker
Looking for Gamma-Ray sources using the L3+Cosmics experiment at CERN
NNV najaarsvergadering, Lunteren, October 26, 2001

[2] M. Botje
Error Estimates on Parton Density Distritubions
New Trends in Hera Physics 2001, Ringberg Castle, Tegernsee (Germany), June 17-22, 2001.

[3] J.F.J. van den Brand and M. Merk
Topical Lectures on Discrete Symmetries
NIKHEF, Amsterdam, June 14, 2001

[4] M. Bruinsma
Charmonium physics at Hera-B
Hard Probe Collaboration meeting, NBI, Copenhagen (Denmark), May 18, 2001.

[5] M. Bruinsma
Quarkonium suppression at Hera-B
Seminar, CERN Heavy Ion Forum, CERN, Geneva (Switserland), July 5, 2001.

[6] H.J. Bulten
Distributed Computing and LHCb
NIKHEF, Amsterdam, June 26, 2001

[7] J. van Dalen
Bose-Einstein correlations in WW events at LEP
XXXIst Int. Symposium on Multiparticle Dynamics (ISMD 2001), Datong (China), September 1-7, 2001

[8] J. van Dalen
Bose-Einstein correlations: the only known tool to obtain information about the space-time structure of the hadron source from the measured particle momenta
Hua-Zhong Normal University, Wuhan, (China), September 13, 2001

[9] J. van Dalen
Bose-Einstein correlations in e^+e^- events at LEP
Hua-Zhong Normal University, Wuhan (China), September 14, 2001

[10] J. van Dalen
Bose-Einstein correlations in WW events at LEP
NNV najaarsvergadering, Lunteren, October 26, 2001

[11] M. Dierckxsens
Resonance Production in gamma-gamma collisions at L3
EPS Conf. Budapest (Hungary), July 12-18, 2001

[12] A. Doubi
Magnetic Monopoles Search with the ANTARES detector
HEFIN Colloquium, June 7, 2001

[13] S. Duensing
Tau identification at D0
NNV najaarsvergadering, Lunteren, October 26, 2001

[14] N.J.A.M. van Eijndhoven
Heavy-Ion Physics at CERN: From SPS to the ALICE LHC experiment
Physics colloquium University of Bergen, Bergen (Norway), April 18, 2001.

[15] N.J.A.M. van Eijndhoven
Physics Aspects of Heavy-Ion Collisions
Physics colloquium, Nikhef Amsterdam, October 19,2001.

[16] N.J.A.M. van Eijndhoven
From Woodblock to Expanding Universe
Invited evening lecture, Kiwanis Utrecht, November 20, 2001.

[17] N.J.A.M. van Eijndhoven
In the Light of the Quark-Gluon Plasma : A Thermometer in the Big Bang
Astrophysics department Utrecht, December 3, 2001.

[18] N.J.A.M. van Eijndhoven
The Quest for the Quark Soup
Third North West Europe Nuclear Physics Conf., Bergen (Norway), April, 2001

[19] J.J. Engelen
ep Scattering at 300 GeV
Colloquium, KVI Groningen, October 16, 2001

[20] J.J. Engelen
De detectie van kosmische neutrino's
Koninklijk Natuurkundig Gezelschap, Groningen, October 16, 2001

[21] J.J. Engelen
Antares: een detector voor kosmische neutrino's
Diligentia, Den Haag, September 24, 2001

[22] J.J. Engelen
Status of the LHC Experimental Programme
7th Workshop on Electronics for LHC Experiments, Stockholm (Sweden), September 2001

[23] T.O. Eynck
Resummation and polarized heavy quark production
Natl. Theoretical Physics Seminar, NIKHEF Amsterdam, October 12, 2001

[24] T.O. Eynck
Comparison of phase space slicing and dipole subtraction methods
NNV najaarsvergadering, Lunteren, October 2001

[25] R. Hart
Communication between Trigger/DAQ and DCS in ATLAS
CHEP01, Beijing (China), September 2001

[26] E. Garutti
Fisica dello spin ad HERMES
Lecture at the University of Ferrara, Ferrara (Italy), May 26, 2001

[27] E. Garutti
Hadron Formation in Nuclei in Deep-Inelastic Scattering
NNV najaarsvergadering, Lunteren, The Netherlands, October 26, 2001

[28] E. Garutti
Physics at HERMES (an experiment to study the structure function of the nucleon)
ZEUS PhD Colloquia, DESY, Hamburg (Germany), December 1, 2001

[29] F. Hartjes
Diamond as a Detector for High Energetic Particles
University of Florence, Florence (Italy), November 23, 2001

[30] J.W. van Holten
Worldline deviations and epicycles
Journees Relativistes, Dublin (Ireland), September 2001

[31] J.W. van Holten
Aspects of BRST-Quantization
Lectures at the summerschool "Geometry and Topology in Physics" Rot a/d Rot (Germany), September 2001

[32] Y. Hu
Searches of the Standard Model Higgs Boson in e^+e^- collisions with the L3 detector at LEP
HEFIN Colloquium, February 8, 2001

[33] Y. Hu
Searches for the SM Higgs boson with leptons in the final state with L3 detector at LEP
NNV najaarsvergadering, Lunteren, October 26, 2001

[34] L. Huiszoon
The Geometry of WZW Orientifolds
Univ. of Rome 'Tor Vergata', Rome (Italy), December 3, 2001

[35] L. Huiszoon
The Geometry of WZW Orientifolds
RUG, Groningen, December 11, 2001

[36] W. Hulsbergen
Status of the Hera-B Experiment
Cracow Epiphaniy Conf on b-Physics and CP violation, Cracow (Poland), January 5-7, 2001

[37] E. Jans
What can one learn from ^{3}He(e,e'pp)n about correlations and currents in the three-nucelon system?
Fifth Workshop on "Electromagnetically induced Two-Hadron Emission", Lund (Sweden), June 13-16, 2001

[38] S.J. de Jong
IT uses and developments in Experimental High Energy Physics
CSI Colloquium, KUN, Nijmegen, February 12, 2001

[39] S.J. de Jong
The Tevatron: Hadron collider physics
Hua-Zhong Normal University, Wuhan (China), June 13, 2001

[40] S.J. de Jong
D0: Run 1 results
Hua-Zhong Normal University, Wuhan (China), June 14, 2001

[41] S.J. de Jong
D0: Run 2 prospects
Wuhan central normal university, Wuhan (China), June 14, 2001

[42] S.J. de Jong
Standard Model Higgs
Hua-Zhong Normal University, Wuhan (China), June 15, 2001

[43] S.J. de Jong
Non-SM Higgses and SUSY
Hua-Zhong Normal University, Wuhan (China), June 18, 2001

[44] S.J. de Jong
Semiconductor tracking detector techniques
Hua-Zhong Normal University, Wuhan (China), June 19, 2001

[45] S.J. de Jong
The TESLA project
Hua-Zhong Normal University, Wuhan (China), June 20, 2001

[46] W. Kittel
Introductory review of correlations and fluctuations
XXXIst Int. Symposium on Multiparticle Dynamics (ISMD 2001), Datong (China), September 1-7, 2001

[47] W. Kittel
Review of experimental constraints on Bose-Einstein modelling
WW Physics Workshop, Cetraro (Italy), October 12-17, 2001

[48] W. Kittel
Correlations in e^+e^- collisions
Symposium in Honor of N. Antoniou, Univ. of Athens (Greece), November 9, 2001

[49] W. Kittel
Correlations in e^+e^-, hp and AA collisions
Winterschool on Heavy Ion Physics, Budapest, (Hungary), December 5-7, 2001

[50] W. Kittel
Introduction to correlations and fluctuations
IPP Workshop on Multiparticle Production in QCD Jets, Durham (UK), December 12-15, 2001

[51] P.M. Kluit
B_s oscillations
Int. Conf. on Flavor Physics (ICPF2001), Zhang-Jia-Jie (China)

[52] E. Laenen
The strong interaction
Lectures at the University of Iceland (Reykjavik), April 2001

[53] E. Laenen
Resummation in QCD and summary talk
Les Houches workshop on Physics at TeV Colliders, Les Houches (France), May 2001

[54] E. Laenen
Opportunities in Heavy Flavour Physics with HERA II
DESY, Hamburg (Germany), July 2001

[55] E. Laenen
Heavy Flavour Production at HERA
Bonn University, Bonn (Germany), July 2001

[56] E. Laenen
The Standard Model and the Strong Force
Physics Colloquium, RUG (Groningen), September 2001

[57] E. Laenen
Threshold Effects in Heavy Quark Production
Torino University, Torino (Italy), October 2001

[58] L. Lapikás
Radiative corrections in A(e,e')
Workshop on Radiative Corrections, Hamburg (Germany), February 2, 2001

[59] L. Lapikás
Rescattering and the ^{208}Pb(e,e'p) reaction
Miniworkshop on Rescattering, Tübingen (Germany), October 22, 2001

[60] W. Lavrijsen
COmBined muon Reconstruction for Atlas
Atlas Software Workshop, Frascati (Italy), May 16, 2001

[61] W. Lavrijsen
COmBined muon Reconstruction for Atlas
Atlas Physics Workshop, Lund (Sweden), September 13, 2001

[62] W. Lavrijsen
ComBined muon reconstruction for Atlas
NNV najaarsvergadering, Lunteren, October 26, 2001

[63] W.J. Metzger
New Bose-Einstein results from L3
XXXIst Int. Symposium on Multiparticle Dynamics (ISMD 2001), Datong (China), September 1-7, 2001

[64] W.J. Metzger
Tuning QCD Monte Carlo programs in L3
WW Physics Workshop, Cetraro (Italy), October 15, 2001

[65] W.J. Metzger
FSI Outlook
WW Physics Workshop, Cetraro (Italy), October 17, 2001

[66] W.J. Metzger
Rapidity Gaps and Colour (Re-)Connection
IPP Workshop on Multiparticle Production in QCD Jets, Durham (UK), December 14, 2001

[67] V. Mexner
Spin-asymmetry of photo-produced high-p_T hadron pairs in HERMES
NNV najaarsvergadering, Lunteren, The Netherlands, October 26th, 2001

[68] N.A. Naumann
HEP Particle Classes in ROOT
ROOT2001, Int. HENP ROOT Users Workshop, Fermilab, Batavia Ill. (USA), June 14, 2001

[69] T.S. Nyawelo
Supersymmetric hydrodynamics
Inst. Theor. Physics RUG (Groningen), November 30, 2001

[70] M.P. Sanders
Measurement of Bose-Einstein correlations between neutral (and charged) pions from hadronic Z decays
University of Manchester, Manchester (UK), March, 2001

[71] M. Sanders
Bose-Einstein correlations of neutral and charged pions in hadronic Z decays
NNV najaarsvergadering, Lunteren, October 26, 2001

[72] A.N. Schellekens
Open ends in string theory
Univ. of Rome 'Tor Vergata', Rome (Italy), April 4, 2001

[73] A.N. Schellekens
Open ends in string theory
Univ. di Firenze, Florence (Italy), April 16, 2001

[74] A.N. Schellekens
Open ends in string theory
Univ. di Genova, Genua (Italy), April 23, 2001

[75] A.N. Schellekens
Open ends in string theory
Vrije Univ. Amsterdam, May 23, 2001

[76] M.C. Simani
Spin physics at HERMES
Advanced study institute: symmetries and spin, Int. school-workshop 'Prague-Spin-2001', Prague (Czech Republic), July 15-28, 2001

[77] N. Sousa
Recent advances in string theory
Univ. Coimbra, Coimbra (Portugal), January 5, 2001

[78] G. van der Steenhoven
Skewed Parton Distributions at HERMES, ELFE and TESLA-N
Workshop on "Skewed Parton Distributions", European ESOP RTM network, Orsay (France), January 18, 2001

[79] G. van der Steenhoven
Deep-inelastic scattering on nuclei
Workshop on "Correlations in nucleons and nuclei", Institute for Nuclear Theory (INT), Seattle, Washington (USA), March 19, 2001

[80] G. van der Steenhoven
The role of the nucleus in (polarized) deep-inelastic scattering
Third North West Europe Nuclear Physics Conf., Bergen (Norway), April 18, 2001

[81] G. van der Steenhoven
De nieuwe kernfysica: een spel van quarks en gluonen
Inaugurele rede, Rijksuniversiteit Groningen, Groningen, June 5, 2001

[82] G. van der Steenhoven
Introduction
Symposium ter gelegenheid van het afscheid van prof. dr. Ger van Middelkoop als directeur van NIKHEF: "Past and future policies on facilities for nuclear and high energy physics research", Amsterdam, 22 June 2001

[83] G. van der Steenhoven
Hard Exclusive Processes at HERMES
Eighth Conf. on Mesons and Light Nuclei, Prague, (Czech Republic), July 4, 2001

[84] G. van der Steenhoven
Spin Physics: where will we be in 2006?
IPPP Workshop on Future Physics at HERA, Durham (UK), December 6-7, 2001

[85] J.A.M. Vermaseren
How to compute three-loop QCD structure functions
University of Helsinki, Helsinki (Finland), March 2001

[86] J.A.M. Vermaseren
Modern Computer Algebra
Symposium in honour of prof. dr. M. Veltman, University of Amsterdam, May 2001

[87] J.A.M. Vermaseren
Ingredients of a three-loop structure functin calculation
University of Tokyo, Tokyo (Japan), November 2001

[88] J. Visser
Nuclear Effects in Deep Inelastic Scattering
Workshop on Perspectives in Hadronic Physics, Trieste (Italy), May 7-11, 2001

[89] H. Wilkens
Preliminary results from L3+Cosmics
NNV najaarsvergadering, Lunteren, October 26, 2001

[90] B. Wijngaarden
b-Tagging at D0
NNV najaarsvergadering, Lunteren, October 26, 2001

[91] B. Zihlmann
Nuclear Effects on $R = \sigma_L/\sigma_T$ in Deep Inelastic Scattering
Department of Physics, University of Basel, Basel (Switzerland), June 7, 2001

4 Seminars at NIKHEF

[1] January 19, 2001
M. Mulders
The Art of W mass reconstruction in Delphi

[2] January 23, 2001
D. Reid
The Lorentz structure of τ decays

[3] January 24, 2001
S. Soldner-Rembold
The Hunt for the Higgs Boson at LEP

[4] January 29, 2001
M. Vreeswijk
The Making of Atlas Muon Chambers and the World Wide Higgs Hunt

[5] February 1, 2001
F. Sanchez
HERA B: an experiment to measure CP violation

[6] February 2, 2001
D. Zer Zion
Non Standard Model Higgs searches at LEP

[7] February 5, 2001
C. Padilla
CP violation and HERA-B: experiences for future experiments

[8] February 5, 2001
R. Nisius
The Structure of the Photon

[9] February 7, 2001
U. Uwer
HERA-B, a Spectrometer for High Rates: Achievements and Prospects

[10] February 21, 2001
A. Pellegrino
Inclusive Deep Inelastic Scattering Studies at HERA

[11] February 23, 2001
C. Tully
The Higgs search at LEP

[12] March 1, 2001
G. Raven
Measurement of CP violating Asymmetries and $B^0 - \bar{B^0}$ Mixing at Babar

[13] March 1, 2001
P. Gorham
Extreme Astronomy : Neutrinos from the edge

[14] March 9, 2001
A. de Roeck
The physics potential of CLIC

[15] March 12, 2001
T. Azemoon
The L3 Simulation Facility

[16] March 12, 2001
Ch. Loomis
Visualization of High-Energy Physics

[17] March 23, 2001
O. Melzer
Charm production at CHORUS

[18] March 26, 2001
J. Templon
Few-Body Nuclear Physics at Jefferson Lab

[19] March 30, 2001
J. Ralston
The Case for Zero Spin of the Gauge Sector

[20] April 12, 2001
M. Amarian
Deeply Virual Compton Scattering and Exclusive Meson Production at Hermes

[21] April 26, 2001
E. do Couto e Silva
Particle Astrophysics at SLAC

[22] May 11, 2001
F.E. Close
Glueballs: A central mystery

[23] May 15, 2001
Chr. Korthals Altes
Extra compact dimensions, or how to avoid domain walls

[24] May 18, 2001
J. Harris
First Glimpses of the Primordial Quark Gluon Soup?

[25] June 1, 2001
H. Stroeher
Hadron physics at COSY/Jülich

[26] June 6, 2001
W. Giele
Parton Density Function Uncertainties

[27] June 8, 2001
J. Dainton
Experimental Quantum Chromodiffraction

[28] June 27, 2001
Y. Gouz
Luminosity measurements in DELPHI with the STIC detector

[29] June 27, 2001
H.J. Bulten
Physics and Computing at LHCb

[30] June 29, 2001
R. Vogt
Charmonium production at HERA B

[31] June 29, 2001
M. Bouwhuis
Recent results from Hermes

[32] August 31, 2001
H. Chang (FOM)
Accenten voor 2001/2002

[33] September 7, 2001
R. Oldeman
B-physics at CDF: status and prospects

[34] September 14, 2001
R. Yoshida
Hard QCD and Structure Functions

[35] September 21, 2001
E. Richter-Was
Higgs bosons at LHC

[36] September 28, 2001
F. J. Yndurain
NNLO evaluations of DIS and precision calculations of α-strong

[37] October 5, 2001
N. de Groot
From Pixels to Physics

[38] October 18, 2001
E. Leader
First ever extraction of Fragmentation Functions without assumptions concerning favoured/unfavoured transitions

[39] October 19, 2001
N. van Eijndhoven
Heavy Ion Physics

[40] November 2, 2001
D. Cassel
Recent results from CLEO and plans for CLEO-c

[41] November 9, 2001
P. Kluit
Status of the CKM matrix; impact of LEP

[42] November 16, 2001
P. Katgert
Recent evidence for an acceleration of the expansion of the Universe

[43] November 30, 2001
J. Walraven
Properties of the Bose Einstein Condensates

[44] December 7, 2001
G. Raven
CP violation at Babar

5 NIKHEF Annual Scientific Meeting December 13-14, 2001, Amsterdam

[1] A. Bacchetta
A Transverse Look at the Proton

[2] T. Bauer
Overview of the B-physics program

[3] W. Beenakker
Large electroweak corrections at TeV-scale linear colliders

[4] S. Bentvelsen
ATLAS software

[5] M. Bruinsma
Recent results from HERA-B

[6] M. Dierckxsens
W selection/cross section/Anom. couplings at LEP

[7] S. Duensing
D0 analysis report

[8] J.J. Engelen
NIKHEF: today and tomorrow

[9] J. Ferreira Montenegro
W mass measurement at LEP

[10] F. Filthaut
D0 running report

[11] S. Grijpink
Charged Current interactions

[12] L. Huiszoon
D-branes and O-planes in String Theory

[13] R. Hierck
Track reconstruction at LHCb

[14] M. de Jong
Status of the Antares project

[15] E. Koffeman
Developments in vertex detection

[16] P. Kuijer
Status of the Alice program

[17] M. van Leeuwen
Status of NA49

[18] F. Linde
ATLAS progress report

[19] F. Linde
Recent ECFA and HEPAP reports

[20] S. Peeters
ATLAS tracker

[21] E. van der Pijll
Direct photons at WA98

[22] M.C. Simani
Flavour decomposition of the nucleon spin

[23] F. Spada
neutrino-charm physics

[24] J. Templon
The EU DataGrid Project at NIKHEF

[25] H. Tiecke
Status ZEUS

[26] C. Timmermans
Cosmic ray physics with the L3 muon spectrometer

[27] G. de Vries
Gamma Ray Burst detection with the Antares detector

F Resources and Personnel

1 Resources

In 2001 the NIKHEF income was 39.9 Mfl. The budget figures of the NIKHEF partners were: FOM-institute 26.1 Mfl, universities 9.6 Mfl of which 3.2 Mfl through the FOM Research Division of Subatomic Physics. In addition, third parties contributed 4.2 Mfl to the NIKHEF income.

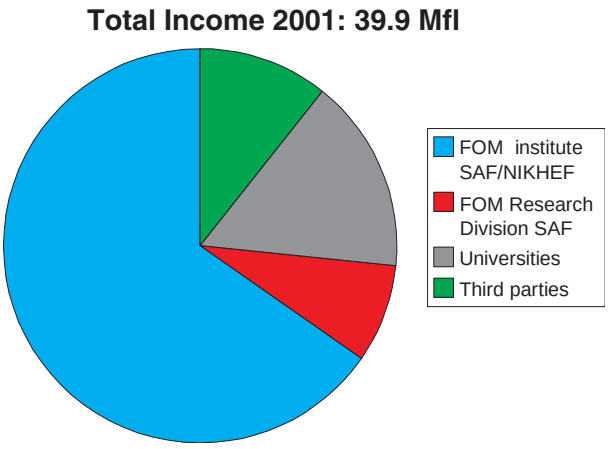

Figure 1.1: *NIKHEF funding*

The largest program, Atlas, represents about a quarter of the total budget. Antares appears for the first time as an approved FOM-program. Capital investments in 2001 were made for Atlas, LHCb and Antares.

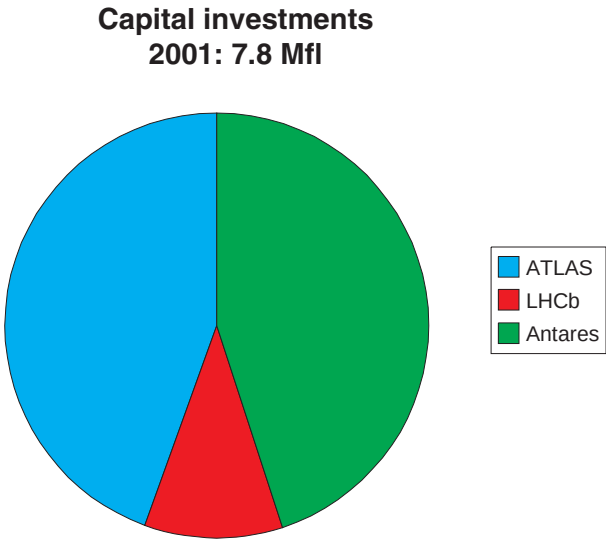

Figure 1.3: *Capital investments*

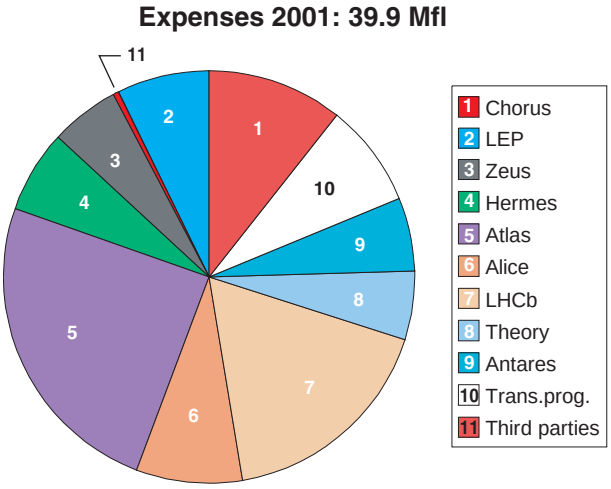

Figure 1.2: *Exploitation budget*

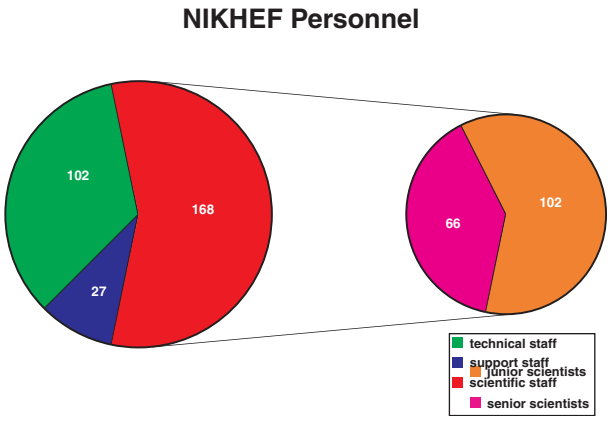

Figure 1.4: *Personnel as of December 31, 2001 (left). Subdivision of personnel: the scientists divided into senior and junior scientists (right).*

2 Membership of Councils and Committees during 2001

NIKHEF Board
F. T. M. Nieuwstadt (FOM, chairman)
K. H. Chang (FOM)
J. J. M. Franse (UvA)
S. Groenewegen (VU)
C. W. P. M. Blom (KUN)
J. G. F. Veldhuis (UU)
H. G. van Vuren (secretary, FOM)

Scientific Advisory Committee NIKHEF
G. Goggi (CERN)
K. Pretzl (Bern) from Oct. 2001
D. von Harrach (Univ. Mainz) until Oct. 2001
G. Ross (Univ. Oxford), chair, from Oct. 2001
M. Spiro (IN2P3)
J. Stachel (Univ. Heidelberg), chair, until Oct. 2001
J. Dainton (Univ. Liverpool) from Oct. 2001

NIKHEF Works Council
P. de Jong (chairman)
M. Vreeswijk (2nd chairman)
R. Hart (1st secretary)
J. Hogenbirk (2nd secretary)
A. Boucher
J. Dokter
E. van Kerkhoff
R. Kluit
S. Schagen
H. Schuijlenburg
J. Velthuis

FOM Board
J. J. Engelen until 1 July 2001
S. de Jong starting 1 January 2001

SPC-CERN
J. J. Engelen until 1 September 2001
K. J. F. Gaemers

LHCC-CERN
J. J. Engelen (chairman) until 1 September 2001
H. Tiecke (member) starting 1 September 2001

SPSC-CERN
B. Koene until 1 February 2001
M. de Jong

Extended Scientific Council, DESY
K. J. F. Gaemers
J. J. Engelen

ECFA
J. J. Engelen (also in Restricted ECFA starting 1 July 2001)
K. J. F. Gaemers
R. Kamermans
E. W. Kittel
G. van Middelkoop (also in Restricted ECFA until 1 July 2001)

NuPECC
G. van Middelkoop

HEP Board EPS
J. J. Engelen

Research Board CERN
J. J. Engelen (until 1 September 2001)

EPAC G. Luijckx

Beleidsadvies college KVI
G. Luijckx
P. Mulders

Scientific Committee Frascati Laboratory
G. van Middelkoop

Scientific Advisory Committee, Physique Nucleaire, Orsay
P. K. A. de Witt Huberts

Scientific Advisory Committee DFG Hadronen Physik
J. H. Koch
P. K. A. de Witt Huberts

Program Advisory Committee, ELSA (Bonn)/MAMI (Mainz)
H. P. Blok

Program Advisory Committee, Jefferson Laboratory
H. P. Blok

NNV Board
E. W. A. Lingeman
J. Konijn

OECD Global Science Forum Consultative Group
G. van Middelkoop until 1 July 2001
J. J. Engelen starting 1 July 2001

Other committees
St. CAN : J. Vermaseren
CERN, Task Force 2 : G. van Middelkoop
EPCS : W. Heubers
ESRF : G. Luijckx
HTASK : K. Bos
ICANN : R. Blokzijl
ICHEP2002 : G. van Middelkoop (chairman)
IRI : J. H. Koch
IWoRID : J. Visschers
JINR Scientific Council : G. van Middelkoop
Kuratorium HEPHY , Vienna : E. W. Kittel
NOMINET : R. Blokzijl
Physical Review Letters editorial Board : G. van der Steenhoven
RIPE : R. Blokzijl
St. Physica Board : J. Konijn
WAC KVI : G. van der Steenhoven
WCW Board : A. J. van Rijn

3 Personnel as of December 31, 2001

FOM, and the universities UVA, VU, KUN and UU are partners in NIKHEF (See colofon). UL and UT denote the universites of Leiden and Twente. GST stands for guest. Other abbreviations refer to the experiments, projects and departments.

1. Experimental Physicists

Akker, Drs. M. van den	KUN	L-3
Apeldoorn, Dr. G.W. van	UVA	B-Phys.
Baak, Drs. M.	VU	B-Phys.
Bakel, Drs. N.A. van	FOM	B-Phys.
Baldew, Drs. S.V.	UVA	L-3
Balm, Drs. P.W.	FOM	ATLAS
Barisonzi, Drs. M.	UT	ATLAS
Barneo González, Drs. P.J.	FOM	Other Projects
Bauer, Dr. T.S.	FOM	B-Phys.
Bentvelsen, Dr. S.C.M.	FOM	ATLAS
Blekman, Drs.Mw. F.	FOM	ATLAS
Blok, Dr. H.P.	VU	HERMES.
Blom, Drs. H.M.	FOM	DELPHI
Blouw, Dr. J.	Other	HERMES
Bobbink, Dr. G.J.	FOM	L-3
Boer, Dr. F.W.N. de	GST	ALGEMEEN
Boersma, Drs. D.J.	GST	AmPS-Phys.
Bokel, Drs. C.H.	GST	ZEUS
Bos, Dr. K.	FOM	ATLAS
Botje, Dr. M.A.J.	FOM	ALICE
Bouwhuis, Drs. Mw. M.C.	FOM	ANTARES
Brand, Prof.Dr. J.F.J. van den	VU	Other Projects
Bruinsma, Drs. M.	FOM	B-Phys.
Bruinsma, Ir. P.J.T.	GST	ANTARES
Buis, Drs. E.J.	GST	ATLAS
Bulten, Dr. H.J.	FOM-VU	B-Phys.
Buuren, Drs. L.D. van	FOM	Other Projects
Calvet, Dr. D.	GST	ATLAS
Cârloganu, Dr. Mw. F.C.	FOM	ANTARES
Crijns, Dipl.Phys.F.J.G.H.	FOM-KUN	ATLAS
Dalen, Drs. J. van	FOM-KUN	L-3
Dam, Dr. P.H.A. van	UVA	DELPHI
Dantzig, Dr. R. van	GST	CHORUS
Daum, Prof.Dr. C.	GST	ATLAS
Diddens, Prof.Dr. A.N.	GST	DELPHI
Dierckxsens, Drs. M.E.T.	FOM	L-3
Dierendonck, Drs. D.N. van	GST	L-3
Duensing, Drs. Mw. S.	KUN	ATLAS
Duinker, Prof.Dr. P.	GST	L-3
Eijk, Prof.Dr. B. van	FOM	ATLAS
Eijk, Ir. R.M. van der	FOM	B-Phys.
Eldik, Drs. J.E. van	GST	DELPHI
Engelen, Prof.Dr. J.J.	UVA	DIR
Erné, Prof.Dr.Ir F.C.	GST	L-3
Eyndhoven, Dr. N. van	FOM-UU	Other Projects
Ferreira Montenegro, Drs. Mw. J.	FOM	DELPHI
Filthaut, Dr. F.	KUN	ATLAS
Fornaini, Drs. A.	FOM	ATLAS
Garutti, Drs. Mw. E.	FOM	HERMES
Gouz, Dr. I	GST	B-Phys.
Graaf, Dr.Ir. H. van der	FOM	ATLAS
Grijpink, Drs. S.J.L.A.	FOM	ZEUS
Groep, Dr. D.L.	FOM	Other Projects
Gulik, Ir. R.C.W. van	UL	ATLAS
Hartjes, Dr. F.G.	FOM	ATLAS
Heesbeen, Drs. D.	FOM	HERMES
Heijboer, Drs. A.J.	UVA	ANTARES
Hesselink, Dr. W.H.A.	VU	HERMES
Hessey, Dr. N.P.	FOM	ATLAS
Hierck, Drs. R.H.	FOM-VU	B-Phys.
Hommels, Ir. L.B.A.	FOM	B-Phys.
Hu, Drs. Y.	FOM-KUN	L-3
Hulsbergen, Drs. W.D.	FOM	B-Phys.
Jans, Dr. E.	FOM	AmPS-Phys.
Jong, Dr. M. de	FOM	ANTARES
Jong, Dr. P.J.	FOM	ATLAS
Jong, Prof.Dr. S.J.	KUN	ATLAS
Kamermans, Prof.Dr. R.	FOM-UU	ALICE
Ketel, Dr. T.J.	FOM-VU	B-Phys.
Kittel, Prof.Dr. E.W.	KUN	L-3
Klok, Drs. P.F.	FOM-KUN	ATLAS
Klous, Drs. S.	FOM-VU	B-Phys.
Kluit, Dr. P.M.	FOM	ATLAS
Koene, Dr. B.K.S.	FOM	B-Phys.
Koffeman, Dr.Ir. Mw. E.N.	FOM	ZEUS
König, Dr. A.C.	KUN	ATLAS
Konijn, Dr.Ir. J.	GST	CHORUS
Kooijman, Prof.Dr. P.M.	UVA	ZEUS
Kuijer, Dr. P.G.	FOM	ALICE
Laan, Dr. J.B. van der	FOM	Other Projects
Lapikás, Dr. L.	FOM	HERMES
Lavrijsen, Drs. W.T.L.P.	FOM-KUN	ATLAS
Laziev, Drs. A.E.	FOM-VU	HERMES
Leeuwen, Drs. M. van	FOM	ALICE
Linde, Prof.Dr. F.L.	UVA	ATLAS
Luijckx, Ir. G.	FOM	ATLAS
Maas, Dr. R.	FOM	Other Projects
Maddox, Drs. E.	UVA	ZEUS
Mangeol, Drs. D	GST	L-3
Massaro, Dr. G.G.G.	FOM	ATLAS
Merk, Dr. M.H.M.	FOM	B-Phys.
Metzger, Dr. W.J.	KUN	L-3
Mevius, Drs. Mw. M.	FOM-UU	B-Phys.
Mexner, Drs. Mw. I.V.	FOM-BR	HERMES
Middelkoop, Prof.Dr. G. van	GST	Other Projects
Naumann, Drs. A.	FOM	ATLAS
Needham, Dr. M.D.	FOM	B-Phys.
Nooren, Dr.Ir. G.J.L.	FOM-UU	ALICE
Ouchrif, Dr. M.	FOM	B-Phys.
Peeters, Ir. S.J.M.	FOM	ATLAS
Pellegrino, Dr. A.	FOM	B-Phys
Peters, Drs. O.	UVA	ATLAS
Petersen, Drs. B.	GST	L-3
Phaf, Drs. L.K.	FOM	ATLAS
Pijll, Drs. E.C. van der	FOM-UU	Other Projects
Putte, Dr.Ir. M.J.J. van den	FOM	Other Projects
Reid, Dr. D.W.	FOM	DELPHI

Reischl, Drs. A.J.	FOM	HERMES
Rens, Drs. B.A.P. van	FOM	ANTARES
Rijke, Drs. P. de	FOM-UU	ALICE
Roux, Drs. Mw. B.	FOM-KUN	L-3
San Segundo Bello, Drs. D.	FOM-HCM	Other Projects
Sanders, Drs. M.	GST	L-3
Sbrizzi, Drs. A.	FOM	B-Phys.
Schagen, Drs. S.E.S.	FOM	ZEUS
Schillings, Drs. E.	FOM-UU	ALICE
Scholte, Ir. R.C.	UT	ATLAS
Schotanus, Dr. D. J.	KUN	L-3
Simani, Drs. Mw. M.C.	FOM-VU	HERMES
Sokolov, Drs. A.	UU	ALICE
Spada, Dr. Mw. F.R.	GST	CHORUS
Steenbakkers, Drs. M.F.M.	GST	Other Projects
Steenhoven, Prof.Dr. G. van der	FOM	HERMES
Steijger, Dr. J.J.M.	FOM	HERMES
Stonjek, Dipl. Phys. S.	Other	ZEUS
Tassi, Dr. E.	FOM	ZEUS
Templon, Dr. J.A.	FOM	B-Phys
Tiecke, Dr. H.G.J.M.	FOM	ZEUS
Tilburg, Drs. J.A.N.	FOM	B-Phys.
Timmermans, Dr. J.J.M.	FOM	DELPHI
Toet, Dr. D.Z.	GST	Other Projects
Tvaskis, Drs. V.	VU	HERMES
Uiterwijk, Ir. J.W.E.	GST	CHORUS
Velthuis, Ir. J.J.	FOM	ZEUS
Vermeulen, Dr.Ir. J.C.	UVA	ATLAS
Vavrik, Dr. D.	FOM-HCM	Other Projects
Visschers, Dr. J.L.	FOM	Other Projects
Visser, Drs. E.	KUN	ATLAS
Visser, Drs. J.	FOM	HERMES
Vos, Drs. M.A.	UT	ATLAS
Vreeswijk, Dr. M.	FOM	ATLAS
Vries, Drs. G. de	UU	ANTARES
Vries, Dr. H. de	FOM	B-Phys.
Vulpen, Drs. I.B. van	FOM	DELPHI
Wahlberg, Drs. H.	UU	B-Phys.
Wiggers, Dr. L.W.	FOM	ZEUS
Wijngaarden, Drs. D.A.	KUN	ATLAS
Wilkens, Drs. H.G.S.	FOM-KUN	L-3
Witt Huberts, Prof.Dr. P.K.A.	FOM	ANTARES
Wolf, Dr. Mw. E. de	UVA	ZEUS
Woudstra, Ir. M.J.	GST	ATLAS
Zihlmann, Dr. B.	FOM-VU	HERMES

2. Theoretical Physicists

Bachetta, Drs. A.	FOM-VU
Eynck, Dipl.Phys. T.O.	FOM
Fuster, Drs. Mw. A.	GST
Gaemers, Prof.Dr. K.J.F.	UVA
Gato-Rivera, Dr. Mw. B.	GST
Heide, Drs. J. van der	FOM
Henneman, Drs. A.	GST
Holten, Prof.Dr. J.W. van	FOM
Huiszoon, Drs. L.R.	FOM
Iersel, Drs. M. van	FOM-VU
Kleiss, Prof.Dr. R.H.P.	KUN
Koch, Prof.Dr. J.H.	FOM
Laenen, Dr. E.	FOM
Marques de Sousa, Drs. N.M.	GST
Metz, Dr. A.	FOM-VU
Mulders, Prof.Dr. P.J.G.	VU
Nyawelo, B.Sc. T.S.	FOM
Pijlman, Drs. F.	VU
Riccioni, Dr. F.	FOM
Schellekens, Prof.Dr. A.N.J.J.	FOM
Veltman, Prof.Dr. M.J.G.	GST
Vermaseren, Dr. J.A.M.	FOM
Vogt, Dr. A.	Other
Warringa, Drs. H.	VU
Wit, Prof.Dr. B.Q.P.J. de	UU
Zhou, Dr. M.	FOM

3. Computer Technology Group

Akker, T.G.M. van den	FOM
Antony, A.T.	FOM
Blokzijl, Dr. R.	FOM
Boterenbrood, Ir. H.	FOM
Damen, Ing. A.C.M.	FOM
Geerts, M.L.	FOM
Harapan, Drs. D.	FOM
Hart, Ing. R.G.K.	FOM
Heubers, Ing. W.P.J.	FOM
Huyser, K.	FOM
Joosten, Dr. Mw. K.	Other
Kuipers, Drs. P.	FOM
Leeuwen, Drs. W.M. van	FOM
Oudolf, J.D.	QUADO
Schimmel, Ing. A.	FOM
Steenbakkers, Ir. M.F.M.	FOM
Tierie, Mw. J.J.E.	FOM
Venekamp, Drs. G.M.	FOM
Wijk, R.F. van	FOM

4. Electronics Technology Group

Berkien, A.W.M.	FOM
Beuzekom, Ing. M.G.van	FOM
Boer, J. de	FOM
Boerkamp, A.L.J.	FOM
Born, E.A. van den	FOM
Es, J.T. van	GST
Evers, G.J.	FOM
Fransen, J.P.A.M.	FOM
Gotink, G.W.	FOM
Groen, P.J.M. de	FOM
Groenstege, Ing. H.L.	FOM
Gromov, Drs. V.	FOM
Haas, Ing. A.P. de	FOM
Harmsen, C.J.	FOM
Heine, Ing. E.	FOM

Heutenik, B.	FOM
Hogenbirk, Ing. J.J.	FOM
Jansen, L.W.A.	FOM
Jansweijer, Ing. P.P.M.	FOM
Kieft, Ing. G.N.M.	FOM
Kluit, Ing. R.	FOM
Kok, Ing. E.	FOM
Koopstra, J.	UVA
Kroes, Ir. F.B.	FOM
Kruijer, A.H.	FOM
Kuijt, Ing. J.J.	FOM
Mos, Ing. S.	FOM
Peek, Ing. H.Z.	FOM
Reen, A.T.H. van	FOM
Rewiersma, Ing. P.A.M.	FOM
Schipper, Ing. J.D.	FOM
Sluijk, Ing. T.G.B.W.	FOM
Stolte, J.	FOM
Timmer, P.F.	FOM
Verkooijen, Ing. J.C.	FOM
Vink, Ing. W.E.W.	FOM
Wieten, P.	FOM
Zwart, Ing. A.N.M.	FOM
Zwart, F. de	FOM

5. Mechanical Engineering Group

Arink, R.P.J.	FOM
Band, H.A.	FOM
Boer Rookhuizen, H.	FOM
Boomgaard-Hilferink, Mw. J.G.	FOM
Boucher, A.	FOM
Buskop, Ir. J.J.F.	FOM
Doets, M.	FOM
Hover, Ing. E.P.	FOM
Kaan, Ir. A.P.	FOM
Korporaal, A.	FOM
Kraan, Ing. M.J.	FOM
Lassing, P.	FOM
Lefévere, Y.	FOM
Munneke, Ing. B.	FOM
Riet, Ing. M.	FOM
Schuijlenburg, Ing. H.W.A.	FOM
Snippe, Ir. Q.H.C.	FOM
Thobe, P.H.	FOM
Verlaat, Ing. B.A.	FOM
Verschuijl, J.R.	Other
Werneke, Ing. P.J.M.	FOM
Zegers, Ing. A.J.M.	FOM

6. Mechanical Workshop

Apel, A.W.	FOM
Berbee, Ing. E.M.	FOM
Beumer, H.	FOM
Boer, R.P. de	FOM
Bron, M.	FOM
Brouwer, G.R.	FOM
Bruijn, E.J.	FOM
Buis, R.	FOM
Ceelie, L.	UVA
Homma, J.	FOM
Jacobs, J.	FOM
Jaspers, M.J.F.	UVA
John, D.	FOM
Kok, J.W.	FOM
Kuilman, W.C.	FOM
Langedijk, J.S.	FOM
Leguyt, R.	FOM
Mul, F.A.	FOM-VU
Overbeek, M.G. van	FOM
Petten, O.R. van	FOM
Rietmeijer, A.A.	FOM
Roeland, E.	FOM
Römers, L.W.E.G.	FOM
Rövekamp, J.C.D.F.	UVA
Veen, J. van	FOM

7. Management and Administration

Berg, A. van den	FOM
Buitenhuis, W.E.J.	FOM
Bulten, F.	FOM
Cossee, Mw. N.	Other
Doest, Mw. C.J.	Other
Dokter, J.H.G.	FOM
Dulmen, Mw. A.C.M. van	FOM
Echtelt, Ing. H.J.B. van	FOM
Egdom, T. van	FOM
Geerinck, Ir. J.	GST
Greven-v.Beusekom, Mw. E.C.L.	FOM
Heuvel, Mw. G.A. van den	FOM
Hooff, F.B. van	Other
Kerkhoff, Mw. E.H.M. van	FOM
Kesgin-Boonstra, Drs. Mw. M.J.	FOM
Langelaar, Dr. J.	UVA
Langenhorst, A.	FOM
Lemaire-Vonk, Mw. M.C.	FOM
Louwrier, Dr. P.W.F.	FOM
Mulders, Mw. P.N.	FOM
Mors, A.G.S.	UVA
Pancar, M.	FOM
Post, Mw. E.C.	FOM
Rijksen, C.	FOM
Rijn, Drs. A.J. van	FOM
Rooij, Mw. T.J. La	QUADO
Spelt, Ing. J.B.	FOM
Visser, J.	FOM
Vries, W. de	FOM
Woortmann, E.P.	Other

8. Apprentices in 2001

Aeijelts Averink, R.

Afework, Y.
Amasslam, M.
Azouagh, Mw. S.
Barisonzi, M.
Bobeldijk, A.
Boer, Y.R. de
Boezaart, T.J.
Bruijn, R.
Dalhuizen, J.M.
Davidse, F.
Davidse, M.
Demey, M.
Dirks, B.P.F.
Donders, R.S.
Dongen, B.J. van
Fosse, D. Hadri, A.
Hagebeuk, J.C.
Hal, M.C. van
Huiting, R.
Hulsman, M.
Jansen, F.M.
Jeukens, S.
Kappert, Mw. L.
Kop, A.
Krijger, Mw. E.
Kruijtzer, G.L.
Lim, G.
Mejdoubi, K.
Nat, P.B. van der
Nijenhuis, Mw. N.
Oudolf, H.
Pronk, M.
Rantwijk, J. van
Schouten, S.S.
Silkens, I.M.A.
Snoek, H.L.
Spoor, V.
Tascon Lopez, D.
Timmer, R.
Vliet, E. van
Vogelvang, M.

9. They left us

Adamus, Dr. M.
Agasi, Dr. E.E.
Amaryan, Dr. M.
Bakker, C.N.M. † 30/7/01
Batenburg, Dr. M.F. van
Bouhali, Dr. O.
Brammerloo, A.V.
Buijs, Prof.Dr. A.
Buis, Drs. E.J.
Buskens, J.P.M.
Derrick, Prof.Dr. M.
Geerinck, Ir. J.
Duinker, Prof.Dr. P.
Gerritsen - Visser, Mw. J.
Gulik, Ir. R.C.W. van
Haan, M.
Heijne, Dr.H.M.
Jarvis, Dr. P.
Kruiper, H.A.
Laan, Mw. F.M.
Lutterot, Drs. M.
Mangeol, Drs. D.
Melzer, Dr. O.
Middelkoop, Prof. Dr. G. van
Mil, Drs. A. van
Muigg, Dr. Mw. D.
Muijs Dr. Mw. A.J.M.
Mulders, Dr. M.P.
Noomen, Ir. J.G.
Pesen, Dr. E.
Ploeg, F.
Reid, Dr. D.W.
Römers, L.W.E.G.
Schalm, Dr. K.E.
Sichtermann, Dr. E.P.
Trigt, J.H. van
Tuning, Dr. N.
Ven, Drs. P.A.G. van de
Yndurain, Dr. F.
Zupan, Drs. M.